Towards Understanding the Role of Branched Ubiquitin Chains in Cellular Signaling

By

Sean O. Crowe

A dissertation submitted in partial fulfillment of the requirements for the degree of

Doctor of Philosophy

(Chemistry)

At the University of Wisconsin-Madison

2018

Date of final oral examination: August 8, 2018 2:00 PM

The dissertation is approved by the following members of the Final Oral Committee:

Eric R. Strieter, Associate Professor, Chemistry

Ying Ge, Associate Professor, Chemistry

Lloyd Smith, Professor, Chemistry

Judith Burstyn, Professor, Chemistry

Acknowledgments

Working towards a PhD in any field is a selfish endeavor and awards should be given to the people who support those of us who attempt it. As I do not have the power to grant such awards hopefully, this section of my thesis will suffice. I have been incredibly lucky with the amount of help and support I have been shown throughout my life and time in graduate school, and it will be impossible to mention everyone without making this section the length of a chapter, so I will *try* to be brief.

There are several groups of people whom I need to thank, the first one being my family. Thank you to my parents who have always worked and sacrificed so I can have a better life. You have always inspired me to work hard to achieve my dreams. Growing up, you taught me to find enjoyment in learning new things and because of that I have continued to try to learn new things every day. Without those experiences I do not think I would be here today. Also thank you to my sister Veronica, you are an incredibly strong person and you inspire me every day. And thank you to my nephew John and niece Ariel. I have loved watching you grow up and look forward to seeing what amazing things you will do in the future. Finally, thank you to my brother in law, Matt for being there for my sister and the kids.

I have also been extraordinarily fortunate to have two grandfathers who have been exceptionally inspirational to me. Thank you to my Grandpa John. You are one of the hardest working people I have ever met. You have taught me many lessons including the value of hard work and the importance of learning as much as I can. You have also been one person who I can always depend on and I will forever be grateful of that. Also thank you my Grandpa Jerry, another person whom I respect greatly and have learned a lot from. I know that I can always come to you for advice and I will never forget how much you have done for me over the years.

Next up on the list is my advisor Eric Strieter. Thank you for teaching me to be a critical thinker and better scientist. Also thank you for somehow finding the perfect balance of both giving me the freedom

and independence to design and work on my projects while also knowing exactly when I need to be pointed in the right direction. I will miss your ability to think of the perfect experiment to test something that I am stuck on. Finally, I will also miss your excitement for science and I hope to find another mentor that is as passionate about the work I am doing as you are.

I would also like to thank the members of the Strieter Lab past and present. You have all been influential to my time in graduate school and I have enjoyed having you as colleagues and collaborators. Science cannot be performed in a vacuum, and you always need help to achieve anything of value, so without this team of people I would have never made it off the ground. To Drs. Vivian Trang, Ellen Valkevich, Grace Pham, Robert Guenette, and Ambar Rana, thank you for accepting me into the lab and training me. Without your help I would have never transitioned from a bumbling first year into a scientist. Also Thank you to the current Strieter Lab members: Dr. Jiian Liu, Lin Hui Chang, Kirandeep Deol, Jiale Du, Sándor Babik, Yanfeng Li, and Heather Bisbee. It has been a pleasure to work with and learn from such a hardworking and dedicated group of scientists. I know it will be sad to leave such an amazing group of people. Finally, thank you to the undergrad that I had the honor to work with, Jacob Ziegler. It was a pleasure being able to help you grow as a scientist and it was always fun having you around. I miss having your help and infectious personality in the lab.

There are not a lot of benefits to relocating your life in the middle of graduate school, but one thing that I have appreciated about the move from Madison to Amherst is that I have had the pleasure of working in two great environments. This has given me the ability to take advantage of resources and expertise while at both schools. Starting with Madison, I need to thank the members of the Kiessling, Gellman, Blackwell, Ge, Fredrickson, Smith, and Cavagnero Labs whom I have interacted with and learned from over the years. Whether it was sharing reagents, expertise, or time, I enjoyed having such a supportive community to work and be a part of. Also thank you to Martha Vestling for all your help while

I was at UW. I was able to lean on your experience and expertise more than a few times and I have appreciated it greatly.

While at UMass, I have also had great experiences with the excellent community here. Special thanks to the labs we share the 7th floor with (Chen and Hardy) for helping us transition to our new home and accepting us as colleagues and friends. Also thank you to the attendees of the CS3 (Chien, Stratton, Serio and Strieter) group meeting. This has been one of the most enjoyable aspects of our move as every week I get to experience new perspectives and opinions and I am exposed to completely different techniques and projects. The discussions had during these meetings have resulted in many new ideas, I would have never come up without these experiences. Thank you to Drs. Stephen Eyles and Lizz Bartlett for helping me with many aspects of my project and sharing your expertise with me and also having patience with me while I learn to use your instruments even when I may have made extra work for you. Special thanks to Bob Sabola and Ryan Feyrer, who have at this point fixed an uncountable number of instruments and problems for the lab and have basically kept our lab running. Finally, thank you to all the friends that I have been able to make while in UMass, I truly appreciate you accepting Meg and me into your lives and making us feel welcome.

Thank you to the people who have served on various committees. It takes a lot of time and patience to help graduate students become scientists. And even though in the moment, many of these exams are stressful, I have always found the advice and suggestions given to be incredibly helpful in my development as a scientist. Thank you for your time, advice, and help throughout my PhD.

Outside of work and science, there are several friends that have had an impact on my life. Perhaps the most obvious of these is Ambar Rana and Dan Araki, with whom I have had countless enjoyable experiences and discussions. Thank you for making life in Madison more enjoyable. I also need to thank

Franky Alvarado. You have been a great friend ever since we were young and you are another person I can always talk to when I am struggling with science or life.

This list would not be complete without mention of my second family, the McHales. Jim and Nancy, you have been incredibly welcoming of me and I have come to feel at home whenever I am at your house. I truly appreciate all of the support you have shown me throughout the years and I do not know where I would be without it. Also, Sean and Danny, you have become like brothers to me and exceptional friends. Thank you for welcoming me into your family.

There is no one more deserving of my gratitude than Megan McHale. Thank you, Meg, for always being there for me. Even on the hardest days you are always there to make me smile. Also, thank you for all of the sacrifices you have had to endure so I can achieve my dream. You have stuck with me through this roller coaster and never gave up. Finally, thank you for just being a wonderful person. I have never met someone who can adapt to any situation like you can and I doubt I ever will. I have been very lucky to have you in my life and I have enjoyed having you with me for all of the good times and the tough ones, and I look forward to whatever the future brings.

Abstract

The covalent attachment of the small protein, ubiquitin (Ub), to proteins represents one of the most versatile post-translational modifications in eukaryotic cells. This modification occurs between the C-terminus of Ub and the ε-amino group of lysine residues on target proteins by an enzymatic cascade involving three classes of enzymes, E1, E2, and E3. This modification is dynamic and the removal of Ub from substrates is facilitated by a special class of protease known as deubiquitinases or DUBs. As Ub has eight potential modification sites including its seven lysine residues (Lys6, Lys11, Lys27, Lys29, Lys33, Lys48, and Lys63) as well as its N-terminal methionine (Met1), Ub itself can be ubiquitinated resulting in the formation of Ub polymers. These polymers can adopt a vast array of potential configurations, including both unbranched and branched Ub chains. These various configurations allow Ub chains to fill a large amount of chemical space, giving Ub unparalleled versatility in cellular signaling. To date, the study of Ub chains has largely been limited to characterizing the role of unbranched homotypic chains in cellular signaling. This limitation is due to a lack of suitable tools available for the study of the more complicated Ub chain configurations. The goal of this thesis is to introduce new tools that will allow us to better study branched Ub chains. The first chapter of this thesis describes a fluorescence labeling strategy that allows us to examine substrate selectivity when a DUB hydrolyzes branched chains. The next chapter introduces an analytical workflow called Ubiquitin Chain Enrichment Middle-Down Mass Spectrometry (UbiChEM-MS) to detect and characterize branched chains in a cellular context. The final chapter of this thesis combines these tools and others to explore how branched chains are regulated in the cell. Herein we examine a novel activity for the proteasome associated DUB, UCH37, using a combination of protein chemistry, enzymology, and analytical chemistry to show this enzyme selectively debranches Ub chains containing Lys48 linkages.

Table of Contents

List of Figures

List of Tables

List of Schemes

1 Introduction

1.1 Overview of Ubiquitin Signaling

Cells use a variety of means to sense and respond to their environment. One of the key mechanisms they employ is the post-translational modification (PTM) of proteins. PTMs increase the versatility of expressed proteins by altering their cellular function and providing spatial and temporal control over protein function.[1] Perhaps the most versatile PTM is the modification of proteins with ubiquitin (Ub). This modification termed ubiquitination regulates nearly every signaling pathway in eukaryotic cells, including many critical events such as progression through the cell cycle,[2] repair of damaged DNA,[3, 4] maintenance of protein quality and proteostasis,[5] and the immune response.[6-10] The Ub protein is highly conserved amongst all eukaryotic organisms with only three amino acid substitutions between the yeast and human protein. Consistent with this high degree of conservation, malfunctions in the ubiquitination machinery are implicated in the pathogenesis of several human diseases including many cancers and neurodegenerative diseases.[11-13] Additionally, it is widely accepted that pathogenic bacteria have also evolved to manipulate the ubiquitination machinery to evade the immune response.[14-17] As such there is a lot of interest in understanding how Ub regulates these signaling pathways.

Ub is a relatively small, 76 amino acid protein, installed on lysine residues of substrate proteins resulting in the formation of an isopeptide bond between the C-terminus of Ub and the ε-amino group of the modified lysine. This modification is highly abundant with over 63,000 unique ubiquitination sites on over 9,000 proteins identified in a recent proteomic study.[18] Ubiquitination is also highly regulated, requiring the coordinated effort of three classes of enzymes: 1) ubiquitin activating enzymes known as E1 (2 enzymes) 2) ubiquitin conjugating enzymes known as E2s (~40 enzymes) and 3) ubiquitin ligating enzymes known as E3s (>600 enzymes) (Figure 1.1).[7, 8, 19] Ubiquitination is also dynamic and can be reversed by a special class of proteases known as deubiquitinases or DUBs (~ 100 enzymes).[20, 21] In total cells dedicate nearly 5% of their genome to the proper maintenance of Ub modifications.[19] It is through

combinations of this vast set of ubiquitination/deubiquitination machinery that cells can modify such a large portion of its proteome in a highly selective manner.

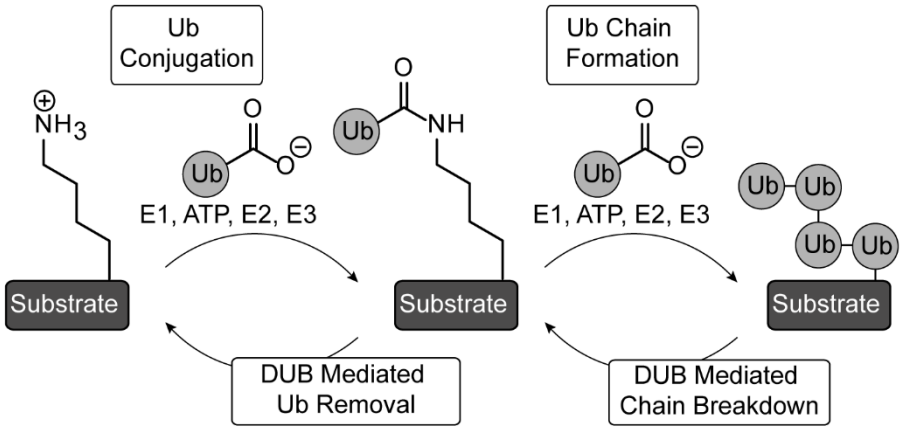

Figure 1.1: Ubiquitin is a dynamic post-translational modification. The post-translational modification of proteins by Ub occurs through the coordinated efforts of three classes of enzymes: E1, E2, and E3 in an ATP dependent manner. Repeated events can result in ubiquitination of any of Ub's seven lysine residues or N-terminal Met, resulting in the formation of Ub chains. Modification of proteins by Ub is reversed by a special class of proteases known as DUBs, which can either break down Ub chains or remove Ub from modified substrates. The dashes in between Ub subunits represent an isopeptide linkage and are drawn this way for clarity.

The versatility of Ub stems from its structure. Ub adopts a β-grasp fold with two exposed hydrophobic patches centered around Ile36 and Ile44. These patches mediate interactions between Ub and the Ub regulatory machinery.[22, 23] The flexible C-terminus serves as the attachment point for its substrate proteins (Figure 1.2 A). Additionally, Ub has eight reactive amines including its seven lysine residues (Lys6, Lys11, Lys27, Lys29, Lys33, Lys48, or Lys63) and N-terminus (Met1), all of which all can serve as attachment points for further ubiquitination resulting in the formation of polymeric Ub chains (Figure 1.2 A).[7, 8] In fact, all eight Ub chain types have been detected in proteomic studies.[24] The different polymers can adopt several unique configurations including uniform unbranched chains, where a single Ub linkage is formed

throughout, heterotypic (mixed) unbranched chains, and branched chains, in which a single Ub subunit is modified at multiple positions (Figure 1.2 B). To further complicate matters, a single substrate can be modified at multiple lysine residues with one or more Ub modifications to produce complex signals. Interestingly, structural studies have shown that Ub chains adopt unique structures depending on their linkage types.[7] These differences result in unique orientations of the hydrophobic patches of different Ub subunits relative to one another.[7, 23] This difference in orientation of the Ub surface allows for selective Ub binding proteins to recognize and interact with different Ub chain types to promote cellular signaling. These selective interactions have led to the hypothesis of a Ub code where different chain types promote unique aspects of cellular signaling.[7] To date several features of this code have been deciphered including the roles of Met1 chains in NF-κB signaling,[10, 25, 26] Lys6 chains in the DNA damage response,[27-29] Lys11 chains as cell cycle regulators,[2, 30-32] Lys48 chains as degradation tags,[33-35] and Lys63 in non-proteasomal signaling including protein trafficking[36, 37] and DNA damage repair pathways.[38-41]

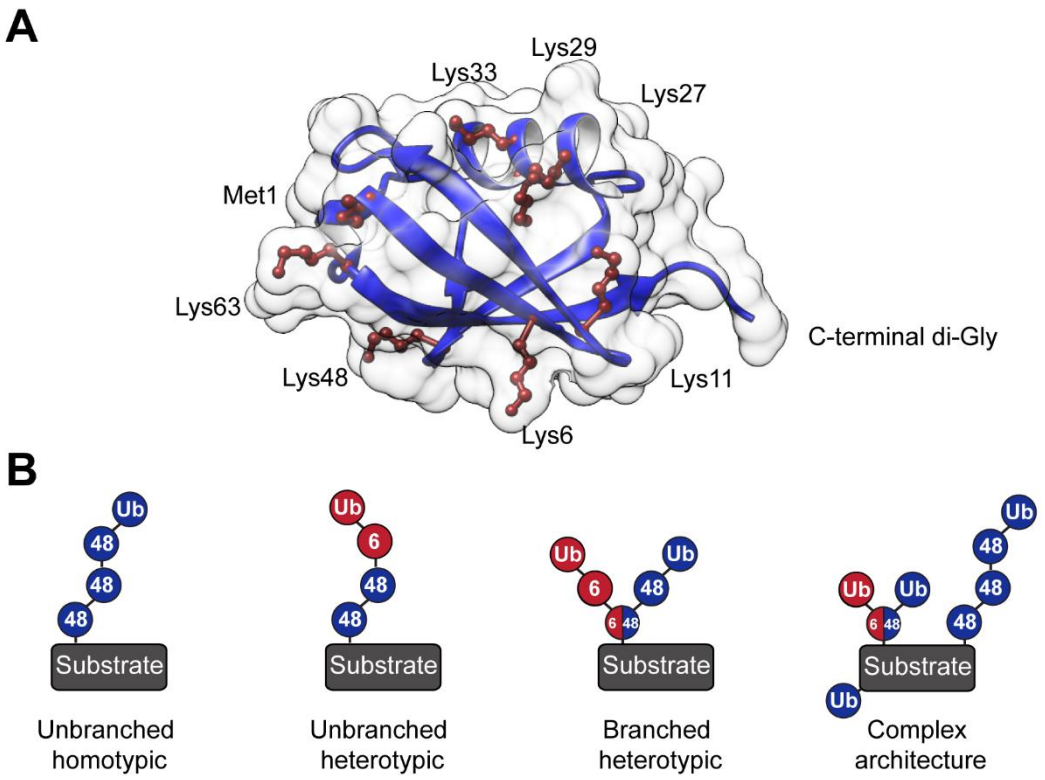

Figure 1.2: The versatility of Ub modifications is encoded in Ub's structure. A) Crystal structure of Ub (PDB ID: 1UBQ)[42] showing the eight amino groups of Ub and its flexible C-terminus. **B**) Ub polymers can adopt a wide variety of configurations including both unbranched and branched chains. Additionally, substrates can be modified with multiple Ub modifications at once resulting in complex signals. The number labeled on individual subunits represents the Lys residue that is modified on that Ub subunit, the dash between monomers represents the isopeptide linkage holding individual monomers together.

The strongest evidence for different Ub chains encoding for different signaling outputs is the comparison between Lys48 and Lys63 linked chains. Chains linked through Lys48 tend to adopt dynamic and compact structures with strong contacts at the interface between individual monomers.[43-45] Lys63 linked chains, on the other hand adopt open conformations with little contact between the individual subunits of a chain (Figure 1.3).[46] This results in specific positioning of the Ub hydrophobic patches along the Ub chain (Figure 1.3). These exposed hydrophobic surfaces serve as the binding sites for many DUBs

and Ub interacting proteins. In the case of Lys48 and Lys63 linked chains, the positions of these patches differ in both the distance between patches as well as the orientation of the patches along the surface of the chain.[7] This gives Lys48 and Lys63 linked chains unique surface properties that can be recognized by specialized Ub binding domains (UBDs) which translate the information in individual chains into separate signaling events e.g., proteasomal degradation for Lys48 chains and non-degradative signals for Lys63.[7, 23]

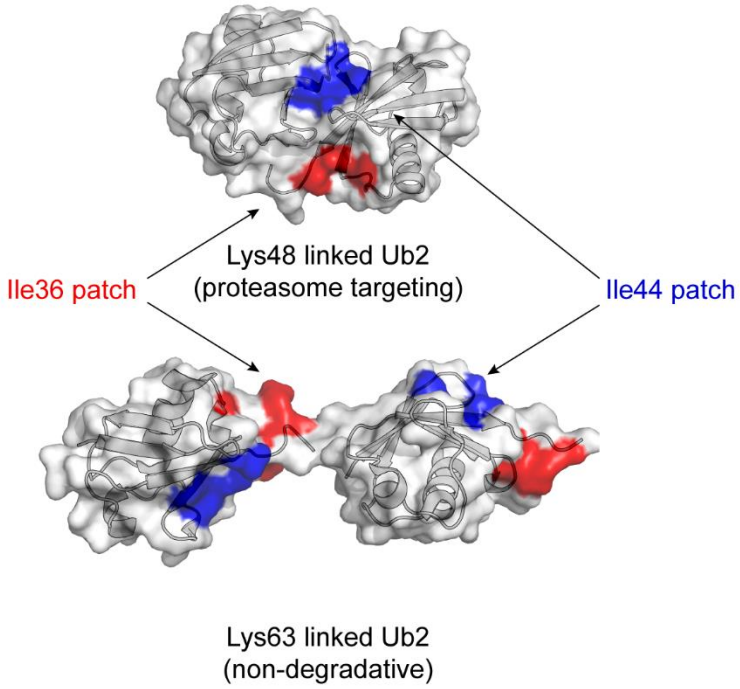

Figure 1.3: Ub linkages encode different signals by adopting unique conformations. Ub chains linked through different Lys residues adopt unique structures relative to one another. The top structure shows one conformation of the Lys48 linked Ub dimer (PDB ID: 1AAR)[44] and the bottom shows the structure of a Lys63 linked dimer (PDB ID: 2JF5).[46] The Lys48 chain adopts a compact structure while the Lys63 linked chain adopts an open structure. This results in unique orientations of the Ile36 and Ile44 hydrophobic patches shown in red and blue respectively.

Although there is a lot of evidence supporting individual roles for Lys48 and Lys63 chains in cellular signaling, it has been difficult to assign individual functions for many of the other Ub chain types. For

example, a recent proteomics study has shown that all Ub linkage types except for Lys63 chains accumulate upon proteasomal inhibition, suggesting that many chain types target proteins to the proteasome.[47] In agreement, Lys11 linked Ub chains are known to be necessary to drive proteasomal degradation of cell cycle regulating proteins and misfolded proteins.[32] However, Lys11 linked chains can only become potent degradation signals when combined with Lys48 linked chains in a branched configuration.[31] Additionally, substrates modified by Lys63 or Lys29 chains can also be transformed into potent degradation signals by the addition of Lys48 branch points, suggesting that the cell can fine tune or edit Ub signaling by incorporating branch points.[48, 49]

The observations that branched Ub chains can alter the fate of ubiquitinated proteins suggests that there must be unique properties associated with this chain configuration. As branching increases the density of Ub subunits, new conformations might emerge. The proximity of multiple Ub chains to one another also results in a high local concentration of Ub surrounding the branch point, suggesting a possible mechanism by which branched chains affect cellular signaling by acting as higher affinity docking sites for various signaling molecules.

Evidence for specialized binding surfaces can be found in the transcriptional response to activation of the innate immune system. This signaling pathway is regulated by the transcription factor, nuclear factor-κB (NF-κB), which remains inactive until binding of stimulatory molecules e.g., lipopolysaccharide (LPS).[50] Upon recognition of these molecules, the cell rapidly activates transcription by degrading IκB (inhibitor of κB), which frees NF-κB to enter the nucleus and activate the transcriptional response. This process is highly regulated and involves the recruitment of multiple ubiquitin ligases and kinases. Briefly, upon binding of LPS, the immune receptor undergoes multiple layers of ubiquitination resulting in the formation both Lys63 and Met1 linked Ub chains. This ubiquitination results in the recruitment of and activation of NF-κB essential modulator (NEMO). NEMO then recruits the IκB kinase (IKK) complex allowing IKK to

phosphorylate IκB, promoting IκB's ubiquitination and subsequent degradation. NEMO contains multiple UBDs including both a Lys63 specific Npl4 zinc finger (NZF) and a Met1 selective UBAN (ubiquitin binding in ABIN and NEMO) domain.[51] Evidence suggests the formation of Lys63 and Met1 Ub chains is hierarchical, with Lys63 linked chains formed first, followed by the synthesis of Met1 chains from the existing Lys63 chains resulting in the formation of Met1/Lys63 branched chains.[52, 53] The nature of how these chains are built suggests a potential mechanism of regulation in which NEMO selectively recognizes a special surface at a Met1/Lys63 junction using its multiple linkage selective UBDs, allowing for both spatial and temporal control of IKK activation in the cell.

It has also been suggested that branched chains result in high local Ub concentrations and act as high affinity ligands to Ub receptors in the cell.[8] Evidence of this mode can be found in recruitment of ubiquitinated substrates to the proteasome for their degradation. A recent kinetic study has shown that the density of Ub modifications on a substrate is more important for driving degradation than the length of a Ub chain.[54] Additionally, it has also been suggested that the mechanism of proteasomal preference for Lys11/Lys48 linked branched chains over their linear counterparts is primarily driven through an increase in the affinity for the substrate upon chain branching.[55] Finally, substrates modified with Lys29 and Lys63 chains can also be targeted to the proteasome, upon editing of the signal by Lys48 branching.[48, 49] This general preference for branched chains regardless of linkage, suggests that there is a mechanism for branched chain recognition where a high local concentration of Ub is important for driving proteasomal degradation over recognition of specific Ub chain types, although more work is needed to prove such a model.

The dynamic modification of proteins by Ub and Ub chains represents a complex signaling pathway in the cell. Even though our understanding of how ubiquitination promotes cellular signaling has greatly evolved over the past few decades, there is still much to learn. Already it is clear that alterations in Ub homeostasis coincides with many disease phenotypes including progression of cancer and

neurodegenerative diseases, as well as the spread of infectious disease. As we continue to uncover more details about how Ub modulates signaling pathways, we need to continuously update our arsenal of tools to study this fascinating modification. The need for new tools is especially true now that new Ub signals, such as branched chains, are becoming appreciated as important modulators in a variety of pathways. New tools are needed to study this complex architecture as much of the current toolbox is geared towards uncovering the role of homotypic chains. The work presented in this thesis aims to both expand the arsenal of tools to study branched Ub chains (Chapters 2 and 3) as well as to use these tools to understand how branched chains are regulated in the cell (Chapter 4).

1.2 Chemical Tools for Studying Branched Ubiquitin Chains

The study of how Ub modifications affect cellular signaling requires access to well defined ubiquitinated substrates and chains. Like most PTMs, the installation of Ub on substrate proteins is highly regulated and requires the coordinated efforts of many cellular components. With the exception of Met1 linked chains, Ub polymers are linked through isopeptide bonds and cannot be generated using recombinant strategies. As a result, Ub chains need to be generated synthetically, making the study of Ub chains an exciting and important challenge for chemists.

To date, many strategies have been developed to synthesize Ub chains including both branched and unbranched chains of defined linkages. Generally, these approaches can be broken up into three major categories 1) ubiquitination using reconstituted ubiquitination machinery 2) semi-synthetic approaches and 3) total synthesis of Ub conjugates. Many advances have been made in the realm of reconstituted cellular components, including the discovery of enzymatic strategies for the synthesis of all Ub chains except for Lys27 chains.[56] These strategies are straightforward for the synthesis of Met1, Lys11, Lys48, and Lys63 linked chains.[57, 58] However, the synthesis of homotypic Lys6, Lys29 and Lys33 linked chains still requires combinations of linkage selective ligases and DUBs, or Lys to Arg mutations of Ub.[59-61]

Additionally, the synthesis of defined branched Ub chains using these enzymes is nearly impossible without significant mutation of Ub's lysine residues and C-terminus.

Many new strategies for semisynthetic Ub chain synthesis have also been developed. These approaches can be used to incorporate native-isopeptide linkages or isopeptide mimetics between Ub subunits without the need for mutating any of the surface residues found in the Ub chain. The general strategy involves incorporating selective reactive handles onto the C-terminus of one Ub monomer and a complementary reactive handle onto the desired lysine residue of another. An example of a reaction that results in a native isopeptide bond uses native chemical ligation (NCL) by combining Ub-thioesters generated through intein-chemistry with Ub-monomers where a specific lysine residue is replaced with δ-thio-L-lysine using Amber codon suppression.[62] This results in a completely native isopeptide bond after subsequent desulfurization. Although useful for generation of Ub-dimers, chains of other lengths are difficult to make. Moreover, the chemistry suffers from the low efficiency of unnatural amino acid incorporation and the use of denaturing conditions. Another example uses orthogonal lysine protection chemistries to generate Ub monomers with differentially reactive lysine residues.[63] Selective deprotection followed by silver mediated condensation between the deprotected lysine residue and a Ub-thioester with globally protected lysine residues results in the properly modified Ub conjugate. Although this approach can be repeated in a linear fashion to produce nearly any unbranched Ub chain (homotypic or heterotypic), it is limited in its ability to furnish branched polymers.

In comparison to the installation of the natural isopeptide linkage, isopeptide mimetics are relatively easy to install. Many of these approaches take advantage of the fact that Ub does not have any natural cysteine residues. This fact allows chemists to use the unique chemistry associated with the thiol group of cysteine by simply replacing a lysine of interest with a cysteine through site-directed mutagenesis.[64] An example from our lab uses a thiol-ene coupling (TEC) reaction between the thiol of a cysteine and an alkene functionalized Ub.[65, 66] This chemistry involves two major steps 1) the enzymatic installation of

allylamine at the C-terminus of Ub and 2) the photoinitiated radical coupling between the installed alkene and the free thiol of the incorporated cysteine (Figure 1.4 B). This results in an isopeptide mimetic that differs from a native isopeptide linkage by a single sulfur atom. Our lab has shown that this linkage functions as the native bond and is readily cleaved by DUBs.[67] Importantly, this chemistry can be used to rapidly build branched Ub chains in a selective manner by simply replacing two lysine residues with cysteines. (Figure 1.4 C).

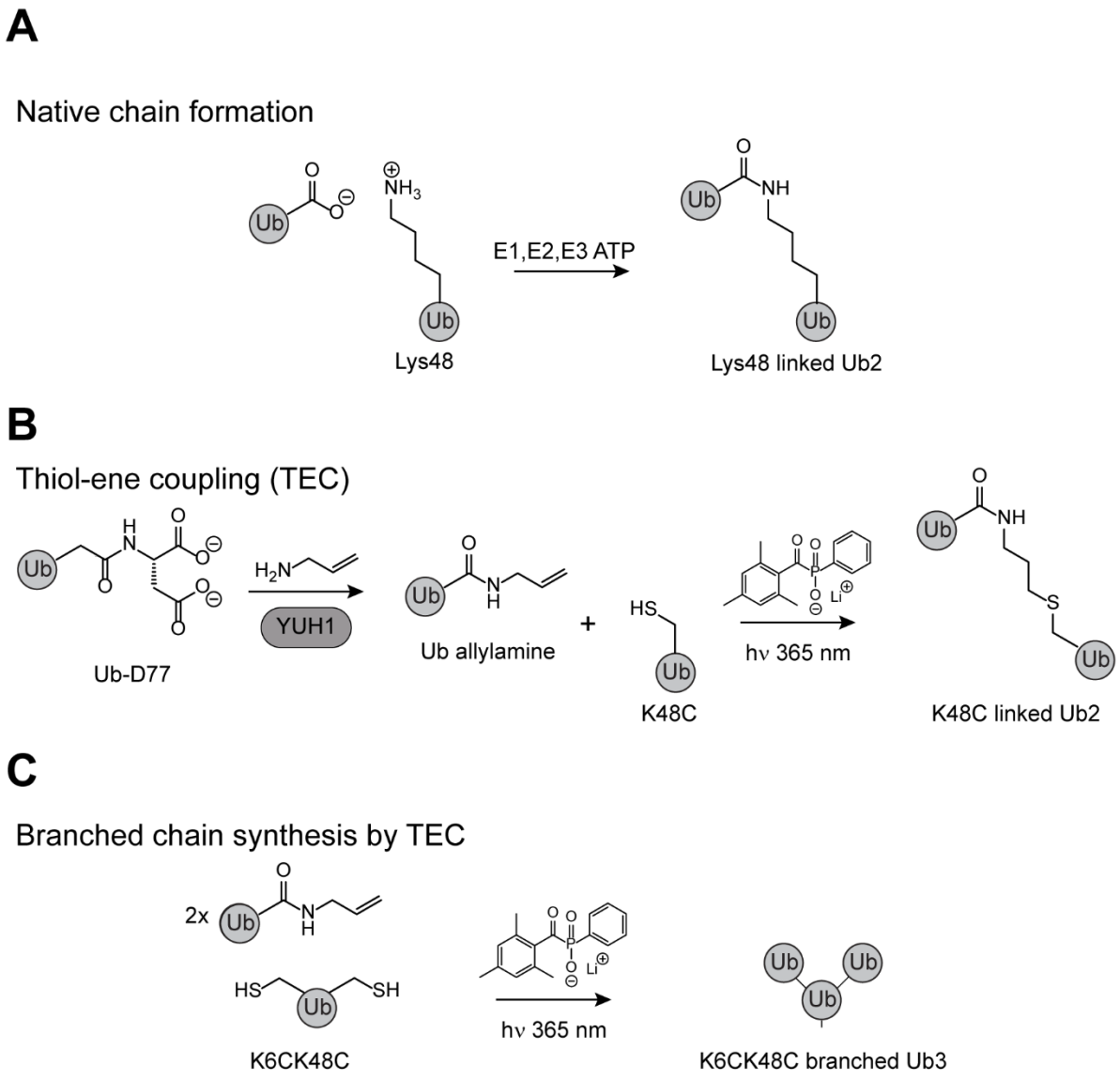

Figure 1. 4: Thiol-ene coupling (TEC) is a useful tool for synthesizing branched Ub chains. A) Native chain synthesis requires multiple enzymes and results in the formation of a native isopeptide bond. **B**) Scheme showing the steps involved in building Ub dimers using TEC and the structure of the resulting isopeptide mimic. **C**) TEC can be adapted for the synthesis of branched Ub chains using a Ub containing two Lys to Cys mutations.

Although new technologies have granted access to the vast library of potential Ub chain types, the study of these chains often requires the incorporation of reactive handles or subunit-specific labeling

chemistries to gain insight into the dynamics and selectivity of the machinery that processes these signals. Branched chains for example, contain two chemically distinct isopeptide bonds that can be recognized differently by various regulators of Ub signaling. For example, when a DUB encounters a branched Ub chain, cleavage can be selective or promiscuous (Figure 1.5 A). This is important because the different chains that result from cleavage have distinct functions.

Although each isopeptide linkage is chemically distinct, there are few ways to readily identify different Ub chains in a complex mixture. The current state of the art includes analyzing Ub chains by western blot using linkage selective antibodies, sequential digests of chain mixtures with linkage selective DUBs, or characterization of the mixture by tandem mass spectrometry (MS^2). Analysis of reaction products by linkage selective antibodies or DUBs is limited by the availability of linkage-specific reagents. Antibodies are only available for Met1, Lys11, Lys48 and Lys63 linked chains, and many "linkage selective DUBs" display poor reaction kinetics and their selectivity has only been characterized using short Ub chains so it is unclear if they maintain selectivity against longer chains or those with branch points.[68] Additionally, both western blotting and DUB based chain digestion fail to offer quantitative data. These short comings are generally overcome by MS^2, but this method of analysis requires access to specialized equipment and expertise.

One way to circumvent these limitations is to chemically tag different subunits of a Ub chain (Figure 1.5 B). Although, several strategies for the chemical modification of Ub chains have been reported, many of these methods require the use of total synthesis of modified Ub monomers and subsequent installation of these monomers into Ub chains using strategies such as NCL.[69] This chemistry is difficult and requires expertise not found in many biochemistry labs and have thus far mostly been limited to the study of Ub dimers. Ideally, it would be possible to subunit-specifically incorporate chemical labels into Ub chains using a semisynthetic approach rather than total synthesis. This approach would have to take advantage

of a labeling strategy that is bioorthogonal to the native ubiquitination machinery as well as many of the common semi-synthetic approaches to building defined Ub chains.

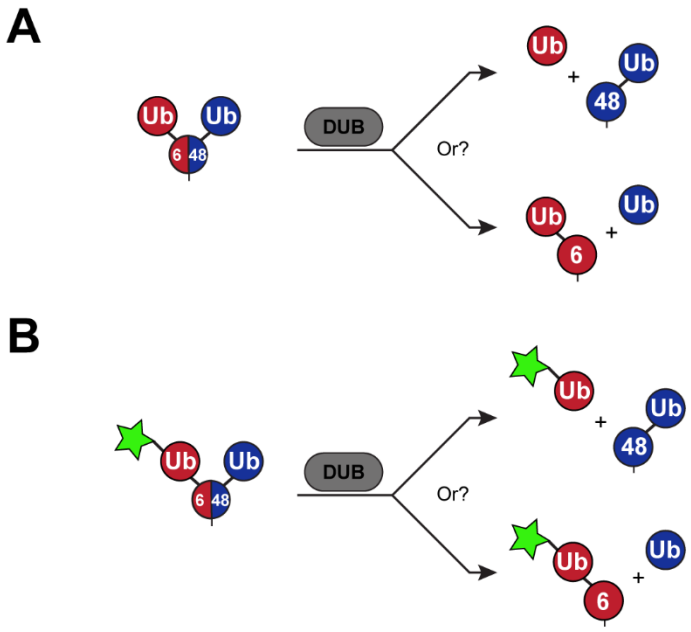

Figure 1.5: Cleavage of branched Ub chains results in multiple reaction pathways. A) When a DUB attempts to cleave a branched chain, it can prefer to cleave one linkage over the other, resulting in two chemically distinct products depending on the preferred reaction pathway. **B**) Example of how a subunit-specific label can help to distinguish between these two reaction pathways.

Chapter 2 of this thesis discusses the development of such a tool, which takes advantage of the bacterial transpeptidase, Sortase A (SrtA), to install fluorophores at every position of a branched Ub trimer and characterize how DUBs interact with these chains. SrtA itself can be used as a highly selective labeling tool as it only recognizes a specific peptide motif (LPXTG), where X can be any amino acid.[70] Upon recognition of this motif, SrtA cleaves the Thr-Gly bond resulting in the formation of an acyl-enzyme intermediate between Thr-and the reactive-site Cys residue of SrtA.[70, 71] This intermediate is then intercepted by peptides or proteins bearing an N-terminal oligo-glycine motif, creating a new peptide bond (Figure 1.6).[72] When fluorescent building blocks are used, this method represents a convenient way

to add new functionality to Ub chains in a site-specific manner that is also orthogonal to both native and chemical means of Ub chain synthesis.

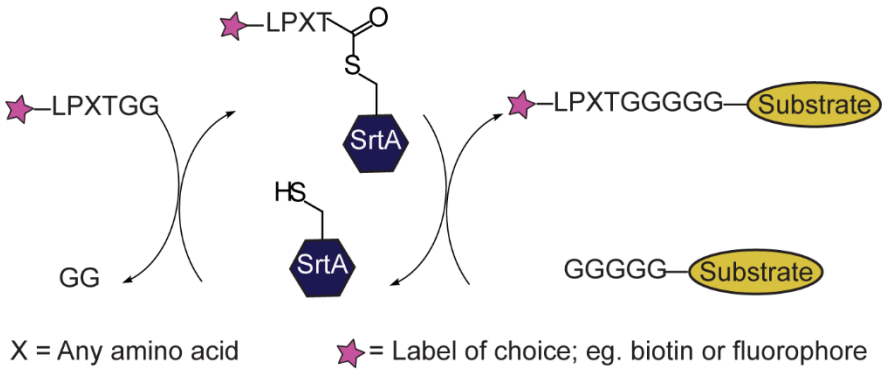

Figure 1.6: Sortase is a bioorthogonal strategy for site-specific labeling of proteins. Sortase recognizes substrates bearing an LPXTG amino acid sequence and fuses them to substrates that have N-terminal Gly residues resulting in new peptide bond.

1.3 Background on Cellular Ubiquitin Chain Characterization

Protein ubiquitination regulates several aspects of cellular biology. As such it is necessary to develop tools that allow us to study Ub chains isolated from their native cellular environment. To date many tools have been described, each having their own advantages and limitations. As the structure of Ub chains is linked to their function, new tools that allow for the characterization of chain configuration i.e., unbranched vs branched are needed.

As briefly described in section 1.2, there are the three commonly employed technologies to characterize the nature of Ub chains. These technologies typically rely on either high-specificity reagents (Ub binding proteins or DUBs) or mass spectrometry (MS).[8, 68] The most commonly used non-MS-based technique to analyze Ub chains isolated from cell culture are linkage specific affinity reagents e.g., antibodies and affimers.[2, 29, 32, 73-75] Linkage specific Ub antibodies, have been incredibly useful for studying the roles of different Ub chains in several signaling pathways. These reagents have been developed against

several homotypic Ub chains (Met1, Lys11, Lys48, Lys63) and one heterotypic Ub linkage (Lys11/Lys48).[2, 32, 73, 74] Recently, there has also been two linkage specific affimer reagents reported in the literature that have specificity for Lys6 and Lys33 linked Ub chains, as well as several linkage-specific UBDs.[23, 29] Typically, these reagents are used detect specific Ub linkages built in response to different cellular conditions in either an immunoblot or immunofluorescence experiment. For example, the anti-Lys11 Ub antibody developed by Genentech was recently used to show that Lys11 linked Ub chains are built to drive cell cycle progression during mitosis.[2] The recent development of a bispecific antibody against Lys11/Lys48 linked heterotypic chains has further clarified our understanding of Lys11 linked chains.[32] It had been a long-standing question how Lys11 chains can target cell cycle regulators to the proteasome for degradation despite reports that Lys11 linked chains are poor substrates of the proteasome. Using this bispecific reagent, researchers were able to confirm that the Lys11 chains built during mitosis are actually mixed (likely branched) Ub chains, and that these chains act as very potent degradation signals for these cell cycle regulators.

Another common tool that uses linkage selective reagents to identify the types of Ub linkages in cellular extract is Ubiquitin Chain Restriction (UbiCRest) analysis.[75] Briefly, Ub chains isolated from cell lysates are subjected to digestion by a series of different DUBs. These DUBs can either selectively or non-selectively cleave Ub chains. Analysis of cleavage products by either SDS-PAGE or western blot sheds light on the type of linkages present in a heterogenous mixture. For example, if digestion of a sample with the Lys48 selective DUB, OTUB1, results in the formation of smaller Ub products, then the sample is likely to contain Lys48 linkages. To date DUBs that cleave Met1, Lys11, Lys48, and Lys63 linked chains with high specificity, as well as DUBs that preferentially cleave Lys29, Lys33 and Lys6 over other chain types albeit with lower selectivity have been described.[75] Using these reagents in combination with other non-selective DUBs it is possible to identify the types of Ub chains present in a sample. It is also possible to show whether a substrate is modified with a homogenous or mixed Ub chain. This technology has been

successfully used to identify the bacterial E3 ligase, NleL, as an enzyme that builds Lys6/Lys48 branched chains[59], to show that mixed Met1/Lys63 linked chains are built in response to NF-kB signaling,[53] and to demonstrate that Lys29 linked chains primarily form mixed chains with Lys48 linkages.[60]

Despite their usefulness in expanding our understanding of how Ub chains regulate cellular signaling, these reagents do not inform on the relative abundance of different chain types under different conditions. Perhaps the most commonly employed tool to study Ub chain dynamics is the use of MS in bottom-up proteomics experiments. In bottom-up proteomics, proteases are used to fragment proteins into small peptides, which can be identified by tandem mass spectrometry.[68] In the case of Ub, trypsin is commonly used because it cleaves after Lys and Arg residues. When Ub is attached to its substrates the connection occurs via Ub's C-terminus, which has the following sequence: Leu73-Arg74-Gly75-Gly76. The cleavage after Arg74 thus releases a di-Gly motif. This motif remains covalently attached to the modified Lys residue of a ubiquitinated protein and typically results in a missed cleavage by trypsin at the modified Lys. This cleavage results in a new di-Gly-modified tryptic peptide containing the missed cleavage; allowing for the identification of a ubiquitinated lysine (Figure 1.6). There are several benefits to this approach including the ability to obtain a global understanding of the Ub landscape under different cellular conditions. Additionally, quantitative experiments have been developed that allow for both relative and absolute quantification of protein ubiquitination.[24, 47, 68, 76, 77] Examples of relative quantification include the use of stable isotope labeled media, isobaric tagging of tryptic peptides, as well as label free quantification. Absolute quantification (AQUA) of Ub chains can be achieved by doping samples with known amounts of isotopically labeled peptides as internal standards for expected ubiquitination events.[77] Together these approaches have resulted in the identification thousands of ubiquitinated proteins modified with all eight possible Ub linkages, as well as branched Ub chains where neighboring Lys residues are adjacent to one another (Met1/Lys6, Lys27/Lys29, and Lys29/Lys33).[68]

Because these approaches rely on complete trypsinization of protein samples into small peptides, it is difficult to characterize proteins that are modified at multiple positions on the same polypeptide chain i.e., branched Ub chains. This is because total proteolysis of the protein sample destroys the structural information held in the protein, making it impossible to determine if such modifications occurred on a single protein or multiple proteins within a complex sample (Figure 1.7). This means that the study of Ub chain structure has lagged relative to the study of Ub chain linkages. Currently, the best tool for studying multiple modifications on the same protein is top-down proteomics. In these experiments, intact proteins are analyzed directly in a mass spectrometer where the proteins can be chemically fragmented and analyzed for PTMs.[78] Together, the intact mass of the protein as well as characterization of resultant fragment ions can be used to characterize proteins containing multiple PTMs. This technology has indeed been employed to characterize branched Ub chains but is limited to chemically synthesized unanchored tetramers and trimers.[79, 80] This limitation is largely due to our ability to analyze the data, as each monomer in a Ub chain contains the same amino acid sequence, it becomes nearly impossible to assign modifications once the chain becomes longer than four subunits.

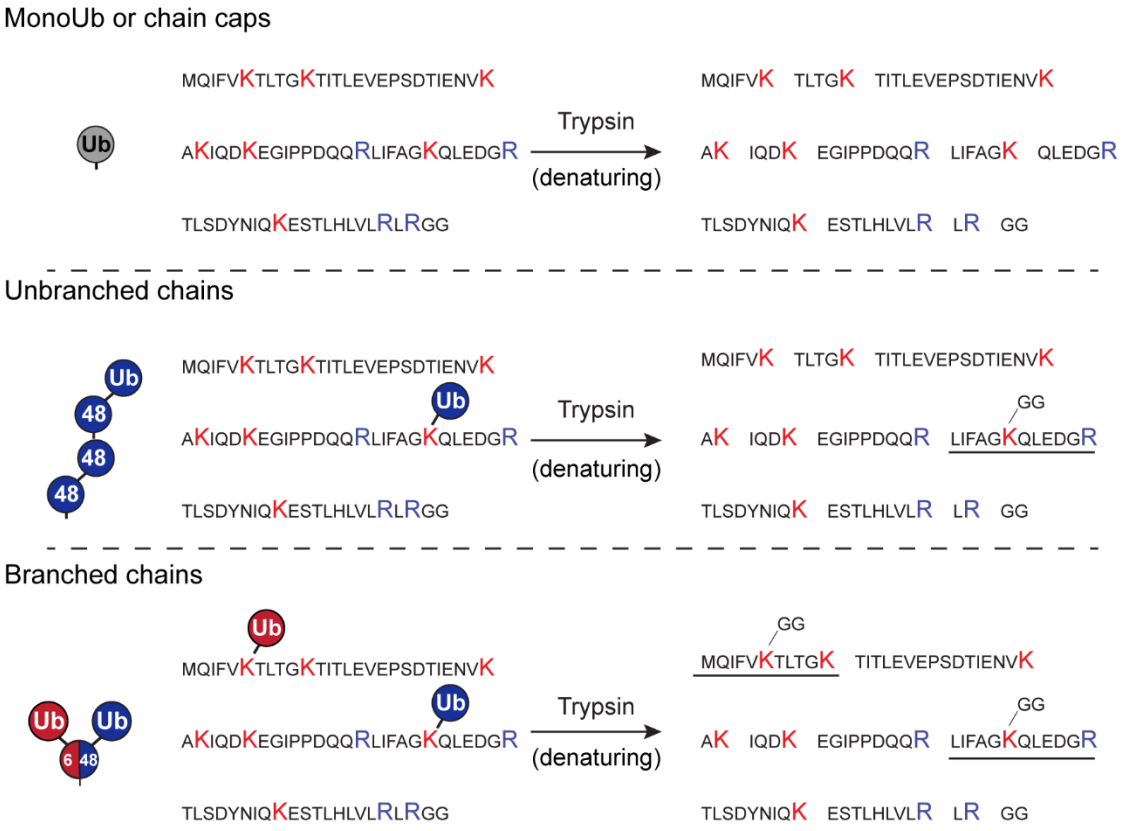

Figure 1.7: Bottom-up mass spectrometry enables characterization of Ub modifications. Top) Amino acid sequence of Ub highlighting the positively charged amino acids Lys and Arg in red and blue respectively. Cleavage by the protease trypsin under denaturing conditions results in the tryptic peptides shown on the right. **Middle**) When a Ub chain is subjected to trypsin, a Lys residue is modified by the C-terminus of its neighboring Ub. This results in a new tryptic peptide containing a di-Gly modified Lys, which can be measured by MS^2 analysis. **Bottom**) Trypsinolysis destroys the structural information encoded in the chain resulting in identical peptides as those found in an unbranched chain.

The use of middle-down MS offers a compromise between the versatility and robustness of the bottom-up approach, while still maintaining useful structural characteristics of the analyzed protein. Typically, middle-down analysis of proteins involves limited digestion of proteins to be analyzed under non-denaturing conditions or the use of specialized proteases that are chosen based on their ability to

produce few cleavages. In the case of Ub modifications, the core of the Ub protein is one of the most tightly folded proteins in the proteome. Under non-denaturing conditions trypsin can only access Arg74 at the flexible C-terminus of the protein. This stability results in a single cleavage site in the protein, while still liberating the diagnostic di-Gly motif. The remaining core of the Ub protein, which contains all possible modification sites (Ub_{1-74}), remains intact; allowing for the simultaneous detection of multiple modifications on a single subunit.[81] In the event of a Ub chain, the di-Gly motif remains on the modified Lys residue resulting in a Ub_{1-74} fragment containing a single di-Gly motif ($^{GG}Ub_{1-74}$) (Figure 1.8). If a branched chain is present, two Lys residues will be modified by di-Gly motifs ($^{2xGG}Ub_{1-74}$). This allows for unambiguous detection of branched chains within a complex mixture without restraints on chain length or distance between modified Lys residues.[82] Further analysis of the Ub_{1-74} species by tandem MS allows for the characterization of the linkages in these chains. Our lab has previously shown that this method of chain analysis can indeed be used to identify and characterize branched chains within a complex mixture of chains generated *in vitro*.[82] However, attempts by another lab to identify branched chains using middle-down MS in yeast cell extract proved unsuccessful.[81]

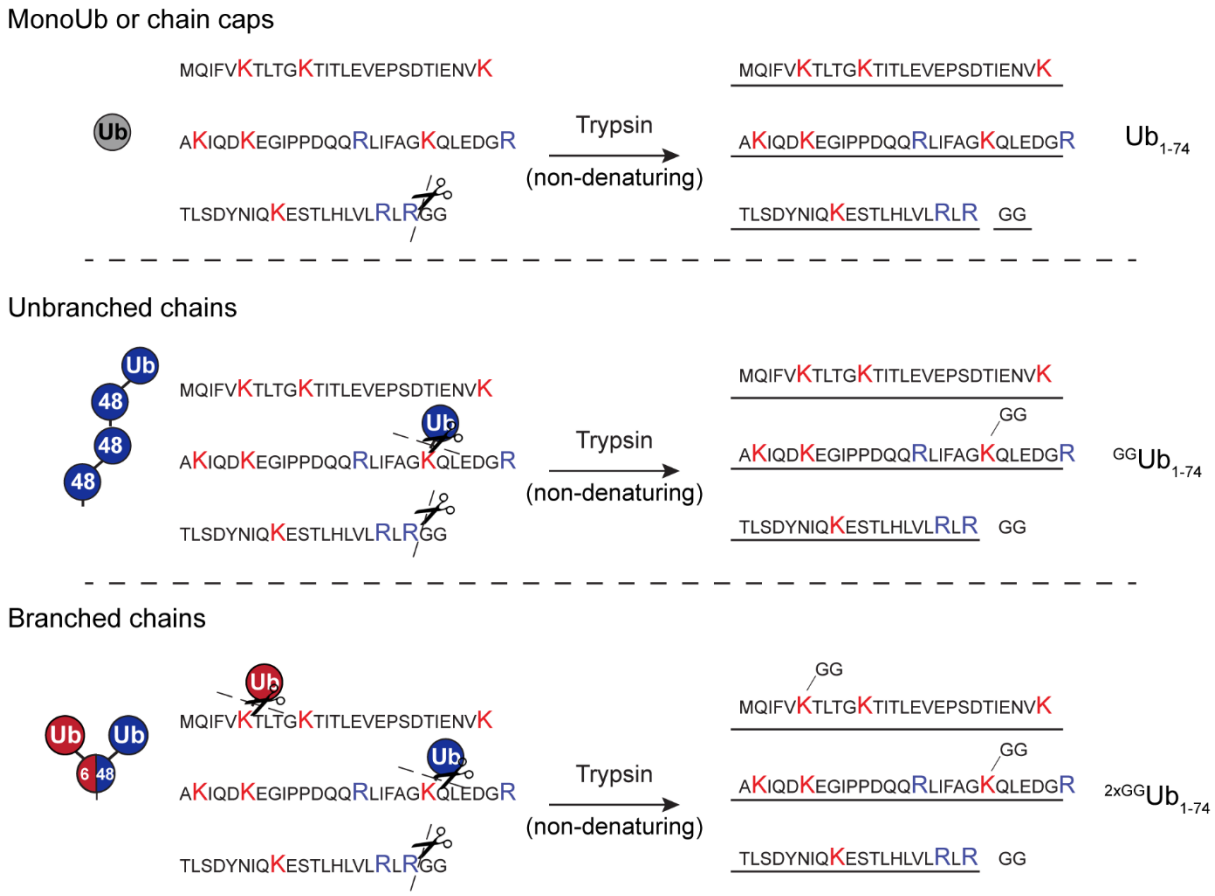

Figure 1.8: Middle-down mass spectrometry allows for the characterization of branched Ub chains. Top) Under native conditions, treatment with trypsin results in a single cleavage event releasing a di-Gly and a Ub_{1-74} fragment. **Middle**) When unbranched chains are treated with trypsin under native conditions, a Ub_{1-74} fragment containing a single di-Gly modification ($^{GG}Ub_{1-74}$) is observed. **Bottom**) When branched chains are treated with trypsin under native conditions, a Ub_{1-74} fragment containing two di-Gly modifications ($^{2xGG}Ub_{1-74}$) is observed. All three Ub1-74 species are chemically distinct and can be characterized by tandem mass spectrometry.

One of the key difficulties in attempting to directly analyze Ub chains in cell culture using middle-down MS is interference from unconjugated mono-Ub in the cell. It has been estimated that only 11% of the total Ub pool in common cell culture models is involved in Ub chains, with an even smaller percentage

expected to contain branch points.[19] The remaining 89% exists as either unconjugated monoUb, charged E1-Ub thioesters, or as a mono-Ub modification on a substrate protein.[19] Indeed, previous attempts to use middle-down MS to detect branched chains in cells proved unsuccessful resulting in an approximately 4:1 ratio of Ub_{1-74}: $^{GG}Ub_{1-74}$, consistent with the notion that the high amount of monoUb interferes with the ability to detect branched Ub chains.[81] One way to circumvent this would be to enrich for poly-Ub chains prior to analysis by middle-down MS. Chapter 3 of this thesis describes our approach to this problem, which we call Ubiquitin Chain Enrichment Middle-down-MS or UbiChEM-MS. This workflow takes advantage of linkage-specific UBDs to isolate individual populations of Ub chains and simultaneously remove unconjugated Ub from the sample (Figure 1.9). These individual chain populations can then be interrogated by middle-down MS to characterize the structure and linkages present in the isolated chains.

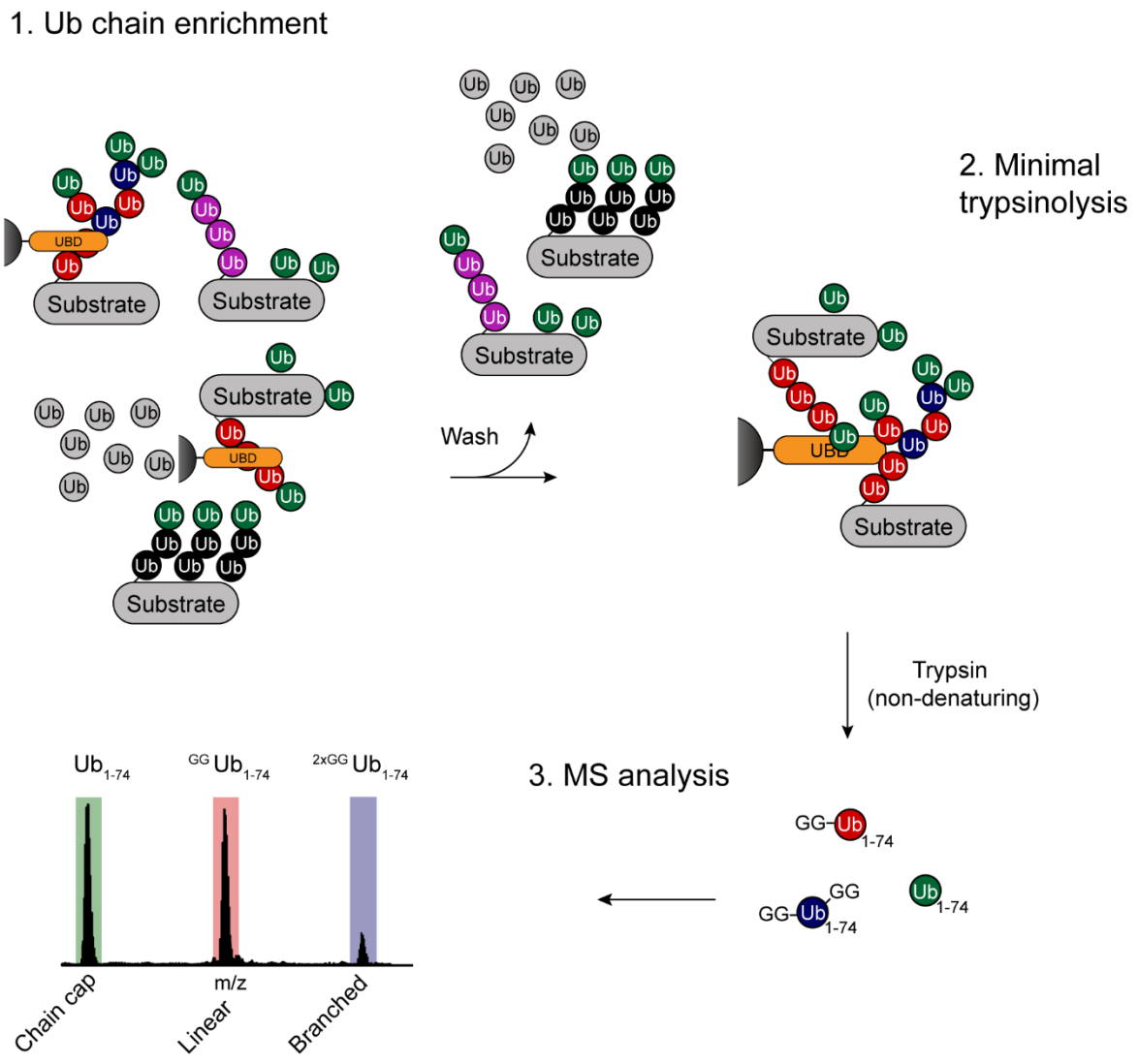

Figure 1.9: Ubiquitin chain enrichment can be used to analyze chain topology of distinct Ub populations in cell extract. Linkage selective UBDs can be used to enrich for specific subsets of Ub chains in a complex mixture such as cell extract resulting in a much less complex subset of chains that can be minimally trypsinized and characterized by mass spectrometry.

1.4 UCH37 and the Proteasome

As mentioned above, one major fate of proteins tagged with branched Ub chains is degradation via the 26S proteasome. Interestingly, there is no obvious subunit that is known to selectively interact with

branched Ub chains despite the observations that branched chains are more potent degradation signals. The proteasome is a 2.6 MDa complex that contains two major subcomplexes. The first is the 20S core particle (CP) which contains the proteolytic subunits.[83] Sitting on either end of the CP is the 19S regulatory particle (RP), which holds the machinery responsible for recognizing and processing ubiquitinated substrates to control their unfolding and degradation (Figure 1.10 A). The CP is made up of four heptameric rings (α and β rings), assembled in a stacked $\alpha\beta\beta\alpha$ pattern.[84] The α rings serve as gates to prevent unregulated access of substrates to the catalytic β subunits. The RP can be subdivided into lid and base subcomplexes. The base subcomplex is made from three Ub binding proteins that function to recruit ubiquitinated proteins to the proteasome, where they can be engaged by a hexameric ring of AAA+ ATPases that unfold substrates and thread them into the catalytic pore of the 20S subcomplex.[85] The lid subcomplex, allosterically activates the base upon substrate binding.[86-88] This complex contains several scaffolding proteins that interact with the base as well as three DUBs: RPN11, USP14, and UCH37.[89] Of the three DUBs, we know the most about the role of RPN11. This DUB cleaves Ub chains *en bloc* (removing the entire chain) from substrates as they are about to enter the ATPase ring. *En bloc* removal prevents clogging of the pore and allows for recycling of Ub.[90] Less is known about the roles of USP14 and UCH37. It is believed that the effects of USP14 and UCH37 on proteasomal degradation are substrate specific, where they can either rescue proteins from degradation by removing Ub chains from improperly ubiquitinated substrates or promote degradation by allosterically activating the ATPase activity of the proteasome.[89] To date, most of the evidence to support this hypothesis has been gathered for USP14's role and little is actually understood about how UCH37 regulates degradation. This disparity results from USP14 being easily removed from proteasome preparations, which allows for biochemical studies to be performed.[8] Additionally, yeast have a USP14 ortholog (Ubp6) which allows for easy genetic studies of the effect of USP14/Ubp6 on proteasomal degradation in cells.[5] UCH37 on the other hand, is tightly bound to the proteasome and *S. cerevisiae* do not have a UCH37 ortholog, making the study of its role in

degradation difficult. Further complicating the study of UCH37 is its involvement in the INO80 chromatin remodeling complex, which functions to regulate gene transcription. In the INO80 complex, UCH37 appears to adopt an inactive conformation, but other than that its role is essentially unknown.[91-93]

UCH37 belongs to the four-member UCH family of DUBs. This class of DUBs includes UCHL1, UCHL3, UCH37 (also known as UCHL5) and BAP1.[94] These enzymes are grouped together based on the homology of their catalytic domains. In addition to their catalytic centers, UCH37 and BAP1 also have a regulatory domain known as the ULD domain (UCH37-like domain), which serves to restrict catalytic activity of these proteins until they are part of the correct complexes.[20] UCH37's interaction with the proteasome occurs via its ULD which has a high affinity for the DEUBAD (deubiquitinase adaptor domain) of the Ub receptor RPN13 (also referred to as ADRM1) (Figure 1.10 A and C).[91, 92, 95] RPN13 itself contains two domains, an N-terminal PRU (pleckstrin-like receptor for Ub) domain, and its DUEBAD domain, which are connected by a long flexible linker (Figure 1.10 B).[96] The PRU domain serves as the docking site for RPN13 to the proteasome as well as a high affinity receptor for ubiquitinated proteins.[96, 97] Upon interaction between the ULD of UCH37 and DEUBAD of RPN13, the ULD domain rearranges, allowing for regulatory segment known as the active site crossover loop (ASCL) to adopt a productive catalytic conformation (Figure 1.10 D).[91, 92] Interestingly, the activity of this enzyme has been assayed against all eight homotypic Ub linkages and only displays catalytic activity against Lys48 linked chains, albeit with very low efficiency.[89] When tested against poorly defined high molecular weight chains however, catalytic activity can be observed, suggesting that this DUB does have the ability to cleave Ub substrates.[98, 99] As the chains tested are of unknown topology it is possible that UCH37 might have selectivity for one topology over the others. In fact, unpublished data from our lab suggests that this is indeed the case and that UCH37 has exquisite preference for branched chains over their unbranched counterparts. Chapter 4 of this thesis explores the

potential of UCH37 as a debranching-specific enzyme and sets the stage for looking into the implications of such an enzyme on the dynamics of protein degradation.

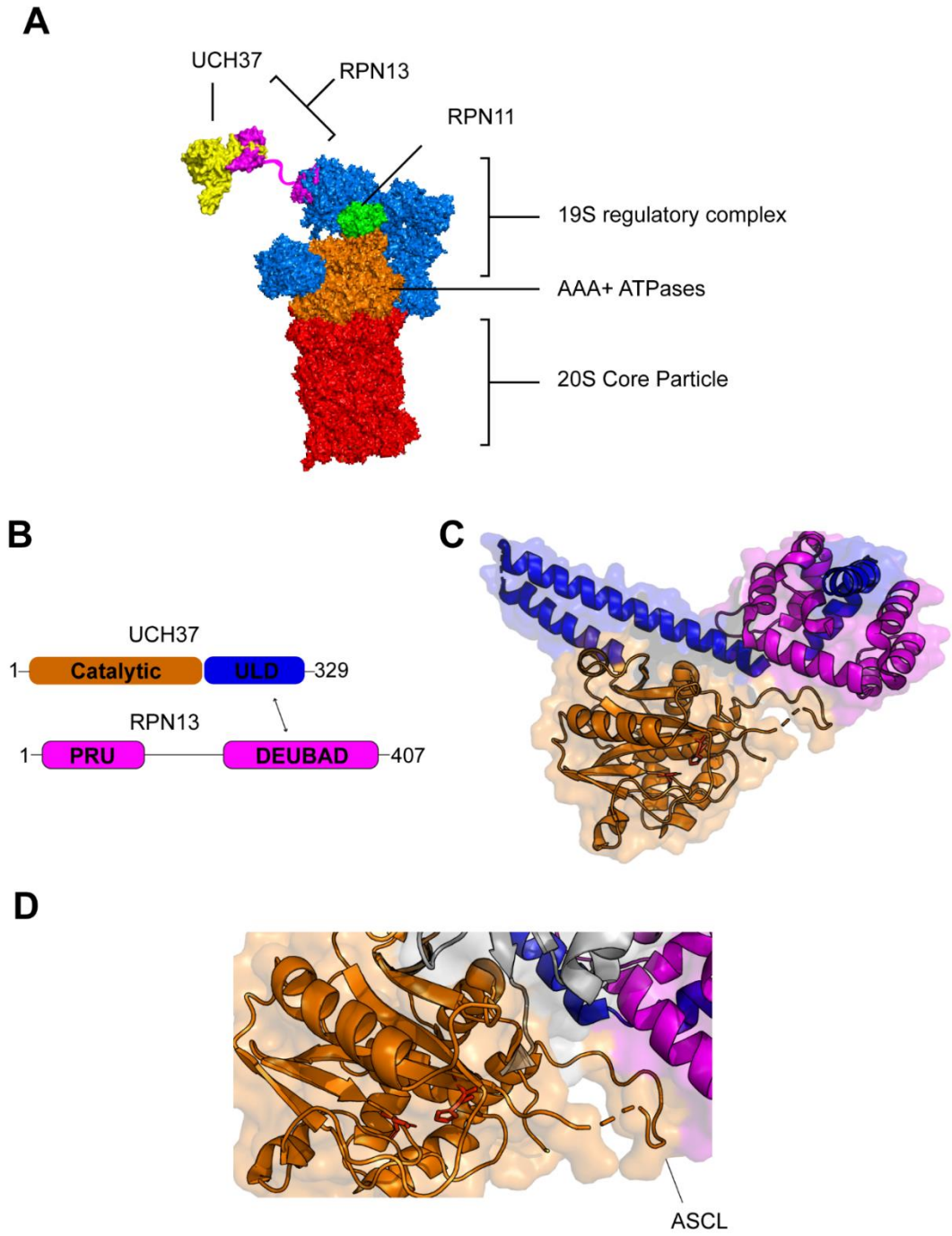

Figure 1.10: UCH37 is a proteasome associated DUB. A) The proteasome (PDB ID: 5T0C)[100] is a multi-protein complex built from two subcomplexes, the CP (red) and RP (Blue and orange). UCH37 (yellow, PDB

ID: 4WLQ)[92] is one of three DUBs that are part of the RP, RPN11 shown in green is another, USP14 is not shown. UCH37 and binds to the proteasome via its interaction with RPN13 (magenta, PDB IDs: 4WLQ (DEUBAD domain) 6CO4(PRU domain)).[101] **B**) Cartoon depicting the domains of UCH37 and RPN13, the arrow indicates the domains that interact with one another. **C**) Crystal structure of UCH37-RPN13 DEUBAD complex covalently bound to Ub propargylamine (PDB ID: 4UEL)[91] showing the interaction between the ULD of UCH37 (blue) and DEUBAD of RPN13 (magenta), Ub is omitted. **D**) Close up of the UCH37 catalytic site showing the active site crossover loop (ASCL) adopting an ordered conformation allowing the C-terminus of Ub (gray) to enter. Catalytic residues of UCH37 are shown as red sticks.

1.5 Conclusion and Foreword to Thesis

Ubiquitin represents one of the most complex and versatile signaling molecules in the cell. With nearly 5% of the human genome dedicated to the installation, interaction, and removal of this modification it also represents one of the most highly regulated signaling molecules as well.[19] Much of the versatility of Ub signaling comes from its complexity, as Ub is known to form polymeric chains through self-modification. These polymers adopt unique architectures which are associated with distinct functional consequences. With recent advancements in the technology to study Ub chain architecture, it has become appreciated that cells can edit the signals encoded in Ub chains by the installation of branch points. These branched chains can serve as new scaffolds for protein binding or higher affinity binding surfaces for Ub receptors due to increased Ub density. As the study of chain branching is still in its infancy, the field will benefit from the development of new tools dedicated to the study of how these chains interact with DUBs and other proteins in the cell as well as tools that will allow for the measurement of the dynamics of branched Ub chains. With these tools in hand, the field will better be able to understand how the structure of Ub chains affects their function and begin to characterize the proteins that are responsible for their regulation.

As discussed throughout the introduction, the goal of this thesis is to introduce new methods that will allow us to link Ub chain structure to function. Chapters 2 introduces new methods to build Ub chains with fluorescent labels installed in at different subunits of that chain and shows how these substrates can be used to characterize DUBs. Chapter 3 shows how middle-down MS can be combined with Ub affinity reagents allowing for the study of Ub chain structure and dynamics in cell extract. Finally, Chapter 4 combines tools outlined in the previous chapters to show that UCH37 is a DUB that selectively hydrolyzes branched chains and sets the stage for understanding how this activity regulates proteasomal degradation.

1.6 References

1. Deribe, Y. L.; Pawson, T.; Dikic, I., Post-translational modifications in signal integration. *Nat. Struct. Mol. Biol.* **2010,** *17*, 666.

2. Matsumoto, M. L.; Wickliffe, K. E.; Dong, K. C.; Yu, C.; Bosanac, I.; Bustos, D.; Phu, L.; Kirkpatrick, D. S.; Hymowitz, S. G.; Rape, M.; Kelley, R. F.; Dixit, V. M., K11-Linked Polyubiquitination in Cell Cycle Control Revealed by a K11 Linkage-Specific Antibody. *Mol. Cell* **2010,** *39* (3), 477-484.

3. Jackson, Stephen P.; Durocher, D., Regulation of DNA Damage Responses by Ubiquitin and SUMO. *Mol. Cell* **2013,** *49* (5), 795-807.

4. Elia, Andrew E. H.; Boardman, Alexander P.; Wang, David C.; Huttlin, Edward L.; Everley, Robert A.; Dephoure, N.; Zhou, C.; Koren, I.; Gygi, Steven P.; Elledge, Stephen J., Quantitative Proteomic Atlas of Ubiquitination and Acetylation in the DNA Damage Response. *Mol. Cell* **2015,** *59* (5), 867-881.

5. Powers, E. T.; Morimoto, R. I.; Dillin, A.; Kelly, J. W.; Balch, W. E., Biological and Chemical Approaches to Diseases of Proteostasis Deficiency. *Annu. Rev. Biochem.* **2009,** *78* (1), 959-991.

6. Hershko, A.; Ciechanover, A., The Ubiquitin System. *Annu. Rev. Biochem.* **1998,** *67* (1), 425-479.

7. Komander, D.; Rape, M., The Ubiquitin Code. *Annu. Rev. Biochem.* **2012,** *81* (1), 203-229.

8. Swatek, K. N.; Komander, D., Ubiquitin modifications. *Cell Res.* **2016,** *26*, 399.

9. Yau, R.; Rape, M., The increasing complexity of the ubiquitin code. *Nat. Cell Biol.* **2016,** *18*, 579.

10. Gerlach, B.; Cordier, S. M.; Schmukle, A. C.; Emmerich, C. H.; Rieser, E.; Haas, T. L.; Webb, A. I.; Rickard, J. A.; Anderton, H.; Wong, W. W. L.; Nachbur, U.; Gangoda, L.; Warnken, U.; Purcell, A. W.; Silke, J.; Walczak, H., Linear ubiquitination prevents inflammation and regulates immune signalling. *Nature* **2011,** *471*, 591.

11. Hoeller, D.; Dikic, I., Targeting the ubiquitin system in cancer therapy. *Nature* **2009,** *458*, 438.

12. Deshaies, R. J., Proteotoxic crisis, the ubiquitin-proteasome system, and cancer therapy. *BMC Biol.* **2014,** *12* (1), 94.

13. Popovic, D.; Vucic, D.; Dikic, I., Ubiquitination in disease pathogenesis and treatment. *Nat. Med.* **2014,** *20*, 1242.

14. Maculins, T.; Fiskin, E.; Bhogaraju, S.; Dikic, I., Bacteria-host relationship: ubiquitin ligases as weapons of invasion. *Cell Res.* **2016,** *26*, 499.

15. Bhogaraju, S.; Kalayil, S.; Liu, Y.; Bonn, F.; Colby, T.; Matic, I.; Dikic, I., Phosphoribosylation of Ubiquitin Promotes Serine Ubiquitination and Impairs Conventional Ubiquitination. *Cell* **2016,** *167* (6), 1636-1649.e13.

16. Pruneda, Jonathan N.; Durkin, Charlotte H.; Geurink, Paul P.; Ovaa, H.; Santhanam, B.; Holden, David W.; Komander, D., The Molecular Basis for Ubiquitin and Ubiquitin-like Specificities in Bacterial Effector Proteases. *Mol. Cell* **2016,** *63* (2), 261-276.

17. Angot, A.; Vergunst, A.; Genin, S.; Peeters, N., Exploitation of eukaryotic ubiquitin signaling pathways by effectors translocated by bacterial type III and type IV secretion systems. *PLoS Pathog.* **2007,** *3* (1), e3.

18. Akimov, V.; Barrio-Hernandez, I.; Hansen, S. V. F.; Hallenborg, P.; Pedersen, A.-K.; Bekker-Jensen, D. B.; Puglia, M.; Christensen, S. D. K.; Vanselow, J. T.; Nielsen, M. M.; Kratchmarova, I.; Kelstrup, C. D.; Olsen, J. V.; Blagoev, B., UbiSite approach for comprehensive mapping of lysine and N-terminal ubiquitination sites. *Nat. Struct. Mol. Biol.* **2018,** *25* (7), 631-640.

19. Clague, M. J.; Heride, C.; Urbé, S., The demographics of the ubiquitin system. *Trends Cell Biol.* **2015,** *25* (7), 417-426.

20. Mevissen, T. E. T.; Komander, D., Mechanisms of Deubiquitinase Specificity and Regulation. *Annu. Rev. Biochem.* **2017,** *86* (1), 159-192.

21. Clague, M. J.; Barsukov, I.; Coulson, J. M.; Liu, H.; Rigden, D. J.; Urbé, S., Deubiquitylases From Genes to Organism. *Physiol. Rev.* **2013,** *93* (3), 1289-1315.

22. Dikic, I.; Wakatsuki, S.; Walters, K. J., Ubiquitin-binding domains — from structures to functions. *Nat. Rev. Mol. Cell Biol.* **2009,** *10*, 659.

23. Husnjak, K.; Dikic, I., Ubiquitin-Binding Proteins: Decoders of Ubiquitin-Mediated Cellular Functions. *Annu. Rev. Biochem.* **2012,** *81* (1), 291-322.

24. Kim, W.; Bennett, Eric J.; Huttlin, Edward L.; Guo, A.; Li, J.; Possemato, A.; Sowa, Mathew E.; Rad, R.; Rush, J.; Comb, Michael J.; Harper, J. W.; Gygi, Steven P., Systematic and Quantitative Assessment of the Ubiquitin-Modified Proteome. *Mol. Cell* **2011,** *44* (2), 325-340.

25. Ikeda, F.; Deribe, Y. L.; Skånland, S. S.; Stieglitz, B.; Grabbe, C.; Franz-Wachtel, M.; van Wijk, S. J. L.; Goswami, P.; Nagy, V.; Terzic, J.; Tokunaga, F.; Androulidaki, A.; Nakagawa, T.; Pasparakis, M.;

Iwai, K.; Sundberg, J. P.; Schaefer, L.; Rittinger, K.; Macek, B.; Dikic, I., SHARPIN forms a linear ubiquitin ligase complex regulating NF-κB activity and apoptosis. *Nature* **2011,** *471*, 637.

26. Tokunaga, F.; Nakagawa, T.; Nakahara, M.; Saeki, Y.; Taniguchi, M.; Sakata, S.-i.; Tanaka, K.; Nakano, H.; Iwai, K., SHARPIN is a component of the NF-κB-activating linear ubiquitin chain assembly complex. *Nature* **2011,** *471*, 633.

27. Wu-Baer, F.; Lagrazon, K.; Yuan, W.; Baer, R., The BRCA1/BARD1 Heterodimer Assembles Polyubiquitin Chains through an Unconventional Linkage Involving Lysine Residue K6 of Ubiquitin. *J. Biol. Chem.***2003,** *278* (37), 34743-34746.

28. Morris, J. R.; Solomon, E., BRCA1 : BARD1 induces the formation of conjugated ubiquitin structures, dependent on K6 of ubiquitin, in cells during DNA replication and repair. *Hum. Mol. Genet.* **2004,** *13* (8), 807-817.

29. Michel, M. A.; Swatek, K. N.; Hospenthal, M. K.; Komander, D., Ubiquitin Linkage-Specific Affimers Reveal Insights into K6-Linked Ubiquitin Signaling. *Mol. Cell* **2017,** *68* (1), 233-246.e5.

30. Jin, L.; Williamson, A.; Banerjee, S.; Philipp, I.; Rape, M., Mechanism of Ubiquitin-Chain Formation by the Human Anaphase-Promoting Complex. *Cell* **2008,** *133* (4), 653-665.

31. Meyer, H.-J.; Rape, M., Enhanced Protein Degradation by Branched Ubiquitin Chains. *Cell* **2014,** *157* (4), 910-921.

32. Yau, R. G.; Doerner, K.; Castellanos, E. R.; Haakonsen, D. L.; Werner, A.; Wang, N.; Yang, X. W.; Martinez-Martin, N.; Matsumoto, M. L.; Dixit, V. M.; Rape, M., Assembly and Function of Heterotypic Ubiquitin Chains in Cell-Cycle and Protein Quality Control. *Cell* **2017,** *171* (4), 918-933.e20.

33. Chau, V.; Tobias, J. W.; Bachmair, A.; Marriott, D.; Ecker, D. J.; Gonda, D. K.; Varshavsky, A., A multiubiquitin chain is confined to specific lysine in a targeted short-lived protein. *Science* **1989,** *243* (4898), 1576.

34. Finley, D.; Sadis, S.; Monia, B. P.; Boucher, P.; Ecker, D. J.; Crooke, S. T.; Chau, V., Inhibition of proteolysis and cell cycle progression in a multiubiquitination-deficient yeast mutant. *Mol. Cell. Biol.* **1994,** *14* (8), 5501-5509.

35. Thrower, J. S.; Hoffman, L.; Rechsteiner, M.; Pickart, C. M., Recognition of the polyubiquitin proteolytic signal. *EMBO J.* **2000,** *19* (1), 94.

36. Ren, X.; Hurley, J. H., VHS domains of ESCRT-0 cooperate in high-avidity binding to polyubiquitinated cargo. *EMBO J.* **2010,** *29* (6), 1045.

37. Raiborg, C.; Stenmark, H., The ESCRT machinery in endosomal sorting of ubiquitylated membrane proteins. *Nature* **2009,** *458*, 445.

38. Chen, Z. J.; Sun, L. J., Nonproteolytic Functions of Ubiquitin in Cell Signaling. *Mol. Cell* **2009,** *33* (3), 275-286.

39. Kim, H.; Chen, J.; Yu, X., Ubiquitin-Binding Protein RAP80 Mediates BRCA1-Dependent DNA Damage Response. *Science* **2007,** *316* (5828), 1202.

40. Sobhian, B.; Shao, G.; Lilli, D. R.; Culhane, A. C.; Moreau, L. A.; Xia, B.; Livingston, D. M.; Greenberg, R. A., RAP80 Targets BRCA1 to Specific Ubiquitin Structures at DNA Damage Sites. *Science* **2007,** *316* (5828), 1198.

41. Wang, B.; Matsuoka, S.; Ballif, B. A.; Zhang, D.; Smogorzewska, A.; Gygi, S. P.; Elledge, S. J., Abraxas and RAP80 Form a BRCA1 Protein Complex Required for the DNA Damage Response. *Science* **2007,** *316* (5828), 1194.

42. Vijay-Kumar, S.; Bugg, C. E.; Cook, W. J., Structure of ubiquitin refined at 1.8Åresolution. *J. Mol. Biol.* **1987,** *194* (3), 531-544.

43. Varadan, R.; Walker, O.; Pickart, C.; Fushman, D., Structural Properties of Polyubiquitin Chains in Solution. *J. Mol. Biol.* **2002,** *324* (4), 637-647.

44. Cook, W. J.; Jeffrey, L. C.; Carson, M.; Chen, Z.; Pickart, C. M., Structure of a diubiquitin conjugate and a model for interaction with ubiquitin conjugating enzyme (E2). *J. Biol. Chem.* **1992,** *267* (23), 16467-16471.

45. Ryabov, Y. E.; Fushman, D., A model of interdomain mobility in a multidomain protein. *J. Am. Chem. Soc.* **2007,** *129* (11), 3315-3327.

46. Komander, D.; Reyes-Turcu, F.; Licchesi, J. D. F.; Odenwaelder, P.; Wilkinson, K. D.; Barford, D., Molecular discrimination of structurally equivalent Lys 63-linked and linear polyubiquitin chains. *EMBO Rep.* **2009,** *10* (5), 466.

47. Xu, P.; Duong, D. M.; Seyfried, N. T.; Cheng, D.; Xie, Y.; Robert, J.; Rush, J.; Hochstrasser, M.; Finley, D.; Peng, J., Quantitative Proteomics Reveals the Function of Unconventional Ubiquitin Chains in Proteasomal Degradation. *Cell* **2009,** *137* (1), 133-145.

48. Ohtake, F.; Tsuchiya, H.; Saeki, Y.; Tanaka, K., K63 ubiquitylation triggers proteasomal degradation by seeding branched ubiquitin chains. *Proc. Natl Acad. Sci. USA***2018,** *115* (7), E1401.

49. Liu, C.; Liu, W.; Ye, Y.; Li, W., Ufd2p synthesizes branched ubiquitin chains to promote the degradation of substrates modified with atypical chains. *Nat. Commun.* **2017,** *8*, 14274.

50. Hayden, M. S.; Ghosh, S., Shared Principles in NF-κB Signaling. *Cell* **2008,** *132* (3), 344-362.

51. Laplantine, E.; Fontan, E.; Chiaravalli, J.; Lopez, T.; Lakisic, G.; Véron, M.; Agou, F.; Israël, A., NEMO specifically recognizes K63-linked poly-ubiquitin chains through a new bipartite ubiquitin-binding domain. *EMBO J.* **2009,** *28* (19), 2885.

52. Emmerich, C. H.; Ordureau, A.; Strickson, S.; Arthur, J. S. C.; Pedrioli, P. G. A.; Komander, D.; Cohen, P., Activation of the canonical IKK complex by K63/M1-linked hybrid ubiquitin chains. *Proc. Natl Acad. Sci. USA* **2013,** *110* (38), 15247.

53. Emmerich, C. H.; Bakshi, S.; Kelsall, I. R.; Ortiz-Guerrero, J.; Shpiro, N.; Cohen, P., Lys63/Met1-hybrid ubiquitin chains are commonly formed during the activation of innate immune signalling. *Biochem. Biophys. Res. Commun.* **2016,** *474* (3), 452-461.

54. Lu, Y.; Lee, B.-h.; King, R. W.; Finley, D.; Kirschner, M. W., Substrate degradation by the proteasome: A single-molecule kinetic analysis. *Science* **2015,** *348* (6231).

55. Grice, Guinevere L.; Lobb, Ian T.; Weekes, Michael P.; Gygi, Steven P.; Antrobus, R.; Nathan, James A., The Proteasome Distinguishes between Heterotypic and Homotypic Lysine-11-Linked Polyubiquitin Chains. *Cell Rep.* **2015,** *12* (4), 545-553.

56. Faggiano, S.; Alfano, C.; Pastore, A., The missing links to link ubiquitin: Methods for the enzymatic production of polyubiquitin chains. *Anal. Biochem.* **2016,** *492*, 82-90.

57. Reyes-Turcu, F. E.; Shanks, J. R.; Komander, D.; Wilkinson, K. D., Recognition of Polyubiquitin Isoforms by the Multiple Ubiquitin Binding Modules of Isopeptidase T. *J. Biol. Chem.* **2008,** *283* (28), 19581-19592.

58. Dong, Ken C.; Helgason, E.; Yu, C.; Phu, L.; Arnott, David P.; Bosanac, I.; Compaan, Deanne M.; Huang, Oscar W.; Fedorova, Anna V.; Kirkpatrick, Donald S.; Hymowitz, Sarah G.; Dueber, Erin C., Preparation of Distinct Ubiquitin Chain Reagents of High Purity and Yield. *Structure* **2011,** *19* (8), 1053-1063.

59. Hospenthal, M. K.; Freund, S. M. V.; Komander, D., Assembly, analysis and architecture of atypical ubiquitin chains. *Nat. Struct. Mol. Biol.* **2013,** *20*, 555.

60. Kristariyanto, Yosua A.; Abdul Rehman, Syed A.; Campbell, David G.; Morrice, Nicholas A.; Johnson, C.; Toth, R.; Kulathu, Y., K29-Selective Ubiquitin Binding Domain Reveals Structural Basis of Specificity and Heterotypic Nature of K29 Polyubiquitin. *Mol. Cell* **2015,** *58* (1), 83-94.

61. Michel, Martin A.; Elliott, Paul R.; Swatek, Kirby N.; Simicek, M.; Pruneda, Jonathan N.; Wagstaff, Jane L.; Freund, Stefan M. V.; Komander, D., Assembly and Specific Recognition of K29- and K33-Linked Polyubiquitin. *Mol. Cell* **2015,** *58* (1), 95-109.

62. Virdee, S.; Kapadnis, P. B.; Elliott, T.; Lang, K.; Madrzak, J.; Nguyen, D. P.; Riechmann, L.; Chin, J. W., Traceless and Site-Specific Ubiquitination of Recombinant Proteins. *J. Am. Chem. Soc.* **2011,** *133* (28), 10708-10711.

63. Castañeda, C.; Liu, J.; Chaturvedi, A.; Nowicka, U.; Cropp, T. A.; Fushman, D., Nonenzymatic Assembly of Natural Polyubiquitin Chains of Any Linkage Composition and Isotopic Labeling Scheme. *J. Am. Chem. Soc.* **2011,** *133* (44), 17855-17868.

64. Pham, G. H.; Strieter, E. R., Peeling away the layers of ubiquitin signaling complexities with synthetic ubiquitin–protein conjugates. *Curr. Opin. Chem. Biol.* **2015,** *28*, 57-65.

65. Valkevich, E. M.; Guenette, R. G.; Sanchez, N. A.; Chen, Y.-c.; Ge, Y.; Strieter, E. R., Forging Isopeptide Bonds Using Thiol–Ene Chemistry: Site-Specific Coupling of Ubiquitin Molecules for Studying the Activity of Isopeptidases. *J. Am. Chem. Soc.* **2012,** *134* (16), 6916-6919.

66. Trang Vivian, H.; Valkevich Ellen, M.; Minami, S.; Chen, Y.-C.; Ge, Y.; Strieter Eric, R., Nonenzymatic Polymerization of Ubiquitin: Single-Step Synthesis and Isolation of Discrete Ubiquitin Oligomers. *Angew. Chem. Int. Ed.* **2012,** *51* (52), 13085-13088.

67. Pham Grace, H.; Rana Ambar, S. J. B.; Korkmaz, E. N.; Trang Vivian, H.; Cui, Q.; Strieter Eric, R., Comparison of native and non-native ubiquitin oligomers reveals analogous structures and reactivities. *Protein Sci.* **2015,** *25* (2), 456-471.

68. Ordureau, A.; Münch, C.; Harper, J. W., Quantifying Ubiquitin Signaling. *Mol. Cell* **2015,** *58* (4), 660-676.

69. Hameed, D. S.; Sapmaz, A.; Ovaa, H., How Chemical Synthesis of Ubiquitin Conjugates Helps To Understand Ubiquitin Signal Transduction. *Bioconjugate Chem.* **2017,** *28* (3), 805-815.

70. Mazmanian, S. K.; Liu, G.; Ton-That, H.; Schneewind, O., Staphylococcus aureus Sortase, an Enzyme that Anchors Surface Proteins to the Cell Wall. *Science* **1999,** *285* (5428), 760.

71. Ton-That, H.; Liu, G.; Mazmanian, S. K.; Faull, K. F.; Schneewind, O., Purification and characterization of sortase, the transpeptidase that cleaves surface proteins of Staphylococcus aureusat the LPXTG motif. *Proc. Natl. Acad. Sci.* **1999,** *96* (22), 12424.

72. Huang, X.; Aulabaugh, A.; Ding, W.; Kapoor, B.; Alksne, L.; Tabei, K.; Ellestad, G., Kinetic Mechanism of Staphylococcus aureus Sortase SrtA. *Biochemistry* **2003,** *42* (38), 11307-11315.

73. Matsumoto, M. L.; Dong, K. C.; Yu, C.; Phu, L.; Gao, X.; Hannoush, R. N.; Hymowitz, S. G.; Kirkpatrick, D. S.; Dixit, V. M.; Kelley, R. F., Engineering and Structural Characterization of a Linear Polyubiquitin-Specific Antibody. *J. Mol. Biol.* **2012,** *418* (3), 134-144.

74. Newton, K.; Matsumoto, M. L.; Wertz, I. E.; Kirkpatrick, D. S.; Lill, J. R.; Tan, J.; Dugger, D.; Gordon, N.; Sidhu, S. S.; Fellouse, F. A.; Komuves, L.; French, D. M.; Ferrando, R. E.; Lam, C.; Compaan, D.; Yu, C.; Bosanac, I.; Hymowitz, S. G.; Kelley, R. F.; Dixit, V. M., Ubiquitin Chain Editing Revealed by Polyubiquitin Linkage-Specific Antibodies. *Cell* **2008,** *134* (4), 668-678.

75. Hospenthal, M. K.; Mevissen, T. E. T.; Komander, D., Deubiquitinase-based analysis of ubiquitin chain architecture using Ubiquitin Chain Restriction (UbiCRest). *Nat. Protoc.* **2015,** *10*, 349.

76. Kaiser, S. E.; Riley, B. E.; Shaler, T. A.; Trevino, R. S.; Becker, C. H.; Schulman, H.; Kopito, R. R., Protein standard absolute quantification (PSAQ) method for the measurement of cellular ubiquitin pools. *Nat. Meth.* **2011,** *8*, 691.

77. Kirkpatrick, D. S.; Gerber, S. A.; Gygi, S. P., The absolute quantification strategy: a general procedure for the quantification of proteins and post-translational modifications. *Methods* **2005,** *35* (3), 265-273.

78. Catherman, A. D.; Skinner, O. S.; Kelleher, N. L., Top Down proteomics: Facts and perspectives. *Biochem. Biophys. Res. Commun.* **2014,** *445* (4), 683-693.

79. Lee Amanda, E.; Geis-Asteggiante, L.; Dixon Emma, K.; Kim, Y.; Kashyap Tanuja, R.; Wang, Y.; Fushman, D.; Fenselau, C., Preparing to read the ubiquitin code: characterization of ubiquitin trimers by top-down mass spectrometry. *J. Mass Spectrom.* **2016,** *51* (4), 315-321.

80. Lee Amanda, E.; Geis-Asteggiante, L.; Dixon Emma, K.; Miller, M.; Wang, Y.; Fushman, D.; Fenselau, C., Preparing to read the ubiquitin code: top-down analysis of unanchored ubiquitin tetramers. *J. Mass Spectrom.* **2016,** *51* (8), 629-637.

81. Xu, P.; Peng, J., Characterization of Polyubiquitin Chain Structure by Middle-down Mass Spectrometry. *Anal. Chem.* **2008,** *80* (9), 3438-3444.

82. Valkevich, E. M.; Sanchez, N. A.; Ge, Y.; Strieter, E. R., Middle-Down Mass Spectrometry Enables Characterization of Branched Ubiquitin Chains. *Biochemistry* **2014,** *53* (30), 4979-4989.

83. Tomko, R. J.; Hochstrasser, M., Molecular Architecture and Assembly of the Eukaryotic Proteasome. *Annu. Rev. Biochem.* **2013,** *82* (1), 415-445.

84. Budenholzer, L.; Cheng, C. L.; Li, Y.; Hochstrasser, M., Proteasome Structure and Assembly. *J. Mol. Biol.* **2017,** *429* (22), 3500-3524.

85. Collins, G. A.; Goldberg, A. L., The Logic of the 26S Proteasome. *Cell* **2017,** *169* (5), 792-806.

86. Śledź, P.; Förster, F.; Baumeister, W., Allosteric Effects in the Regulation of 26S Proteasome Activities. *J. Mol. Biol.* **2013,** *425* (9), 1415-1423.

87. Peth, A.; Besche, H. C.; Goldberg, A. L., Ubiquitinated Proteins Activate the Proteasome by Binding to Usp14/Ubp6, which Causes 20S Gate Opening. *Mol. Cell* **2009,** *36* (5), 794-804.

88. Peth, A.; Kukushkin, N.; Bossé, M.; Goldberg, A. L., Ubiquitinated Proteins Activate the Proteasomal ATPases by Binding to Usp14 or Uch37 Homologs. *J. Biol. Chem.* **2013,** *288* (11), 7781-7790.

89. de Poot, S. A. H.; Tian, G.; Finley, D., Meddling with Fate: The Proteasomal Deubiquitinating Enzymes. *J. Mol. Biol.* **2017,** *429* (22), 3525-3545.

90. Verma, R.; Aravind, L.; Oania, R.; McDonald, W. H.; Yates, J. R.; Koonin, E. V.; Deshaies, R. J., Role of Rpn11 Metalloprotease in Deubiquitination and Degradation by the 26S Proteasome. *Science* **2002,** *298* (5593), 611.

91. Sahtoe, Danny D.; van Dijk, Willem J.; El Oualid, F.; Ekkebus, R.; Ovaa, H.; Sixma, Titia K., Mechanism of UCH-L5 Activation and Inhibition by DEUBAD Domains in RPN13 and INO80G. *Mol. Cell* **2015,** *57* (5), 887-900.

92. VanderLinden, R. T.; Hemmis, C. W.; Schmitt, B.; Ndoja, A.; Whitby, F. G.; Robinson, H.; Cohen, R. E.; Yao, T.; Hill, C. P., Structural Basis for the Activation and Inhibition of the UCH37 Deubiquitylase. *Mol. Cell* **2016,** *61* (3), 487.

93. Yao, T.; Song, L.; Jin, J.; Cai, Y.; Takahashi, H.; Swanson, S. K.; Washburn, M. P.; Florens, L.; Conaway, R. C.; Cohen, R. E.; Conaway, J. W., Distinct Modes of Regulation of the Uch37 Deubiquitinating

Enzyme in the Proteasome and in the Ino80 Chromatin-Remodeling Complex. *Mol. Cell* **2008,** *31* (6), 909-917.

94. Nijman, S. M. B.; Luna-Vargas, M. P. A.; Velds, A.; Brummelkamp, T. R.; Dirac, A. M. G.; Sixma, T. K.; Bernards, R., A Genomic and Functional Inventory of Deubiquitinating Enzymes. *Cell* **2005,** *123* (5), 773-786.

95. Yao, T.; Song, L.; Xu, W.; DeMartino, G. N.; Florens, L.; Swanson, S. K.; Washburn, M. P.; Conaway, R. C.; Conaway, J. W.; Cohen, R. E., Proteasome recruitment and activation of the Uch37 deubiquitinating enzyme by Adrm1. *Nat. Cell Biol.* **2006,** *8*, 994.

96. Chen, X.; Lee, B.-H.; Finley, D.; Walters, K. J., Structure of Proteasome Ubiquitin Receptor hRpn13 and Its Activation by the Scaffolding Protein hRpn2. *Mol. Cell* **2010,** *38* (3), 404-415.

97. Husnjak, K.; Elsasser, S.; Zhang, N.; Chen, X.; Randles, L.; Shi, Y.; Hofmann, K.; Walters, K. J.; Finley, D.; Dikic, I., Proteasome subunit Rpn13 is a novel ubiquitin receptor. *Nature* **2008,** *453*, 481.

98. Lam, Y. A.; DeMartino, G. N.; Pickart, C. M.; Cohen, R. E., Specificity of the Ubiquitin Isopeptidase in the PA700 Regulatory Complex of 26 S Proteasomes. *J. Biol. Chem.* **1997,** *272* (45), 28438-28446.

99. Lam, Y. A.; Xu, W.; DeMartino, G. N.; Cohen, R. E., Editing of ubiquitin conjugates by an isopeptidase in the 26S proteasome. *Nature* **1997,** *385*, 737.

100. Chen, S.; Wu, J.; Lu, Y.; Ma, Y.-B.; Lee, B.-H.; Yu, Z.; Ouyang, Q.; Finley, D. J.; Kirschner, M. W.; Mao, Y., Structural basis for dynamic regulation of the human 26S proteasome. *Proc. Natl. Acad. Sci. USA* **2016,** *113* (46), 12991.

101. Lu, X.; Nowicka, U.; Sridharan, V.; Liu, F.; Randles, L.; Hymel, D.; Dyba, M.; Tarasov, S. G.; Tarasova, N. I.; Zhao, X. Z.; Hamazaki, J.; Murata, S.; Burke, J. T. R.; Walters, K. J., Structure of the Rpn13-Rpn2 complex provides insights for Rpn13 and Uch37 as anticancer targets. *Nat. Commun.* **2017,** *8*, 15540.

2 Subunit-Specific Labeling of Ubiquitin Chains Using Sortase: Insights into the Selectivity of Deubiquitinases

This chapter has been published:

Crowe S.O., Pham G. H., Ziegler J. C., Deol K. K., Guenette R. G., Ge Y., and Strieter E. R., *ChemBioChem* **2016**, 17, 1525-1531.

Author contributions:

SOC and ERS designed the experiments and wrote the manuscript.

SOC designed the synthesis, optimized the chemistry, performed the labeling, and enzymatic assays.

GHP made the initial observations with USP15.

JCZ synthesized small molecules.

KKD performed middle-down MS analysis.

RGG performed some labeling experiments.

YG and ERS supervised the acquisition of data.

All authors read and approved the final manuscript.

2.1 Abstract

Information embedded in different ubiquitin chains is transduced by proteins with ubiquitin-binding domains (UBDs) and erased by a set of hydrolytic enzymes referred to as deubiquitinases (DUBs). Understanding the selectivity of UBDs and DUBs is necessary for decoding the functions of different ubiquitin chains. Critical to these efforts is the access to chemically defined ubiquitin chains bearing site-specific fluorescent labels. One approach toward constructing such molecules involves peptide ligation using sortase (SrtA), a bacterial transpeptidase responsible for covalently attaching cell surface proteins to the cell wall. Here, we demonstrate the utility of SrtA in modifying individual subunits of ubiquitin chains. Using ubiquitin derivatives in which an N-terminal glycine is unveiled after protease-mediated digestion, we synthesized ubiquitin dimers, trimers, and tetramers with different isopeptide linkages. SrtA was then used in combination with fluorescent depsipeptide substrates to effect the modification of each subunit in a chain. By constructing branched ubiquitin chains with individual subunits tagged with a fluorophore, we provide evidence that the ubiquitin specific protease USP15 prefers Ub trimers but has little preference for a particular isopeptide linkage. Our results emphasize the importance of subunit-specific labeling of Ub chains when studying how DUBs process Ub chains.

2.2 Introduction

The human genome encodes ~80 active deubiquitinating enzymes that remove ubiquitin (Ub) modifications and disassemble Ub chains.[1-3] The precise timing of their action is critical, as aberrant activity is associated with several human diseases, including many cancers and neurological disorders.[4-7] While the importance of DUBs in disease pathology has been well documented, molecular details underlying the activity of these enzymes remain poorly understood. Central to the challenge in studying DUBs is the diversity of potential substrates. Proteomics studies have identified over ~19,000 ubiquitination sites on 5,000 human proteins. Moreover, there is tremendous complexity just within Ub chains. Each of the eight amino groups of Ub (Met1, Lys6, Lys11, Lys27, Lys29, Lys33, Lys48, and Lys63) can be used to extend a Ub chain from a particular substrate.[8-11] As a result, chains of varying length can be generated bearing a single linkage (homotypic) or a mixture of linkages (heterotypic) in a linear or branched configuration.

Given the diversity in both substrate proteins and Ub chains, DUBs have the ability to regulate Ub-dependent pathways on several levels.[2, 3, 12, 13] For instance, a DUB may directly recognize a specific ubiquitinated substrate and remove mono-Ub. In the context of Ub chains, DUBs have been shown to discriminate between the eight different linkages and selectively act on the end (exo) or in the middle (endo) of a chain. Many of these discoveries have been made using a limited set of defined Ub conjugates. A comprehensive biochemical characterization of DUBs requires access to a large array of substrates.

To address this issue a number of research groups, including ours, have been interested in developing chemical methods to synthesize Ub chains.[14-21] Recently we discovered that by replacing a lysine of interest with cysteine and installing an alkene at the C-terminus of Ub, free-radical thiol-ene coupling (TEC) could be used to effect isopeptide bond formation between Ub molecules.[14, 22] This method is straightforward to carry out, as it requires standard recombinant proteins, minimal synthetic

manipulations, and can be conducted under non-denaturing conditions. Most importantly, thiol-ene coupling provides access to large quantities of all linkage types and topologies that serve as functional surrogates of native oligomers.

In this study, we sought to expand the utility of Ub chains derived from TEC chemistry by installing fluorophores on individual subunits in a site-specific manner. Fluorescent labeling of Ub chains facilitates efforts to better understand the selectivity of DUBs. Current approaches to the site-specific installation of fluorophores employ cysteine reactive dyes.[18, 23-26] Although these methods have been successfully applied to the study of homotypic chains, this strategy is not compatible with TEC chemistry. The bacterial transpeptidase, sortase (SrtA), is a powerful tool for site-specific labeling of proteins and is orthogonal to TEC chemistry.[27-33] We demonstrate that SrtA can be used to install fluorophores on specific subunits within a large variety of Ub chains. Our work has led to the discovery that the ubiquitin specific protease USP15 prefers branched trimers over dimers but does not have a preference for a particular isopeptide linkage.

2.3 Results and Discussion

SrtA recognizes the small pentapeptide motif LPXTG (*X* is any amino acid) and cleaves the scissile bond between Thr and Gly.[34, 35] The resulting acyl-enzyme intermediate is intercepted by an N-terminal oligoglycine motif to furnish a new bioconjugate. Utilizing SrtA to catalyze fluorophore-labeling of Ub chains therefore requires a Ub monomer carrying an N-terminal oligo-Gly appendage. To prepare chains for SrtA-mediated modification, we introduced a tobacco etch virus (TEV) protease recognition sequence (ENLYFQ) at the N-terminus of Ub followed by a pentaglycine (5xGly) motif. We also synthesized depsipeptides **I** and **II** using Fmoc solid phase peptide synthesis (SPPS) (Scheme 1). Recent studies have shown that peptides containing a depsipeptide linkage between the scissile Thr-Gly bond greatly enhance the efficiency of N-terminal SrtA ligation by rendering the reaction irreversible.[28, 36]

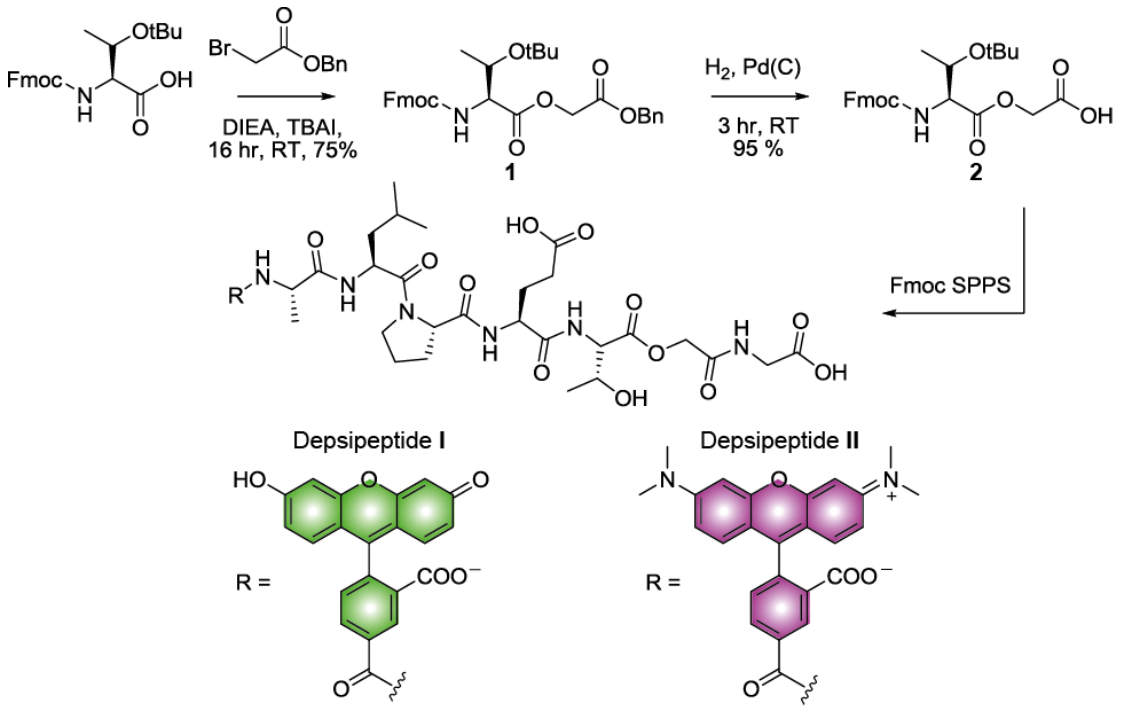

Scheme 2.1: Synthesis of depsipeptides I and II. DIEA; diisopropylethylamine, TBAI; tetrabutylammonium iodide, rt; room temperature, SPPS; solid phase peptide synthesis.

With building blocks in hand, we explored the SrtA-catalyzed fluorophore-labeling of Lys63-linked Ub dimers. After the dimers were synthesized using TEC chemistry, TEV protease was used to unmask the 5xGly motif. Labeling experiments were then performed using 0.5 and 10 equivalents of SrtA and depsipeptide **I**, respectively. Under these conditions, we observe two new bands by Coomassie and fluorescence imaging at early time points (Figures 2.1 B and 2.1 C). The lower molecular weight band corresponds to a singly labeled species, whereas the higher molecule weight band represents a doubly labeled dimer. By ninety minutes the unlabeled and singly labeled dimers are completely converted to fully labeled dimers. To confirm the SDS-PAGE results, we obtained the intact mass of the products by MALDI-TOF mass spectrometry (Figure 2.S.1). The results of this analysis indicate that both subunits are indeed conjugated to a fluorescein-labeled peptide. Encouraged by these findings, we synthesized Lys6-, Lys11-, and Lys48-linked dimers using TEC chemistry, and subjected them to our optimized labeling

conditions (Figure 2.S.1). As judged by SDS-PAGE and MALDI-TOF analysis, both subunits of the dimers are efficiently labeled with fluorophores; only trace amounts of the singly labeled species are detected.

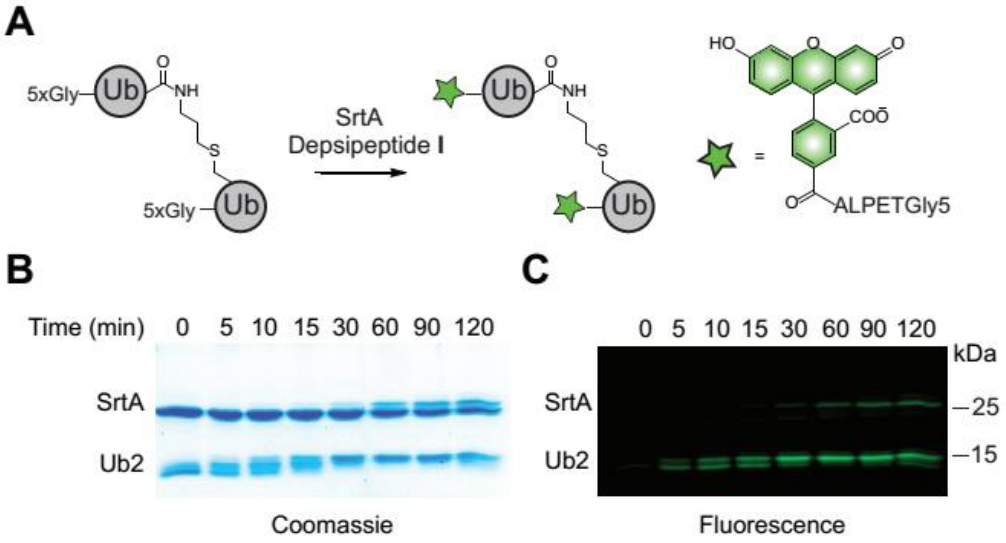

Figure 2. 1: Site-specific labeling of Ub dimers using SrtA. A) Labeling schematic. **B**) Coomassie-stained 15 % SDS-PAGE gel showing the transition from unlabeled to singly labeled to fully labeled Ub dimer. **C**) Fluorescence image of the same gel. Fluorescence was detected using the blue laser (473 nm) on a Typhoon FLA 9500 imager (GE Healthcare) equipped with a 515-545 nm filter.

Next, we sought to label longer chains. A series of Lys63-linked chains were generated by TEC chemistry, ranging in length between two and five subunits. After incubating with TEV protease, the chains were labeled at their individual N-termini using depsipeptide **I** (Figure 2.2 B). It is important to note the amounts of SrtA and depsipeptide **I** had to be adjusted to account for the total concentration of Ub monomer in each reaction. As with the Ub dimers, we detect robust labeling of chains of different length. Fluorescence imaging shows single bands for each of the discrete oligomers. To measure the extent of labeling, we then purified the chains and measured the dye to protein ratio. This required removal of excess depsipeptide, TEV, and SrtA and TEV (Figure 2.S.2 and 2.S.3). Ratios of dye to protein indicate that individual subunits are conjugated to the fluorophore (Figure 2.2 C). In this case, the resulting products

are similar to those obtained using N-terminal fluorophore-labeled mono-Ub and Ub conjugating enzymes.[37, 38] However, since thiol-ene coupling is more versatile than enzymatic methods, the site-specific installation of fluorophores can be applied toward the synthesis of fluorescent chains bearing different linkages and topologies.

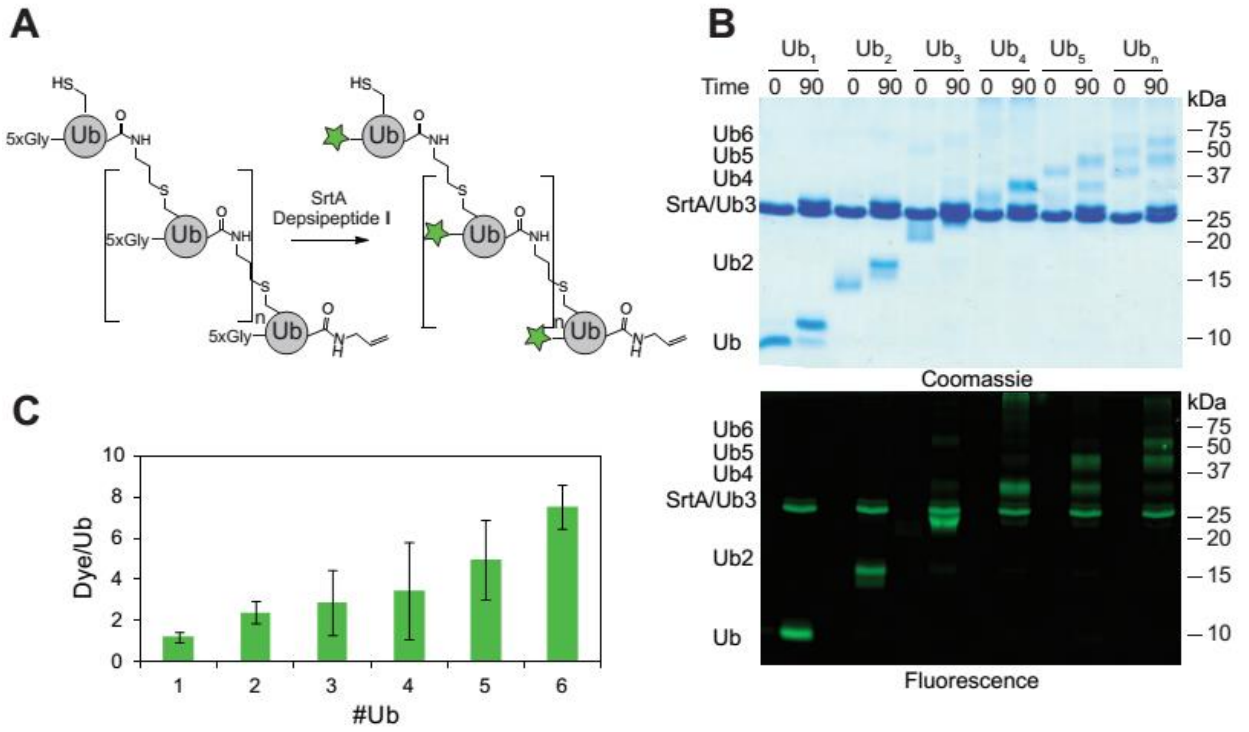

Figure 2.2: Site specific labeling of Ubiquitin chains of discrete length. A) General scheme for the labeling of Ub chains of different length. **B**) SDS-PAGE analysis of labeling reactions. Ub oligomers (40 µM adjusted for the relative concentration of monoUb) were incubated with TEV protease (2 µM) for 2 hours at room temperature prior to the addition of SrtA (20 µM) and I (400 µM). Time points were taken at the indicated times by quenching an aliquot with 6x Laemmli loading buffer and separated on a 15 % SDS-PAGE gel. The top gel is the Coomassie-stained SDS-PAGE gel of labeled Ub chains before and after 90 min incubation with SrtA and depsipeptide **I**. In each reaction a discrete band can be seen for the labeled oligomer with a mass shift consistent with that of the added peptides. The bottom image is the fluorescence scan of the

same gel. **C**) Quantification of labeled Ub chains. Chains were separated from SrtA, TEV protease, and excess peptide **I** using a two-step purification strategy employing Ni^{2+} affinity chromatography to remove His-tagged enzymes and a desalting column to remove excess **I**. The ratio of dye to protein is plotted for each oligomer of different length. Error bars show the replicates of three measurements.

A topology of particular interest is a branched Ub chain. Branched Ub chains in which a single Ub has been modified at positions Lys11 and Lys48 have been shown to advance the cell cycle through enhanced degradation by the proteasome.[39] The mechanisms by which Lys11/Lys48 branched chains trigger degradation are, however, unclear. Recent data suggests that single linkage (homotypic) Lys11 chains bind to Ub receptors on the proteasome with low affinity, whereas mixed linkage (heterotypic) Lys11 chains strongly interact with the proteasome.[39] These results suggest that in contrast to the prevailing view that branched Ub chains may adopt distinct conformations relative to their linear counterparts.[40] Access to fluorescent, branched chains is therefore important for testing this hypothesis. We constructed branched Lys6/Lys48 and Lys11/Lys48 Ub trimers containing a single oligoglycine motif at the base of the chain. Introduction of fluorescent labels at the base proceeds efficiently (Figure 2S.4), demonstrating that SrtA-mediated modification enables unprecedented access to fluorophore-labeled branched oligomers.

Having established a method for the synthesis and labeling of Ub chains, we evaluated whether DUBs accept the modified dimers as substrates. We performed a series of assays comparing the hydrolysis of labeled dimers to that of unmodified dimers (Figures 2.3 A and B). For these experiments, we chose two different members of the ubiquitin-specific protease (USP) family of DUBs, USP7 and USP15. The USP DUBs have previously been shown to display little selectivity toward different Ub dimers, making them ideal candidates for testing whether a fluorophore label on different dimers perturbs activity.[41-43] With both USP7 and USP15, we observe robust chain hydrolysis similar to that of the unmodified dimers. These results indicate that the introduction of a fluorophore does not impede the ability to cleave dimers.

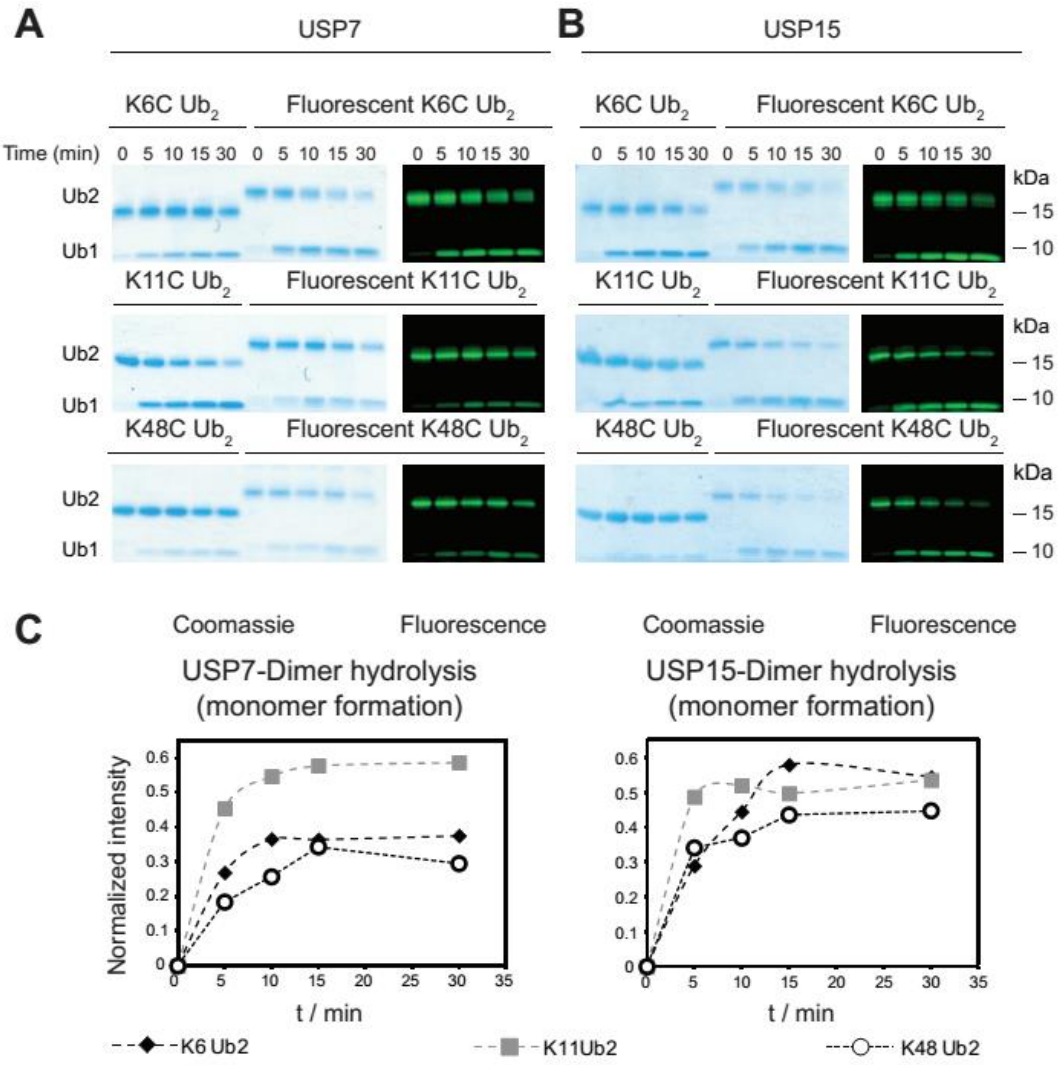

Figure 2.3: Ub dimers labeled with SrtA are suitable substrates for DUBs. A) USP7-catalyzed hydrolysis of Lys6-, Lys11-, and Lys48-linked unlabeled and fluorescently labeled Ub dimers. **B**) USP15-catalyzed hydrolysis of Lys6-, Lys11-, and Lys48-linked unlabeled and fluorescently labeled Ub dimers. For both sets of DUB assays, Ub dimer (10 µM) was incubated with the indicated DUB (100 nM) at 37 °C. Time points were taken at the indicated time by quenching an aliquot of reaction mixture with 6x Laemmli loading buffer. Samples were then separated on a 12 % Bis-Tris NuPAGE gel (Invitrogen). **C**) Densitometric analysis of fluorescent gels in panel B following the appearance of fluorescent monoUb over time. The intensity of the monomer band was normalized against the intensity of the fluorescent dimer at t = 0. The dotted lines

do not represent a fit to a mathematical expression. Densitometry was performed on the fluorescence image using ImageJ (NIH) to quantify the relative amounts of monoUb.

We then tested branched trimers as substrates. As with the fluorescently labeled dimers, the fluorophore-labeled trimers were hydrolyzed by USP7 and USP15 with similar efficiency as the unlabeled oligomers (Figures 2.4 B and C). With USP15, the fluorescent gels show the TEC-derived Lys6/Lys48 branched trimer is rapidly converted from trimer to dimer, however, hydrolysis of the resulting dimer occurs at a much slower rate. Densitometric analysis confirmed these observations, showing fast appearance of fluorescent dimer and a significant a delay before the appearance of fluorescent monomer in the gels (Figure 2.4 C). Considering the fluorophore is tethered to the base of the trimer, complete hydrolysis from trimer to monomer is necessary for the appearance of fluorescent monomer. The delay in monomer formation was also observed when the TEC-derived Lys11/Lys48 branched trimer was tested against USP15, but to a lesser extent than the Lys6/Lys48 trimer. Selective hydrolysis of branched chains was not observed with USP7. The results with USP15 were unexpected, as this DUB displays little selectivity toward homotypic chains,[43] but here it appears that cleavage of a branched chain is preferred over that of the dimer product.

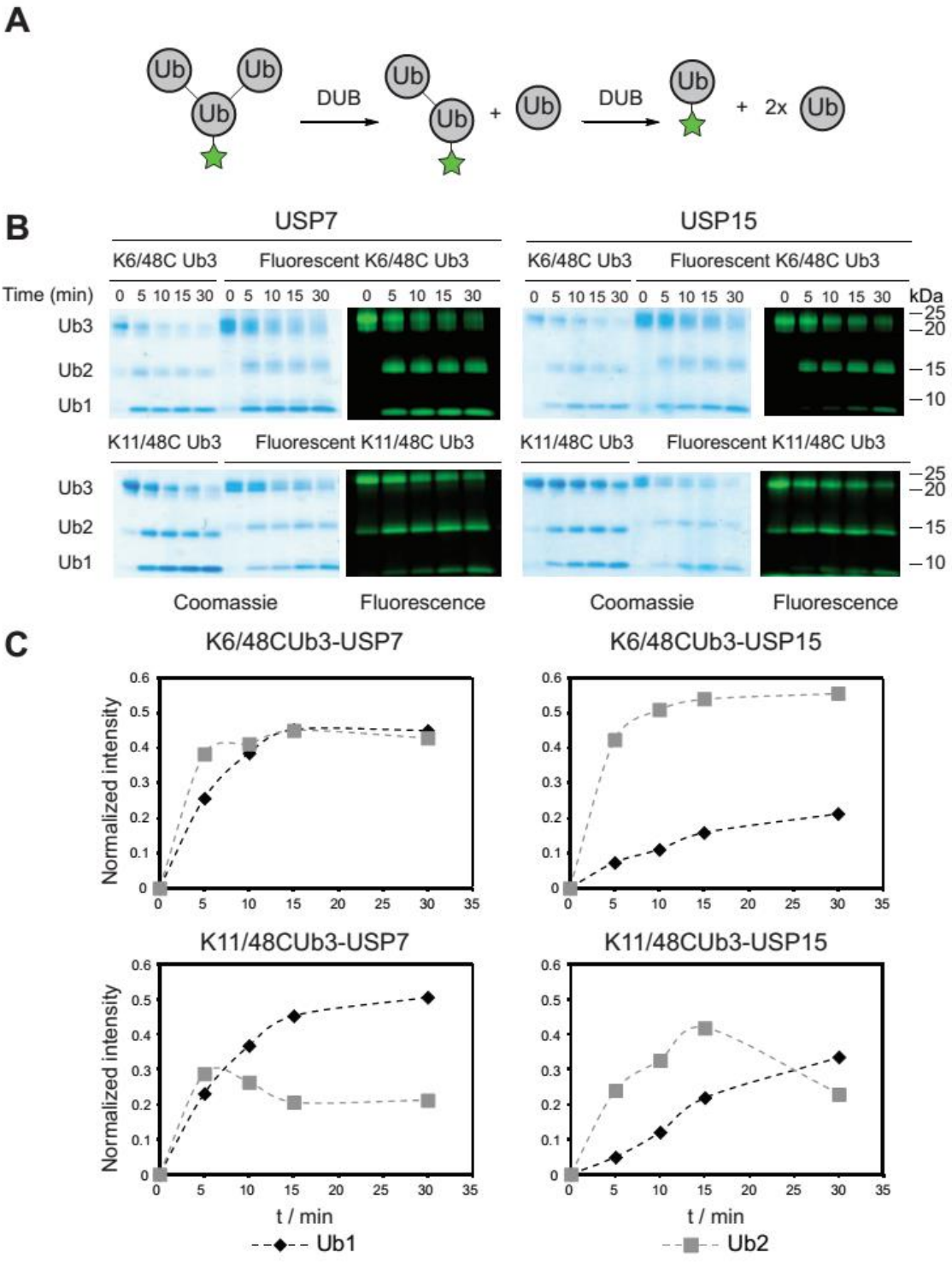

Figure 2.4: DUB-catalyzed hydrolysis of labeled branched Ub chains. A) General scheme for the DUB-catalyzed hydrolysis of branched Ub labeled with peptide **I** at the base. **B**) Time-course analysis of the USP7- and USP15-catalyzed hydrolysis of TEC-derived Lys6/Lys48 and Lys11/Lys48 branched trimers. For

both sets of DUB assays, the branched trimer (10 μM) was incubated with the indicated DUB (100 nM) at 37 °C. Aliquots of reaction mixture were quenched by the addition of 6x Laemmli loading buffer at the indicated time points and separated on a 12 % Bis-Tris NuPAGE gel (Invitrogen). **C**) Densitometric analysis of fluorescent gels in panel B following the appearance of fluorescent mono- and di-Ub over time. The intensities of the bands are normalized to the intensity of the fluorescent branched trimer at t = 0 min.

To confirm our findings with TEC-derived chains and ensure trimer hydrolysis is a consequence of preferential branched chain hydrolysis—and not simply a preference for a specific linkage within the trimer—we synthesized segmentally, fluorophore-labeled native isopeptide-linked trimers. The bacterial E3 ligase NleL was recently shown to build primarily Lys6- linked chains.[44] Thus, we used NleL in conjunction with the Lys48 linkage-specific conjugating enzyme UBE2R1 to synthesize Lys6/Lys48 branched trimers modified with an N-terminal 5xGly motif at specific subunits (Figure 2.5 A). The connectivity of each of the native branched trimers was confirmed using minimal trypsinolysis followed by high-resolution tandem mass spectrometry (MS/MS) on a Fourier-transform ion cyclotron resonance mass spectrometer (FT-ICR) (Figures 2S.5-8).[45] SrtA was then employed to append a peptide carrying either fluorescein (depsipeptide **I**) or 5-carboxytetramethylrhodamine (TAMRA; depsipeptide **II**).

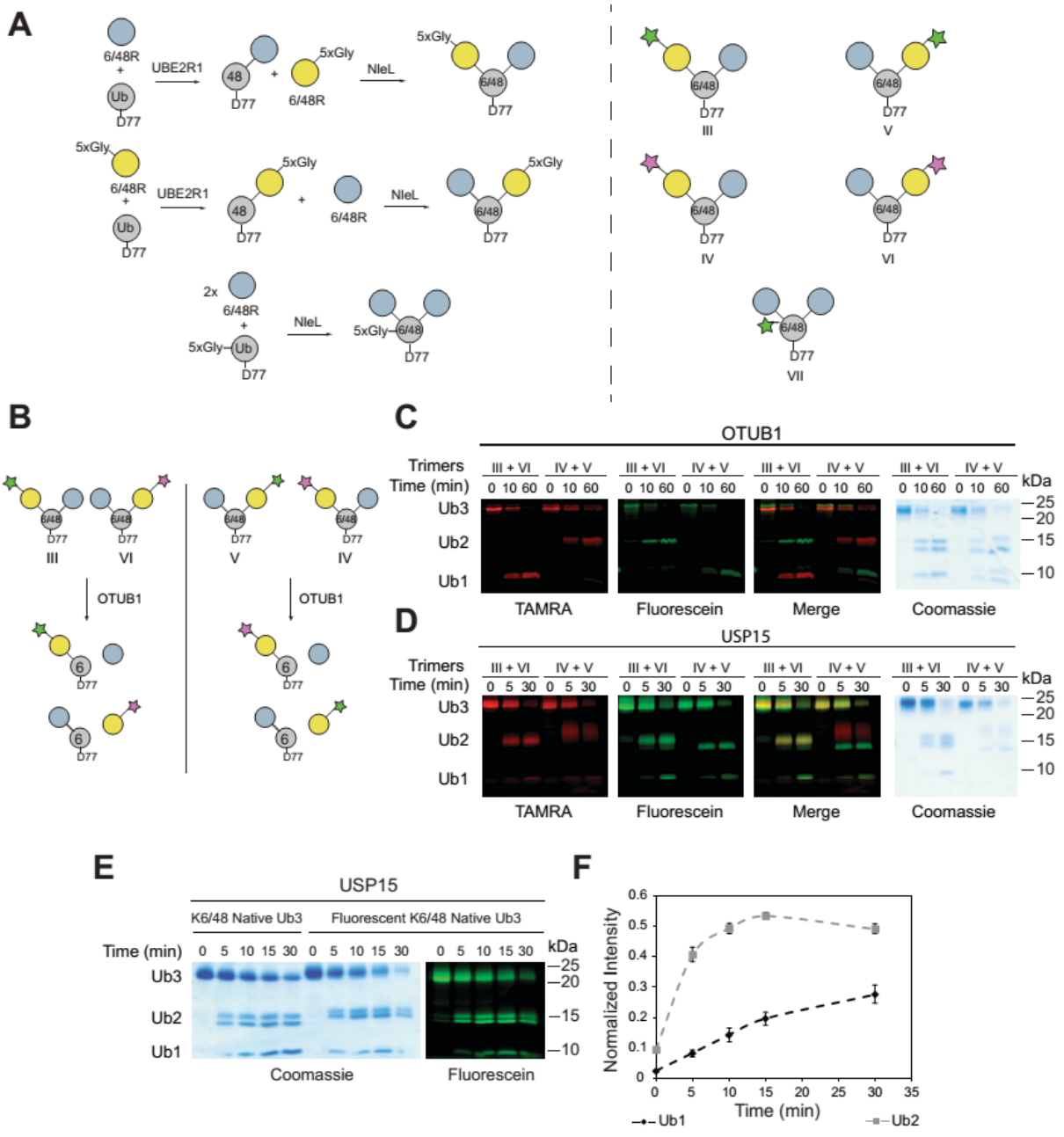

Figure 2.5: Selectivity of USP15 toward native isopeptide-linked branched trimers. A) Scheme depicting the synthesis of segmentally labeled native isopeptide-linked branched trimers (left). Structures of the segmentally labeled branched trimers used in this study (right). **B**) Scheme showing how segmental labeling informs on the linkage selectivity of a DUB. The green star denotes Ub labeled with depsipeptide **I**, the pink start denotes Ub labeled with depsipeptide **II**. **C**) Complementary branched trimers labeled with

either depsipeptide **I** or **II** were mixed at an equal ratio and subjected to hydrolysis by the Lys48 selective DUB OTUB1. Aliquots were taken at indicated time points and quenched by the addition of 6 x Laemmli loading buffer prior to separation on a 12 % Bis-Tris NuPAGE gel (Invitrogen). Gels were then imaged using a Typhoon FLA 9500 imager (GE Healthcare). **D**) USP15 hydrolysis of complementary labeled branched trimers shows that USP15 does not display linkage selectivity when hydrolyzing Lys6/Lys48 linked branched trimers. **D**) Time-course analysis of the USP15-catalyzed hydrolysis of native Lys6/Lys48 branched trimer labeled with depsipeptide **I** at the base (left). **E**) Densitometric analysis of the fluorescent gel in Figure 2.S.9 following the appearance of fluorescent mono- and di-Ub over time. The error bars represent the standard deviation of three replicates.

Since the Ub subunits are essentially "color-coded" in segmentally labeled native branched trimers we devised a competition-based DUB assay to report on the linkage selectivity. Differentially labeled trimers were mixed and subjected to the Lys48 linkage-specific DUB OTUB1 (Figure 2.5 B). When either fluorescein or TAMRA are attached to the Lys48-linked distal Ub subunit, a fluorescent monomer rapidly appears in the presence of OTUB1 (Figure 2.5 C). By contrast, labeling of the Lys6-linked distal Ub subunit results in the formation of only fluorescent dimers, indicative of Lys48 linkage specificity. Using USP15 instead of OTUB1 shows there is little selectivity for the Lys6 or Lys48 isopeptide bond, as fluorescent dimers and monomers are formed regardless of the position of the fluorescent Ub subunit (Figure 2.5 D). Thus, our results demonstrate that segmental labeling can inform on the linkage selectivity of DUBs and USP15 does not have a predilection for a particular linkage within a branched trimer.

We then sought to reaffirm that USP15 has a proclivity for branched trimers by shifting our focus on native trimers labeled with a fluorophore at the base of the chain. The experiments are identical to those performed with TEC-derived chains. USP15-catalyzed hydrolysis of the native trimers shows the two possible fluorescent dimers appear simultaneously, again indicating a lack of linkage selectivity (Figure 2.5

E). More importantly, however, the formation of fluorescent mono-Ub is significantly postponed relative to the dimer, similar to the USP15-catalyzed hydrolysis of TEC-derived chains (Figures 2.5 E and 2.5 F). These results further demonstrate that TEC-derived Ub oligomers are a good model for native chains and suggest USP15 prefers branched trimers over Ub dimers. The analysis of Coomassie stained gels does not yield this level of insight, as it is difficult to discern which Ub moiety is represented by the mono-Ub species. Our findings with USP15 therefore underscore the importance of subunit-specific labeling of Ub chains when studying how DUBs process Ub chains.

Our observation that USP15 rapidly cleaves branched trimers leaving behind a dimer that is transformed more slowly into monomers likely has physiological significance. Recent studies have shown that USP15 counteracts the ability of the E3 Ub ligase Parkin to promote the clearance of damaged mitochondria through a degradative process referred to as mitophagy.[46] Parkin synthesizes heterogeneous chains with Lys6, Lys11, Lys48, and Lys63 linkages.[47] Failure to produce these linkages, particularly Lys6 and Lys63, reduces the efficiency of mitophagy.[48, 49] Although the precise topology of the chains Parkin generates is unknown, the finding that USP15 exhibits little linkage selectivity but prefers a branched trimer suggests this DUB might mitigate mitophagy by removing branched conjugates. Another possibility is that USP15 could restrict the length of Ub chains produced by Parkin through an odd-even effect. With an even number of Ub molecules in a chain there is the possibility to form multiple inter-subunit contacts, which may preclude interactions with USP15. With an odd number there will always be a Ub molecule unable to form inter-subunit contacts, making it accessible to USP15. The ramifications of an odd-even effect would be an accumulation of proteins decorated with Ub dimers, which may not be sufficient to drive mitophagy. Future work will focus on how the biochemical activity of USP15 relates to its biological function.

In conclusion, we demonstrate the utility of SrtA in catalyzing the installation of fluorophores on individual subunits of homotypic and heterotypic chains. By combining TEC with SrtA chemistry, we now

have the ability to probe the selectivity of a number of DUBs. We highlight this by using SrtA to site-specifically install a fluorophore at each individual subunit of a branched Ub trimer. We further demonstrate the utility of these novel probes by showcasing their ability to reveal insight into the linkage selectivity of DUBs when processing a branched Ub chains using both a linkage selective DUB (OTUB1) and non-selective DUB (USP15). Furthermore, we provide evidence that USP15 may have a preference for branched trimers over their linear counterparts.

2.4 Acknowledgments

This work was supported by research grant RO1GM110543 from the National Institutes of Health. The purchase of the Bruker ULTRAFLEX™ III in 2008 was partially funded by NIH NCRR 1S10RR024601-01 Award to the University of Wisconsin-Madison Department of Chemistry.

2.5 References

1. Nijman, S. M. B.; Luna-Vargas, M. P. A.; Velds, A.; Brummelkamp, T. R.; Dirac, A. M. G.; Sixma, T. K.; Bernards, R., A Genomic and Functional Inventory of Deubiquitinating Enzymes. *Cell* **2005,** *123* (5), 773-786.

2. Komander, D.; Clague, M. J.; Urbe, S., Breaking the chains: structure and function of the deubiquitinases. *Nat. Rev. Mol. Cell Biol.* **2009,** *10* (8), 550-563.

3. Clague, M. J.; Barsukov, I.; Coulson, J. M.; Liu, H.; Rigden, D. J.; Urbé, S., Deubiquitylases From Genes to Organism. *Physiol. Rev.* **2013**, *93,* 1289-1315.

4. Hoeller, D.; Dikic, I., Targeting the ubiquitin system in cancer therapy. *Nature* **2009,** *458* (7237), 438-444.

5. Heideker, J.; Wertz, Ingrid E., DUBs, the regulation of cell identity and disease. *Biochem. J.* **2015,** *465* (1), 1-26.

6. Tai, H.-C.; Schuman, E. M., Ubiquitin, the proteasome and protein degradation in neuronal function and dysfunction. *Nat. Rev. Neurosci.* **2008,** *9* (11), 826-838.

7. Popovic, D.; Vucic, D.; Dikic, I., Ubiquitination in disease pathogenesis and treatment. *Nature medicine* **2014,** *20* (11), 1242-1253.

8. Komander, D.; Rape, M., The ubiquitin code. *Annu. Rev. Biochem.* **2012,** *81*, 203-29.

9. Husnjak, K.; Dikic, I., Ubiquitin-Binding Proteins: Decoders of Ubiquitin-Mediated Cellular Functions. *Annu. Rev. Bio.* **2012,** *81* (1), 291-322.

10. Pickart, C. M., Mechanisms Underlying Ubiquitination. *Annu. Rev. Biochem.* **2001,** *70* (1), 503-533.

11. Clague, M. J.; Heride, C.; Urbé, S., The demographics of the ubiquitin system. *Trends Cell Biol.* **2015,** *25* (7), 417-426.

12. Clague, M. J.; Coulson, J. M.; Urbé, S., Cellular functions of the DUBs. *J. Cell Sci.* **2012,** *125* (2), 277-286.

13. Reyes-Turcu, F. E.; Ventii, K. H.; Wilkinson, K. D., Regulation and Cellular Roles of Ubiquitin-Specific Deubiquitinating Enzymes. *Annu. Rev. Biochem.* **2009,** *78* (1), 363-397.

14. Valkevich, E. M.; Guenette, R. G.; Sanchez, N. A.; Chen, Y.-c.; Ge, Y.; Strieter, E. R., Forging Isopeptide Bonds Using Thiol–Ene Chemistry: Site-Specific Coupling of Ubiquitin Molecules for Studying the Activity of Isopeptidases. *J. Am. Chem. Soc.* **2012,** *134* (16), 6916-6919.

15. Dixon, E. K.; Castañeda, C. A.; Kashyap, T. R.; Wang, Y.; Fushman, D., Nonenzymatic assembly of branched polyubiquitin chains for structural and biochemical studies. *Bioorg. Med. Chem.* **2013,** *21* (12), 3421-3429.

16. Castañeda, C.; Liu, J.; Chaturvedi, A.; Nowicka, U.; Cropp, T. A.; Fushman, D., Nonenzymatic Assembly of Natural Polyubiquitin Chains of Any Linkage Composition and Isotopic Labeling Scheme. *J. Am. Chem. Soc.* **2011,** *133* (44), 17855-17868.

17. Virdee, S.; Kapadnis, P. B.; Elliott, T.; Lang, K.; Madrzak, J.; Nguyen, D. P.; Riechmann, L.; Chin, J. W., Traceless and Site-Specific Ubiquitination of Recombinant Proteins. *J. Am. Chem. Soc.* **2011,** *133* (28), 10708-10711.

18. Virdee, S.; Ye, Y.; Nguyen, D. P.; Komander, D.; Chin, J. W., Engineered diubiquitin synthesis reveals Lys29-isopeptide specificity of an OTU deubiquitinase. *Nat. Chem. Biol.* **2010,** *6* (10), 750-757.

19. Eger, S.; Scheffner, M.; Marx, A.; Rubini, M., Synthesis of Defined Ubiquitin Dimers. *J. Am. Chem. Soc.* **2010,** *132* (46), 16337-16339.

20. Schneider, T.; Schneider, D.; Rösner, D.; Malhotra, S.; Mortensen, F.; Mayer, T. U.; Scheffner, M.; Marx, A., Dissecting Ubiquitin Signaling with Linkage-Defined and Protease Resistant Ubiquitin Chains. *Angew. Chem. Int. Ed.* **2014,** *53* (47), 12925-12929.

21. Hameed, D. S.; Sapmaz, A.; Ovaa, H., How Chemical Synthesis of Ubiquitin Conjugates Helps To Understand Ubiquitin Signal Transduction. *Bioconjugate Chem.* **2016,** *28*, 805-815.

22. Trang, V. H.; Valkevich, E. M.; Minami, S.; Chen, Y.-C.; Ge, Y.; Strieter, E. R., Nonenzymatic Polymerization of Ubiquitin: Single-Step Synthesis and Isolation of Discrete Ubiquitin Oligomers. *Angew. Chem. Int. Ed.* **2012,** *51* (52), 13085-13088.

23. Gururaja, T. L.; Pray, T. R.; Lowe, R.; Dong, G.; Huang, J.; Daniel-Issakani, S.; Payan, D. G., A Homogeneous FRET Assay System for Multiubiquitin Chain Assembly and Disassembly. In *Methods Enzymol.*, Raymond, J. D., Ed. Academic Press: 2005; Vol. Volume 399, pp 663-682.

24. Yang, L.-L.; Kao, M.; Chen, H.-L.; Lim, T.-S.; Fann, W.; Chen, R., Observation of protein folding/unfolding dynamics of ubiquitin trapped in agarose gel by single-molecule FRET. *Eur. Biophys. J.* **2012,** *41* (2), 189-198.

25. Kao, M. W.-P.; Yang, L.-L.; Lin, J. C.-K.; Lim, T.-S.; Fann, W.; Chen, R. P. Y., Strategy for Efficient Site-Specific FRET-Dye Labeling of Ubiquitin. *Bioconjugate Chem.* **2008,** *19* (6), 1124-1126.

26. Trang, V. H.; Rodgers, M. L.; Boyle, K. J.; Hoskins, A. A.; Strieter, E. R., Chemoenzymatic Synthesis of Bifunctional Polyubiquitin Substrates for Monitoring Ubiquitin Chain Remodeling. *Chembiochem : a Eur. J. Chem. Biol.* **2014,** *15* (11), 1563-1568.

27. Li, Y.-M.; Li, Y.-T.; Pan, M.; Kong, X.-Q.; Huang, Y.-C.; Hong, Z.-Y.; Liu, L., Irreversible Site-Specific Hydrazinolysis of Proteins by Use of Sortase. *Angew. Chem.* **2014,** *126* (8), 2230-2234.

28. Williamson, D. J.; Fascione, M. A.; Webb, M. E.; Turnbull, W. B., Efficient N-Terminal Labeling of Proteins by Use of Sortase. *Angew. Chem. Int. Ed.* **2012,** *51* (37), 9377-9380.

29. Antos, J. M.; Chew, G.-L.; Guimaraes, C. P.; Yoder, N. C.; Grotenbreg, G. M.; Popp, M. W.-L.; Ploegh, H. L., Site-Specific N- and C-Terminal Labeling of a Single Polypeptide Using Sortases of Different Specificity. *J. Am. Chem. Soc.* **2009,** *131* (31), 10800-10801.

30. Witte, M. D.; Theile, C. S.; Wu, T.; Guimaraes, C. P.; Blom, A. E. M.; Ploegh, H. L., Production of unnaturally linked chimeric proteins using a combination of sortase-catalyzed transpeptidation and click chemistry. *Nat. Protoc.* **2013,** *8* (9), 1808-1819.

31. Claessen, J. H. L.; Witte, M. D.; Yoder, N. C.; Zhu, A. Y.; Spooner, E.; Ploegh, H. L., Catch-and-Release Probes Applied to Semi-Intact Cells Reveal Ubiquitin-Specific Protease Expression in Chlamydia trachomatis Infection. *Chembiochem* **2013,** *14* (3), 343-352.

32. Swee, L. K.; Guimaraes, C. P.; Sehrawat, S.; Spooner, E.; Barrasa, M. I.; Ploegh, H. L., Sortase-mediated modification of αDEC205 affords optimization of antigen presentation and immunization against a set of viral epitopes. *Proc. Natl. Acad. Sci. USA* **2013,** *110* (4), 1428-1433.

33. David Row, R.; Roark, T. J.; Philip, M. C.; Perkins, L. L.; Antos, J. M., Enhancing the efficiency of sortase-mediated ligations through nickel-peptide complex formation. *Chem. Commun.* **2015**.

34. Mazmanian, S. K.; Liu, G.; Ton-That, H.; Schneewind, O., Staphylococcus aureus Sortase, an Enzyme that Anchors Surface Proteins to the Cell Wall. *Science* **1999,** *285* (5428), 760-763.

35. Ton-That, H.; Liu, G.; Mazmanian, S. K.; Faull, K. F.; Schneewind, O., Purification and characterization of sortase, the transpeptidase that cleaves surface proteins of Staphylococcus aureus at the LPXTG motif. *Proc. Natl. Acad. Sci. USA* **1999,** *96* (22), 12424-12429.

36. Williamson, D. J.; Webb, M. E.; Turnbull, W. B., Depsipeptide substrates for sortase-mediated N-terminal protein ligation. *Nat. Protoc.* **2014,** *9* (2), 253-262.

37. Lu, Y.; Lee, B.-h.; King, R. W.; Finley, D.; Kirschner, M. W., Substrate degradation by the proteasome: A single-molecule kinetic analysis. *Science* **2015,** *348* (6231).

38. Lu, Y.; Wang, W.; Kirschner, M. W., Specificity of the anaphase-promoting complex: A single-molecule study. *Science* **2015,** *348* (6231).

39. Meyer, H.-J.; Rape, M., Enhanced Protein Degradation by Branched Ubiquitin Chains. *Cell* **2014,** *157* (4), 910-921.

40. Nakasone, Mark A.; Livnat-Levanon, N.; Glickman, Michael H.; Cohen, Robert E.; Fushman, D., Mixed-Linkage Ubiquitin Chains Send Mixed Messages. *Structure* **2013,** *21* (5), 727-740.

41. Faesen, Alex C.; Dirac, Annette M. G.; Shanmugham, A.; Ovaa, H.; Perrakis, A.; Sixma, Titia K., Mechanism of USP7/HAUSP Activation by Its C-Terminal Ubiquitin-like Domain and Allosteric Regulation by GMP-Synthetase. *Mol. Cell 44* (1), 147-159.

42. Faesen, Alex C.; Luna-Vargas, Mark P. A.; Geurink, Paul P.; Clerici, M.; Merkx, R.; van Dijk, Willem J.; Hameed, Dharjath S.; El Oualid, F.; Ovaa, H.; Sixma, Titia K., The Differential Modulation of USP Activity by Internal Regulatory Domains, Interactors and Eight Ubiquitin Chain Types. *Chem. Biol.* **2011,** *18* (12), 1550-1561.

43. Ritorto, M. S.; Ewan, R.; Perez-Oliva, A. B.; Knebel, A.; Buhrlage, S. J.; Wightman, M.; Kelly, S. M.; Wood, N. T.; Virdee, S.; Gray, N. S.; Morrice, N. A.; Alessi, D. R.; Trost, M., Screening of DUB activity and specificity by MALDI-TOF mass spectrometry. *Nat. Commun.* **2014,** *5*.

44. Hospenthal, M. K.; Freund, S. M. V.; Komander, D., Assembly, analysis and architecture of atypical ubiquitin chains. *Nat. Struct. Mol. Biol.* **2013,** *20* (5), 555-565.

45. Valkevich, E. M.; Sanchez, N. A.; Ge, Y.; Strieter, E. R., Middle-Down Mass Spectrometry Enables Characterization of Branched Ubiquitin Chains. *Biochemistry* **2014,** *53* (30), 4979-4989.

46. Cornelissen, T.; Haddad, D.; Wauters, F.; Van Humbeeck, C.; Mandemakers, W.; Koentjoro, B.; Sue, C.; Gevaert, K.; De Strooper, B.; Verstreken, P.; Vandenberghe, W., The deubiquitinase USP15 antagonizes Parkin-mediated mitochondrial ubiquitination and mitophagy. *Hum. Mol. Genet.* **2014,** *23* (19), 5227-5242.

47. Cunningham, C. N.; Baughman, J. M.; Phu, L.; Tea, J. S.; Yu, C.; Coons, M.; Kirkpatrick, D. S.; Bingol, B.; Corn, J. E., USP30 and parkin homeostatically regulate atypical ubiquitin chains on mitochondria. *Nat. Cell Biol.* **2015,** *17* (2), 160-169.

48. Ordureau, A.; Sarraf, Shireen A.; Duda, David M.; Heo, J.-M.; Jedrychowski, Mark P.; Sviderskiy, Vladislav O.; Olszewski, Jennifer L.; Koerber, James T.; Xie, T.; Beausoleil, Sean A.; Wells, James A.; Gygi, Steven P.; Schulman, Brenda A.; Harper, J. W., Quantitative Proteomics Reveal a Feedforward Mechanism for Mitochondrial PARKIN Translocation and Ubiquitin Chain Synthesis. *Mol. Cell* **2014,** *56* (3), 360-375.

49. Ordureau, A.; Heo, J.-M.; Duda, D. M.; Paulo, J. A.; Olszewski, J. L.; Yanishevski, D.; Rinehart, J.; Schulman, B. A.; Harper, J. W., Defining roles of PARKIN and ubiquitin phosphorylation by PINK1 in mitochondrial quality control using a ubiquitin replacement strategy. *Proc. Natl. Acad. Sci. USA* **2015,** *112* (21), 6637-6642.

2.6 Supplemental information

2.6.1. Synthesis of Precursor for Depsipeptide.

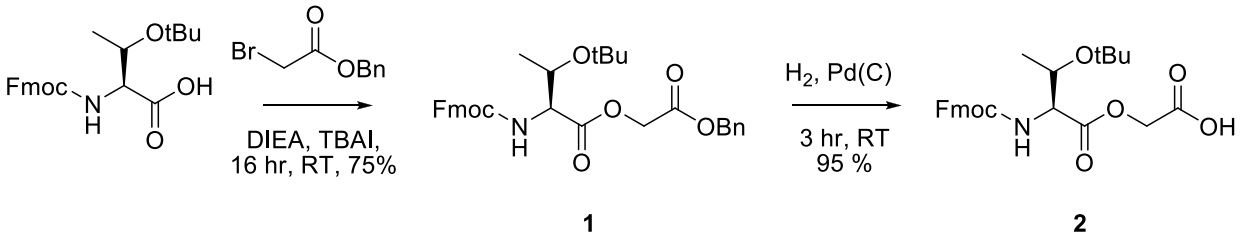

*2.6.1.a. Fmoc-Thr(OtBu)-OGly-OBz (**1**)*

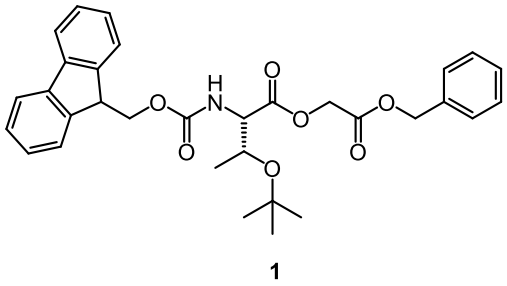

Compound **1** was synthesized according to the protocol described by Williamson et al.[1, 2] Triethylamine (2.4 mL, 16 mmol) was added to a stirring solution of Fmoc-Thr(OtBu)-OH (5.3 g, 13 mmol), benzyl-2-bromoacetate (3.2 mL, 20.5 mmol), and tetrabutylammonium iodide (1.9 g, 5.2 mmol) in 20 mL THF. The reaction was allowed to stir overnight at room temperature. The resultant yellow solution was diluted into 200 mL of water and extracted with ethyl acetate (2 x 200 mL). The combined organic fractions were then washed with 10 % sodium thiosulfate (2 x 200 mL), brine (2 x 200 mL), and dried over $MgSO_4$. The solvent was removed using a rotary evaporator yielding a viscous oil. The crude oil was purified by flash column chromatography (silica, 4:1 hexanes: ethyl acetate) yielding 5.4 g of **1** (75 %) as a white solid. ^{1}H NMR (400 MHz, Chloroform-*d*) δ 7.76 (d, *J* = 7.5 Hz, 2H), 7.63 (t, *J* = 7.4 Hz, 2H), 7.39 (t, *J* = 7.6 Hz, 2H), 7.36 – 7.28 (m, 7H), 5.63 (d, *J* = 9.5 Hz, 1H), 5.19 (s, 2H), 4.76 (d, *J* = 15.9 Hz, 1H), 4.65 (d, *J* = 15.9 Hz, 1H), 4.46 – 4.34 (m, 3H), 4.32 – 4.23 (m, 2H), 1.25 (d, *J* = 6.2 Hz, 3H), 1.14 (s, 8H).

^{13}C NMR (101 MHz, $CDCl_3$) δ 170.54, 167.02, 156.64, 144.05, 141.30, 128.65, 127.68, 127.07, 125.20, 119.96, 74.25, 67.27, 61.26, 59.81, 47.20, 28.43, 20.93.

HRMS (ESI) calculated for $C_{32}H_{39}N_2O_7^+$ $[M+NH_4]^+$ 563.2752, found 563.2752.

*2.6.1.b Fmoc-Thr(OtBu)-OGly-OH (**2**)*

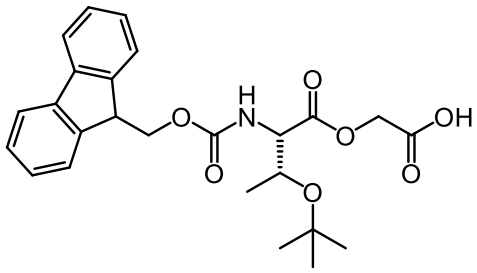

2

Compound **2** was synthesized using a modified procedure of the protocol described by Williamson et al.[1, 2] Compound **1** (2.0 g, 3.6 mmol) was dissolved in 40 mL of a 3:1 mixture of THF and water. To this solution Pd/C (0.2 g, 10 % wt) was added and the reaction was placed under a N_2 atmosphere. The flask was then evacuated and replaced with a H_2 atmosphere. The mixture was allowed to stir at room temperature with careful monitoring by TLC (2:1 hexanes: ethyl acetate). Once the consumption of the starting material was observed, the reaction atmosphere was immediately replaced with N_2 before being opened to the atmosphere. The mixture was then filtered over a plug of celite to remove the catalyst. The plug was further washed with THF (3 x 100 mL), and the organic solvent was removed using a rotary evaporator resulting in a clear oil. The oil was dissolved in ethyl acetate (200 mL), washed with 5 % HCl (2 x 50 mL), brine (1 x 50 mL), dried over $MgSO_4$ and the solvent removed using a rotary evaporator yielding a foamy solid. This solid was resuspended in 10 mL of water and lyophilized to yield 1.5 g of **2** as a white crystalline solid. ^{1}H NMR (400 MHz, Chloroform-*d*) δ 7.77 (d, *J* = 7.5 Hz, 2H), 7.61 (dd, *J* = 7.6, 3.7 Hz, 2H), 7.41 (t, *J* = 7.5 Hz, 2H), 7.36 – 7.28 (m, 2H), 5.62 (d, *J* = 8.6 Hz, 1H), 4.91 (d, *J* = 16.3 Hz, 1H), 4.64 (d, *J* = 16.3 Hz, 1H), 4.42 (td, *J* = 5.8, 4.7, 3.0 Hz, 2H), 4.30 – 4.21 (m, 2H), 1.21 (s, 9H).

^{13}C NMR (126 MHz, $CDCl_3$) δ 171.47, 170.23, 156.84, 143.89, 143.67, 141.30, 127.73, 127.09, 125.17, 119.98, 74.77, 67.40, 67.26, 60.86, 47.13, 30.32, 28.32, 20.43.

HRMS (ESI) calculated for $C_{25}H_{33}N_2O_7^+$ $[M+NH_4]^+$ 473.2282, observed 473.2281.

2.6.2 Synthesis of 5-Carboxytetramethyl rhodamine (TAMRA).

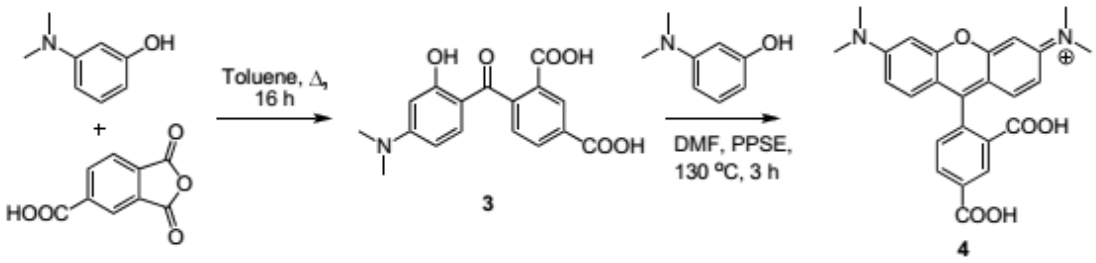

*2.6.2.a. 4-(4-(dimethylamino)-2-hydroxybenzoyl)isophthalic acid (**3**).*

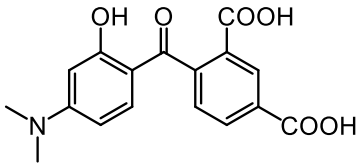

Compound **3** was synthesized according to the protocol reported by Kvach et al.[3] 3-dimethylamino phenol (13.7 g, 100 mmol) was dissolved in 300 mL of toluene with gentle heating and trimellitic anhydride (23.3 g, 120 mmol) was added. The resulting solution was allowed to reflux for 24 h. The solution was cooled, and the resultant residue was filtered and washed with toluene. The solid was dissolved in 300 mL of MeOH and heated to reflux for 10 min followed by the addition of 100 mL of acetic acid. Solvent was removed under reduced pressure yielding a purple solid of mixed isomers. This solid was resuspended in 200 mL of MeOH and allowed to reflux for 2 hours followed by cooling at 4 °C overnight. The resulting solid was filtered and washed with chilled MeOH yielding pure **3** as a purple solid (4.0 g, 12.2 %). ^{1}H NMR (400 MHz, DMSO-d_6) δ 13.48 (s, 2H), 12.43 (s, 1H), 8.55 (d, *J* = 1.7 Hz, 1H), 8.27 (dd, *J* = 7.9, 1.7 Hz, 1H), 7.59 (d, *J* = 7.9 Hz, 1H), 6.87 (d, *J* = 9.1 Hz, 1H), 6.28 (dd, *J* = 9.2, 2.5 Hz, 1H), 6.18 (d, *J* = 2.4 Hz, 1H), 3.08 (s, 6H). ^{13}C NMR (101 MHz, DMSO) δ 198.10, 166.57, 164.68, 156.30, 144.21, 134.27, 133.16, 132.11,

131.16, 130.47, 128.74, 109.91, 104.99, 97.48. HRMS (ESI-) calculated for $C_{17}H_{14}NO_6^-$ $[M-H]^-$ 328.0826, found 328.0831.

*2.6.2.b. 5-CarboxyTAMRA (**4**).*

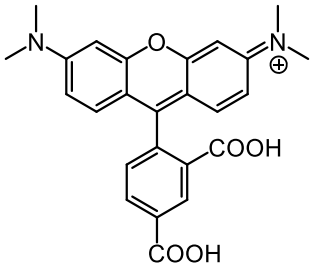

Compound **4** was synthesized according to the procedure described by Kvach et al.[3] To a solution of **3** (3.8 g, 11.7 mmol) and dimethylamino phenol (2.1 g, 15.2 mmol) in DMF (44 mL) was added trimethylsilylpolyphosphite (10 g as a 1 g/mL solution in chloroform). The solution was then heated to 130 ^oC for 3.5 h and the solvent was removed under reduced pressure yielding a purple solid. The solid was dissolved in 5 % NaOH (82 mL) and stirred overnight. The solution was diluted with 175 mL of water and acidified by the addition of 5.9 mL of conc. HCl. The resulting solid was filtered, washed with water, and allowed to dry yielding **4** as a purple-brown solid (4.4 g, 87 %). ^1H NMR (400 MHz, Methanol-d_4) δ 8.74 (d, *J* = 1.7 Hz, 1H), 8.22 (dd, *J* = 7.8, 1.8 Hz, 1H), 7.34 (d, *J* = 7.8 Hz, 1H), 7.15 (d, *J* = 9.4 Hz, 2H), 6.98 (dd, *J* = 9.5, 2.5 Hz, 2H), 6.88 (d, *J* = 2.5 Hz, 2H), 3.23 (s, 12H).

^{13}C NMR (126 MHz, MeOD) δ 169.90, 169.00, 160.98, 158.49, 158.27, 137.65, 134.85, 132.11, 132.05, 131.83, 130.56, 114.69, 114.20, 96.82, 40.31.

HRMS (ESI) Calculated for $C_{25}H_{23}N_2O_5^+$ $[M]^+$ 431.1602, found 431.1588.

2.6.3. Solid Phase Peptide Synthesis

2.6.3.a. Reagents and Equipment

All Fmoc protected amino acids, coupling reagents, and Fmoc-Gly-Wang resin (0.62mmol/g) were purchased from Chem-Impex International and used without further purification. Reactions were performed in fritted polypropylene tubes (Grace and Co.). Coupling and deprotection reactions were performed in a MARS multimode microwave reactor (CEM) using microwave assisted solid-phase reaction conditions adapted from the procedure described in Horne et al.[4] Depsipeptide precursor **2** was incorporated into peptides using the standard coupling conditions described below.

2.6.3.b General Fmoc Deprotection Protocol

Fmoc-Gly-Wang resin (0.16 g, 100 µM) and a magnetic stir bar were added to a polypropylene reaction vessel and the resin was allowed to swell in DMF for 30 min while stirring. The solvent was aspirated from the reaction vessel and 20 % piperidine in DMF (3 mL) was added. The tube was then placed into the microwave. Deprotections were carried out at 80 ^{o}C in the microwave (2 min ramp to 80 ^{o}C, 2 min hold at 80 ^{o}C). Upon completion of the reaction, the piperidine mixture was removed by filtration, and the resin was washed with DMF (3 x 5 mL).

2.6.3.c. General Coupling Protocol

Fmoc protected amino acid (400 µmol, 4 eq), HCTU (370 µmol, 3.7 eq), Cl-HOBt (400 µmol, 4 eq), and diisopropylethylamine (800 µmol, 8 eq) were dissolved in DMF (3 mL), and vortexed until the amino acid was fully dissolved, and a color change was observed. The activated amino acid solution was then added to the reaction vessel containing the resin and the vessel was placed in the microwave reactor. Couplings were performed at 70 ^{o}C in the microwave (2 min ramp to 70 ^{o}C, 4 min hold at 70 ^{o}C). Upon completion of the reaction, the activated amino acid mixture was removed by filtration, and the resin was washed with DMF (3 x 5 mL).

2.6.3.d. Peptide Elongation

Peptides were elongated by performing couplings and deprotections as described above in an alternating fashion until all the desired sequence had been achieved.

2.6.3.e. Peptide Cleavage and Purification

After the final coupling step, the resin was washed with DMF (3 x 5 mL), CH_2Cl_2 (3 x 5 mL), MeOH (3 x 5 mL), and the resin was allowed to dry. Upon drying the resin was stored at -20 ^oC until cleavage was performed. Cleavage was performed by stirring the resin in 4 mL of a cocktail containing 95:2.5:2.5 TFA:H_2O:Triisopropylsilane for 2 h at room temperature after which the resin was filtered and washed with TFA (2 x 2 mL). The mixture was concentrated to < 2 mL under a stream of N_2 and the crude peptide was precipitated by the addition of 30 mL of cold diethyl ether. The precipitated peptide was pelleted at 3000 x g for 10 minutes and the ether was decanted. The peptide was further washed by re-suspending in ice cold ether (25 mL) followed by centrifugation at 3000 x g for ten minutes and decanting the liquid 3 more times. Further purification was performed using semi-preparative reverse- phase HPLC on a C-18 column (solvent A = 0.05 % TFA in H_2O, solvent B = 0.05% TFA in ACN) as described below. Peptide identity was confirmed by ESI-MS.

*2.6.3.f. Fluorescein-Ala-Leu-Pro-Glu-Thr-OGly-Gly-OH (Depsipeptide **I**)*

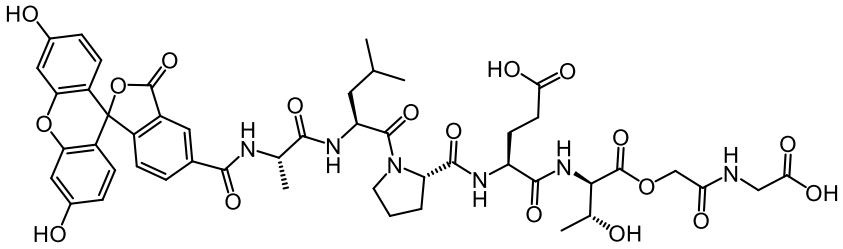

I

Depsipeptide **I** was purified using semi-prep HPLC using a linear gradient of 35 % to 45 % B. Fractions containing **I** were identified by MALDI-TOF MS, frozen and lyophilized yielding **I** as a yellow powder. HRMS (ESI) calculated for $C_{48}H_{55}N_6O_{18}^+$ $[M+H]^+$ 1003.3567, observed 1003.3582.

*2.g.3.g. TAMRA-Ala-Leu-Pro-Glu-Thr-OGly-Gly-OH (Depsipeptide **II**)*

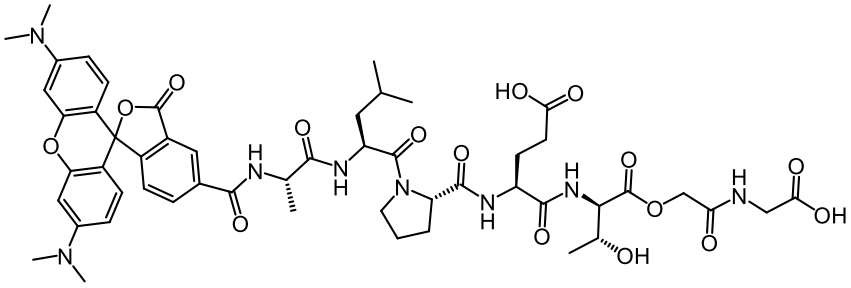

II

Depsipeptide **II** was precipitated from ether, dissolved in water, lyophilized and used without further purification. HRMS (ESI) calculated for $C_{52}H_{64}N_8O_{16}^+$ $[M+2H]^{2+}$ 529.2293, observed 529.2287.

2.6.4 Protein Expression and Purification

2.6.4.a. Expression and Purification of His_6SrtAΔN25

Purification of His_6SrtAΔN25 (SrtA) was adapted from the procedure outlined by Williamson et al.[1, 2] The cDNA for *S. Aureus* His_6SrtAΔN25 cloned intopQE30 was a generous gift from Professor Schneewind.[5, 6] SrtA was overexpressed in *E. coli* BL21 (DE3) cells at 16 °C for 16 h after induction with 400 µM IPTG at an OD_{600} of 0.6. Cells were pelleted at 5000 x g for 20 min, resuspended in 120 mL of lysis buffer (50 mM Tris, 150 mM NaCl, 10 % glycerol, pH 7.5), and lysed by sonication. Cell lysate was clarified at 30,000 x g for 20 min and His_6 tagged SrtA was applied to Co^{2+} resin pre-equilibrated with lysis buffer. The resin was washed with 25 mL of lysis buffer, 25 mL of high salt lysis buffer (lysis buffer + 500 mM salt), 25 mL lysis buffer containing 50 mM imidazole, and eluted with 35 mL of lysis buffer containing 300 mM imidazole collecting 5 mL fractions. SrtA containing fractions were further purified using a Superdex 75 HiLoad size exclusion column and isocratically eluted with 50 mM HEPES, 150 mM NaCl, and 10 mM $CaCl_2$, pH 7.5. Fractions

were analyzed by SDS-PAGE and SrtA containing fractions were concentrated using a 10,000 MWCO centrifugal filter (Millipore). A 50 % glycerol in water solution was added to the concentrated protein to a final concentration of 10 % glycerol prior to aliquoting and freezing. Protein concentration was measured using BCA assay and estimated to be 3 mg/mL (142 μM).

2.6.4.b. Expression and Purification of AIA His_7TEVΔ238.

Purification of AIA His_7TEVΔ238 (TEV protease) was adapted from the protocol described by Blommel and Fox.[7] TEV protease was overexpressed in *E. coli* BL21 (DE3) cells at 16 °C for 16 h after induction with 300 μM IPTG at an OD_{600} of 0.6. Cells were pelleted at 5000 x g for 20 min, re-suspended in 120 mL of lysis buffer (50 mM Tris, 400 mM NaCl, 20 mM imidazole, 1 mM TCEP, 1 mM benzamidine, pH 7.5), and lysed by sonication. Cell lysate was clarified at 30,000 x g for 20 min and His_7 tagged TEV was applied to Co^{2+} resin pre-equilibrated with lysis buffer. The resin was washed with 25 mL of lysis buffer, 25 mL of wash buffer (lysis buffer containing 50 mM imidazole) and eluted with 35 mL of elution buffer (lysis buffer containing 300 mM imidazole) collecting 5 mL fractions. TEV protease containing fractions were identified by SDS-PAGE, and buffer exchanged into 50 mM Tris, 2 mM DTT pH 7.6, and glycerol was added to a final concentration of 50% before aliquoting and freezing. Protein concentration was estimated by BCA assay to be approximately 2.3 mg/mL (96 μM).

2.6.4.c. General Protocol for Expression of Ubiquitin Mutants

The general protocol for ubiquitin expression and purification is adapted from the methods outlined by Pickart and Raasi.[8] All ubiquitin K-to-C mutants used were cloned into the pET22b vector using Nde1 and Not1 restriction sites without any affinity tags as described in Valkevich et al.[9] The following forward primer was used for the incorporation of the TEVGly_5 sequence for all ubiquitin mutants, TATACATATGGAAAACCTGTATTTTCAGGGCGGTGGCGGTGGTATGCAGATCTTCGTC. Proteins were over-expressed in *E. coli* Rosetta (DE3) cells grown in 2XYT media. Cells were grown at 37 °C to an OD_{600} between 0.5 and 0.9, expression was induced with 300 μM IPTG, and expression was allowed to proceed for 4 h at

37 °C. Cells were pelleted at 5000 x g, resuspended in 120 mL of Ub lysis buffer (50 mM Tris, 5 mM EDTA, 1 mM EGTA, 1 mM PMSF, 1 mM DTT, 0.02 % IGPAL, pH 7.5), and lysed by sonication. Cell lysate was clarified at 8000 x g for 20 min, and proteins were precipitated by the addition of 1.2 mL of 70 % perchloric acid. Precipitated proteins were centrifuged at 8000 x g for 20 min, and the soluble portion was dialyzed against buffer A (50 mM NH_4OAc, 2 mM EDTA, 1 mM DTT, pH 4.4). Dialyzed protein was then applied to Sepharose Fast Flow MonoS resin pre-equilibrated with buffer A. The resin was washed with 25 mL of 5 % buffer B ((50 mM NH_4OAc, 2 mM EDTA, 1 mM DTT, 1 M NaCl, pH 4.4), 25 mL of 10 % buffer B, and protein was eluted using 50 mL 25 % buffer B. Fractions containing ubiquitin as determined by SDS-PAGE were collected, buffer exchanged into water, concentrated, and lyophilized.

2.6.5 Generation and Mass Spectrometric Characterization of Ubiquitin Chains

2.6.5.a. General Protocol for Generation of Ub Allylamine (Ub-AA)

Reactions were performed as described previously by Valkevich et al.[9] $TEVGly_5UbD77$ (800 μM), allylamine (250 mM), and YUH1 (250 nM) were dissolved in a buffer containing 50 mM HEPES (pH 8, final pH ~10 after adding allylamine), 1 mM EDTA, 30 % DMSO, and the reaction was agitated for 2 h at room temp. TFA was added to a final pH of 1-2 and the reaction was frozen and thawed. Precipitated Yuh1 was pelleted at 3000 x g and the reaction was diluted with buffer A to a concentration of 5 % DMSO. This solution was dialyzed against buffer A. The dialyzed protein was concentrated and purified on a MonoS column (GE healthcare). Fractions containing Ub-AA were identified by MALDI-TOF-MS, concentrated, and exchanged into water and lyophilized.

2.6.5.b. General Protocol for Thiol-Ene Ub Dimer Generation

Reactions were performed as described previously.[9] $TEVGly_5$Ub-AA (1 mM) $TEVGly_5$KxCD77 (1 mM; where x is the lysine position that has been mutated), and lithium phenyl-2,4,6-trimethylbenzoylphosphinate (LAP; 1 mM) were dissolved in a 250 mM NaOAc buffer pH 5.1 (2 mL reaction volume in 20 - 100 μL

reaction aliquots) and the samples were placed on ice. Chilled samples were irradiated with 365 nm light for 30 min using an OmniCure series 1500 light source. Samples were concentrated to a volume of 1 mL and purified using a Superdex highload 75 size exclusion column (GE healthcare) by eluting with Ub SEC buffer (50 mM Tris, 300 mM NaCl, 1 mM EDTA, 1 mM DTT). Fractions were analyzed by SDS-PAGE gel and dimer-containing fractions were concentrated and exchanged into water prior to lyophilization.

2.6.5.c. General Protocol for Thiol-Ene Ub Chain Generation.

Reactions were performed as described previously.[10] TEVGly5K63C Ub-AA(2 mM) and LAP (1 mM) were dissolved in a 250 mM NaOAc buffer pH 5.1 (3 mL reaction volume in 30 - 100 μL aliquots) and samples were placed on ice. Chilled samples were irradiated with 365 nm light for 30 min using an OmniCure series 1500 light source. Samples were concentrated to a volume of 1 mL and purified using a Superdex highload 75 SEC column (GE healthcare) by eluting with Ub SEC buffer. Fractions were analyzed by SDS-PAGE and fractions containing oligomers of different lengths were identified, concentrated, and exchanged into water prior to lyophilization.

2.6.5.d. Synthesis of Lys6/Lys48 Native Branched Trimer

Native branched chains were prepared as described previously.[11] Synthesis of the native branched trimer was carried out in a 1 mL reaction. UbD77 (1 mM) K6/48R Ub (2 mM), E1 (150 nM), UBE2L3 (2 μM), and NleL (1 μM) were mixed in ubiquitination buffer (40 mM Tris pH 7.5, 50 mM NaCl, 10 mM $MgCl_2$, 10 mM ATP, and 6 mM DTT) and the reaction was allowed to proceed overnight at 37 ^{o}C. Subsequently, the reaction was quenched by lowering the pH to <5 via addition of 5 M NH_4OAc pH 4.4. Enzymes were then precipitated through multiple freeze thaw cycles. The resulting supernatant was filtered and separated on a Superdex highload 75 SEC column (GE healthcare) by eluting with Ub SEC buffer. Fractions were analyzed by SDS-PAGE and the fractions containing trimer were pooled, concentrated and exchanged into water before lyophilization.

2.6.5.e. Synthesis of Lys6/Lys48 Native Branched Trimer containing a Gly5 Base.

This branched trimer was synthesized as described above using TEVGly5 UbD77 as the base and K6/48RUb as the distal subunits. For a 625 µL reaction, TEVGly5 UbD77 (1 mM) K6/48R Ub (2 mM), E1 (150 nM), UBE2L3 (2 µM), and NleL (1 µM) were mixed in ubiquitination buffer (40 mM Tris pH 7.5, 50 mM NaCl, 10 mM $MgCl_2$, 10 mM ATP, and 6 mM DTT) and the reaction was allowed to proceed overnight at 37 ^oC. The resulting precipitated protein was removed by centrifugation at 16,000 x g for 10 min, and the pH of the supernatant was increased to a pH of 8 via the addition of 1 M NaOH and incubated overnight with TEV protease at room temperature to expose the N-terminal Gly5 on the base of the trimer, after which the pH was again reduced to <5 via the addition of NH_4OAc and precipitated TEV was removed by centrifugation. The resulting supernatant was filtered and separated on a Superdex highload75 SEC column (GE healthcare) by eluting with Ub SEC buffer. Fractions were analyzed by SDS-PAGE and the fractions containing trimer were pooled, concentrated and exchanged into water before lyophilization.

2.6.5.f. Synthesis of Native Lys6/Lys48 Branched trimers Containing Distal Gly5 Motifs.

Branched trimers containing distal oligoglycine motifs were synthesized in two steps. First, a native Lys48 linked Ub dimer was constructed using the Lys48 linkage-specific conjugating enzyme Ube2R1. UbD77 served as the proximal subunit while K6/48R Ub acts as the distal. In brief, UbD77 (2 mM), K6/48R Ub (2mM), E1 (300 nM), and UBE2R1 (2 µM) were mixed in ubiquitination buffer, and the reaction mixture was incubated overnight at 37 ^oC. Subsequently, the reaction was quenched by lowering the pH to <5 via addition of 5 M NH_4OAc pH 4.4 and enzymes were precipitated by multiple freeze-thaw cycles. The resulting precipitated proteins were removed by centrifugation at 16,000 x g for 10 mins. The supernatant was filtered and separated on a Superdex highload75 SEC column (GE healthcare) eluting with Ub SEC buffer. Fractions were analyzed by SDS-PAGE and the fractions containing dimer were pooled, concentrated and exchanged into water before lyophilization. In the second step, the K6 linked Gly5 containing distal subunit was added by incubating the Lys48-linked dimer described above (1 mM) to

Gly5K6/48R Ub (2.5 mM), E1 (150 nM), UbcH7 (2 μM), and NleL (1μM) in ubiquitination buffer (625 μL reaction volume). The reaction was incubated overnight at 37 ^{o}C after which it was quenched and purified by gel filtration chromatography as described above. Fractions containing trimer were identified by SDS-PAGE, concentrated and exchanged into water prior to lyophilization.

The complementary trimer containing an oligoglycine motif on the Lys48 distal subunit was synthesized as described above by first building a Gly5 containing Lys48-linked dimer via the substitution of K6/48R Ub with Gly5K6/48R Ub. The K6 distal subunit was attached using NleL and substituting K6/48R Ub for Gly5K6/48R Ub.

2.6.5.g. General Procedure for Minimal Trypsinolysis of Branched Trimers

Minimal trypsinolysis was performed as described previously.[12] A 100 μL reaction was performed by incubating 20 μM of the desired branched trimer with 0.5 μg sequencing grade modified trypsin (Promega) in DUB buffer overnight at room temperature. Reactions were quenched by the addition of acetic acid to a final concentration of 10% and were subsequently dialyzed into water using Slide-A-lyzer MINI dialysis unit (3.5 kDa MWCO, Thermo Fisher Scientific Inc.).

2.6.5.h. Middle-Down Mass Spectrometry Analysis

Samples were dissolved in a water/acetonitrile/acetic acid (45:45:10) solution and injected into a 7T linear ion trap/Fourier transform ion cyclotron resonance (LTQ/FT-ICR) hybrid mass spectrometer (Thermo Scientific Inc.) equipped with an automated chip-based nanoESI source (Triversa NanoMate, Advion BioSciences, Ithaca, NY). The resolving power of the FT-ICR mass analyzer was set at 200000. All FT-ICR spectra were processed with in-house software (MASH Suite)[13] using a signal-to-noise threshold of 3 and a fit factor of 60% and then validated manually.

2.6.5.i. Electron Capture Dissociation (ECD) Analysis of Ub Chain Linkages

For tandem mass spectrometry (MS/MS) experiments using ECD, individual charge states of protein molecular ion were first isolated. Then, the ions were dissociated by ECD using 5% "electron energy" and a 70 ms duration. All FT-ICR spectra were processed with the MASH software suite using a signal-to-noise threshold of 3 and a fit factor of 60% and then validated manually. The resulting mass lists were further assigned on the basis of the protein sequence of Ub with or without the diglycine (GG) modification at each lysine using a tolerance of 10 ppm for precursor and fragment ions. All reported calculated (calc'd) and experimental (expt'l) values correspond to the most abundant molecular weights.

2.6.6 Sortase Labeling and DUB Assays

2.6.6.a. General Protocol for Sortase Labeling and Purification.

TEVGly$_5$K63C Ub$_2$ (20 μM dimer, 40 μM reactive equivalent of Gly$_5$Ub) was incubated with TEV protease for 2 h at room temperature in a buffer containing 50 mM HEPES pH 7.5, 150 mM NaCl, and 10 mM $CaCl_2$. Depsipeptide **I** or **II** (400 μM) and SrtA (20 μM) were added to the mixture and the reaction was incubated at 37 ^oC for 1.5-2 h. Reactions were quenched by the addition of acetic acid until the pH was <4 and peptide was removed and sample buffer exchanged into 50 mM HEPES pH 7.5 using a Zeba™ Spin desalting column (Life Technologies) according to the manufacturer's instructions. The resulting solution was incubated with Ni^{2+} resin for 30 min at 4 ^oC with agitation followed by pelleting of the resin at 800 x g for 5 min to remove His-tagged SrtA and TEV. The supernatant was collected, and subsequent washes were performed using 50 mM HEPES pH 7.5. Fractions were separated on an SDS-PAGE gel, and those containing fluorescent oligomer were pooled and concentrated yielding the fluorescently labeled Ub conjugate.

2.6.6.b. SrtA Time Course Reactions.

TEVGly$_5$K63C Ub$_2$ (20 μM dimer, 40 μM reactive equivalent of Gly$_5$Ub) was incubated with His$_7$TEV protease for 2 h at room temperature in a buffer containing 50 mM HEPES pH 7.5, 150 mM NaCl, and 10 mM $CaCl_2$. To this solution was added depsipeptide **I** (400 μM) and SrtA (20 μM) and the reaction was incubated at 37 °C. Aliquots were removed at specific times and quenched by adding 6x Laemmli loading buffer. Samples were separated on an SDS-PAGE gel and fluorescence visualized using a Typhoon imager (GE Healthcare) employing a blue laser (473 nm) with a (515-545 nm filter). After imaging, the gel was Coomassie stained.

2.6.6.c. Deubiquitination Time Course Assays with USPs.

Deubiquitination assays were carried out in parallel at 37 °C. In each case a 10x solution of the DUB of choice (USP7 or USP15, 1 μM) was preincubated at 37 °C in DUB buffer (50 mM Tris, 150 mM NaCl, pH 7.5) containing 10 mM DTT for 30 min prior to the start of the assay. Reactions were initiated by adding the USP master mix to a final concentration of 100 nM DUB into a solution containing Ub oligomer (10 μM) in DUB buffer containing 4 mM DTT. Prior to initiating the reaction, an aliquot of the Ub containing mixture was removed and diluted with 6x loading dye. Aliquots were removed at specific times and quenched by adding 6x Laemmli loading buffer. Samples were separated on a 12 % NuPAGE gel (Invitrogen) and fluorescence was detected using a Typhoon imager (GE Healthcare) employing a blue laser (473 nm) with a (515-545 nm filter). After imaging, the gel was Coomassie stained. Progress curves were generated by densitometric analysis of each fluorescence image using ImageJ (NIH). For dimer hydrolysis the band resulting from fluorescent monomer was normalized against the intensity of the starting dimer band at t = 0 min and plotted against time. For branched trimer hydrolysis, the bands resulting from fluorescent dimer and monomer were normalized against the intensity of the starting branched trimer at t = 0 min and plotted against time.

2.6.6.d. Two-Fluorophore Deubiquitination Assays

Deubiquitination assays were carried out at 37 ^{o}C. In each case a 10x solution of the DUB of choice (1 µM USP15, or 10 µM OTUB1) was preincubated at 37 ^{o}C in DUB buffer (50 mM Tris, 150 mM NaCl, pH 7.5) containing 10 mM DTT for 30 min prior to the start of the assay. Reactions were initiated by adding the DUB master mix to a final concentration of 100 nM DUB into a solution containing differentially labeled ubiquitin trimers (5 µM each trimer; 10 µM total timer concentration) in DUB buffer containing 4 mM DTT. Prior to initiation of the reaction, an aliquot of the Ub containing mixture was removed and diluted with 6x loading dye. Aliquots were removed at specific times and quenched by adding 6x Laemmli loading buffer. Samples were separated on a 12 % NuPAGE gel (Invitrogen) and fluorescence was detected using a Typhoon imager (GE Healthcare). Fluorescein was detected using a 473 nm laser with a 515-545 nm filter and TAMRA was detected using a 532 nm laser with a >575 nm filter. After imaging, the gel was Coomassie stained.

2.6.7 Supplementary Figures

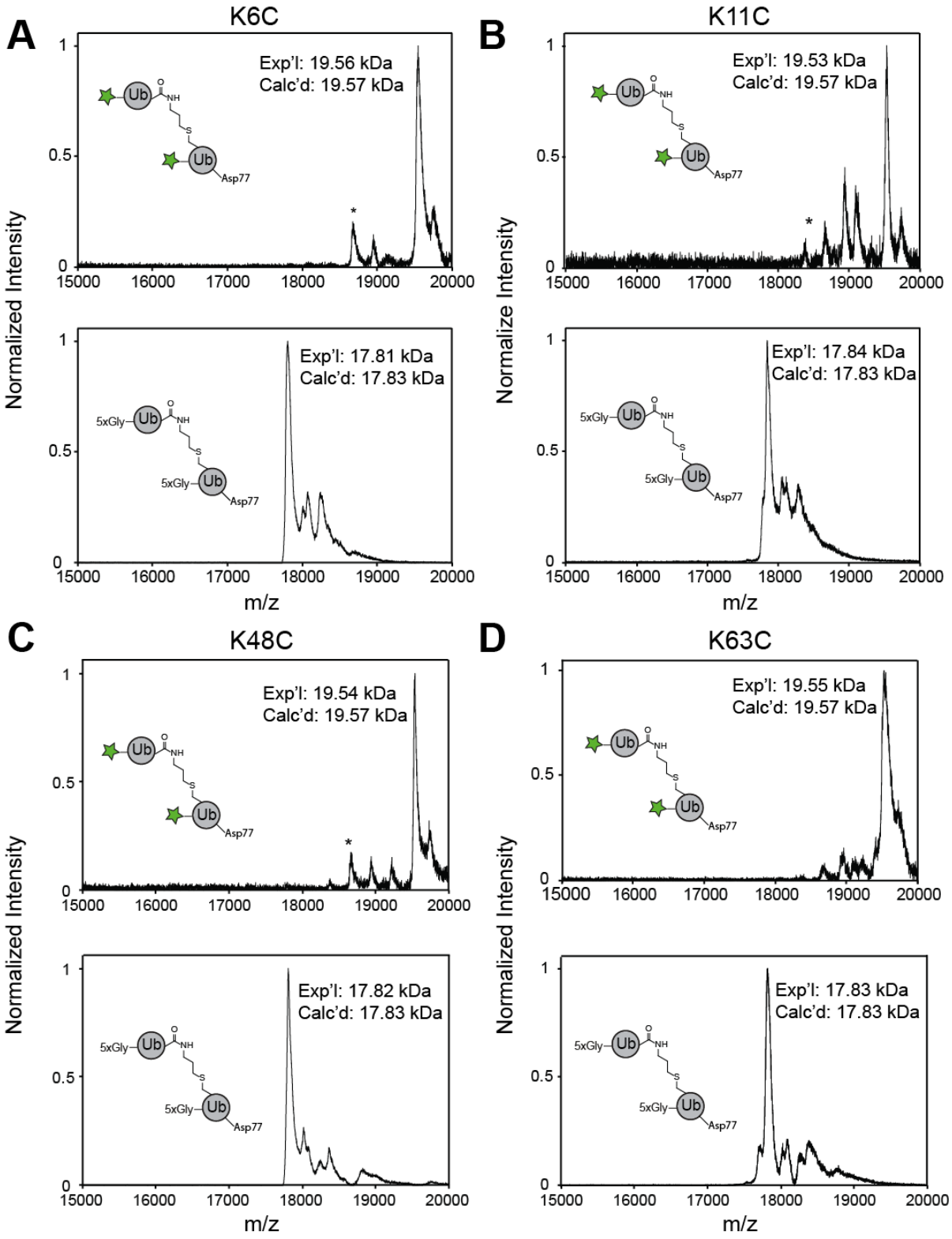

Figure 2. S.1: **MALDI-TOF MS for dimers coupled to depsipeptide I**. **A**) K6C linked Ub. **B**) K11C linked Ub. **C**) K48C linked Ub. The top panels in each set show MALDI-TOF MS data for the labeled dimers. The bottom panels show MALDI-TOF MS data for the unlabeled starting materials. * denotes the singly labeled species.

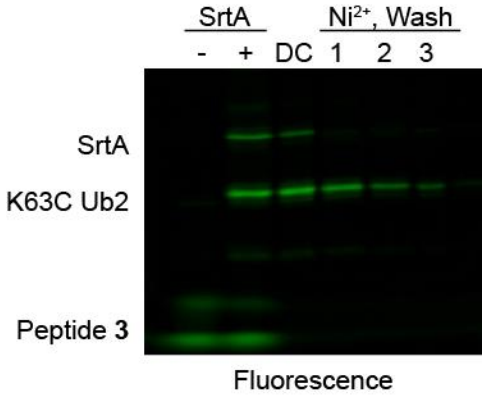

Figure 2. S.2: General strategy for the isolation of fluorescent Ub chains. Reactions were performed as described in the methods. After 90 min, reactions were quenched by the addition of 10 % acetic acid. Peptides were removed, and the solution was buffer exchanged into 50 mM HEPES pH 7.5 using a desalting column (DC). SrtA was removed using Ni^{2+} affinity chromatography.

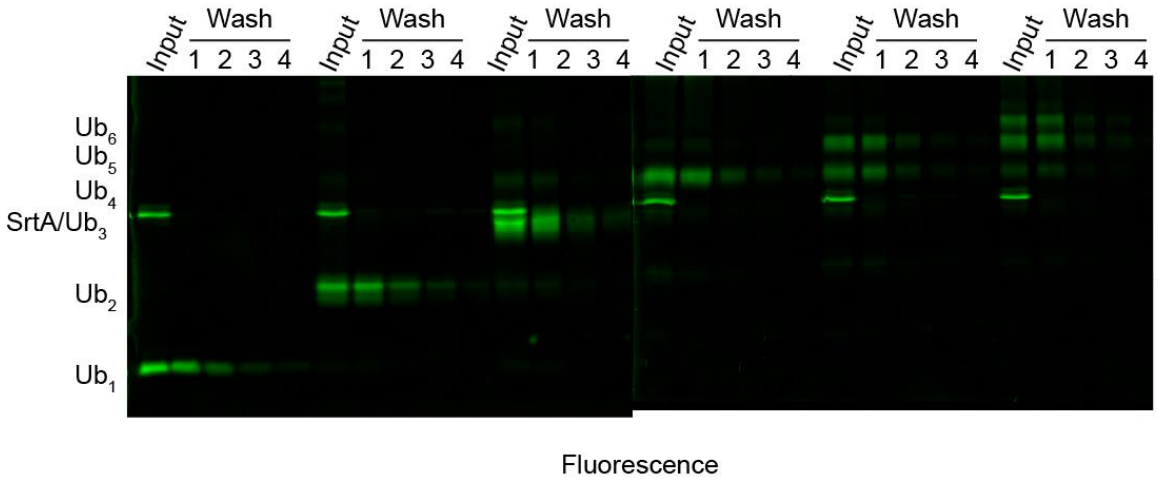

Figure 2. S.3: Purification of ubiquitin oligomers labeled with depsipeptide I. Fluorescence gel showing the purification of chains from SrtA using Ni^{2+} affinity chromatography. Washes containing Ub oligomers were pooled and concentrated.

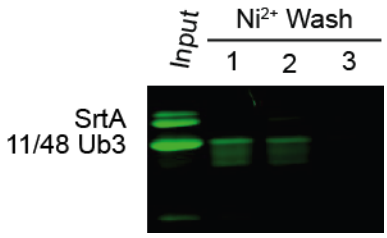

Figure 2. S.4: Isolation of K11/48C branched trimer labeled with depsipeptide I. Fluorescence gel showing the purification of branched chains from SrtA using Ni^{2+} affinity chromatography. Washes containing Ub oligomers were pooled and concentrated.

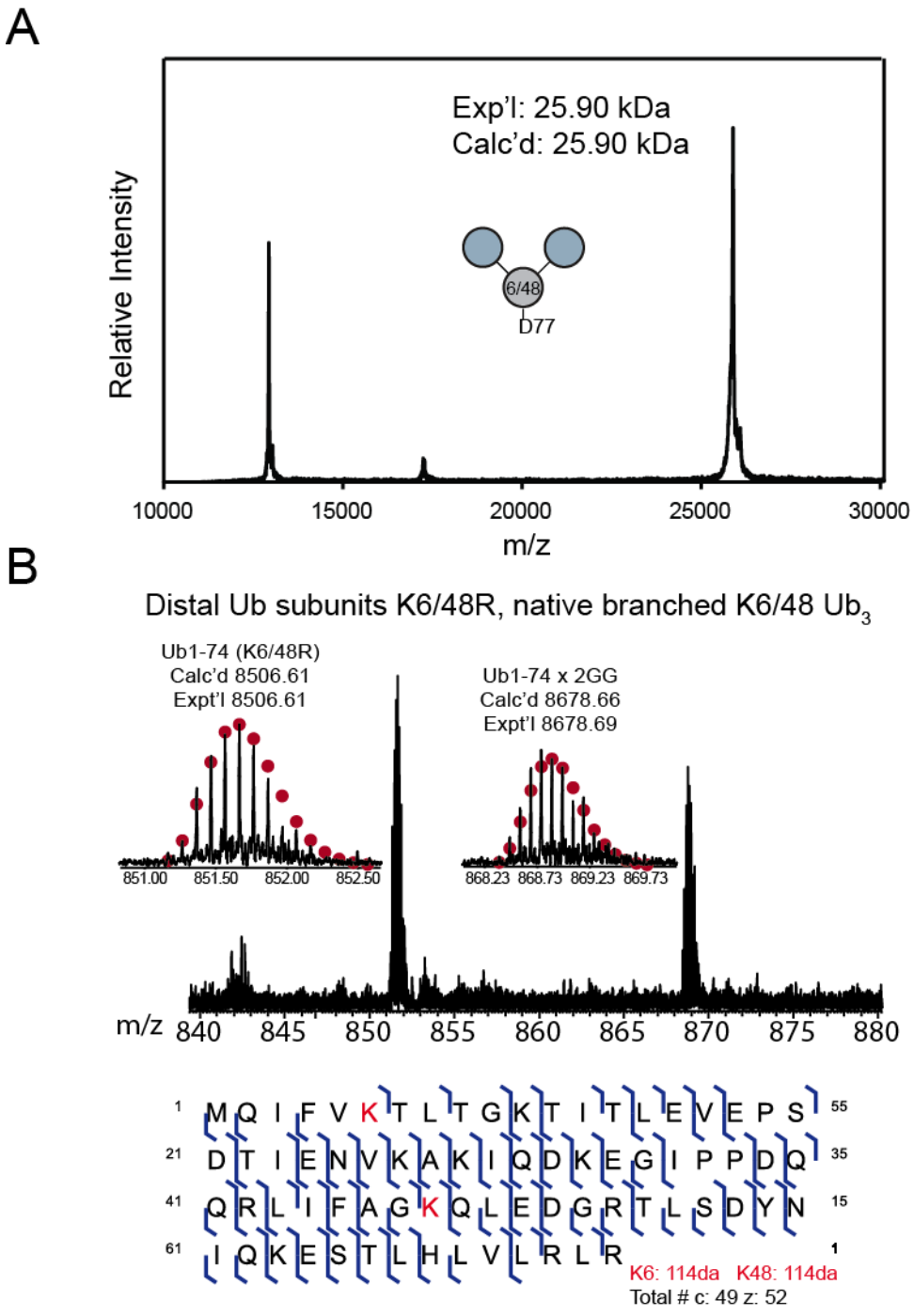

Figure 2. S.5: Characterization of Lys6/Lys48 linked native branched trimer. A) MALDI-TOF mass spectrum of the intact Lys6/Lys48 native branched trimer. **B**) ECD analysis of Ub_{1-74} x 2GG. Isolation of the parent ion (M^{10+} charge state) of each indicated Ub subunit is shown on the top. Circles represent

theoretical isotopic abundance distribution. Calc'd: calculated most abundant molecular weight. Expt'l: experimental most abundant molecular weight. A map of the observed ECD fragments is shown on the bottom. Data analysis includes *N*-ε-GlyGly-Lys modification at lysine 6 and 48 in the *c* and *z* ion predictions (highlighted in red).

A

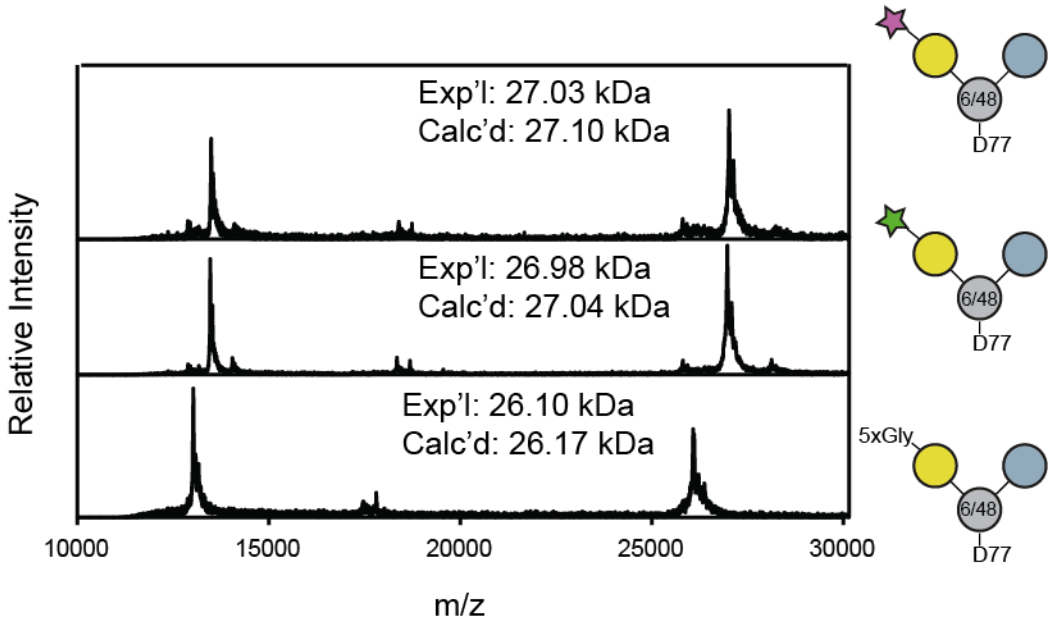
Exp'l: 27.03 kDa
Calc'd: 27.10 kDa
Exp'l: 26.98 kDa
Calc'd: 27.04 kDa
Exp'l: 26.10 kDa
Calc'd: 26.17 kDa
Relative Intensity
10000
15000
20000
25000
30000
m/z
6/48
D77
5xGly

B

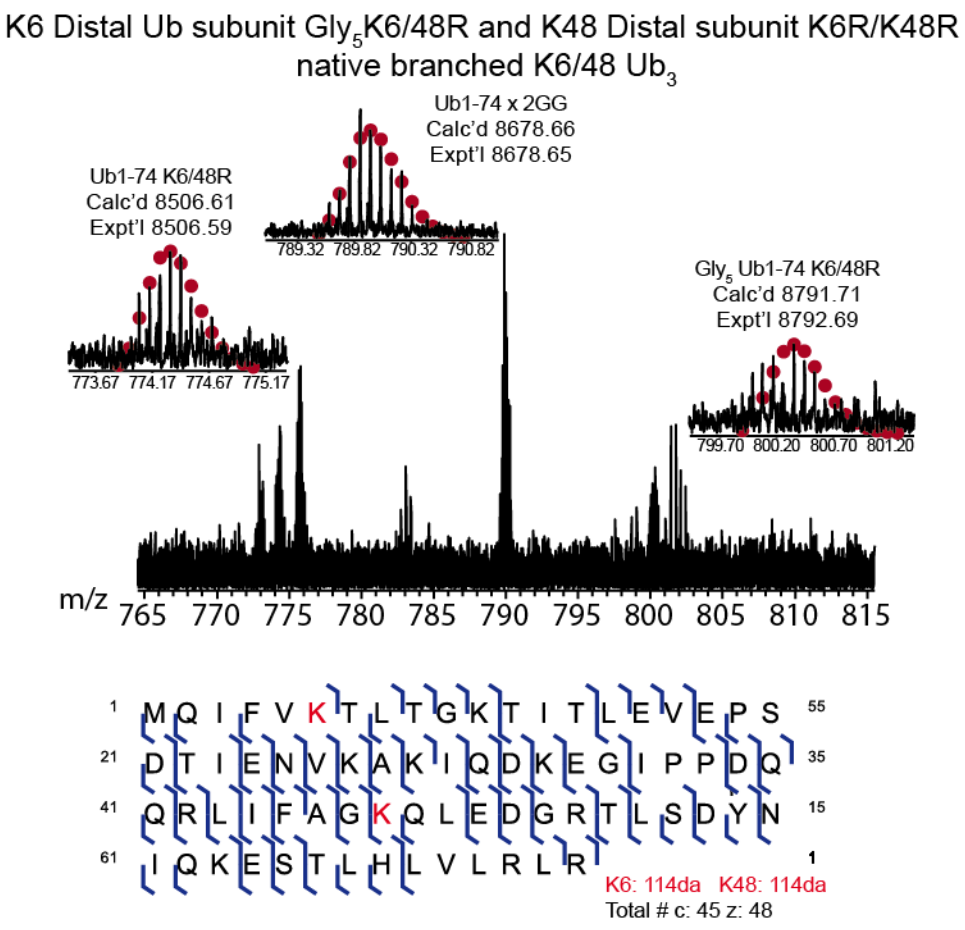
K6 Distal Ub subunit Gly5K6/48R and K48 Distal subunit K6R/K48R
native branched K6/48 Ub3
Ub1-74 x 2GG
Calc'd 8678.66
Expt'l 8678.65
Ub1-74 K6/48R
Calc'd 8506.61
Expt'l 8506.59
Gly5 Ub1-74 K6/48R
Calc'd 8791.71
Expt'l 8792.69
m/z
765 770 775 780 785 790 795 800 805 810 815
M Q I F V K T L T G K T I T L E V E P S
D T I E N V K A K I Q D K E G I P P D Q
Q R L I F A G K Q L E D G R T L S D Y N
I Q K E S T L H L V L R L R
K6: 114da K48: 114da
Total # c: 45 z: 48

Figure 2.S. 6: Characterization of Lys6/Lys48 Native branched trimer containing a 5xGly motif at the 6-distal position. A) MALDI-TOF MS data for the Lys6/Lys48 native branched trimer containing a 5xGly motif at the 6-distal position (bottom). MALDI-TOF MS data for trimer modified with depsipeptide **I** at the 6-distal position (middle). MALDI-TOF MS data for the trimer modified with peptide **II** (top). **B**) ECD analysis of Ub1-74 x 2GG. Isolation of the parent ion (M11+ charge state) of each indicated Ub subunit is shown on the top. Circles represent theoretical isotopic abundance distribution. Calc'd: calculated most abundant molecular weight. Expt'l: experimental most abundant molecular weight. A map of the observed ECD fragments is shown on the bottom. Data analysis includes N-ε-GlyGly-Lys modification at lysine 6 and 48 in the c and z ion predictions (highlighted in red).

A

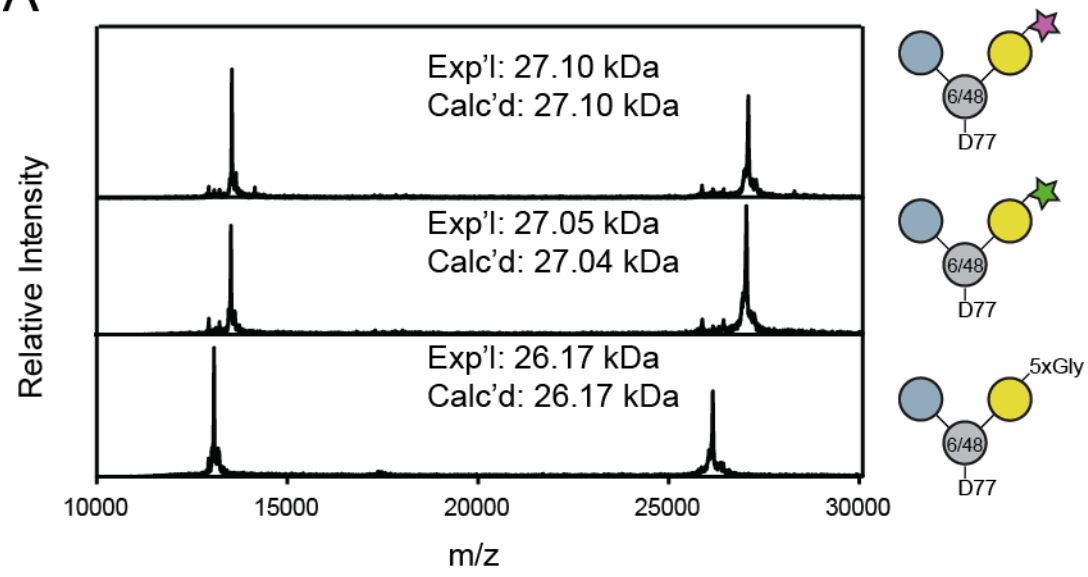
Exp'l: 27.10 kDa
Calc'd: 27.10 kDa
Exp'l: 27.05 kDa
Calc'd: 27.04 kDa
Exp'l: 26.17 kDa
Calc'd: 26.17 kDa
Relative Intensity
10000
15000
20000
25000
30000
m/z
6/48
D77
5xGly

B

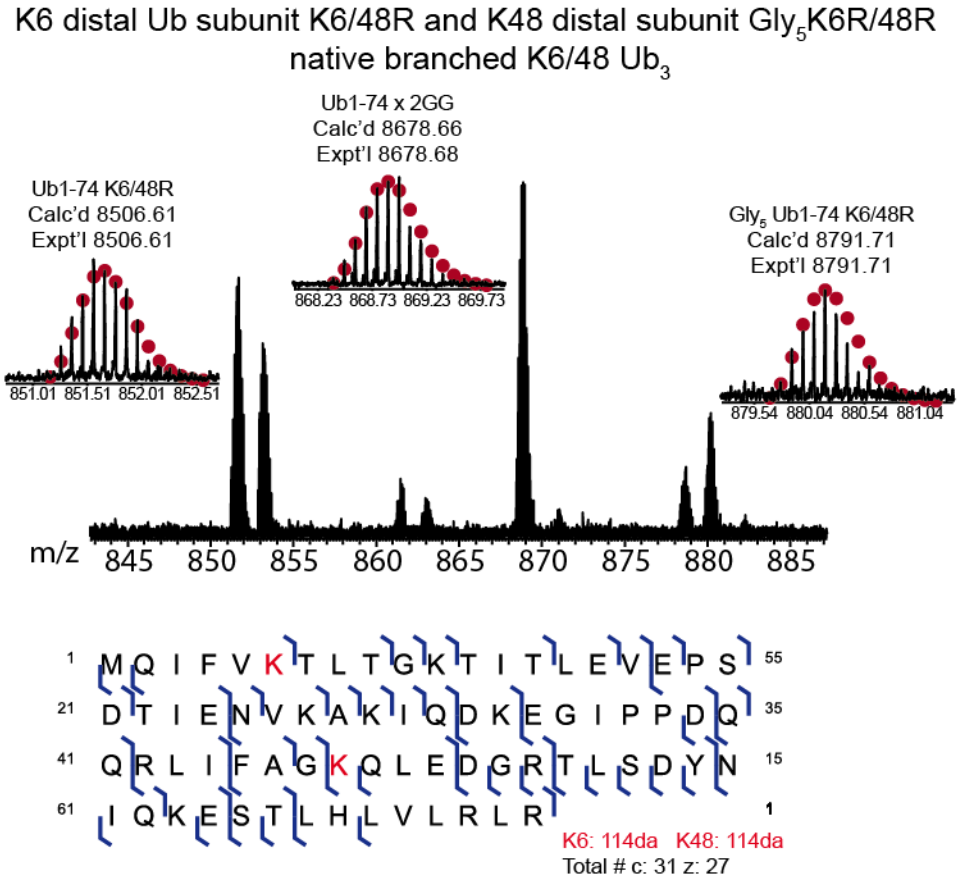
K6 distal Ub subunit K6/48R and K48 distal subunit Gly5K6R/48R
native branched K6/48 Ub3
Ub1-74 x 2GG
Calc'd 8678.66
Expt'l 8678.68
Ub1-74 K6/48R
Calc'd 8506.61
Expt'l 8506.61
Gly5 Ub1-74 K6/48R
Calc'd 8791.71
Expt'l 8791.71
m/z
845 850 855 860 865 870 875 880 885
1 M Q I F V K T L T G K T I T L E V E P S 55
21 D T I E N V K A K I Q D K E G I P P D Q 35
41 Q R L I F A G K Q L E D G R T L S D Y N 15
61 I Q K E S T L H L V L R L R 1
K6: 114da K48: 114da
Total # c: 31 z: 27

Figure 2. S.7: Characterization of Lys6/Lys48 Native branched trimer containing a 5xGly motif at the 48-distal position. A) MALDI-TOF MS data for the Lys6/Lys48 native branched trimer containing a 5xGly motif at the 48-distal position (bottom). MALDI-TOF MS data for the trimer modified with depsipeptide **I** at the 48-distal position (middle). MALDI-TOF MS data for the trimer modified with peptide **II** (top). **B**) ECD analysis of Ub1-74 x 2GG. Isolation of the parent ion (M10+ charge state) of each indicated Ub subunit is shown on the top. Circles represent theoretical isotopic abundance distribution. Calc'd: calculated most abundant molecular weight. Expt'l: experimental most abundant molecular weight. A map of observed ECD fragments is shown on the bottom. Data analysis includes N-ε-GlyGly-Lys modification at lysine 6 and 48 in the c and z ion predictions (highlighted in red).

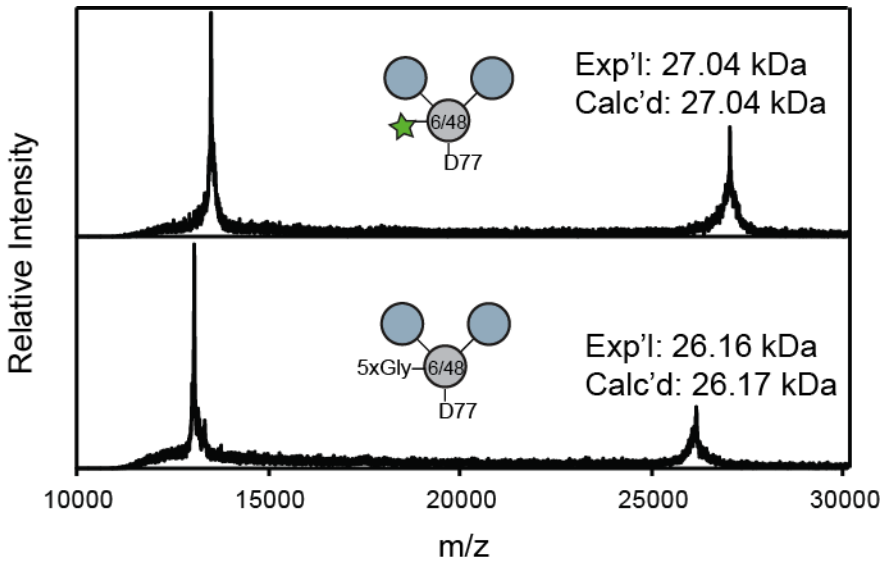

Figure 2.S. 8: Characterization of Lys6/Lys48 native branched trimer containing 5xGly motif at the base. MALDI-TOF MS data of the Lys6/Lys48 native branched trimer containing a 5xGly motif at the base (bottom). MALDI-TOF MS data of the trimer modified with depsipeptide **I** at the base (top).

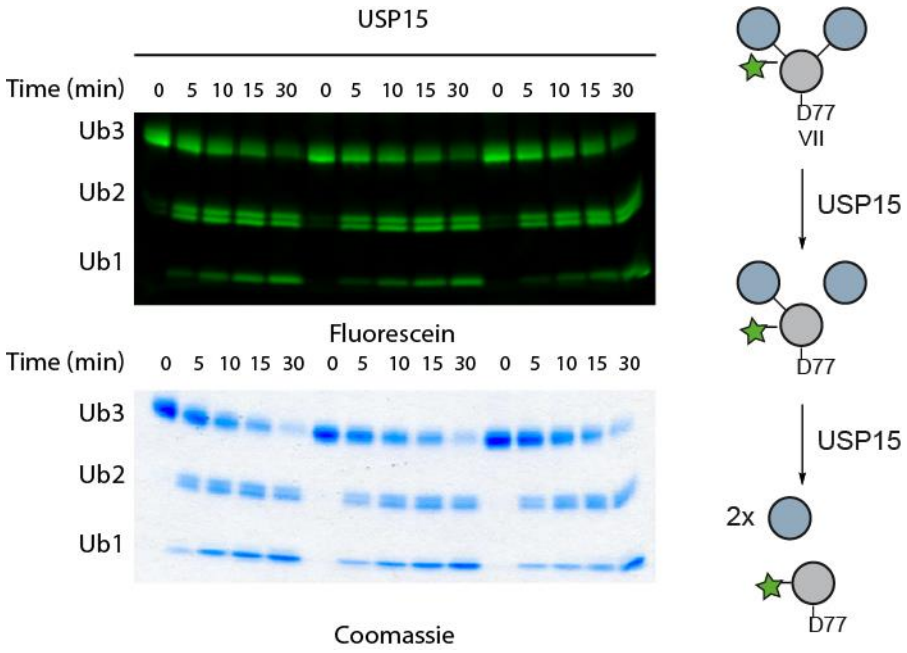

Figure 2.S. 9: USP15 DUB assay of labeled Lys6/Lys48 branched trimer, VII repeated in triplicate. Assays were performed by incubating 10 µM labeled branched trimer with 0.1 µM USP15 at 37°C. Aliquots were removed at the indicated time points and quenched with loading buffer prior to SDS-PAGE analysis.

2.6.8 NMR Spectra

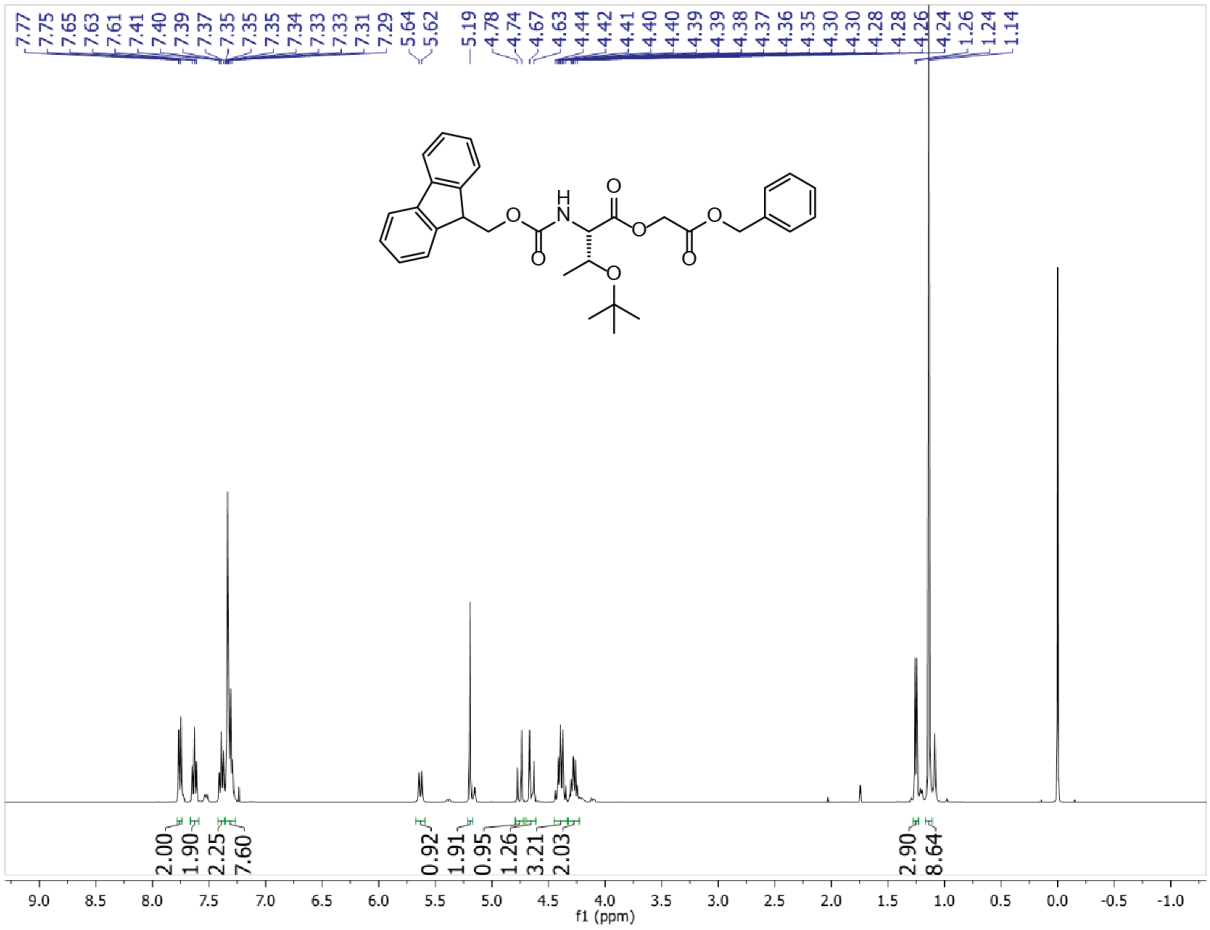

Figure 2. S.10: ^{1}HNMR spectra for Fmoc-Thr(OtBu)-OGly-OBz (1)

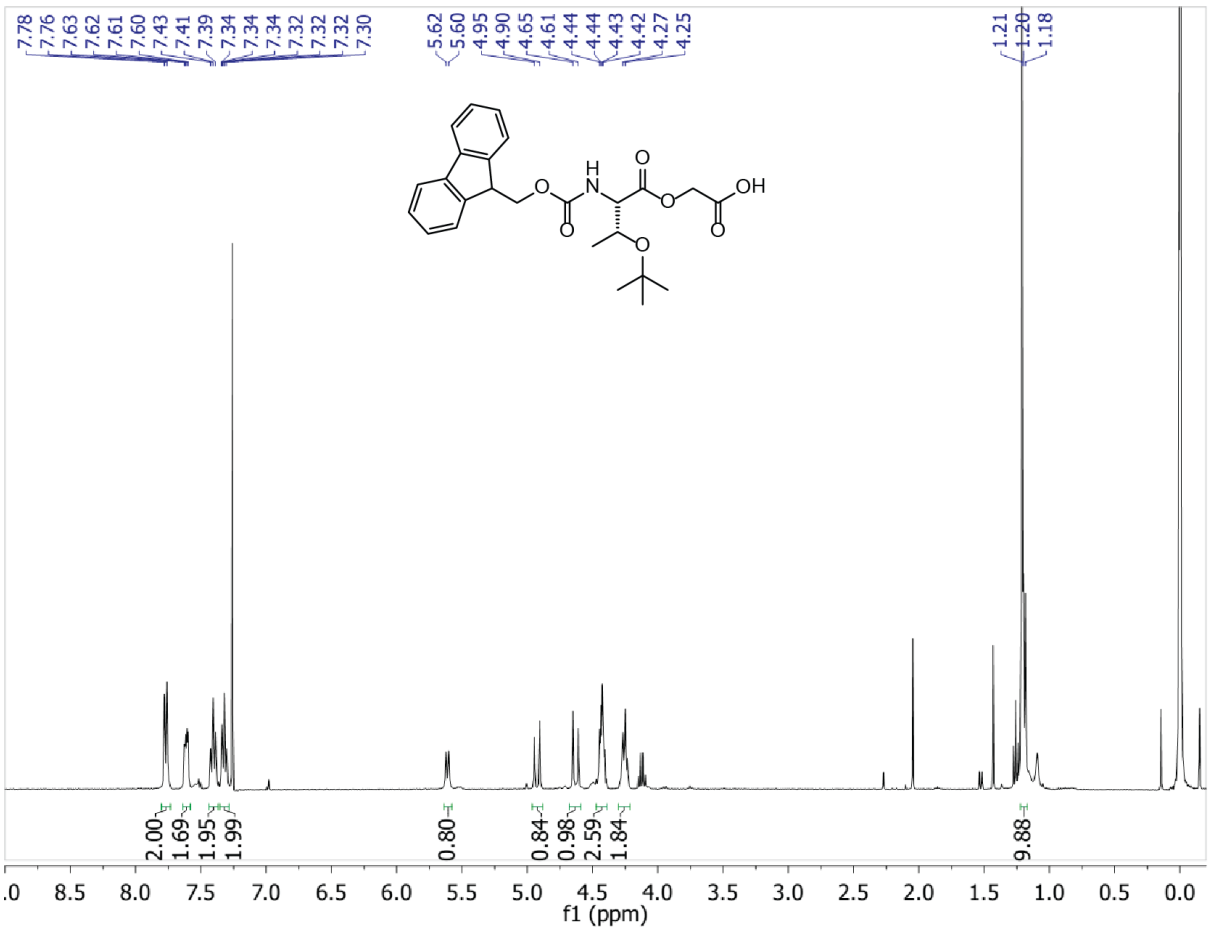

Figure 2.S. 11: ^{1}HNMR spectra for Fmoc-Thr(OtBu)-OGly-OH (2)

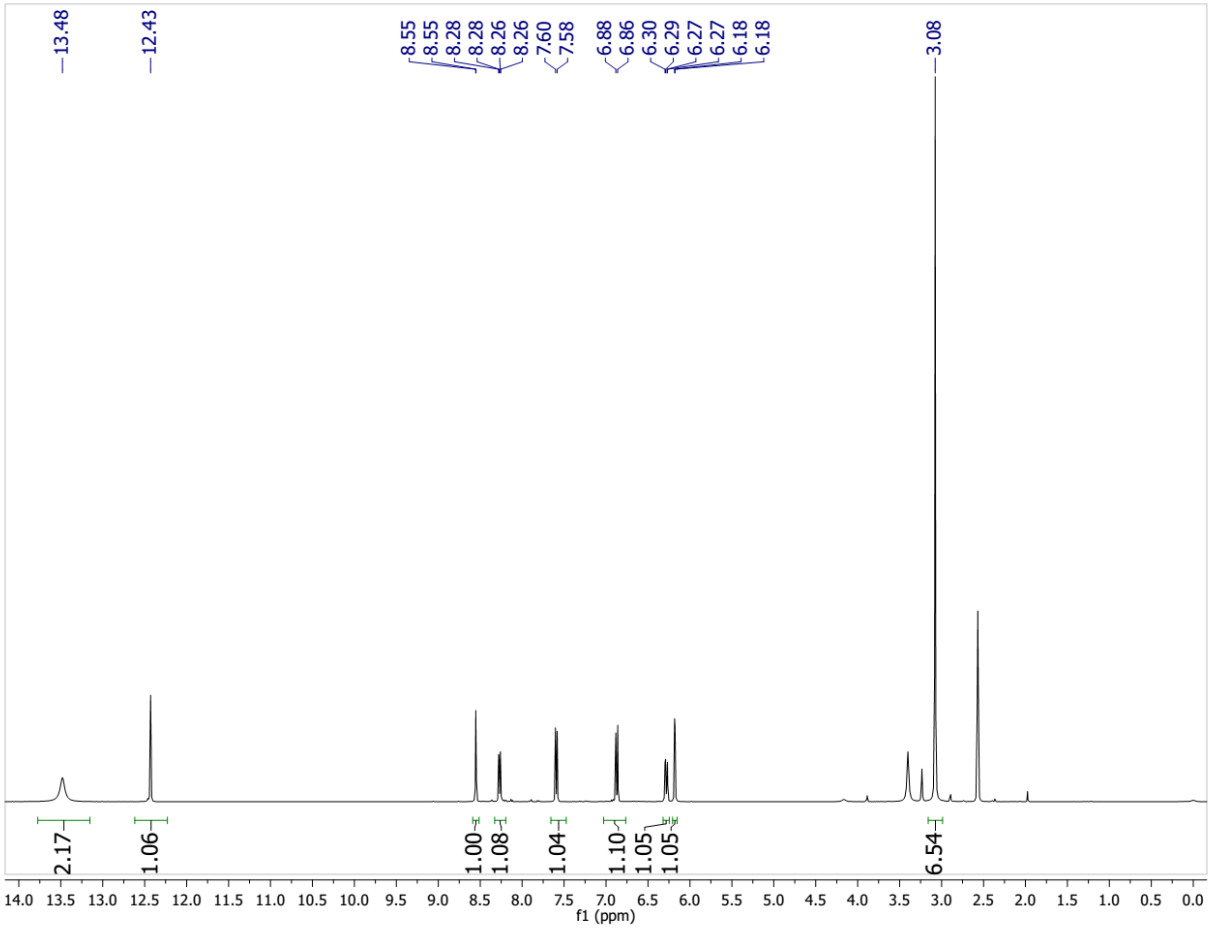

Figure 2. S.12: ^{1}HNMR spectra for4-(4-(dimethylamino)-2-hydroxybenzoyl)isophthalic acid (4).

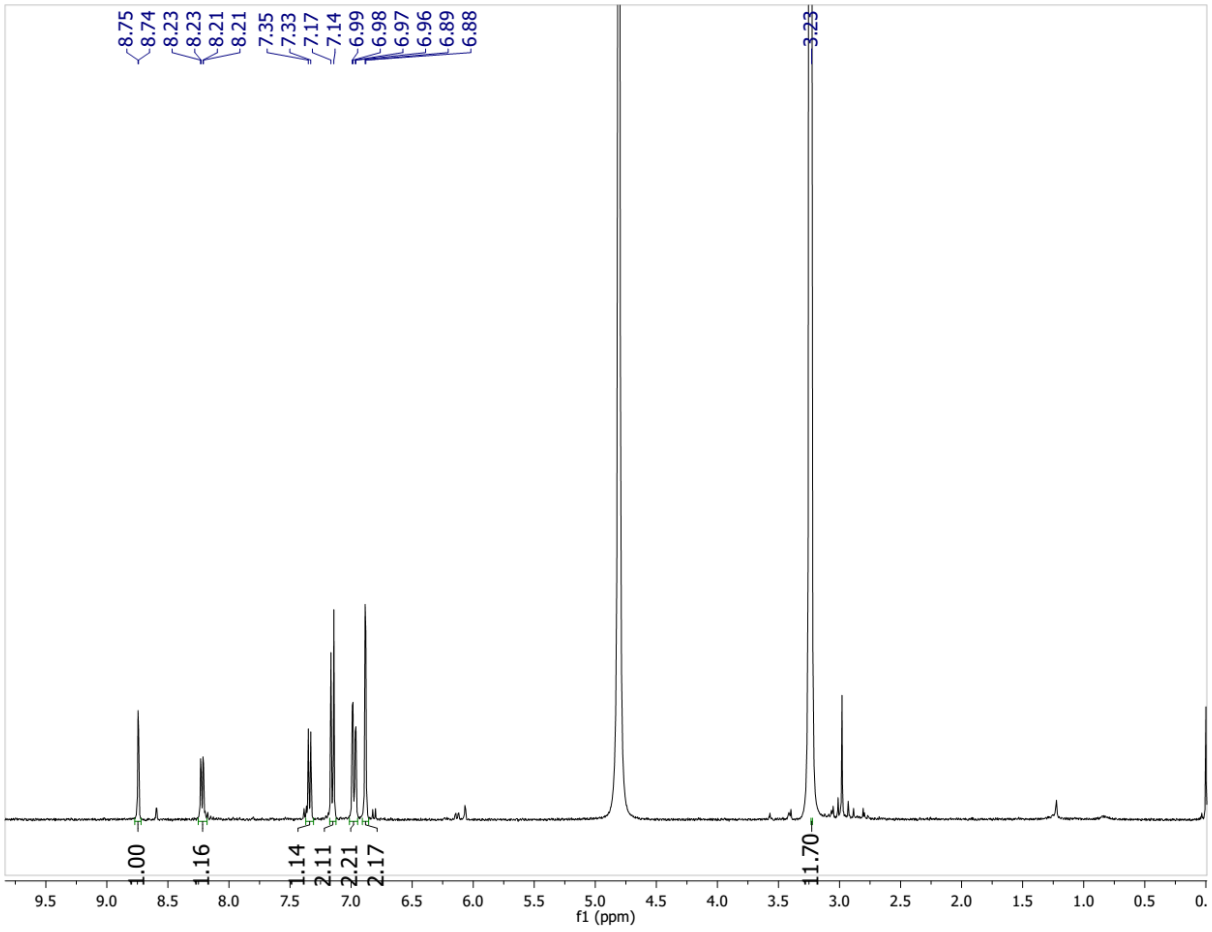

Figure 2.S. 13: ^{1}HNMR spectra for 5-CarboxyTAMRA (5).

2.6.9 Supplemental References

1. Williamson, D. J.; Fascione, M. A.; Webb, M. E.; Turnbull, W. B., Efficient N-Terminal Labeling of Proteins by Use of Sortase. *Angew. Chem. Int. Ed.* **2012,** *51* (37), 9377-9380.

2. Williamson, D. J.; Webb, M. E.; Turnbull, W. B., Depsipeptide substrates for sortase-mediated N-terminal protein ligation. *Nat. Protoc.* **2014,** *9* (2), 253-262.

3. Kvach, M. V.; Stepanova, I. A.; Prokhorenko, I. A.; Stupak, A. P.; Bolibrukh, D. A.; Korshun, V. A.; Shmanai, V. V., Practical Synthesis of Isomerically Pure 5- and 6-Carboxytetramethylrhodamines, Useful Dyes for DNA Probes. *Bioconjugate Chem.* **2009,** *20* (8), 1673-1682.

4. Horne, W. S.; Price, J. L.; Gellman, S. H., Interplay among side chain sequence, backbone composition, and residue rigidification in polypeptide folding and assembly. *Proc. Natl. Acad. Sci. USA* **2008,** *105* (27), 9151-9156.

5. Mazmanian, S. K.; Liu, G.; Ton-That, H.; Schneewind, O., Staphylococcus aureus Sortase, an Enzyme that Anchors Surface Proteins to the Cell Wall. *Science* **1999,** *285* (5428), 760-763.

6. Ton-That, H.; Liu, G.; Mazmanian, S. K.; Faull, K. F.; Schneewind, O., Purification and characterization of sortase, the transpeptidase that cleaves surface proteins of Staphylococcus aureus at the LPXTG motif. *Proc. Natl. Acad. Sci. USA* **1999,** *96* (22), 12424-12429.

7. Blommel, P. G.; Fox, B. G., A combined approach to improving large-scale production of tobacco etch virus protease. *Prot. Expres.Purif.* **2007,** *55* (1), 53-68.

8. Pickart, C. M.; Raasi, S., Controlled Synthesis of Polyubiquitin Chains. In *Methods Enzymol.*, Raymond, J. D., Ed. Academic Press: 2005; Vol. Volume 399, pp 21-36.

9. Valkevich, E. M.; Guenette, R. G.; Sanchez, N. A.; Chen, Y.-c.; Ge, Y.; Strieter, E. R., Forging Isopeptide Bonds Using Thiol–Ene Chemistry: Site-Specific Coupling of Ubiquitin Molecules for Studying the Activity of Isopeptidases. *J. Am. Chem. Soc.* **2012,** *134* (16), 6916-6919.

10. Trang, V. H.; Valkevich, E. M.; Minami, S.; Chen, Y.-C.; Ge, Y.; Strieter, E. R., Nonenzymatic Polymerization of Ubiquitin: Single-Step Synthesis and Isolation of Discrete Ubiquitin Oligomers. *Angew. Chem. Int. Ed.* **2012,** *51* (52), 13085-13088.

11. Hospenthal, M. K.; Freund, S. M. V.; Komander, D., Assembly, analysis and architecture of atypical ubiquitin chains. *Nat. Struct. Mol Biol.* **2013,** *20* (5), 555-565.

12. Valkevich, E. M.; Sanchez, N. A.; Ge, Y.; Strieter, E. R., Middle-Down Mass Spectrometry Enables Characterization of Branched Ubiquitin Chains. *Biochemistry* **2014,** *53* (30), 4979-4989.

13. Guner, H.; Close, P. L.; Cai, W.; Zhang, H.; Peng, Y.; Gregorich, Z. R.; Ge, Y., MASH Suite: A User-Friendly and Versatile Software Interface for High-Resolution Mass Spectrometry Data Interpretation and Visualization. *J. Am. Soc. Mass Spectrom.* **2014,** *25* (3), 464-470.

3 Ubiquitin Chain Enrichment Middle-Down Mass Spectrometry (UbiChEM-MS) Enables Characterization of Branched Ubiquitin Chains *in cellulo*

This chapter has been published:

Crowe S. O.†, Rana A. S. J. B.†, Deol K. K., Ge Y., Strieter, E. R. *Anal. Chem.* **2017**, *89*, 4428-4434.

† These authors contributed equally to this work

Author Contributions:

SOC Performed all Halo-NZF1 experiments.

ASJB performed all TUBEs experiments.

KKD aided in data analysis and protein expression.

SOC, ASJB and ERS wrote the manuscript.

ERS and YG supervised acquisition of data.

All authors edited and approved final manuscript.

3.1 Abstract

Ubiquitin has a broad functional range that has been ascribed to the formation of an array of polymeric ubiquitin chains. Understanding the precise roles of ubiquitin chains, however, is difficult due to their complex chain topologies. Branched ubiquitin chains are particularly challenging, as multiple modifications on a single ubiquitin preclude the use of standard bottom-up proteomic approaches. Developing methods to overcome these challenges is crucial considering evidence suggesting branched chains regulate the stability of proteins. In this study we employ Ubiquitin Chain Enrichment Middle-down Mass Spectrometry (UbiChEM-MS) to identify branched chains that cannot be detected using bottom-up proteomic methods. Specifically, we employ TUBEs and the K29-selective NZF1 domain from the deubiquitinase TRABID to enrich for chains from human cells. Minimal trypsinolysis followed by high resolution mass spectrometric analysis reveals that Ub chain branching can indeed be detected using both UBDs tested at endogenous levels. We find that ~2% of chains isolated with TUBEs contain Ub branch points, with this value rising to ~4% after proteasome inhibition. Electron-Transfer Dissociation (ETD) analysis indicates the presence of K48 in these branched chains. Use of the NZF1 domain reveals that ~4% of the isolated chains contain branch points with no apparent dependence on proteasome inhibition. Our results demonstrate an effective strategy for detecting and characterizing the dynamics of branched conjugates under different cellular conditions.

3.2 Introduction

Over the last few decades it has become widely appreciated that ubiquitin (Ub) plays a major role in regulating nearly every cellular pathway in eukaryotes. The cell cycle, for example, is driven by Ub-mediated degradation[1]; the cellular response to DNA damage[2] and our ability to ward off pathogens are also both intricately linked to Ub signaling.[3] How Ub regulates the dynamics of such diverse biochemical pathways is thought to be a result of Ub chain formation.

Ub chains are generated after consecutive rounds of target protein modification by E1, E2, and E3 enzymes.[4] After Ub is transferred to the ε-amino group of a target lysine, any of the eight amino groups of Ub (M1, K6, K11, K27, K29, K33, K48, and K63) can be attached to the C-terminus of another Ub leading to the formation of a Ub chain.[5] During chain extension there can be tremendous variability in linkage, length, and configuration (i.e., linear versus branched). This versatility is what likely gives rise to the multitude of cellular functions associated with Ub. Mounting evidence suggests that the type of ubiquitin chain determines the cellular fate of a modified protein. For instance, K11- and K48-linked chains signal for protein degradation through the proteasome, whereas M1- and K63-linked chains promote proteasome-independent activities.[6-15]

While there has been significant interest in understanding the functional impact of different chain linkages, much less attention has been paid to the importance of chain configuration. Initial reports on branched chains focused on bifurcations at consecutive lysines of Ub (e.g., K6/K11, K27/K29, or K29/K33) since these modifications can be detected using bottom-up proteomic approaches.[16, 17] Based on *in vitro* proteasome assays, bifurcated chains were found to be less effective at promoting protein degradation compared to chains composed of a single linkage.[16, 18] Whether these observations are solely due to chain branching, however, is unclear given the heterogeneity of the systems under investigations. More recently, there has been evidence suggesting K11/K48 branched chains produced by the anaphase-

promoting complex/cyclosome (APC/C) are capable of triggering proteasomal degradation.[19, 20] In this case, K11/K48 branched chains were detected on APC/C substrates by expressing non-native Ub variants in cells. Other branched chains unamenable to tryptic fragment mass spectrometric analyses have also been implicated in several fundamental cellular pathways. For example, M1/K63 chains have been proposed to regulate NF-κB signaling,[21, 22] K11/K63 conjugates are thought to play a role in receptor internalization,[23, 24] and K29/K48 branched chains have been linked to proteasomal degradation.[25, 26] Further defining the roles of branched chains in regulating protein stability and other cellular pathways requires new methods of detection and characterization.

In this study, we demonstrate the utility of Ubiquitin Chain Enrichment Middle-down Mass Spectrometry (UbiChEM-MS) in characterizing branched Ub chains present in human cell extracts. Previous reports from our lab and others have shown that, when integrated with MS analysis, minimal trypsinolysis and limited acid cleavage retain information on the connectivity of Ub chains, particularly branched chains.[27-31] When Ub is subjected to trypsinolysis under non-denaturing conditions, a single cleavage occurs between Arg74 and Gly75 leaving behind an intact Ub_{1-74} fragment (calc'd 8450.57Da) as well as a Gly-Gly remnant.[32] In the event of minimal trypsinolysis of Ub chains, this Gly-Gly remnant remains attached to the modified lysine resulting in a Ub_{1-74} fragment modified with a single Gly-Gly ($^{GG}Ub_{1-74}$, calc'd 8564.62Da). If a branch point is present within the Ub chain, the Ub moiety bearing the branch point will be modified with two Gly-Gly modifications ($^{2xGG}Ub_{1-74}$, calc'd 8678.66Da), thus enabling characterization of multiple modifications on a single Ub protein. Although useful for characterizing the products of E2-E3 enzymatic activity *in vitro*, these middle-down methods have not led to the identification of branched chains in complex mixtures such as cell extracts. We envisioned that by lysing cells grown under different conditions and enriching particular Ub chains using linkage-selective Ub binding domains (UBDs),[5, 33] branched conjugates could be detected and characterized by middle-down MS. Here we show this strategy is brought to fruition using both the non-selective tandem ubiquitin

binding entities (TUBEs) as well as the K29 linkage-selective NZF1 domain from the deubiquitinase TRABID. Our results reveal that UbiChEM-MS can not only be used to detect previously undetectable branched chains, but also monitor their dynamics. We surmise this same approach can readily be adapted for the detection and characterization of many other branched chains provided a linkage specific binding domain exists.

3.3 Experimental Section

3.3.1 Preparation of Halo-NZF1 resin.

HaloLink resin (1.6mL, Promega) was pelleted at 800x*g* for 2 min and the supernatant removed. The resin was washed four times with binding buffer (2 mL; 50 mM Tris, 150 mM NaCl, 10% glycerol, 0.05% IGEPAL CA-630), and then finally resuspended in binding buffer to yield a 50% slurry. This slurry was then incubated with 800 µL of Halotag-NZF1 fusion protein (115 µM), and the resulting suspension was rocked overnight at 4°C. The suspension was then pelleted at 800x*g* for 2 min; the supernatant was discarded, and the resin was further washed four times with 5 mL of binding buffer.

3.3.2 Isolation of Ubiquitin Chains from HEK Cell Lysate.

Resin bearing the appropriate ubiquitin binding domain (TUBEs 100 µL or NZF1 200µL) was incubated with 45 mg of cell lysate on a revolver overnight at 4°C, after which the resin was pelleted at 800 x*g* for 2min. The resin was then washed three times with 2mL of binding buffer and twice with 2mL of minimal buffer (50 mM Tris, 150 mM NaCl, pH 7.5). The resin was then resuspended in 100 µL of minimal buffer. 6x Laemmli loading buffer was added to aliquots of each step, separated on a 15% SDS-PAGE gel, and analyzed by western blot with anti-Ub antibody (P4D1).

3.3.3 On-Resin Minimal Trypsinolysis of Isolated Ub Chains.

Minimal trypsinolysis were performed on-resin at room temperature for 16 h using empirically determined ratios of lysate to trypsin (Table 3.S.1). These on-resin samples were then acidified to pH 2

with acetic acid to deactivate trypsin. These acidified solutions were incubated in 4 ^{o}C for 15-30 min and then centrifuged for 5 min at 13000 x*g*, 4^{o}C. For samples analyzed by LC MS/MS, the supernatant was concentrated ~5-7 fold using a speedvac. Samples were centrifuged for 30 min at 16000 x*g*, 4^{o}C, prior to injection into the mass spectrometer. For samples analyzed by direct infusion into the mass spectrometer, the supernatant was pipetted into 100 mg SeP-Pak C_{18} column (Waters) which was washed with 10 mL of equilibration solution (0.1% TFA in water). This column was then washed with 3 mL of equilibration solution, followed by collecting 1.5 mL fractions of 10, 20, 30, 40, 50, 60, 70, and 100% acetonitrile in 0.1% TFA solutions. The 0-60% fractions were lyophilized. These lyophilized samples are dissolved in 200 µL of a water/acetonitrile/acetic acid (45:45:10) solution and first analyzed by MALDI-TOF. Then the samples containing Ub species were further analyzed by high resolution mass spectrometry.

3.3.4 Middle-Down Mass Spectrometry and Quantitative Analysis with Orbitrap Fusion.

Samples were directly infused into an Orbitrap Fusion™ Tribrid™ Mass Spectrometer (Thermo Scientific™ Inc), where the resolving power of the mass analyzer was set at 60000. All spectra were processed with in-house software (MASH Suite[34]) using a signal-to-noise (S/N) threshold of 3 and a fit factor of 70% and then validated manually; all reported calculated and experimental values correspond to the most abundant molecular weights. Quantitative analysis of the relative abundance of the three Ub_{1-74} species was performed as described previously.[35, 36] The relative abundances of each Ub species from four different charge states were averaged to obtain the relative percentage. The relative abundances of each Ub species in 700 m/z – 1300 m/z range were averaged to obtain the relative percentage. Percent distribution was calculated from three biological replicates, and data represented as mean ± standard error of the mean (SEM).

3.3.5 Liquid Chromatography Middle-Down Mass Spectrometry and Quantitative Analysis with Bruker Maxis Impact LCMS system.

Minimally digested products were separated using a nanoAcquity LC system (Waters) equipped with replacement capillary custom packed trap (nanoLCMS Solutions LLC) followed by home-packed PLRP-S column and a gradient from 5% B to 95% B over 43 min (solvent A: 0.1% formic acid in water, solvent B: 0.1% formic acid in 1:1 solution of acetonitrile and ethanol). The LC system was coupled online with a Bruker Impact II Q-TOF mass spectrometer, where the resolving power of the mass analyzer was set at 50000. All spectra were processed with in-house software (MASH Suite[34]) using a signal-to-noise (S/N) threshold of 3 and a fit factor of 70% and then validated manually; all reported calculated and experimental values correspond to the most abundant molecular weights. Quantitative analysis of the relative abundance of the three Ub_{1-74} species was performed as described previously.[35, 36] The relative abundances of each Ub species in 600 m/z – 1250 m/z range were averaged to obtain the relative percentage. The percent distribution was calculated from three biological replicates, each with three technical replicates, and data represented as mean (SEM).

3.3.6 Electron-Transfer Dissociation (ETD) Analysis of Ub Chain Linkages on Orbitrap Fusion.

For tandem mass spectrometry (MS/MS) experiments, individual charge states of protein molecular ions were isolated and then dissociated by ETD using a 10 ms reaction time, with a 2.0e5 reagent ion target. ETD was also supplemented by collision induced decay (CID) using a collision energy of 10%. Spectra were recorded in the Orbitrap analyzer over an m/z range 150 to 2000 *m/z* with a resolution setting of 60,000 and AGC setting of 4e5 charges. All spectra were processed with the (MASH suite software)[34] using a S/N threshold of 3 and a fit factor of 70% and then validated manually. The resulting mass lists were further assigned on the basis of the protein sequence of Ub with or without the diglycine (GG) modification at each lysine using a tolerance of 20 ppm for precursor and fragment ions. All reported calculated (calc'd) and experimental (expt'l) values correspond to the monoisotopic molecular weight.

3.3.7 ETD Analysis of Ub Chain Linkages on Bruker Maxis Impact LCMS system.

Minimally digested products were separated using a nanoAcquity LC system (Waters) equipped with replacement capillary custom packed trap (nanoLCMS Solutions LLC) followed by home-packed PLRP-S column and a gradient from 5% B to 95% B over 43 min (solvent A: 0.1% formic acid in water, solvent B: 0.1% formic acid in 1:1 solution of acetonitrile and ethanol). The LC system was coupled online with a Bruker maXis II ETD Q-TOF mass spectrometer. For tandem mass spectrometry (MS/MS) experiments, individual charge states of protein molecular ions were isolated then the ions were dissociated by ETD. The accumulation time, reagent time and reaction time for ETD were determined on case-by-case basis to achieve optimal fragmentation. The ranges for accumulation time, reagent time, reaction time were 1000-4000 ms, 4-20 ms and 1-10 ms respectively. All spectra were processed with the MASH suite software [34] using a S/N threshold of 3 and a fit factor of 70% and then validated manually. The resulting mass lists were further assigned based on the sequence of Ub with or without the diglycine (GG) modification at each lysine using a tolerance of 20 ppm for precursor and fragment ions. All reported calculated (calc'd) and experimental (expt'l) values correspond to the monoisotopic molecular weight.

3.4 Results and Discussion

A general characterization method is needed to understand the various roles that branched Ub chains play in cell signaling. To this end, we sought to develop an approach based on middle-down MS.[27, 28] We envisioned an experimental workflow commencing with the isolation of Ub chains from cells followed by minimal trypsinolysis and MS analysis (Figure 3.1). While there are several methods to enrich Ub chains using Ub binding domains (UBDs), we focused on two UBDs in particular: the non-selective tandem ubiquitin binding entity TUBE2[37] and the NZF1 domain from the K29/K33 selective deubiquitinase TRABID.[38] We reasoned these two UBDs would allow us to monitor both global changes in Ub chain branching as well as changes in specific Ub chains bearing branched linkages.

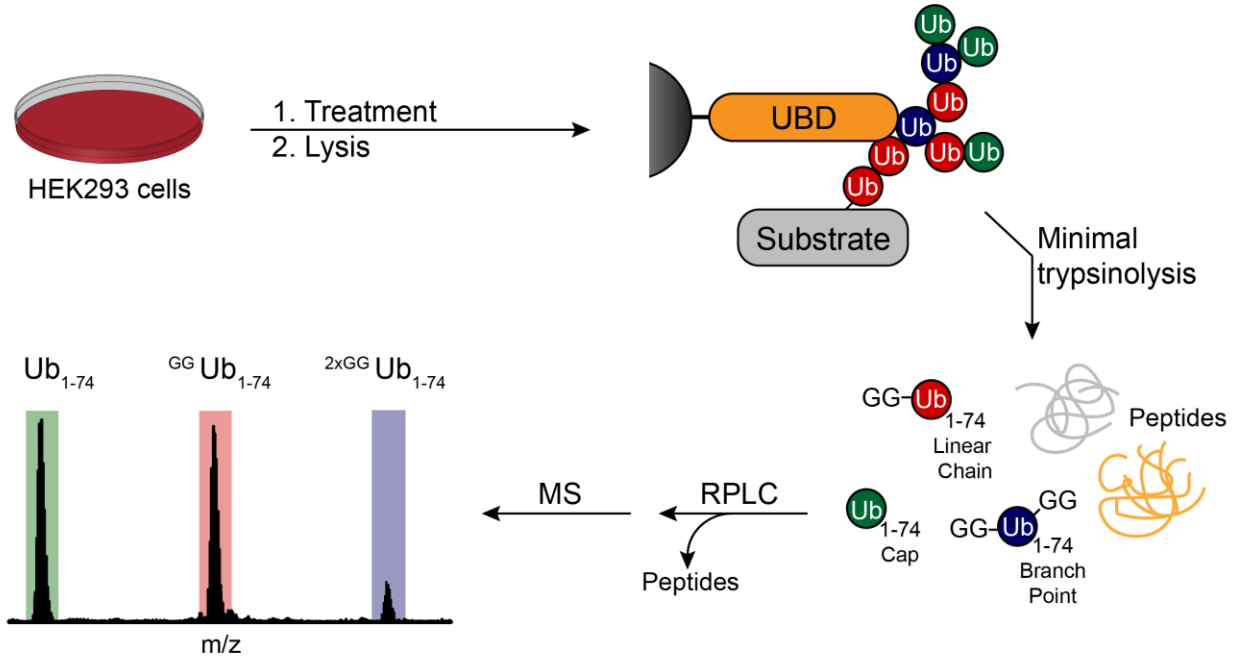

Figure 3. 1: General workflow for isolation and detection of branched Ub chains by UbiChEM-MS. Cells are grown under different treatments and lysed under non-denaturing conditions. Clarified lysates are subsequently incubated with a resin bearing ubiquitin binding domains and the isolated chains are then subjected to minimal trypsinolysis under non-denaturing conditions yielding Ub_{1-74} fragments containing Gly-Gly modifications. These products are enriched for using reverse phase chromatography and characterized by high resolution mass spectrometry.

3.4.1 TUBE2- and NZF1-Based UbiCHEM-MS.

To gain an understanding of the global landscape of Ub chain architecture we captured polyubiquitin chains using the commercially available agarose bound TUBE2. This tandem ubiquitin binding entity is based on the UBA1 domain of Rad23a and has been shown to enrich for Ub chains with little linkage selectivity, thus allowing us to monitor global changes in the Ub pool.[37, 39] Incubation of TUBEs with clarified lysate from HEK293 cells did indeed result in the isolation of high molecular weight chains (Figure 3.S.1). After washing, trypsin was added to achieve minimal digestion of the immobilized chains. The

resulting digests were then subjected to reverse-phase column chromatography to remove salts and smaller peptides prior to high resolution MS analysis. With this strategy, we could detect all three Ub_{1-74} species in untreated HEK293 cell lysates (Figure 3.2 A). Relative quantification reveals that 57% of Ub_{1-74} species exist as either caps or monoUb, 41% are $^{GG}Ub_{1-74}$, and 2% are $^{2xGG}Ub_{1-74}$.

Having established a method that enables characterization of the Ub chain landscape we wanted to explore whether UbiCHEM-MS could be used to monitor chain dynamics. Branched Ub chains have been implicated as potent signals for proteasomal degradation, suggesting that proteasome inhibition would lead to an accumulation of these conjugates.[20] To test this, cells were treated with MG132 for 2, 4, 8, and 16 h and chains were enriched using TUBE2 (Figure 3.2, 3.S.3 and Table 3.S.2). The most significant changes occur after 16 h. Caps/monoUb decrease from 57% to 44%, while $^{GG}Ub_{1-74}$ increase from 41% to 52 % and $^{2xGG}Ub_{1-74}$ rises from 2% to 4% (Figure 3.2 B). These results indicate that long chains harboring branch points accumulate after prolonged proteasome impairment, supporting the idea that branched chains are involved in proteasomal degradation.

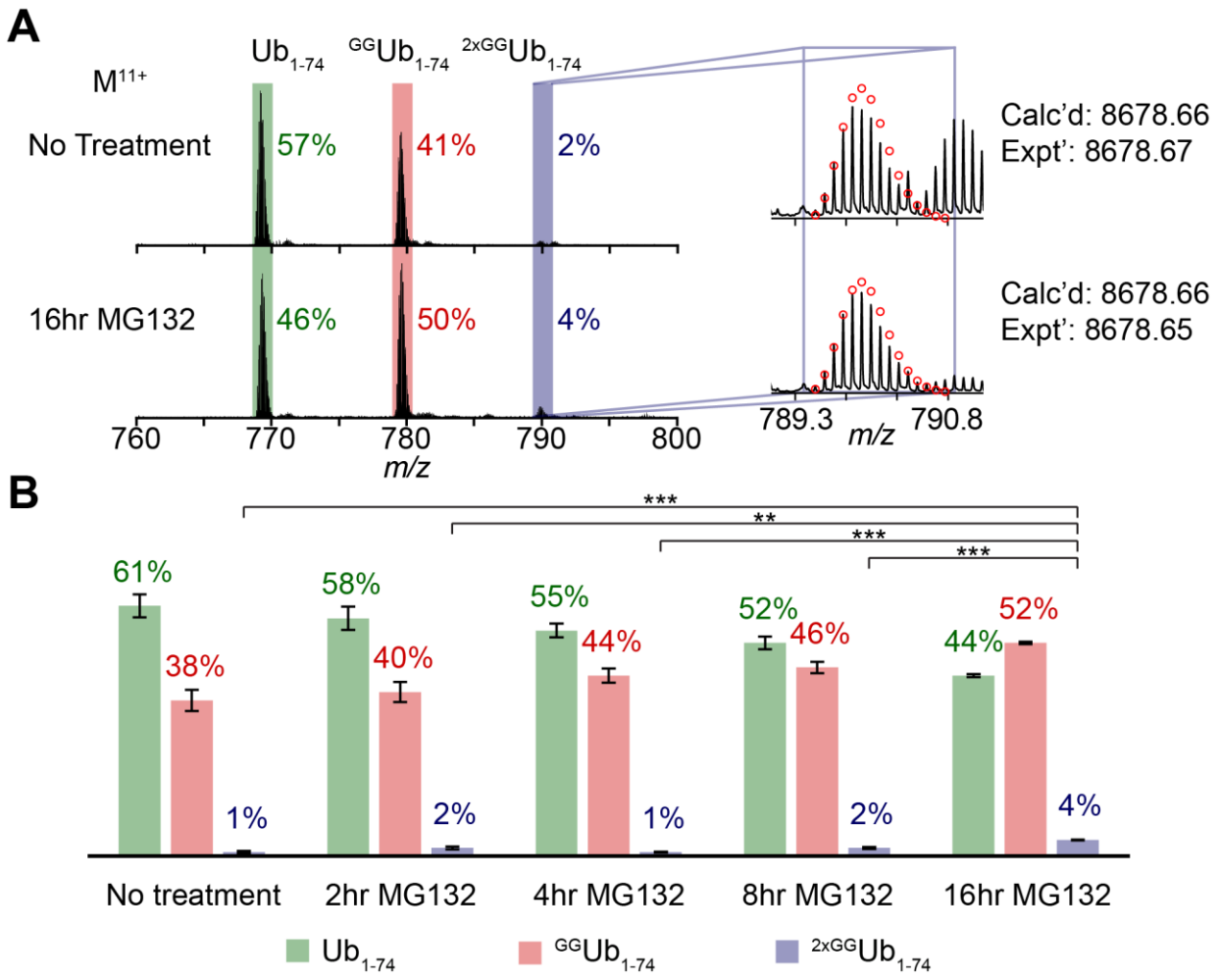

Figure 3. 2: Middle-down MS analysis of Ub chains isolated from HEK cells using agarose bound TUBE2 shows dynamics in Ub chain branching upon proteasome inhibition. **A**) ESI TOF MS spectra showing the presence of all three minimally digested products - Ub_{1-74} (green box), $^{GG}Ub_{1-74}$ (red box), and $^{2xGG}Ub_{1-74}$ (blue box). The spectra correspond to the Ub^{11+} charge state for chains isolated from either untreated or MG132 treated HEK lysate. **B**) Quantification of Ub_{1-74} species at different MG132 time points. The percent distribution is calculated by averaging relative abundance of each Ub_{1-74} species to total abundance of all three species from three biological replicates for each treatment. (Table 3.S.2). Error bars represent standard error of the mean (SEM) for each data set * $p < 0.05$, ** $p < 0.01$, and *** $p < 0.001$ (Student's t-test). Calc'd - calculated most abundant weight; expt'l – experimental most abundant molecular weight.

We then shifted our attention to a UBD with linkage selectivity to capture a specific pool of Ub chains. The NZF1 domain from the deubiquitinase TRABID selectively binds K29-linked Ub chains and has been shown to enrich heterotypic Ub chains from cell lysates.[38] Based on these results we reasoned that a percentage of mixed linkage chains would contain branch points and the dynamics of a specifically linked chain could be monitored. To test this, the NZF1 domain was expressed with an N-terminal fusion to HaloTag and covalently tethered to HaloLink resin as previously reported.[38, 40] The immobilized NZF1 domain was then used to isolate Ub chains from HEK293. As with TUBE2 enrichment, western blot analysis shows the NZF1 domain enables isolation of high molecular weight chains (Figure 3.3, 3.S.1 and 3.S.2). Moreover, all three Ub_{1-74} species are detected by MS. Intriguingly, the Ub chain profile differs from that of the TUBE2 pull-downs. In unstimulated cells, approximately 4% of the NZF1-enriched chains contain branch points ($^{2xGG}Ub_{1-74}$) compared to only 2% in TUBE2 pull-downs (Figure 3.3 B). These differences are indeed significant based on the consistency of results obtained using different mass spectrometers (see below), and the number of biological and technical replicates. Narrowing the scope of chains that can be pulled down thus enables detection of chain architectures that might normally be lost in the noise.

Next, we sought to determine if NZF1-enriched chains are involved in proteasomal degradation. Again, HEK293 cells were treated with the proteasome inhibitor MG132 for 2, 4, 8, and 16 h (Figure 3.3, B.4, and Table 3.S.3).[20] Interestingly, even after 16 h, no significant changes in any of the three Ub_{1-74} species are detected. These results suggest chains enriched by the NZF1 domain do not target substrates to the proteasome.

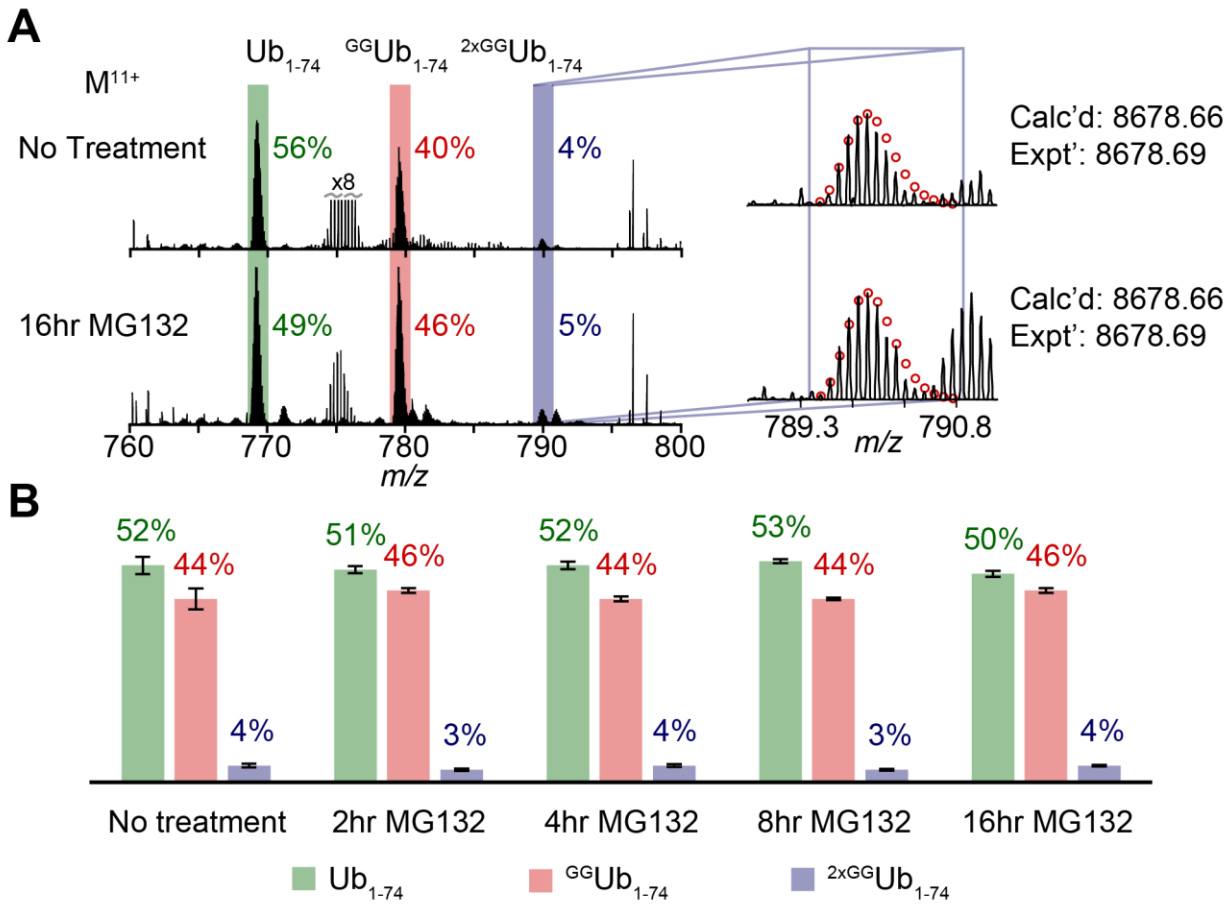

Figure 3. 3: Middle-down MS analysis of Ub chains isolated from HEK cells using Halo-NZF1 resin. A) ESI MS spectra showing the MS spectra of chains isolated using Halo-NZF1 resin. The spectra show the presence of all three minimally digested products - Ub_{1-74} (*green box*), $^{GG}Ub_{1-74}$ (*red box*), and $^{2xGG}Ub_{1-74}$ (*blue box*). The spectra correspond to the Ub^{11+} charge state for chains isolated from either untreated or MG132 treated HEK lysate. **B**) Quantification of Ub_{1-74} species after different lengths of proteasome inhibition. The percent distribution is calculated by averaging relative abundance of each Ub_{1-74} species to total abundance of all three species from three biological replicates for each treatment. (Table 3.S.3). Error bars represent the SEM for each data set. Calc'd - calculated most abundant weight; expt'l – experimental most abundant molecular weight.

3.4.2 MS2 Analysis of Branched Chains.

We sought to characterize the linkages in chains isolated from TUBE2 and NZF1 pull-downs. To this end, we employed electron-transfer dissociation (ETD) fragmentation to generate *c*- and *z*-$^{\bullet}$ type ions.[41, 42] ETD analysis of the $^{GG}Ub_{1-74}$ species points to chains primarily composed of K48 linkages (Figure 3.S.5). Analysis of the $^{2xGG}Ub_{1-74}$ species, however, proved much more difficult, precluding us from identifying specific lysines that comprise the branch points (Figure 3.S.6). This could be due to the non-selective nature of TUBE2, which is likely to enrich for chains composed of multiple linkages.

As the NZF1 domain of TRABID has been shown to selectively isolate K29-linked Ub chains, we hoped to confirm the presence of K29 and identify other linkages within the branch points. Using the sample from MG132 treated cells; we isolated the M^{11+} charge state for $^{2xGG}Ub_{1-74}$ and subjected it to ETD fragmentation (Figure 3.4 A). Accounting for all possible linkage types, the fragmentation pattern best fits a K29/K48 branch point. With these linkages, we identified 31 *c* and 31 $z^{\bullet}$ ions (Figure 3.4 B, C and Figure 3.S.7, 3.S.8). The most important ions for characterization are c_{31} and $z^{\bullet}_{27}$ (Figure 3.4 B). The presence of these two indicates that the Gly-Gly modifications are on K29 and K48. These results are consistent with the previously reported observation that NZF1 enriches heterotypic chains comprised mainly of K29 and K48 linkages.[38]

To provide additional support for the presence of Gly-Gly modifications on K29 and K48, we used Ub chain restriction analysis (UbiCrest).[43, 44] NZF1-enriched chains were digested with the K29/K33 linkage-selective DUB TRABID and the K48 specific DUB OTUB1.[45, 46] As a control, we also employed the non-selective DUB USP15.[47] Western blot analysis shows chains are sensitive to TRABID and OTUB1 with the greatest amount of cleavage occurring when both DUBs are added (Figure 3.4 D). These data confirm that NZF1-enriched chains contain K29 and K48 linkages. Not all high-molecular weight species, however, are removed by TRABID and OTUB1. This suggests that proteins enriched by NZF1 are modified with multiple mono-Ub molecules or chains with linkages other than K29 and K48.

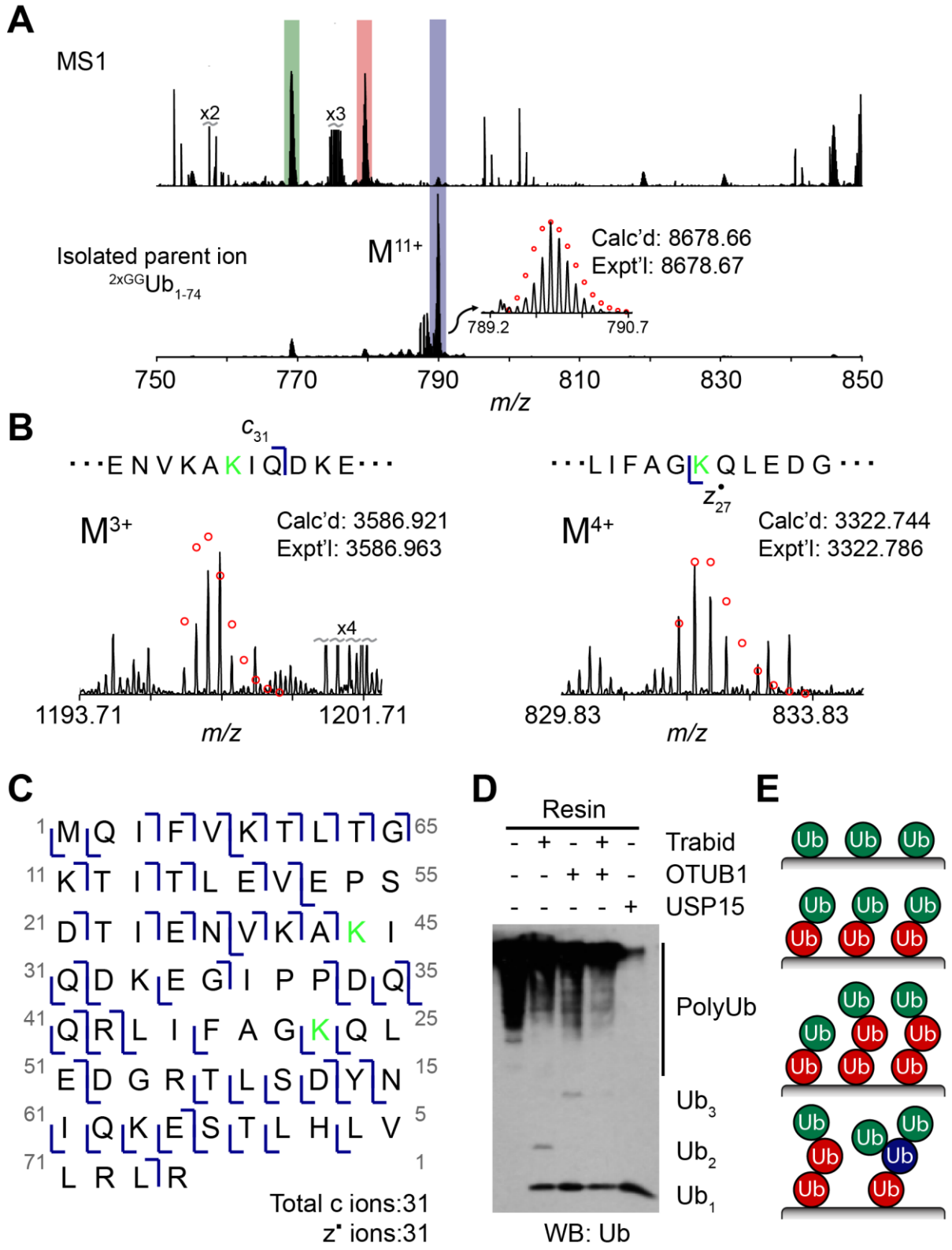
A
MS1
x2
x3
Isolated parent ion
2xGGUb1-74
M11+
Calc'd: 8678.66
Expt'l: 8678.67
789.2
790.7
750
770
790
810
830
850
m/z
B
c31
···E N V K A K I Q D K E···
M3+
Calc'd: 3586.921
Expt'l: 3586.963
x4
1193.71
1201.71
m/z
···L I F A G K Q L E D G···
z•27
M4+
Calc'd: 3322.744
Expt'l: 3322.786
829.83
833.83
m/z
C
1 M Q I F V K T L T G 65
11 K T I T L E V E P S 55
21 D T I E N V K A K I 45
31 Q D K E G I P P D Q 35
41 Q R L I F A G K Q L 25
51 E D G R T L S D Y N 15
61 I Q K E S T L H L V 5
71 L R L R 1
Total c ions:31
z• ions:31
D
Resin
- + - + - Trabid
- - + + - OTUB1
- - - - + USP15
PolyUb
Ub3
Ub2
Ub1
WB: Ub
E
Ub

Figure 3. 4: Characterization of Ub chains isolated with Halo-NZF1 by ECD and DUB restriction analysis uncovers K29/K48 branched chains. A) ESI MS analysis of the minimally digested Ub chains isolated from HEK cells treated with 10µM MG132 for 2 hr. The spectra correspond to the Ub^{11+} charge state, where the top spectrum shows all ions present in the mass range and the bottom spectrum shows the isolated $^{2xGG}Ub_{1-74}$ M^{11+} parent ion. The red circles represent theoretical isotopic abundance distributions of the isotopomer peaks. calc'd – calculated most abundant weight; expt'l – experimental most abundant molecular weight. **B**) Analysis of ECD fragments showing the presence of a di-Gly modification at K29 and K48. The green K shows the position of a modified lysine. **C**) Observed ECD fragments (*c* and *z* $^{\bullet}$ ions) mapped onto the sequence of Ub containing a di-Gly modification at K29 and K48. **D**) DUB restriction analysis of Ub chains isolated from MG132 treated cells using Halo-NZF1 resin. Aliquots of this resin were incubated with the indicated DUBs overnight at 37^{o}C. The reaction mixtures were quenched with 6x Laemmli loading dye, separated on a 15% SDS-PAGE gel and analyzed by western blot using anti-Ub antibody (P4D1). **E**) Cartoon depicting one possible topology of chains isolated with Halo-NZF1, where Ub_{1-74}, $^{GG}Ub_{1-74}$, and $^{2xGG}Ub_{1-74}$ are colored green, red and blue respectively.

We then performed ETD analysis on the M^{11+} charge state of $^{GG}Ub_{1-74}$ to identify other possible linkages. From the fragmentation patterns, it is evident that K48 linkages predominate (Figure 3.S.9), suggesting many of the isolated ubiquitylated proteins are modified with multiple mono Ub that are poor substrates for the linkage selective DUBs employed in our chain restriction digests. Based on these results along with the MS data, we propose that most of the isolated proteins are carrying multi-mono-Ub modifications along with short chains linked through K29 and K48 (Figure 3.4 E). Our middle-down MS approach therefore informs on the overall landscape of Ub modifications and chain configuration.

3.4.3 Ensuring Maximal Detection of the Ub Chain Population by UbiCHEM-MS.

Optimizing the conditions for restricted trypsinolysis is critical for detecting all three Ub_{1-74} species. For instance, the use of denaturants commonly used to elute Ub chains from UBD resins must be avoided to ensure minimal cleavage.[48] In our case, this was achieved by performing trypsinolysis reactions on resin. Another important issue is the amount of lysate required to observe low abundant modifications such as branching. We empirically found a ratio of resin to lysate of 3-4 µL of resin per mg of lysate consistently leads to the detection of branched chains. Over-digestion of resin-bound chains is another problem we encountered. To avoid this, we performed a time course analysis to find the optimal trypsin concentration. As evidenced by the formation of di-Ub and mono-Ub, we observe complete conversion of high molecular weight chains within 16 h using 1 µg of trypsin per 18 mg of lysate for untreated cells and 1 µg of trypsin per 6 mg of lysate for cells treated with MG132 (Figure 3.S.1, 3.S.10 and Table 3.S.1).

Pull-down efficiency is also a concern. This was assessed through recapture experiments in which fractions from a flow through were further incubated with fresh batch of resin. We performed these experiments with cell lysates from both the 0 and 16 h MG132 treatments. Western blot analysis shows that for the untreated cells (0 h) most of the available Ub chains are captured (Figure 3.S.11). However, with cell lysates from the 16 h MG132 treatment, an appreciable amount of Ub species escape the first pull-down and are recaptured by fresh resin (Figure 3.S.11). This is not surprising considering MG132 treatment leads to a dramatic boost in the global levels of Ub chains, which will affect the Ub to resin ratio.[12] Despite the inability to capture all the Ub chains in the initial round of pull-downs, middle-down MS shows the chains isolated from the second round have the same architecture as those from the first. These results indicate that our pull-down conditions are sufficient to yield a complete picture of the Ub landscape.

3.4.4. UbiChEM-MS is Not Limited by Instrumental Setup

For the UbiChEM-MS workflow we used different separation and characterization methods. With the TUBEs, online RPLC separation was coupled to a TOF mass spectrometer. With the NZF1 domain, RPLC was performed offline and analytes were then directly introduced into an Orbitrap mass spectrometer. Despite these differences, similar Ub architectures are observed from experiment-to-experiment and instrument-to-instrument. These results highlight the reproducibility and accessibility of our method.

3.5 Conclusion

Although a number of studies have implicated heterotypic Ub chains in the regulation of fundamental cellular pathways, the precise configuration of these chains has largely remained unknown.[1-3, 5, 13] In this study, we established Ubiquitin Chain Enrichment Middle-down Mass Spectrometry (UbiChEM-MS), as a method for detecting and quantifying the relative abundance of heterotypic branched chains in cell lysates. Using two different UBDs, we demonstrate that the dynamics of Ub chains branched chains containing K29 linkages as well as global Ub pool in response to MG132 treatment. From these experiments we found that while chain branching does indeed increase in response to proteasome inhibition, branched chains containing K29 linkages are likely to be a non-degradative signal. Our work thus expands the known role of branched Ub chains beyond just proteasome targeting signals.

Our strategy of using UBDs coupled with middle-down MS to detect and quantify relative amounts of branched chains has several advantages. First, it enables unambiguous detection of branching using endogenous levels of Ub chains. This avoids the use of Ub mutants, which may provide misleading results. Second, it exploits the selectivity of certain UBDs to examine the architecture of chains harboring specific linkages. Third, it distinguishes between mono-Ub/chain end caps, the linear portion of a chain, and branch points. This is powerful because the relative changes in each of these species can be monitored under different cellular conditions.

3.6 Acknowledgements

This work was supported by research grant RO1GM110543 from the National Institutes of Health (NIH) and the National Science Foundation (NSF) Graduate Research Fellowship Program (GRFP, award number: 1451512). The purchase of the Bruker ULTRAFLEX™ III in 2008 was partially funded by NIH NCRR 1S10RR024601-01 Award to the University of Wisconsin-Madison Department of Chemistry. T*he data described herein were acquired on an Orbitrap Fusion mass spectrometer funded by National Institutes of Health grant 1S10OD010645-01A1.*

3.7 References

1. Nakayama, K. I.; Nakayama, K., Ubiquitin ligases: cell-cycle control and cancer. *Nat. Rev. Cancer* **2006,** *6* (5), 369-381.

2. Jackson, Stephen P.; Durocher, D., Regulation of DNA Damage Responses by Ubiquitin and SUMO. *Mol. Cell* **2013,** *49* (5), 795-807.

3. Liu, Y.-C., Ubiquitin Ligases and the Immune Response. *Annu. Rev. Immunol.* **2004,** *22* (1), 81-127.

4. Hershko, A.; Ciechanover, A., The Ubiquitin System. *Annu. Rev. Biochem.* **1998,** *67* (1), 425-479.

5. Komander, D.; Rape, M., The ubiquitin code. *Annu. Rev. Biochem.* **2012,** *81*, 203-29.

6. Yau, R.; Rape, M., The increasing complexity of the ubiquitin code. *Nat. Cell Biol.* **2016,** *18* (6), 579-586.

7. Swatek, K. N.; Komander, D., Ubiquitin modifications. *Cell. Res.* **2016,** *26* (4), 399-422.

8. Jin, L.; Williamson, A.; Banerjee, S.; Philipp, I.; Rape, M., Mechanism of Ubiquitin-Chain Formation by the Human Anaphase-Promoting Complex. *Cell 133* (4), 653-665.

9. Chau, V.; Tobias, J.; Bachmair, A.; Marriott, D.; Ecker, D.; Gonda, D.; Varshavsky, A., A multiubiquitin chain is confined to specific lysine in a targeted short-lived protein. *Science* **1989,** *243* (4898), 1576-1583.

10. Thrower, J. S.; Hoffman, L.; Rechsteiner, M.; Pickart, C. M., Recognition of the polyubiquitin proteolytic signal. *EMBO J.* **2000**, *19*, 94-102.

11. Jacobson, A. D.; Zhang, N.-Y.; Xu, P.; Han, K.-J.; Noone, S.; Peng, J.; Liu, C.-W., The Lysine 48 and Lysine 63 Ubiquitin Conjugates Are Processed Differently by the 26 S Proteasome. *J. Biol. Chem.* **2009,** *284* (51), 35485-35494.

12. Xu, P.; Duong, D. M.; Seyfried, N. T.; Cheng, D.; Xie, Y.; Robert, J.; Rush, J.; Hochstrasser, M.; Finley, D.; Peng, J., Quantitative Proteomics Reveals the Function of Unconventional Ubiquitin Chains in Proteasomal Degradation. *Cell* **2009,** *137* (1), 133-145.

13. Haglund, K.; Dikic, I., Ubiquitylation and cell signaling. *EMBO J.* **2005,** *24* (19), 3353-3359.

14. Gerlach, B.; Cordier, S. M.; Schmukle, A. C.; Emmerich, C. H.; Rieser, E.; Haas, T. L.; Webb, A. I.; Rickard, J. A.; Anderton, H.; Wong, W. W. L.; Nachbur, U.; Gangoda, L.; Warnken, U.; Purcell, A. W.; Silke, J.; Walczak, H., Linear ubiquitination prevents inflammation and regulates immune signalling. *Nature* **2011,** *471* (7340), 591-596.

15. Ikeda, F.; Deribe, Y. L.; Skanland, S. S.; Stieglitz, B.; Grabbe, C.; Franz-Wachtel, M.; van Wijk, S. J. L.; Goswami, P.; Nagy, V.; Terzic, J.; Tokunaga, F.; Androulidaki, A.; Nakagawa, T.; Pasparakis, M.; Iwai, K.; Sundberg, J. P.; Schaefer, L.; Rittinger, K.; Macek, B.; Dikic, I., SHARPIN forms a linear ubiquitin ligase complex regulating NF-[kgr]B activity and apoptosis. *Nature* **2011,** *471* (7340), 637-641.

16. Kim, H. T.; Kim, K. P.; Lledias, F.; Kisselev, A. F.; Scaglione, K. M.; Skowyra, D.; Gygi, S. P.; Goldberg, A. L., Certain Pairs of Ubiquitin-conjugating Enzymes (E2s) and Ubiquitin-Protein Ligases (E3s) Synthesize Nondegradable Forked Ubiquitin Chains Containing All Possible Isopeptide Linkages. *J. Biol. Chem.* **2007,** *282* (24), 17375-17386.

17. Peng, J.; Schwartz, D.; Elias, J. E.; Thoreen, C. C.; Cheng, D.; Marsischky, G.; Roelofs, J.; Finley, D.; Gygi, S. P., A proteomics approach to understanding protein ubiquitination. *Nat. Biotech.* **2003,** *21* (8), 921-926.

18. Kim, H. T.; Kim, K. P.; Uchiki, T.; Gygi, S. P.; Goldberg, A. L., S5a promotes protein degradation by blocking synthesis of nondegradable forked ubiquitin chains. *EMBO J.* **2009,** *28* (13), 1867-1877.

19. Grice, Guinevere L.; Lobb, Ian T.; Weekes, Michael P.; Gygi, Steven P.; Antrobus, R.; Nathan, James A., The Proteasome Distinguishes between Heterotypic and Homotypic Lysine-11-Linked Polyubiquitin Chains. *Cell Rep. 12* (4), 545-553.

20. Meyer, H.-J.; Rape, M., Enhanced Protein Degradation by Branched Ubiquitin Chains. *Cell* **2014,** *157* (4), 910-921.

21. Emmerich, C. H.; Ordureau, A.; Strickson, S.; Arthur, J. S. C.; Pedrioli, P. G. A.; Komander, D.; Cohen, P., Activation of the canonical IKK complex by K63/M1-linked hybrid ubiquitin chains. *Proc. Natl. Acad. Sc. USA.* **2013,** *110* (38), 15247-15252.

22. Emmerich, C. H.; Bakshi, S.; Kelsall, I. R.; Ortiz-Guerrero, J.; Shpiro, N.; Cohen, P., Lys63/Met1-hybrid ubiquitin chains are commonly formed during the activation of innate immune signalling. *Biochem. Biophys. Res. Commun.* **2016,** *474* (3), 452-461.

23. Boname, J. M.; Thomas, M.; Stagg, H. R.; Xu, P.; Peng, J.; Lehner, P. J., Efficient Internalization of MHC I Requires Lysine-11 and Lysine-63 Mixed Linkage Polyubiquitin Chains. *Traffic* **2010,** *11* (2), 210-220.

24. Goto, E.; Yamanaka, Y.; Ishikawa, A.; Aoki-Kawasumi, M.; Mito-Yoshida, M.; Ohmura-Hoshino, M.; Matsuki, Y.; Kajikawa, M.; Hirano, H.; Ishido, S., Contribution of Lysine 11-linked Ubiquitination to

MIR2-mediated Major Histocompatibility Complex Class I Internalization. *J. Biol. Chem.* **2010,** *285* (46), 35311-35319.

25. Saeki, Y.; Tayama, Y.; Toh-e, A.; Yokosawa, H., Definitive evidence for Ufd2-catalyzed elongation of the ubiquitin chain through Lys48 linkage. *Biochem. Biophys. Res. Commun.* **2004,** *320* (3), 840-845.

26. Koegl, M.; Hoppe, T.; Schlenker, S.; Ulrich, H. D.; Mayer, T. U.; Jentsch, S., A Novel Ubiquitination Factor, E4, Is Involved in Multiubiquitin Chain Assembly. *Cell 96* (5), 635-644.

27. Xu, P.; Peng, J., Characterization of Polyubiquitin Chain Structure by Middle-down Mass Spectrometry. *Anal. Chem.* **2008,** *80* (9), 3438-3444.

28. Valkevich, E. M.; Sanchez, N. A.; Ge, Y.; Strieter, E. R., Middle-Down Mass Spectrometry Enables Characterization of Branched Ubiquitin Chains. *Biochemistry* **2014,** *53* (30), 4979-4989.

29. Lee, A. E.; Castañeda, C. A.; Wang, Y.; Fushman, D.; Fenselau, C., Preparing to read the ubiquitin code: a middle-out strategy for characterization of all lysine-linked diubiquitins. *J. Mass Spectrom.* **2014,** *49* (12), 1272-1278.

30. Lee, A. E.; Geis-Asteggiante, L.; Dixon, E. K.; Kim, Y.; Kashyap, T. R.; Wang, Y.; Fushman, D.; Fenselau, C., Preparing to read the ubiquitin code: characterization of ubiquitin trimers by top-down mass spectrometry. *J. Mass Spectrom.* **2016,** *51* (4), 315-321.

31. Lee, A. E.; Geis-Asteggiante, L.; Dixon, E. K.; Miller, M.; Wang, Y.; Fushman, D.; Fenselau, C., Preparing to read the ubiquitin code: top-down analysis of unanchored ubiquitin tetramers. *J. Mass Spectrom.* **2016,** *51* (8), 629-637.

32. Wilkinson, K. D.; Audhya, T. K., Stimulation of ATP-dependent proteolysis requires ubiquitin with the COOH-terminal sequence Arg-Gly-Gly. *J. Biol. Chem.* **1981,** *256* (17), 9235-9241.

33. Husnjak, K.; Dikic, I., Ubiquitin-Binding Proteins: Decoders of Ubiquitin-Mediated Cellular Functions. *Annu. Rev. Biochem.* **2012,** *81* (1), 291-322.

34. Guner, H.; Close, P. L.; Cai, W.; Zhang, H.; Peng, Y.; Gregorich, Z. R.; Ge, Y., MASH Suite: A User-Friendly and Versatile Software Interface for High-Resolution Mass Spectrometry Data Interpretation and Visualization. *J. Am. Soc. Mass Spectrom.* **2014,** *25* (3), 464-470.

35. Peng, Y.; Gregorich, Z. R.; Valeja, S. G.; Zhang, H.; Cai, W.; Chen, Y.-C.; Guner, H.; Chen, A. J.; Schwahn, D. J.; Hacker, T. A.; Liu, X.; Ge, Y., Top-down Proteomics Reveals Concerted Reductions in Myofilament and Z-disc Protein Phosphorylation after Acute Myocardial Infarction. *Mol. Cell. Proteomics* **2014,** *13* (10), 2752-2764.

36. Chen, Y.-C.; Ayaz-Guner, S.; Peng, Y.; Lane, N. M.; Locher, M. R.; Kohmoto, T.; Larsson, L.; Moss, R. L.; Ge, Y., Effective Top-Down LC/MS+ Method for Assessing Actin Isoforms as a Potential Cardiac Disease Marker. *Anal. Chem.* **2015,** *87* (16), 8399-8406.

37. Hjerpe, R.; Aillet, F.; Lopitz-Otsoa, F.; Lang, V.; England, P.; Rodriguez, M. S., Efficient protection and isolation of ubiquitylated proteins using tandem ubiquitin-binding entities. *EMBO Rep.* **2009,** *10* (11), 1250-1258.

38. Kristariyanto, Y. A.; A. Re, Syed A.; Campbell, D. G.; Morrice, N. A.; Johnson, C.; Toth, R.; Kulathu, Y., K29-Selective Ubiquitin Binding Domain Reveals Structural Basis of Specificity and Heterotypic Nature of K29 Polyubiquitin. *Mol. Cell* **2015**, *58* (1), 83-94.

39. Scott, D.; Oldham, N. J.; Strachan, J.; Searle, M. S.; Layfield, R., Ubiquitin-binding domains: Mechanisms of ubiquitin recognition and use as tools to investigate ubiquitin-modified proteomes. *Proteomics* **2015,** *15* (5-6), 844-861.

40. Los, G. V.; Encell, L. P.; McDougall, M. G.; Hartzell, D. D.; Karassina, N.; Zimprich, C.; Wood, M. G.; Learish, R.; Ohana, R. F.; Urh, M.; Simpson, D.; Mendez, J.; Zimmerman, K.; Otto, P.; Vidugiris, G.; Zhu, J.; Darzins, A.; Klaubert, D. H.; Bulleit, R. F.; Wood, K. V., HaloTag: A Novel Protein Labeling Technology for Cell Imaging and Protein Analysis. *ACS Chem. Biol.* **2008,** *3* (6), 373-382.

41. Zubarev, R. A.; Kelleher, N. L.; McLafferty, F. W., Electron Capture Dissociation of Multiply Charged Protein Cations. A Nonergodic Process. *J. Am. Chem. Soc.* **1998,** *120* (13), 3265-3266.

42. Zubarev, R. A.; Horn, D. M.; Fridriksson, E. K.; Kelleher, N. L.; Kruger, N. A.; Lewis, M. A.; Carpenter, B. K.; McLafferty, F. W., Electron Capture Dissociation for Structural Characterization of Multiply Charged Protein Cations. *Anal. Chem.* **2000,** *72* (3), 563-573.

43. Mevissen, Tycho E. T.; Hospenthal, Manuela K.; Geurink, Paul P.; Elliott, Paul R.; Akutsu, M.; Arnaudo, N.; Ekkebus, R.; Kulathu, Y.; Wauer, T.; El Oualid, F.; Freund, Stefan M. V.; Ovaa, H.; Komander, D., OTU Deubiquitinases Reveal Mechanisms of Linkage Specificity and Enable Ubiquitin Chain Restriction Analysis. *Cell* **2013,** *154* (1), 169-184.

44. Hospenthal, M. K.; Mevissen, T. E. T.; Komander, D., Deubiquitinase-based analysis of ubiquitin chain architecture using Ubiquitin Chain Restriction (UbiCRest). *Nat. Protoc.* **2015,** *10* (2), 349-361.

45. Virdee, S.; Ye, Y.; Nguyen, D. P.; Komander, D.; Chin, J. W., Engineered diubiquitin synthesis reveals Lys29-isopeptide specificity of an OTU deubiquitinase. *Nat. Chem. Biol.* **2010,** *6* (10), 750-757.

46. Wang, T.; Yin, L.; Cooper, E. M.; Lai, M.-Y.; Dickey, S.; Pickart, C. M.; Fushman, D.; Wilkinson, K. D.; Cohen, R. E.; Wolberger, C., Evidence for Bidentate Substrate Binding as the Basis for the K48 Linkage Specificity of Otubain 1. *J. Mol. Biol.* **2009,** *386* (4), 1011-1023.

47. Ritorto, M. S.; Ewan, R.; Perez-Oliva, A. B.; Knebel, A.; Buhrlage, S. J.; Wightman, M.; Kelly, S. M.; Wood, N. T.; Virdee, S.; Gray, N. S.; Morrice, N. A.; Alessi, D. R.; Trost, M., Screening of DUB activity and specificity by MALDI-TOF mass spectrometry. *Nat. Commun.* **2014,** *5*.

48. Emmerich, C. H.; Cohen, P., Optimising methods for the preservation, capture and identification of ubiquitin chains and ubiquitylated proteins by immunoblotting. *Biochem. Biophy. Res. Commun.* **2015,** *466* (1), 1-14.

3.8 Supplemental Information

3.8.1. Supplemental Figures and Tables

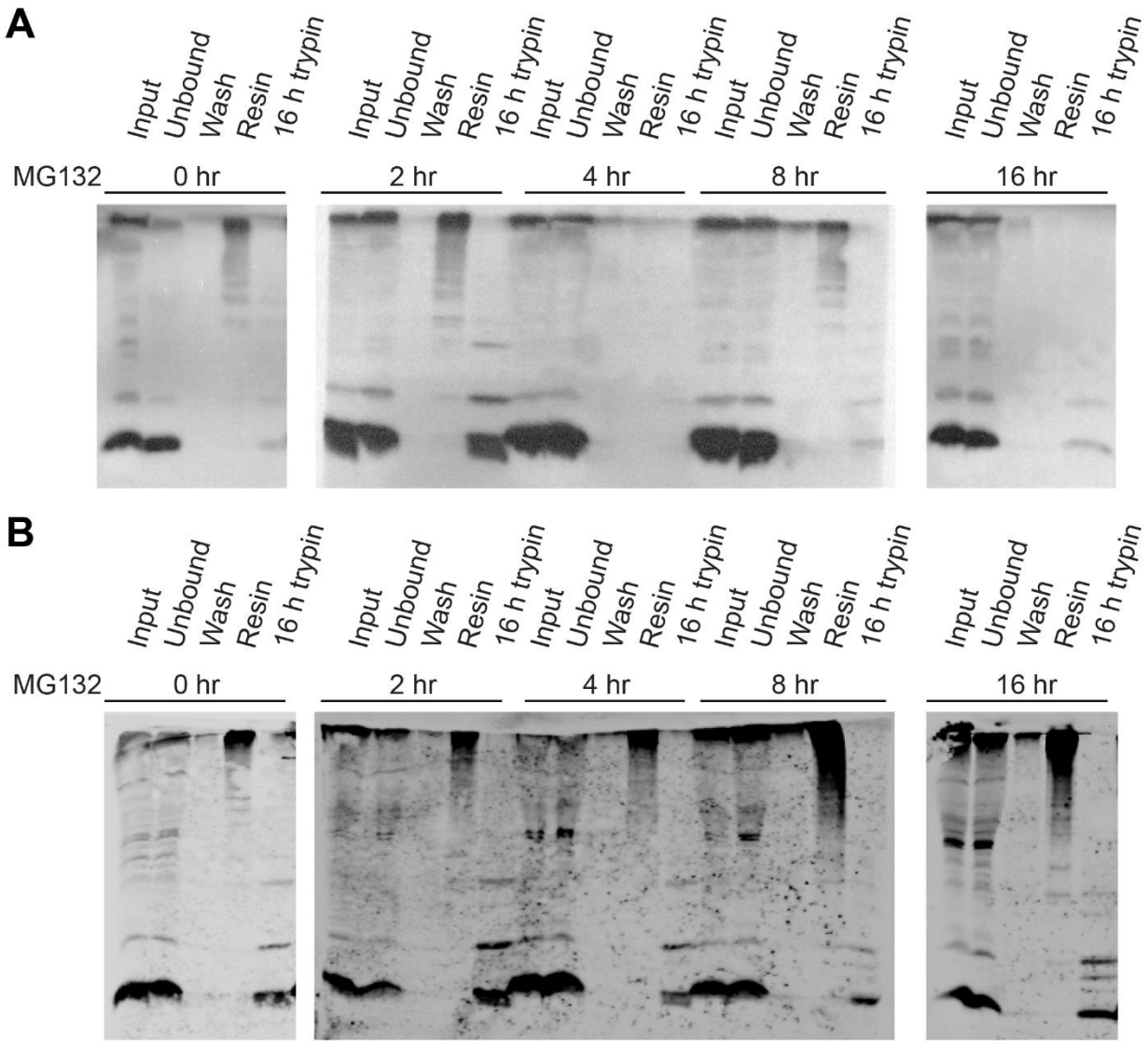

Figure 3.S. 1: Ub chains isolated from cells treated with MG132 at different time points. HEK cells were treated with the proteasome inhibitor MG132 (10 µM) for indicated times prior to harvest and lysis. Lysate was then incubated with **A**) agarose TUBEs and **B**) Halo-NZF1 resin overnight (16hours) at 4°C and

subjected to minimal trypsinolysis described in Table 3. S.1. Samples were separated on a 15 % SDS-PAGE gel and then analyzed by western blot with anti-Ub antibody (P4D1).

Table 3. S.1: Empirically determined optimal ratios of cell lysate to trypsin used throughout this study.

Treatment	Agarose TUBE2 (µL)	Halo-NZF1 resin (µL)	Input lysate (mg)	Trypsin (µg)	Ratio lysate to trypsin (mg:µg)
None	100	-	50	2.5	20:1
None	-	200	45	7.5	18:1
MG132	100	-	50	7.5	6.7:1
MG132	-	200	45	7.5	6:1

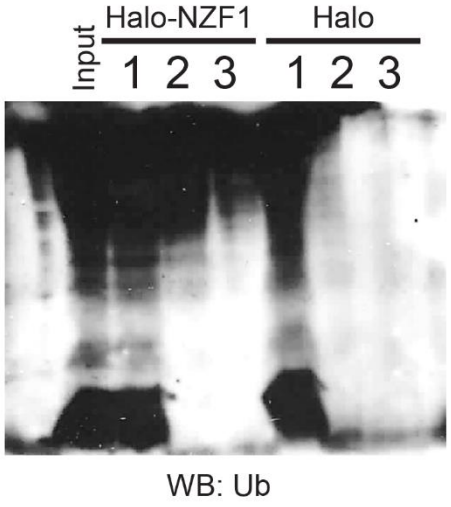

Figure 3. S.2: Halo-NZF1 resin can pull down ubiquitinated proteins from cell lysate while Halo resin alone does not. Lysate from HEK cells treated with MG132 was incubated with HaloLink (Promega) resin modified with either the Halo-NZF1 fusion protein or the Halo protein alone. 1. Flow through 2. Aliquot of

the resin after wash with lysis buffer (see experimental section) 3. Aliquot of supernatant after elution with 0.2M Glycine pH2.5. Samples were analyzed by western blot using anti-Ub antibody (P4D1).

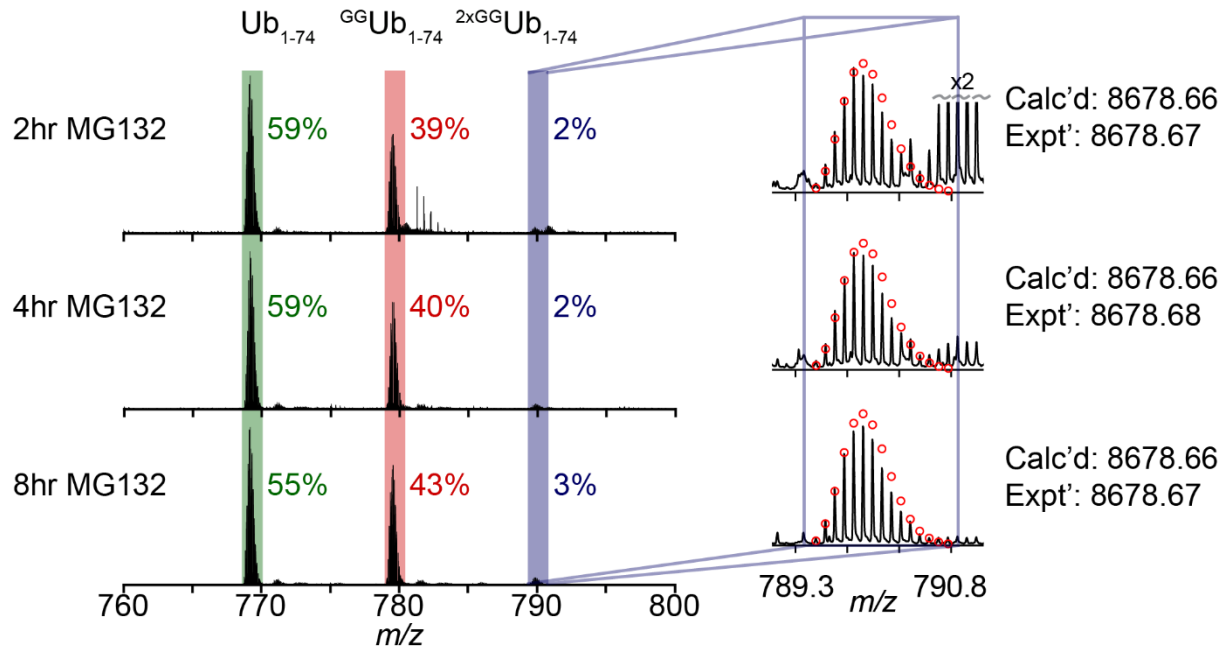

Figure 3. S.3: Representative MS1 data of the M^{11+} charge state for chains isolated from 2hr, 4hr, and 8hr MG132 treatments using agarose TUBEs. HEK cells were treated with 10 µM MG132 for the indicated times followed by UbiChEM-MS workflow using TUBE2. Represented here is the M^{11+} charge state for all three minimally digested Ub products - Ub_{1-74} (green box), $^{GG}Ub_{1-74}$ (red box), and $^{2xGG}Ub_{1-74}$ (blue box). The percentages represent the relative intensities calculated for all three Ub species. Calc'd - calculated most abundant weight; expt'l – experimental most abundant molecular weight.

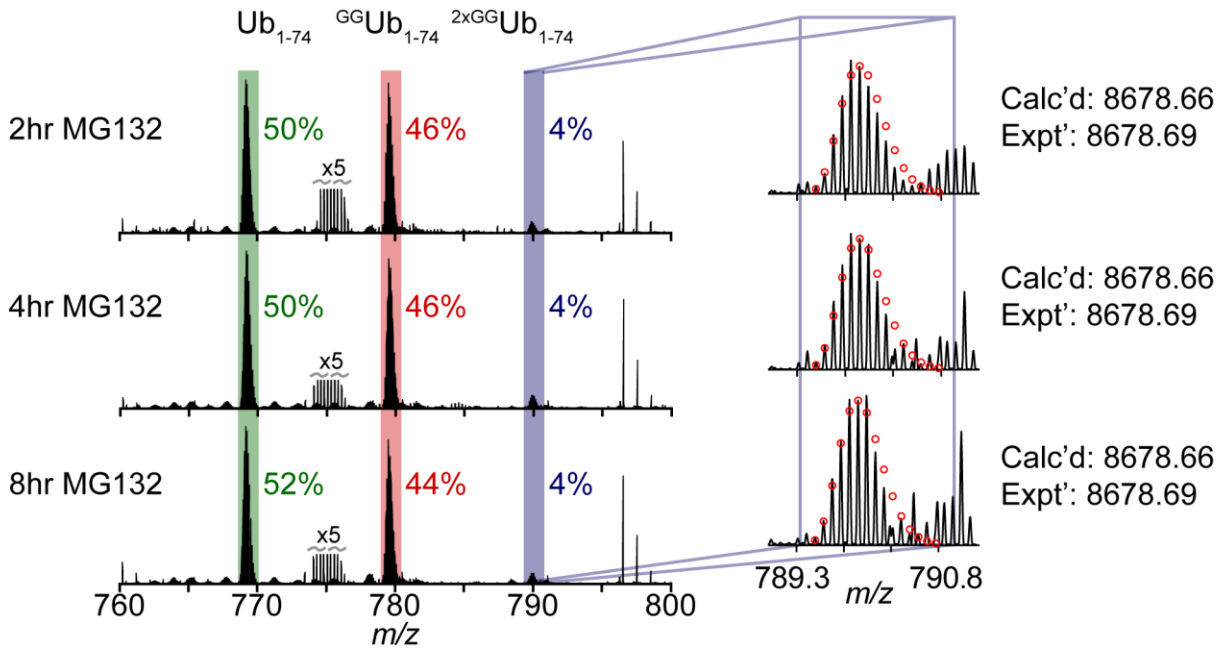

Figure 3. S.4: Representative MS1 data of the M^{11+} charge state for chains isolated from 2hr, 4hr, and 8hr MG132 treatments using Halo-NZF1. HEK cells were treated with 10 µM MG132 for the indicated times followed by UbiChEM-MS workflow using Halo-NZF1. Represented here is the M^{11+} charge state for all three minimally digested Ub products - Ub_{1-74} (green box), $^{GG}Ub_{1-74}$ (red box), and $^{2xGG}Ub_{1-74}$ (blue box). The percentages represent the relative intensities calculated for all three Ub species. Calc'd - calculated most abundant weight; expt'l – experimental most abundant molecular weight.

Table 3. S.2: Table of data used to make bar graph in Figure 3.2 for chains isolated with agarose TUBE2.

	Relative Abundance										
	Bio Rep1			Bio Rep 2			Bio Rep 3			Mean	SEM
	TR1	TR2	TR3	TR1	TR2	TR3	TR1	TR2	TR3		
Untreated											
Ub_{1-74}	56.0%	57.2%	57.2%	71.0%	70.6%	69.4%	45.5%	59.9%	59.6%	60.7%	2.8%
$^{GG}Ub_{1-74}$	42.7%	41.6%	41.6%	28.5%	28.8%	30.0%	51.9%	37.6%	38.3%	37.9%	2.6%
$^{2xGG}Ub_{1-74}$	1.3%	1.2%	1.2%	0.5%	0.5%	0.7%	2.7%	2.5%	2.2%	1.4%	0.3%
2hr MG132											
Ub_{1-74}	59.0%	58.8%	59.6%	66.0%	65.6%	67.7%	47.3%	47.2%	47.1%	57.6%	2.8%
$^{GG}Ub_{1-74}$	39.5%	39.7%	39.1%	33.2%	33.5%	31.3%	49.2%	49.5%	49.7%	40.5%	2.4%
$^{2xGG}Ub_{1-74}$	1.5%	1.5%	1.3%	0.8%	1.0%	1.0%	3.6%	3.3%	3.2%	1.9%	0.4%
4hr MG132											
Ub_{1-74}	58.0%	58.6%	58.3%	58.3%	58.3%	58.2%	48.0%	48.8%	47.9%	54.9%	1.7%
$^{GG}Ub_{1-74}$	40.9%	40.4%	40.7%	40.2%	40.2%	40.3%	50.8%	50.7%	50.8%	43.9%	1.7%
$^{2xGG}Ub_{1-74}$	1.1%	1.0%	1.1%	1.5%	1.5%	1.5%	1.2%	0.6%	1.3%	1.2%	0.1%
8hr MG132											
Ub_{1-74}	55.1%	58.1%	59.2%	51.6%	51.2%	48.4%	48.2%	48.1%	46.6%	51.8%	1.5%
$^{GG}Ub_{1-74}$	43.2%	40.3%	39.3%	45.4%	45.8%	49.9%	49.4%	49.5%	50.7%	45.9%	1.4%
$^{2xGG}Ub_{1-74}$	1.7%	1.5%	1.5%	3.0%	3.0%	1.8%	2.4%	2.4%	2.7%	2.2%	0.2%
16hr MG132											
Ub_{1-74}	45.3%	45.2%	45.0%	43.3%	43.1%	41.6%	43.7%	43.8%	44.3%	43.9%	0.4%
$^{GG}Ub_{1-74}$	51.2%	51.4%	51.6%	52.5%	52.9%	54.3%	52.8%	52.7%	52.1%	52.4%	0.3%
$^{2xGG}Ub_{1-74}$	3.5%	3.4%	3.4%	4.2%	4.0%	4.1%	3.5%	3.5%	3.6%	3.7%	0.1%

Bio Rep – Biological Replicates, TR – Technical Replicates, Mean – average across all biological and technical replicates, SEM – standard error of the mean

Table 3. S.3: Table of data used to make bar graph in Figure 3.3 for chains isolated with Halo-NZF1 domain.

	Relative Abundance				
	Bio Rep1	Bio Rep2	Bio Rep2	Mean	SEM
Untreated					
Ub1-74	54.3 %	47.9 %	53.7 %	51.9 %	2.1 %
Ub1-74 1xGG	41.1 %	49.0 %	42.0 %	44.0 %	2.5 %
Ub1-74 2xGG	4.6 %	3.1 %	4.3 %	4.0 %	0.45 %
2 hr MG132					
Ub1-74	49.7 %	52.3 %	52.1 %	51.4 %	0.83 %
Ub1-74 1xGG	46.5 %	44.7 %	44.9 %	45.4 %	0.56 %
Ub1-74 2xGG	3.8 %	3.0 %	3.1 %	3.3 %	0.26 %
4 hr MG132					
Ub1-74	49.9 %	52.6 %	52.5 %	51.7 %	0.89 %
Ub1-74 1xGG	45.7 %	43.9 %	44.0 %	44.5 %	0.59 %
Ub1-74 2xGG	4.4 %	3.5 %	3.5 %	3.8 %	0.30 %
8 hr MG132					
Ub1-74	52.6 %	53.9 %	54.1 %	53.5 %	0.49 %
Ub1-74 1xGG	44.1 %	43.4 %	43.1 %	43.5 %	0.28 %
Ub1-74 2xGG	3.4 %	2.7 %	2.7 %	2.9 %	0.22 %
16hr MG132					
Ub1-74	48.3 %	50.6 %	50.3 %	49.7 %	0.73 %
Ub1-74 1xGG	47.1 %	45.3 %	45.6 %	46.0 %	0.55 %
Ub1-74 2xGG	4.7 %	4.2 %	4.1 %	4.3 %	0.18 %

Bio Rep – Biological Replicates, Mean – average across all biological replicates, SEM – standard error of the mean

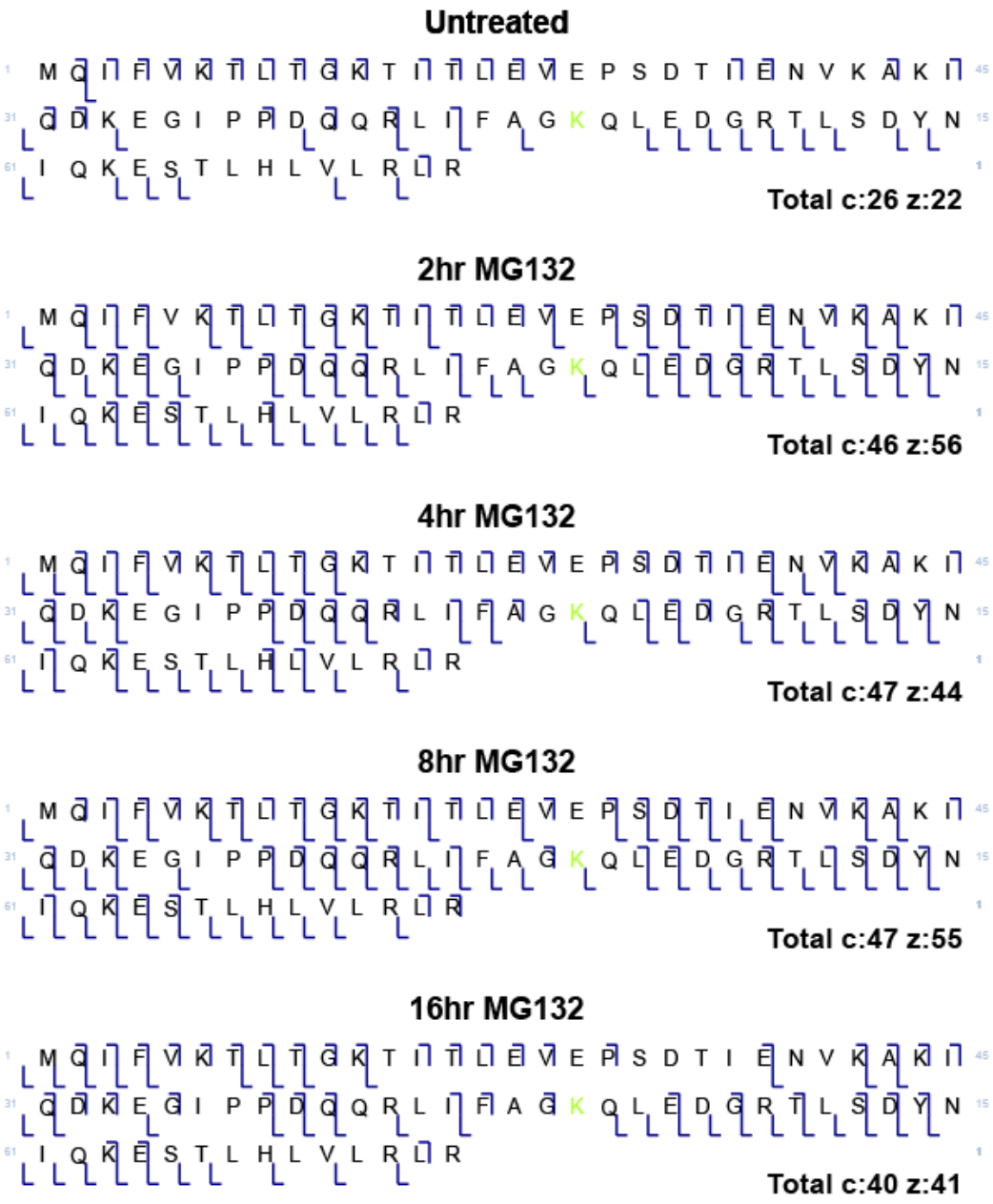

Figure 3.S. 5: ETD analysis of $^{GG}Ub_{1-74}$ for chains isolated using agarose TUBEs. Map of ETD fragments that show $^{GG}Ub_{1-74}$ is primarily K48 linked Ub from untreated and MG132 treated samples.

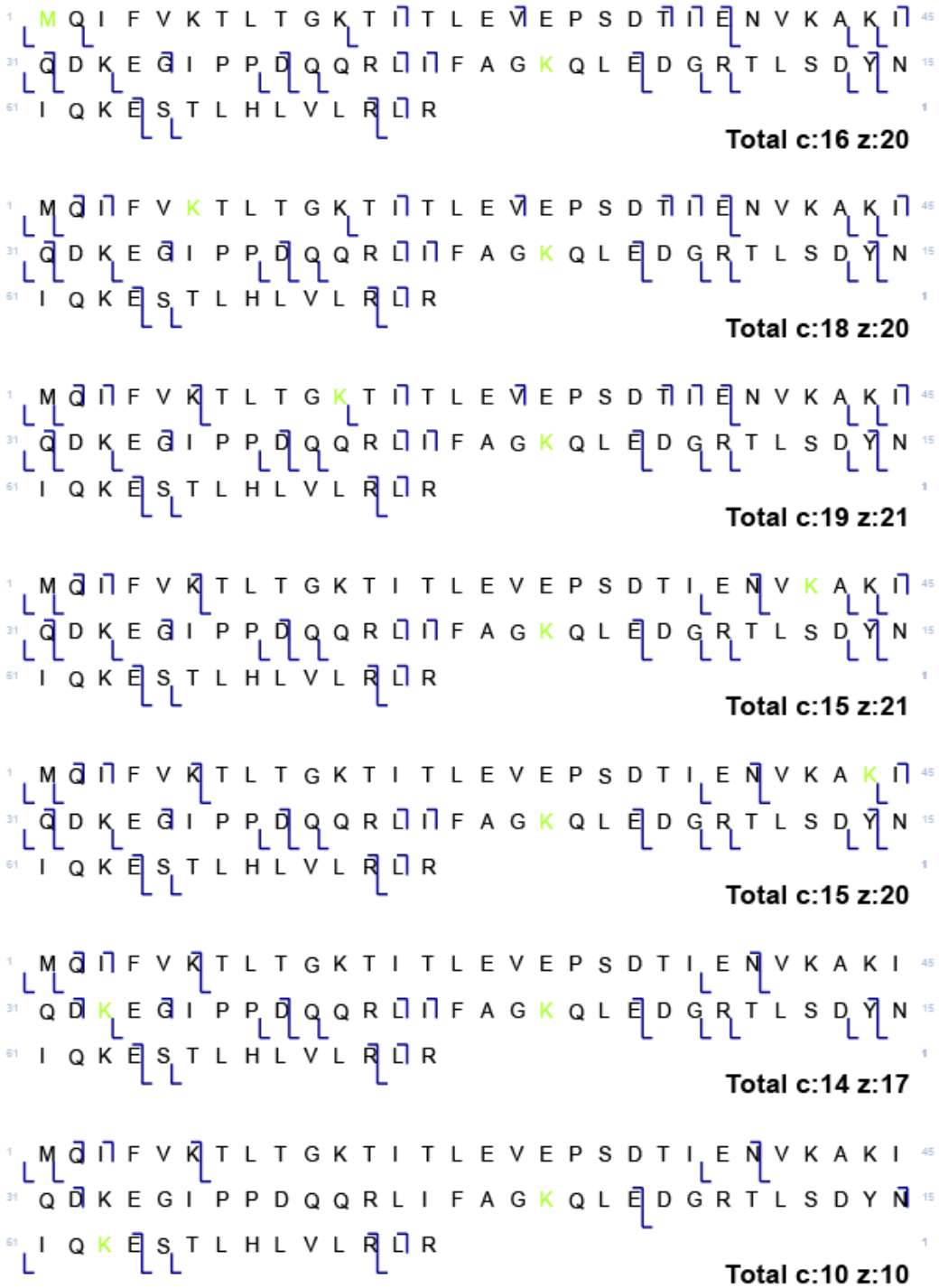

Figure 3. S.6: ETD analysis of $^{2xGG}Ub_{1-74}$ for chains isolated using agarose TUBEs. Map of ETD fragments showing that the absolute configuration for $^{2xGG}Ub_{1-74}$ cannot be unambiguously assigned but is likely to contain a K48 linkage from untreated and MG132 treated samples.

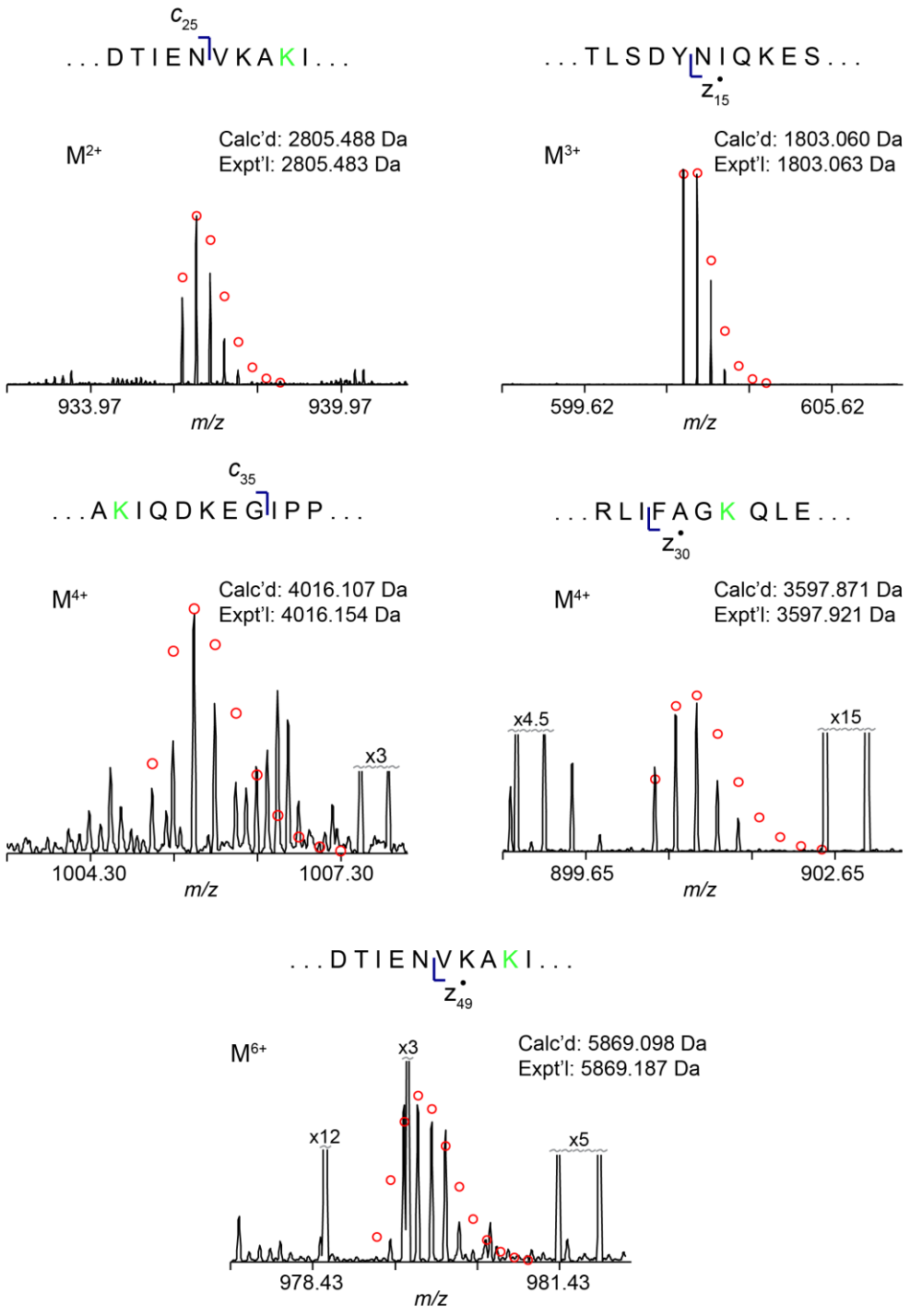

Figure 3. S.7: ETD fragments further supporting the modification of K29 and K48. ETD fragments that show the presence of modification on K29 and K48 as well as a lack of modification on M1, K6, K11, K33 and K63.

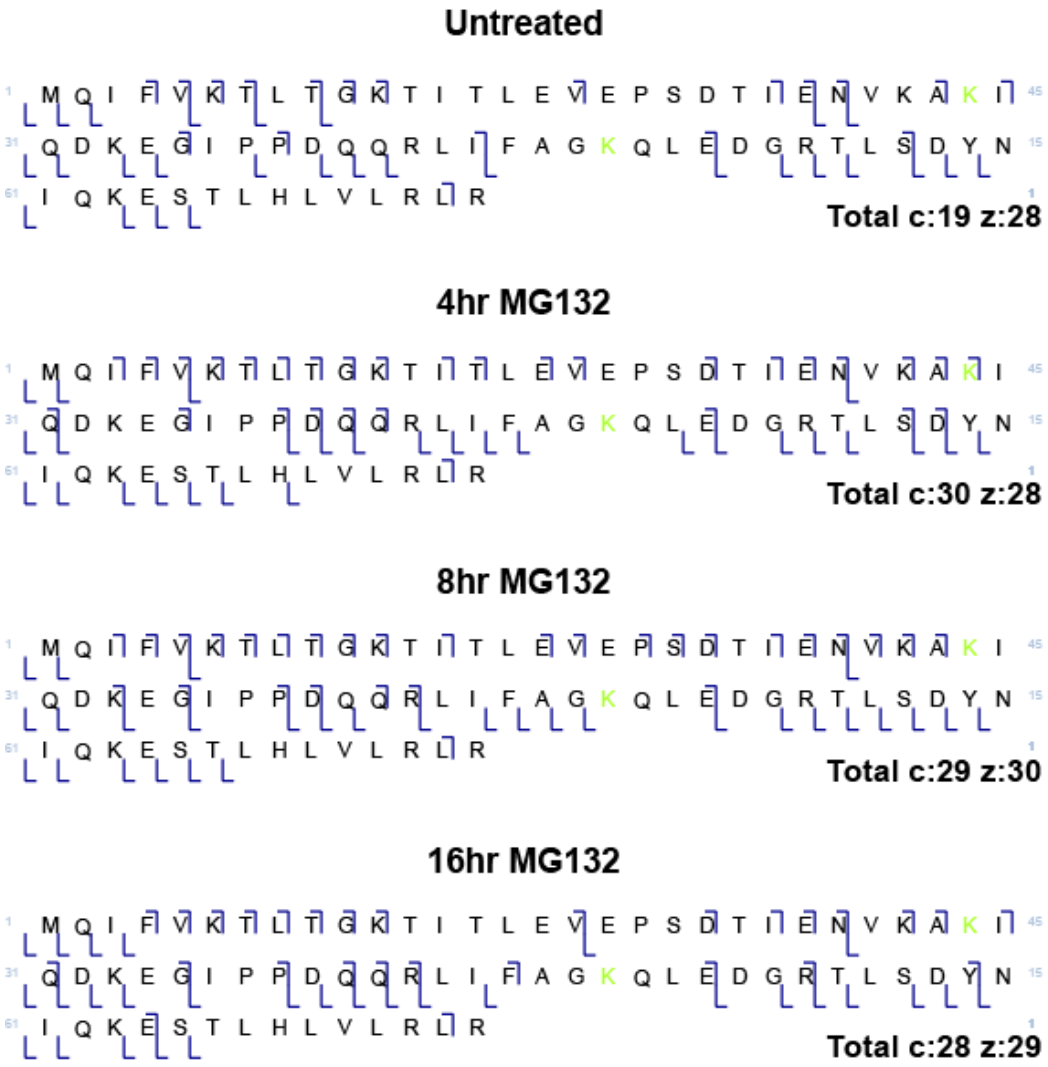

Figure 3. S.8: ETD analysis of $^{2xGG}Ub_{1-74}$ for chains isolated using Halo-NZF1. Map of ETD fragments assigning the $^{2xGG}Ub_{1-74}$ species contains a K29/K48 branched point from untreated and MG132 treated samples.

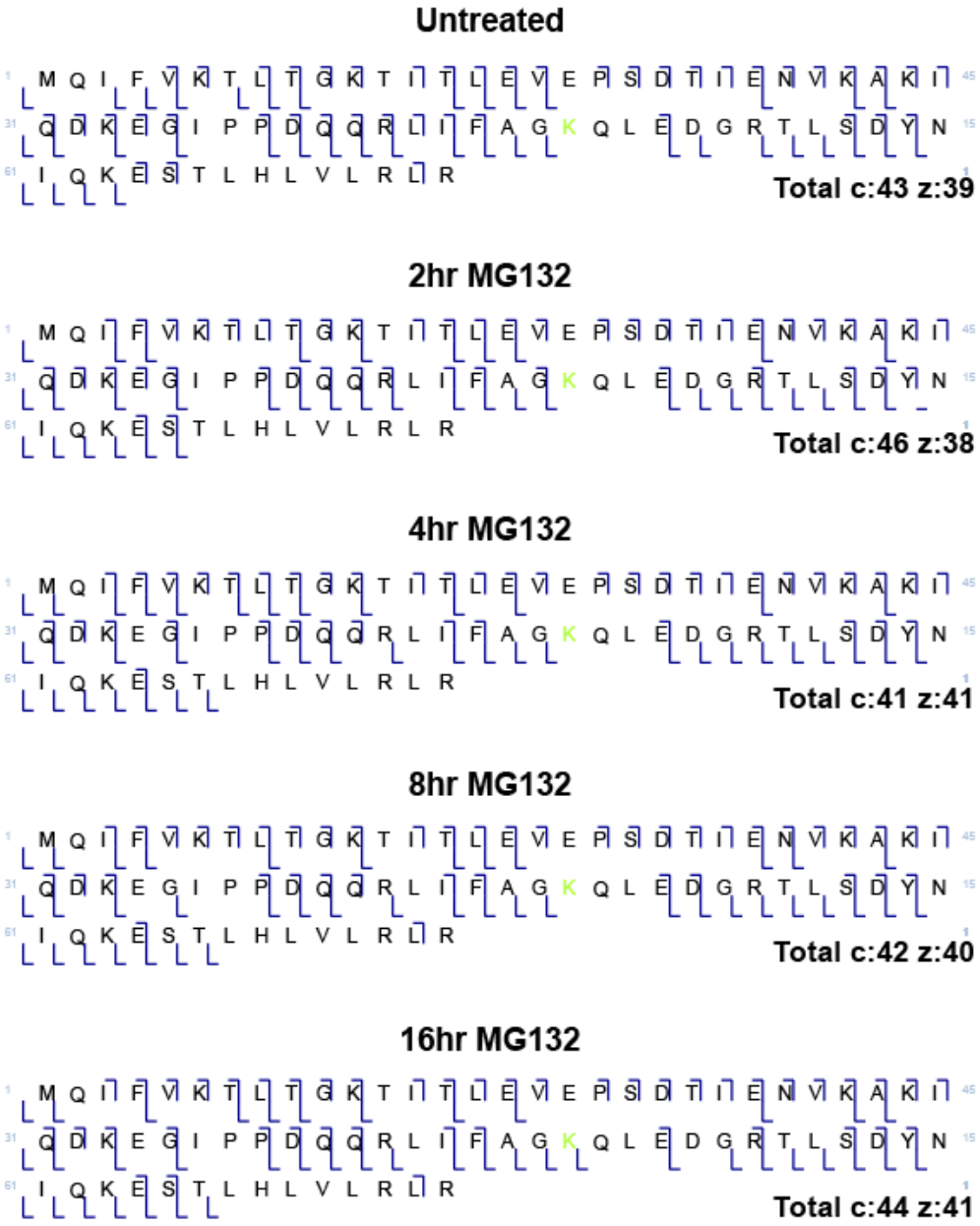

Figure 3. S.9: ETD analysis of $^{GG}Ub_{1-74}$ for chains isolated using Halo-NZF1. Map of ETD fragments that show that $^{GG}Ub_{1-74}$ is primarily K48 linked Ub from untreated and MG132 treated samples.

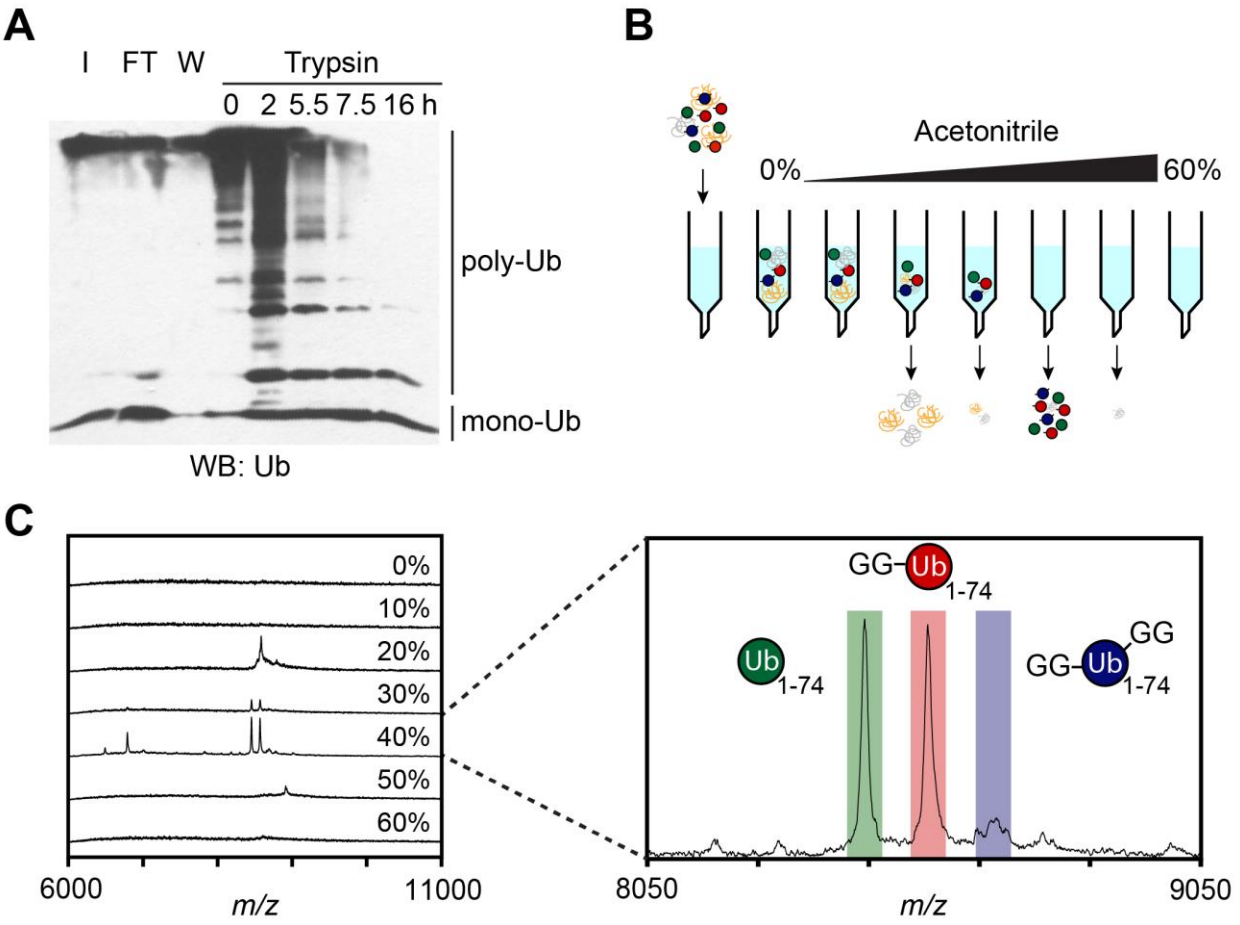

Figure 3. S.10: Optimization of middle-down MS for chains isolated using Halo-NZF1. A) Anti-Ub (P4D1) western blot showing the optimization of minimal tryptic conditions for chains isolated from untreated HEK cells. (left to right) Input lysate, Flow Through, Wash, Resin incubated with 2.5μg trypsin from 0 to 16hours. **B**) Cartoon depicting C18 column purification of minimally digested products. Acidified digests were applied to a 100mg Sep-Pak cartridge (Waters) and washed with an increasing gradient of acetonitrile. **C**) MALDI-TOF analysis of fractions from C18 column (on left). Ub species elutes in the 40% acetonitrile fraction. (on right) A zoomed-in view of 40% acetonitrile fraction showing all three products, Ub_{1-74} (green box), $^{GG}Ub_{1-74}$ (red box), and $^{2xGG}Ub_{1-74}$ (blue box).

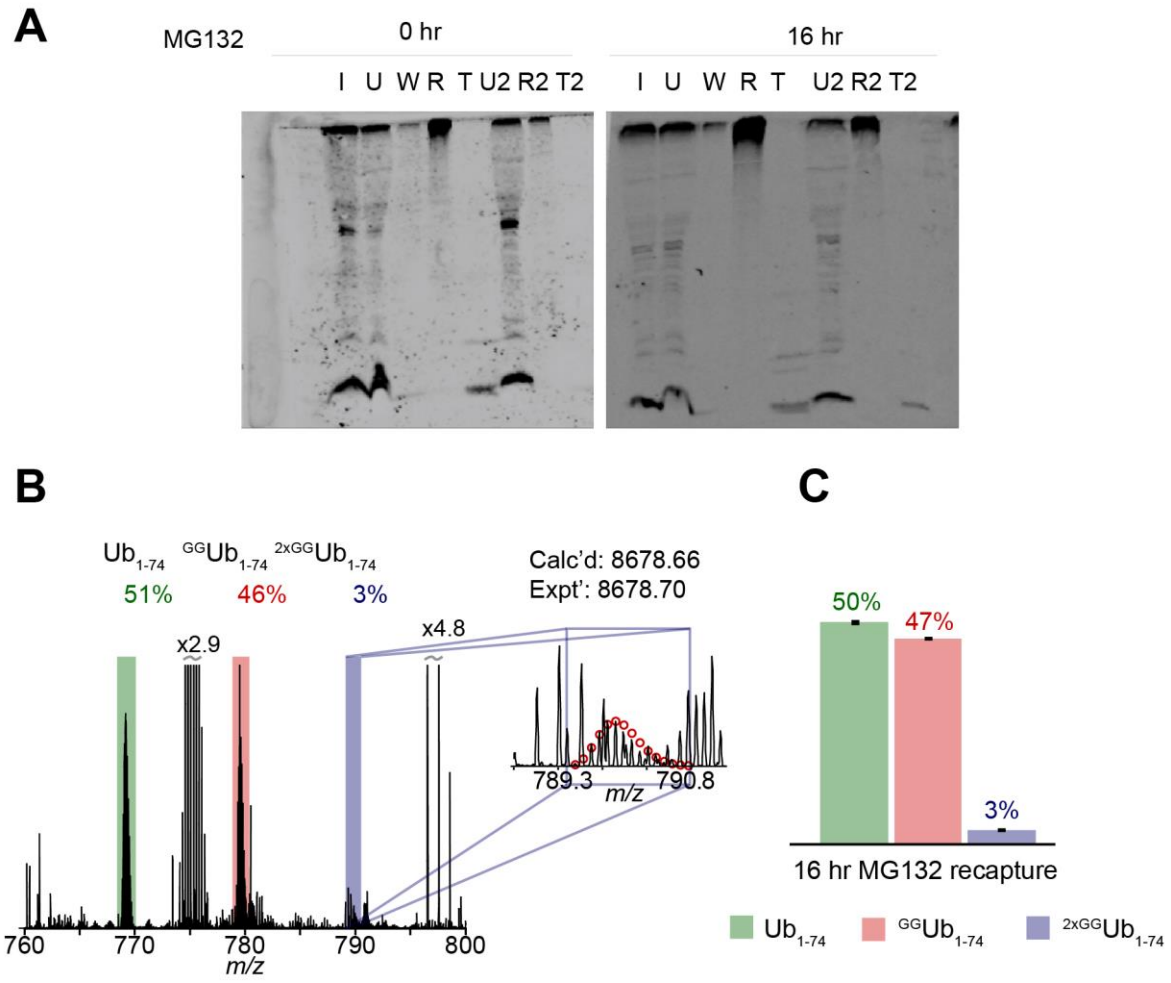

Figure 3. S.11: Results from Halo-NZF1 recapture experiment. A) Western blots analysis of recapture experiments. Ub chains were isolated using Halo-NZF1 by incubating 45mg of HEK lysate with or without 16hr MG132 treatment with 200µL of the resin. The unbound lysate was further incubated with 200µL of fresh resin and the fractions were analyzed by western blot. I = input, U = unbound, W = Wash, R = resin, T = minimal trypsinolysis, U2 = unbound after recapture, R2 = resin after recapture, T2 = minimal tryspinsolysis of recaptured material. **B**) The recaptured minimally trypsinized material from the 16hr MG132 treatment was analyzed by ESI MS. The spectra show the presence of all three minimally digested products - $Ub_{1\text{-}74}$ (green box), $^{GG}Ub_{1\text{-}74}$ (red box), and $^{2xGG}Ub_{1\text{-}74}$ (blue box). The spectra correspond to the Ub^{11+} charge state for chains isolated from either untreated or MG132 treated HEK lysate. **C**)

Quantification of Ub_{1-74} species recaptured by Halo-NZF1 resin. The percent distribution is calculated by averaging relative abundance of each Ub_{1-74} species to total abundance of all three species from three biological replicates for recapture. (Figure 3.S.4). Error bars represent SEM. Calc'd - calculated most abundant weight; expt'l – experimental most abundant molecular weight.

3.8.2 Materials

All reagents from commercial suppliers were – Agarose-TUBE2, purchased from LifeSensors (Cat. No. UM402); Halolink Resin, purchased from Promega (Cat. No. G1914); and MG132, purchased from Enzo Life Sciences (Cat. No. BML-PI102-0025). The antibodies used in this publication, ubiquitin monoclonal antibody (P4D1, Enzo Life Sciences, Cat. No. BML-PW0930-0100), Goat Anti-Mouse IgG Antibody, HRP conjugate (EMD Millipore Cat. No. 12-349), and IRDye® 800CW Goat anti-mouse IgG (Li-Cor Cat. No. 925-32210).

3.8.3. Protein Expression and Purification

3.8.3.a. Expression and purification of His6-MBP-Halo- NZF1 fusion protein.

The Halo-NZF1 (aa1-33 of TRABID) fusion protein was cloned into the pDB.His.MBP vector between the NdeI and NotI restriction sites and purified using a method similar to the one described previously.[1] The fusion protein was expressed in *E. coli* Rosetta (DE3) in LB media supplemented with kanamycin (50µg/mL) and 200 µM $ZnSO_4$. Cells were grown to OD_{600}~0.6 at 37°C and induced with 300µM IPTG. Upon induction, the temperature was lowered to 16°C and protein expressed overnight for 16hours. The cells were centrifuged at 5000 *xg* for 20mins at 4°C and the cell pellet can be stored at -80°C until purification. This cell pellet was resuspended in 40mL lysis buffer (50mM Tris pH 7.5, 300mM NaCl, 0.5mM TCEP, 1mM PMSF, and 1mM benzamidine) and lysed by sonication. The resulting lysate was then clarified at 31,000 x*g* for 45mins at 4°C and the protein was isolated by Ni-NTA chromatography. Fractions containing the MBP-Halo-NZF1 fusion protein were then concentrated and buffer exchanged into a low salt buffer

(50mM Tris pH 7.5, 50mM NaCl). TEV protease was then added to remove the MBP tag, and cleavage was allowed to proceed overnight at 4°C. The cleavage mixture was then poured over Ni-NTA resin to remove 6xHis-MBP as well as any uncleaved fusion protein. The resulting protein was then further purified by ion exchange chromatography (MonoQ, GE Healthcare). Fractions containing the desired protein – Halo-NZF1, were then exchanged into storage buffer (50mM Tris pH 7.5, 50mM NaCl, and 10% glycerol) and stored at -80°C.

3.8.3.b. Expression and purification of His_6-MBP-OTUB1.

OTUB1 was expressed recombinantly in BL21 (DE3) *E. coli.*, with an N-terminal 6xHis-MBP (maltose binding protein) tag. Cells were grown in LB media at 37°C with shaking at 180rpm until OD_{600}~0.6 and subsequently expression was induced with IPTG (100µM). Upon induction, the temperature was lowered to 16°C and protein expressed overnight for 16hours. The cells were centrifuged at 5000 x*g* for 20mins at 4°C. This cell pellet was resuspended in cold lysis buffer (20mM Tris HCl pH7.8, 4mM $MgCl_2$, 100mM NaCl, 1mM TCEP, and 0.25mM PMSF) and lysed by sonication. The resulting lysate was clarified at 75,000 x*g* at 4°C and His6-MBP-OTUB1 was isolated by cobalt affinity chromatography. Fractions containing the fusion protein were buffer exchanged into TEV protease buffer (20mM Tris pH 8.5, 150mM NaCl, 2.5mM NaCl, 2mM DTT) and treated with TEV protease overnight at 4°C to remove the MBP tag. The protein was then buffer exchanged into MonoQ buffer A (20mM Tris pH 7.4, 1mM DTT) and purified by ion exchange chromatography (MonoQ, GE Healthcare) running a gradient of 0 to 50% buffer B (20mM Tris pH 7.4, 1M NaCl, 1mM DTT) over 20 column volumes. Fractions containing OTUB1 were identified by SDS-PAGE, buffer exchanged into storage buffer (50mM HEPES pH 8.0, 50mM NaCl, 2mM DTT and 10% glycerol) and flash frozen and stored at -80°C.

3.8.3.c. Expression and purification of His6-MBP-USP15.

USP15 was expressed recombinantly in BL21 (DE3) *E. coli*., with an N-terminal 6xHis-MBP tag. Cells were grown at 37ºC with shaking at 180rpm until OD_{600}~0.4. Protein expression was induced with isopropyl β-

D-1-thiogalactopyranoside (IPTG, 0.2mM). Cells were then grown overnight at 16ºC and then harvested by centrifugation for 30mins at 4000 x*g*, 4ºC. The cell pellet was resuspended in lysis buffer (50mM Tris pH 7.5, 100mM NaCl, 1mM TCEP, and 0.25mM PMSF) and then lysed by sonication. The lysate was clarified by centrifugation at 75000 x*g* for 30mins at 4ºC. USP15 was then purified using two chromatographic steps: nickel affinity chromatography followed by anion exchange after the MBP fusion was removed using TEV protease.

3.8.3.d. Expression and purification of His_6-GST-OTU+AnkUBD TRABID.

The pOPINK-TRABID plasmid was purchased from Addgene and purified as described previously.[2] OTU+AnkUBD TRABID (aa245-697) was expressed in Rosetta 2(DE3) cells with an N-terminal 6XHis-GST tag. Cells were grown in LB media to an OD_{600} ~0.8-1.0 at 37°C and induced with 1mM IPTG. Upon induction the temperature was lowered to 20°C, protein expressed for 18-20 hr and then the cells were pelleted at 5000 x*g* for 20 minutes at 4°C. The cell pellet was resuspended in cold lysis buffer (25mM Tris pH 8.5, 200mM NaCl, 5mM DTT) and lysed by sonication. The lysate was then clarified by centrifugation at 30000 x*g* for 45min. The clarified lysate was incubated in 2mL pre-equilibrated GST resin for 1.5hr and washed with 25mM Tris pH 8.5, 100mM NaCl, 5mM DTT. The GST tag was cleaved from OTU-AnkUBD TRABID on resin with 50U GST-tagged HRV 3C Protease (Fisher Scientific) overnight at 4°C. Cleaved protein was buffer exchanged into Buffer A (25mM Tris pH 8.5, 5mM DTT) and further purified using anion exchange chromatography (MonoQ, GE healthcare) running a gradient of 0 to 50% buffer B (25mM Tris pH 8.5, 500mM NaCl, 5mM DTT). OTU+AnkUBD TRABID fractions were identified by SDS-PAGE, buffer exchanged into storage buffer (50mM Tris pH 7.5, 75mM NaCl, 2mM DTT, and 10% glycerol), concentrated and flash-frozen.

3.8.4. Cell Culture, Treatment and Lysis

HEK293 cells were grown in high glucose DMEM supplemented with 10% (v/v) fetal bovine serum (FBS), 1x Glutamax (Life Technologies Inc.), and antibiotics (100U/mL penicillin, and 100mg/mL streptomycin) at

37°C in a humidified atmosphere containing 5% CO_2. Once cells reached 80-90% confluency, they were washed with sterile PBS (pre-warmed to 37°C), and then grown in media containing inhibitor 10μM MG132 at 37°C. After four hours, cells were harvested in 2mL cold PBS for every 150mm plate used. Cells were pelleted at 800 x*g* for two minutes and the supernatant decanted. Cell pellets were washed two more times with cold PBS, resuspension and centrifugation at 800 x*g* as previous step. For every 150mm plate of HEK cells, 1mL of cold lysis buffer (50mM Tris pH 7.5, 150mM NaCl, 0.05% IGEPAL® - CA-630 (SIGMA), 10mM 2-chloroacetamide, 10mM N-ethylmaleamide, and 1x protease inhibitor cocktail (Gold Biotechnology)) was added. Cells were incubated in lysis buffer on ice for 30mins prior to sonication and then the resulting lysates were clarified at 16,000 x*g* and 4°C for 30mins.

3.8.5. Enzymatic assays

3.8.5.a. Time course analysis of minimal tryptic digests

Halo-NZF1 resin (200μL) containing Ub chains isolated from 63.4mg of untreated input lysate were resuspended in 100μL of minimal buffer. Sequencing-grade modified trypsin (2.5μg, Promega) was then added to the suspension and the proteolysis was allowed to proceed at room temperature up to 16hours. Aliquots (20μL) of the slurry were then quenched by the addition of 6x Laemmli loading buffer at the indicated time points. The quenched reaction mixtures were then separated on a 15% SDS-PAGE gel and analyzed by western blot with anti-Ub (P4D1). Table 3.S.1 contains empirically determined optimal cell lysate to trypsin ratios for different cellular treatments used in this study.

3.8.5.b. DUB assay analysis of Isolated Ub chain linkages

MG132 treated HEK cell lysate (22.5mg) was incubated with Halo-NZF1 resin (100uL) overnight at 4°C with shaking/stirring. The resin was then washed with 1mL of binding buffer four times followed by 2x washes with 1 mL DUB buffer (50mM Tris pH 7.5, 150mM NaCl, 1mM DTT) and then the resin was resuspended as a 50% slurry in DUB buffer. The resin was aliquoted into four 20μL portions (40μL of the 50% slurry)

and warmed to 37°C for 3mins. After warming, either TRABID (1.7µM final concentration), OTUB1 (3.3µM final concentration), both TRABID and OTUB1 (1.7µM TRABID and 3.3µM OTUB1), or USP15 (1.7µM) were added and the resulting mixtures were rotated at 37°C overnight. The reactions were then quenched by the addition of 6x Laemmli loading dye. The samples were then separated on a 15% SDS-PAGE gel and analyzed by western blot using anti-Ub antibody (P4D1).

3.8.6. Supplemental References

1. Kristariyanto, Y. A.; Rehman, A. Syed A.; Campbell, D. G.; Morrice, N. A.; Johnson, C.; Toth, R.; Kulathu, Y., K29-Selective Ubiquitin Binding Domain Reveals Structural Basis of Specificity and Heterotypic Nature of K29 Polyubiquitin. *Mol. Cell* **2015,** *58* (1), 83-94.

2. Licchesi, J. D. F.; Mieszczanek, J.; Mevissen, T. E. T.; Rutherford, T. J.; Akutsu, M.; Virdee, S.; Oualid, F. E.; Chin, J. W.; Ovaa, H.; Bienz, M.; Komander, D., An ankyrin-repeat ubiquitin-binding domain determines TRABID's specificity for atypical ubiquitin chains. *Nat. Struct. Mol. Biol.* **2011,** *19*, 62.

4 Proteasome-Bound UCH37 Debranches Ubiquitin Chains

Deol K. K.,* Crowe, S. O.* Du J., Guenette R.G., and Strieter E. R.

* These authors contributed equally to this work

This work is in revision at Molecular Cell

Author contributions:

KKD performed Middle down MS, AQUA MS analysis, kinetics with branched trimer and generated high molecular weight chains used throughout the chapter.

SOC performed kinetics using high molecular weight chains, isolated proteasomes, generated CRISPR cell line, and performed cell culture work.

JD performed biochemical experiments and binding studies.

RGG made initial observation of UCH37 debranching activity, and performed biochemical assays related to Figure 4.1 and 4.S.1.

SOC, ERS, KKD and JD all contributed to the writing of the manuscript.

4.1 Abstract

Ubiquitin (Ub) is assembled into a vast array of polymeric chains. The linkage, length, and architecture of chains are all important variables in providing tight control over numerous biological paradigms. Although a role for branched architectures in regulating proteasome-mediated degradation has been described, proteins that selectively recognize and process these atypical chains are unknown. Here, we report that UCH37/UCHL5, a proteasome-associated deubiquitinase, exclusively cleaves K48 branched chains. The debranching activity of UCH37 is markedly enhanced not only by the proteasomal Ub receptor RPN13/ADRM1 but also the proteasome complex itself. We further show that UCH37 interacts with branched Ub chains in cells and is capable of regulating proteasomal degradation of substrates modified by branched Ub chains. Our work, therefore, identifies an enzyme capable of removing K48 branch points and alludes to an important role for chain debranching in regulating proteasomal degradation.

4.2 Introduction

Non-template derived biopolymers have diverse structures that provide precise control over many biological pathways. Polymeric ubiquitin (Ub) chains exemplify this concept.[1, 2] Owing to the eight amino groups of Ub (M1, K6, K11, K27, K29, K33, K48, and K63), substrate proteins can be modified with a single-linkage (homotypic) or a mixed-linkage (heterotypic) polymeric chain in a linear or branched configuration. The cellular fate of ubiquitinated proteins is largely dictated by chain type; K48-linked chains act as the principal proteasome targeting signal, whereas K63-linked chains promote proteasome-independent events during immune signaling and DNA repair.[3] Failure of deubiquitinases (DUBs) to dismantle specific Ub chains at the appropriate time is often detrimental to cellular function.[4-6]

While efforts to elucidate the functions of Ub chains have largely focused on homotypic K48 and K63 Ub chains, little is known about heterotypic chains especially those with branched architectures.[7, 8] Mounting evidence, however, indicates branched chains are important for regulating specific cellular pathways.[9-12] Branched K11/K48 chains are thought to adopt conformations conducive to strong interactions with Ub receptors on the proteasome.[13] There is also evidence that branching interferes with DUB activity.[11, 14] These results raise the possibility that branched conjugates can be selectively recognized and processed. Yet, proteins selective for branched conjugates have not been identified.

UCH37/UCHL5 is a cysteine protease and member of the small family of DUBs referred to as the Ub C-terminal hydrolases (UCHs). Deficiencies in UCH37 lead to embryonic lethality in mice[15] and overexpression has been found in human cancers.[16, 17] At the cellular level, UCH37 has been implicated in several pathways, including TGF-β signaling[18, 19], Wnt signaling[20], DNA double-strand break repair[21], cell cycle progression[22], NF-κB activation[23], and adipogenesis.[24] Most of these functions have been attributed to UCH37's association with either the proteasome[25-27] or INO80 chromatin remodeling complex.[28]

While its precise role in the INO80 complex is unknown, in the case of the proteasome the dogma is that UCH37 trims homotypic K48 chains to regulate degradation.[29] In accord, chains with K48 linkages accumulate in cells upon inhibition of UCH37.[30] However, mounting evidence suggests UCH37 does not simply trim K48 chains; little to no chain disassembly has been observed with free UCH37 or when it is bound to its partner protein the proteasomal Ub receptor RPN13/ADRM1[27, 31, 32], and purified human proteasomes harboring UCH37 as the only non-essential DUB are unable to cleave K48 chains.[33] Considering UCH37 has emerged as a therapeutic cancer target,[34, 35] identifying its substrates is critical.

In the present study, we demonstrate that UCH37 exclusively cleaves branched Ub chains. Using a library of designer Ub chains, we show that K48 linkages are readily removed when presented in the context of a branched chain. Middle-down mass spectrometry combined with quantitative linkage analysis reveals that the K48-specific debranching activity extends to complex chain mixtures. We also find that activity is regained upon addition of RPN13, and more importantly, the proteasome. Our work therefore identifies proteasome-bound UCH37 as a chain debranching enzyme and uncovers a mechanism by which selectivity toward branch points can be achieved.

4.3 Results

4.3.1 UCH37 Cleaves K48 Branched Ub Trimers

Our lab has developed a straightforward method based on thiol-ene coupling (TEC) for synthesizing a diverse set of Ub homo-oligomers with variability in linkage and architecture.[36, 37] Although the Ub-Ub linkage generated through TEC chemistry differs from the native isopeptide bond (Figure 4.1 A), we have shown it acts as a functional surrogate in enzymatic assays with DUBs. [38] We sought to avail our library of TEC-derived Ub homo-oligomers to identify potential targets of UCH37. Through this approach, we found that UCH37 exclusively cleaves branched conjugates (Figure 4.1 B). We confirmed these results by subjecting UCH37 to a native branched trimer with K6 and K48 linkages. Cleavage of this trimer occurs in

a concentration- and time-dependent manner (Figures 4.1 C and D). These results suggest UCH37 targets branched chains and is thus exquisitely sensitive to chain architecture.

Given the importance of chain topology, we surmised that UCH37 might also exhibit linkage specificity. To test this, we used a sortagging approach to selectively label individual Ub subunits of a branched trimer with different fluorophores.[39] With a fluorescent, native K6/K48 branched trimer as a substrate, the logic is that K48 cleavage should furnish a fluorescein-labeled di-Ub and TAMRA-labeled mono-Ub (Figure 4.1 E). By contrast, scission of the K6 linkage should yield a TAMRA-labeled di-Ub and fluorescein-labeled mono-Ub, thus allowing us to interrogate UCH37 linkage selectivity. The results are consistent with K48 linkage specificity, as the products from UCH37-mediated cleavage mirror those generated by the K48 linkage specific DUB OTUB1 (Figure 4.1 F). Cleavage patterns of TEC-derived chains also support this conclusion (Figures 4.S.1 A-B). Our results show that UCH37 is not only selective for the branched topology, but also the K48 linkage.

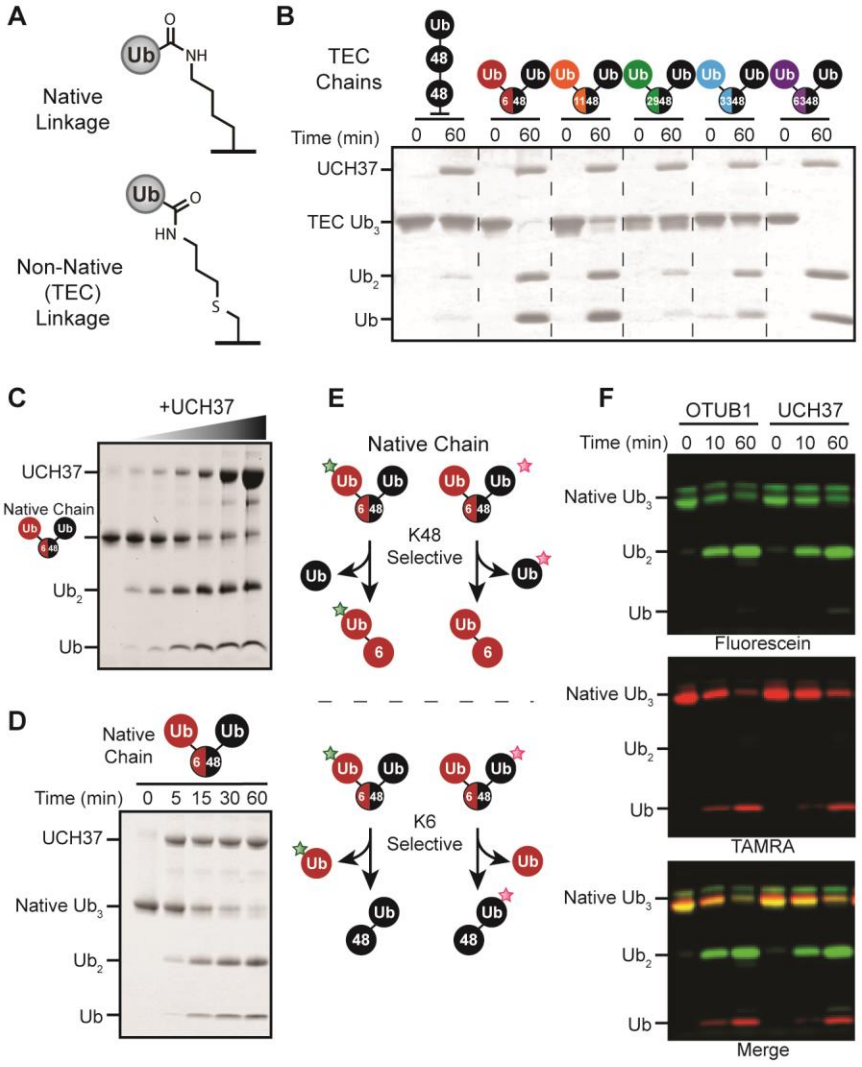

Figure 4. 1: UCH37 Cleaves K48 Linkages in Branched Trimers. A) Chemical depictions of both native and thiol-ene coupled (TEC) isopeptide bonds used in this study. **B**) SDS-PAGE analysis of TEC-derived branch tri-Ub (10 µM) with UCH37 (1 µM). Linkages in branched tri-Ub are represented by X/Y, where X and Y denote the positions of the isopeptide bonds. **C**) SDS-PAGE analysis of native K6/K48 branch tri-Ub (10 µM) with varying concentrations of UCH37 (0, 0.1, 0.25, 0.5, 1, 5, and 10 µM). **D**) SDS-PAGE analysis of the time course for the UCH37-catalyzed cleavage of native K6/K48 branch tri-Ub (10 µM). **E**) Schematic for subunit-specific labeling of native K6/K48 branch tri-Ub with different fluorophores to report on the

linkage specificity of UCH37. F) Fluorescence analysis of cleavage reactions with either OTUB1 (5 μM) or UCH37 (5 μM) and fluorophore-labeled native K6/K48 branch tri-Ub (10 μM).

4.3.2 UCH37 Removes K48 Branch Points in Complex Chains.

While Ub trimers are good model systems, they do not reflect the heterogeneity of ubiquitination observed in cells. Thus, we sought to analyze the debranching activity of UCH37 in the context of heterogeneous chain populations where there is considerable variability in chain length and frequency of branch points. Identifying branch points in complex mixtures of chains, however, is challenging. Chain restriction analysis does not inform on architecture[40] and multiple modifications on a single polypeptide chain are difficult to detect using standard bottom-up proteomic approaches. We turned to middle-down mass spectrometry (Ub MiD MS), as this has proven to be a powerful method for identifying and characterizing branched conjugates.[41]

A set of enzymatic reactions were performed based on their ability to generate chains with a specific mixture of linkages (Figure 4.2 A).[42-47] In each case, high molecular weight (HMW) conjugates were isolated and analyzed by middle-down MS. The extent of branching (2xdiGly-Ub_{1-74}) varies from 4-14% of the total Ub population (Figures 4.2 B-D; top spectra). According to electron capture dissociation (ECD) and electron transfer dissociation (ETD) analysis of the 2xdiGly-Ub_{1-74} peak, NleL generates K6/K48 branch points, the combination of UBE2S and UBE2R1 forms K11/K48 branches, and UBE2N/UBE2V2 with UBE2R1 builds K48/K63 bifurcations (Figures 4.S.2 B-D).

Ub MiD MS analysis of the HMW conjugates after the addition of UCH37 shows a complete loss of the 2xdiGly-Ub_{1-74} species indicative of debranching (Figures 4.2 B-D; bottom spectra). With K6/K48 chains, the disappearance of 2xdiGly-Ub_{1-74} coincides with an increase in diGly-Ub_{1-74}, which represents the linear/unbranched portion of a chain (Figure 4.2 A; bottom spectrum). Subjecting the same chains to OTUB1, which should be immune to chain architecture and cleave any K48 linkage, decreases the branch

point and increases the relative amount of mono-Ub/end caps (Ub_{1-74}) (Figure 4.2 B; middle spectrum). With K11/K48 and K48/K63 chains, both UCH37-catalyzed debranching and the global removal of K48 linkages by OTUB1 afford an increase in Ub_{1-74} (Figures 4.2 C-D; middle and bottom spectra). The difference is that OTUB1 cleavage reveals K48 is the prevailing linkage in K11/K48 chains considering the diGly-Ub_{1-74} peak is reduced from 62% to 23% (Figure 4.2 C; middle spectrum).

To determine whether UCH37 retains specificity toward K48 linkages in these complex chains, we used isotopically labeled, absolute quantitation (AQUA) peptide standards for each linkage of Ub^{48} HMW conjugates were analyzed both prior to and after the addition of OTUB1 and UCH37. The most significant changes occur in the K48 levels for each set of chains, indicating this linkage is the primary target of UCH37 (Figures 4.2 E-G).

Our MS data with HMW chains reveals important features of UCH37's enzymatic activity. First is that the K48-specific debranching activity observed with model Ub trimers holds true for more complex chains. Chains built with non-K48 linkages, e.g., K11 and K63, are not targeted for cleavage by UCH37, nor are K29/K48 chains despite the presence of branch points (Figures 4.S.2 A & 4.S.2 E-H). Second, even in the presence of linear regions of a chain bearing a mixture of linkages, UCH37 cleaves branch points. This is evidenced by the different effects of OTUB1 and UCH37 on the population of Ub_{1-74} variants.

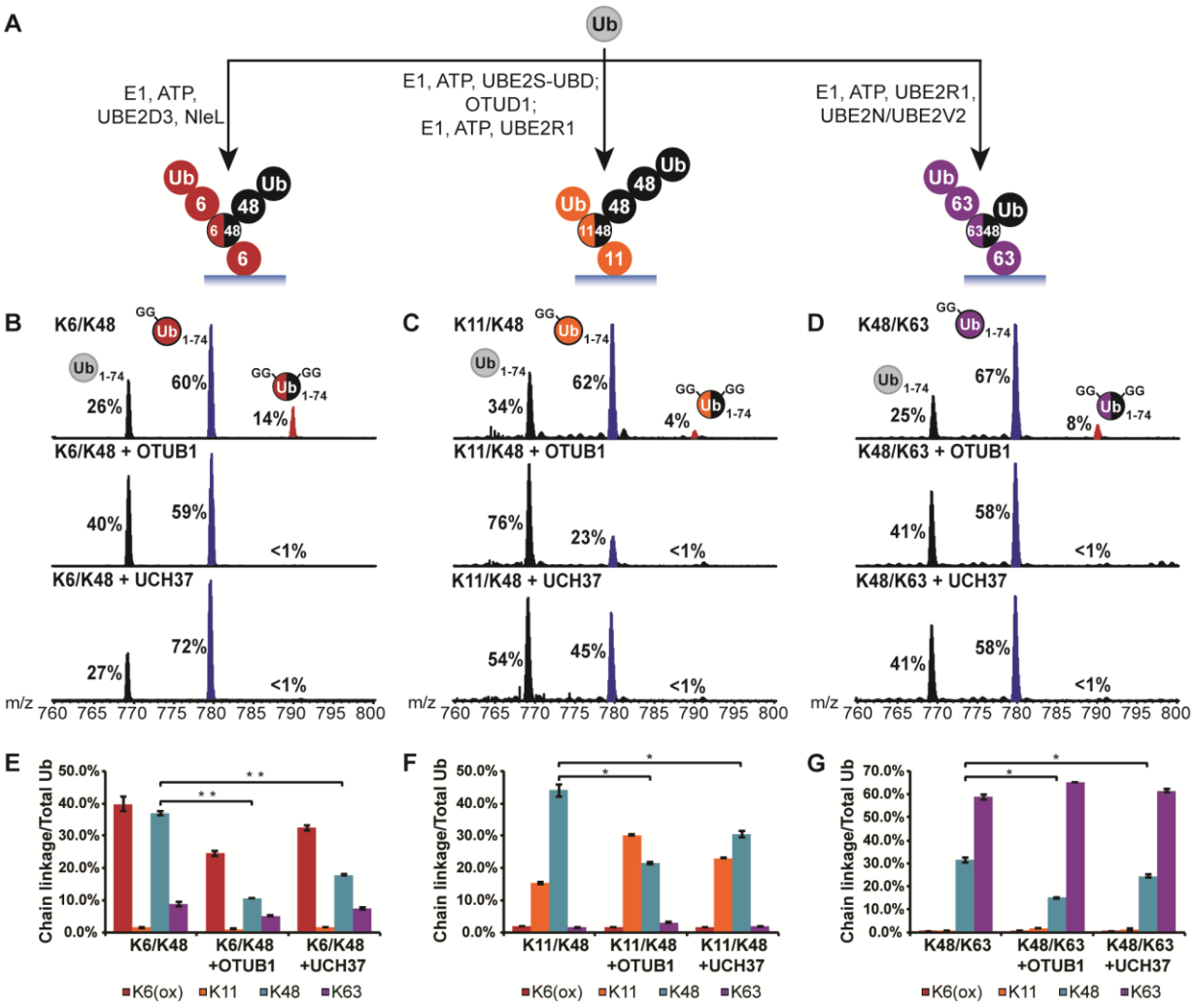

Figure 4. 2: UCH37 Removes K48 Branch Points in Complex Chain Mixtures. A) Schematic showing the assembly of high molecular weight ubiquitin chain mixtures used in this study. **B-D**) Ub middle-down (Ub MiD) MS analysis of HMW K6/K48, K11/K48, and K48/K63 chains (top) followed by treatment with either OTUB1 (middle) or UCH37 (bottom). The spectra correspond to the Ub^{11+} charge state. Percentages correspond to the average relative quantification values of each Ub species: Ub_{1-74}, 1xdiGly-Ub_{1-74}, and 2xdiGly-Ub_{1-74} between the charge states of 8+ to 13+.**E-G**) Ub-AQUA analysis of HMW K6/K48, K11/K48, and K48/K63 chains before and after OTUB1 (middle) or UCH37 (last) treatment. Results are normalized

against total amount of Ub for each linkage type detected and are represented as means ± SEM (standard error of the mean) of two replicates. For all points, *P<0.025, **P<0.01 (Student's T-test).

4.3.3 RPN13 Enhances the Debranching Activity of UCH37

While our data with free UCH37 suggest it could function as a chain debranching enzyme, there is little evidence that UCH37 acts on its own. One of its primary binding partners is the proteasomal Ub receptor RPN13 (Figure 4.3 A).[27] Previous studies have shown that RPN13 enhances UCH37's ability to cleave the fluorogenic substrate Ub-AMC.[27, 28, 49, 50] Thus, we wanted to evaluate the effects of RPN13 on chain debranching. We first attempted to reconstitute the UCH37•RPN13 complex by mixing the purified recombinant proteins; however, we did not observe activity. We then opted to co-purify UCH37 and full length RPN13. This resulted in a 1:1 complex (Figure 4.S.3 A) exhibiting higher activity toward Ub-AMC (3-fold), branched trimers, and HMW chains relative to free UCH37 (Figure 4.3 B and Figure 4.S.3 B).

Encouraged by these results, we sought to obtain more quantitative information. With the native K6/K48 branched trimer as a model substrate we measured the initial rates of debranching using a gel-based assay. The formation of both Ub dimer and monomer were monitored and the resulting data were fit to the Michaelis-Menten equation (Figure 4.3 F). The steady-state parameters reveal a 3-fold decrease in K_m and a 4-fold increase in k_{cat} for UCH37•RPN13 compared to free UCH37 (Figure 4.3 F and 4.S.3 D). RPN13 therefore boosts the overall catalytic efficiency of UCH37 by an order of magnitude from 1200 $M^{-1}•s^{-1}$ to 12000 $M^{-1}•s^{-1}$.

Next, we sought to determine whether RPN13 also affects the cleavage efficiency of complex chains. To test this, UCH37•RPN13 was incubated with K6/K48, K11/K48, and K48/K63 HMW chains. Analysis of these reactions by Ub MiD MS and AQUA confirmed the complex displays the same selectivity for K48 branch points as free UCH37 (Figure 4.3 C and D and Figure 4.S.3 C). We then monitored the formation of mono-, di-, tri-, and tetra-Ub over time by western blot (Figure 4.3 E and Figures 4.S.3 and 4.S.6). For each

species a monotonic increase was observed, and the band intensities were normalized to a synthetic di-Ub standard loaded onto each blot. The resulting progress curves were fit to a pseudo-first-order kinetic expression to obtain an observed rate constant for each of the lower MW Ub species (Figure 4.3 E and Figures 4.S.3). The sum of the rate constants provides a lower limit of the overall rate of chain cleavage, as products larger than tetramers are not accounted for. Remarkably, the rate constants are close to the catalytic efficiencies obtained with branched trimers (within 3- to 5-fold). Moreover, the data indicate that RPN13 enhances the activity of UCH37 toward HMW chains by 5- to 12-fold over free UCH37 (Figure 4.3 F).

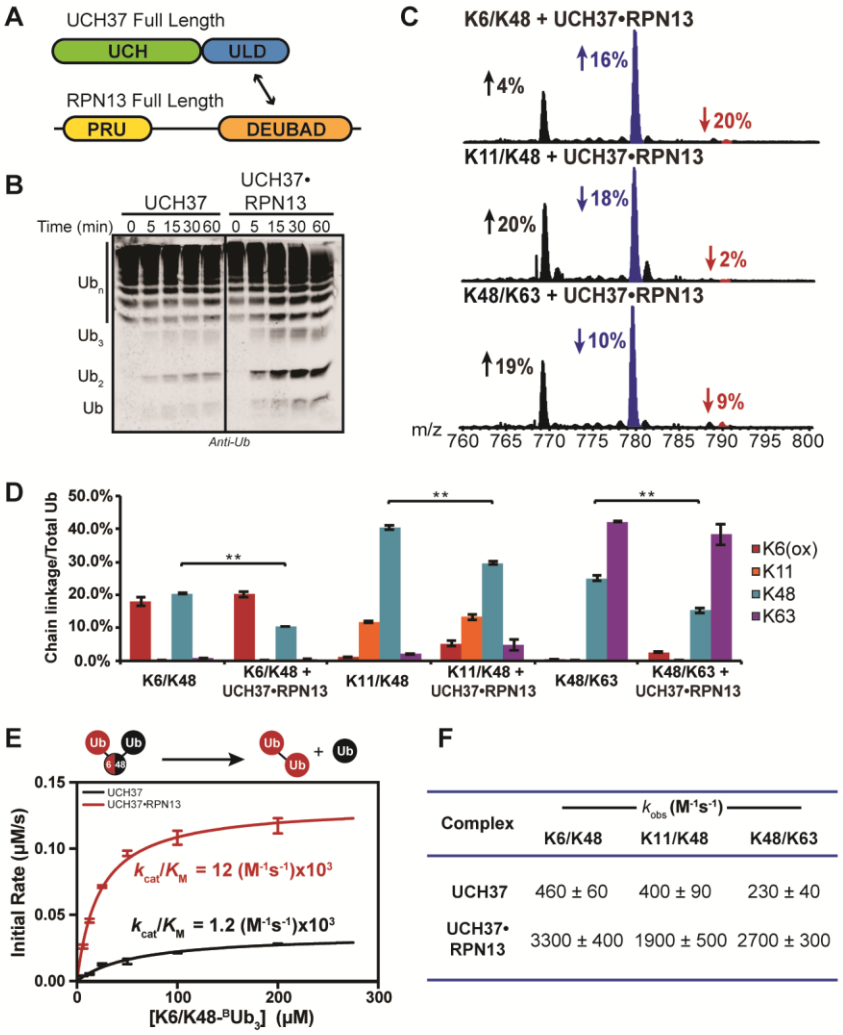

Complex	k_{obs} (M^{-1}s^{-1})		
	K6/K48	K11/K48	K48/K63
UCH37	460 ± 60	400 ± 90	230 ± 40
UCH37•RPN13	3300 ± 400	1900 ± 500	2700 ± 300

Figure 4. 3: Figure 3. Steady-State Kinetic Analysis of Chain Debranching. A) Cartoon of UCH37 and RPN13 domains. Double headed arrow indicates the domains that interact. **B**) Western blot analysis of cleavage reactions with HMW K6/K48 chains (250 ng/μL). Reactions were performed with either UCH37 (1μM), or UCH37•RPN13 complex (1 μM). Time points were taken as indicated before separation on a 15% SDS-PAGE gel and analysis by western blot using the α-Ub P4D1 antibody. **C**) Middle-down analysis confirms that the UCH37•RPN13 complex maintains selectivity for branched Ub chains against K6K48, K11K48, and K48K63 HMW chains. Red arrows indicate the percent loss of the branched peak, Blue arrows indicate the gain of a linear chain, and black arrows indicate the gain in mono-Ub **D**) Ub AQUA analysis confirming that UCH37•RPN13 selectively hydrolyzes K48 linkages in branched Ub chains. **E**) Michaelis-Menten plot for

the hydrolysis of native K6/K48 branched tri-Ub by either free UCH37 (black) or UCH37•RPN13 (red). **F**) Steady-state parameters obtained from the hydrolysis of different HMW chains by either free or RPN13 bound UCH37. Reactions were performed in triplicate by incubating either UCH37 (2.8 μM for K6/K48 and K48/K63 chains and 5 μM for K11/K48 chains) or UCH37•RPN13 (1 μM) with HMW chains (250 ng/μL). Densitometry was measured for lower MW species (Ub1-Ub4) and normalized to an internal di-Ub standard loaded onto each gel. Normalized densitometry values were plotted as a function of time and fit to the pseudo first order kinetics equation to obtain k_{obs} for the formation of each Ub species. Rate constants for Ub1-Ub4 were added to obtain the observed rate constant of debranching.

4.3.4 Proteasome-Bound UCH37 Debranches Chains

Our data showing that RPN13 potentiates chain debranching prompted us to examine proteasome-bound UCH37. We purified wild type proteasomes from a HEK293 cell line stably expressing a HTBH-tagged (6xHis/biotin-tagged) version of the proteasomal DUB RPN11.[51] As anticipated, western blot analysis shows the presence of UCH37 and RPN13 along with other 19S and 20S subunits (Figure 4.4 A). To avoid complications in data interpretation, the other non-essential proteasomal DUB USP14 was depleted under high salt conditions (Figure 4.S.4 A). Adding purified proteasomes to HMW K6/K48 chains results in a concentration-dependent formation of low molecular weight species (Figure 4.4 B). Ub MiD MS shows that branch points decrease in abundance from 20% to 5% in the presence of proteasomes (Figure 4.4 C). A loss of branch points is also observed with other HMW chains containing K48 linkages (Figure 4.S.4 C).

To ascertain whether the debranching activity of purified proteasomes is due to UCH37, we used CRISPR/Cas9 genome editing to remove UCH37 from HEK293 cells expressing HTBH-tagged proteasomes (Figure 4.S.5). As shown by western blot (Figure 4.4 A), proteasomes purified from these cells are indeed devoid of UCH37. Consistent with these results, ΔUCH37 proteasomes have compromised activity toward

Ub-AMC, but not the peptidase reporter Suc-LLVY-AMC (Figure 4.S.4 B). In cleavage reactions with HMW chains, the ΔUCH37 proteasomes are unable to generate smaller products (Figure 4.4 B), and branch points remain intact with all chain types (Figure 4.4 C and 4.S.4 C), indicating that the chain cleavage activity we detect with the proteasome is due to UCH37.

To further cement UCH37 as a chain debranching enzyme, we replenished RPN13-deficient (ΔRPN13) proteasomes, generated by CRISPR/Cas9 genome editing, with recombinant UCH37•RPN13 complexes. This was achieved by adding either catalytically active UCH37•RPN13 or inactive UCH37 C88A•RPN13 to immobilized ΔRPN13 proteasomes and eluting after high salt washes to remove USP14 (Figure 4.4 A and 4.S.4 B). Interrogating the replenished proteasomes with HMW chains shows that chain debranching only occurs when UCH37 is active (Figure 4.4 B-C and 4.S.4 C). There is, however, a slight difference in the population of Ub_{1-74} variants after treatment with replenished (rUCH37•RPN13) and wild type proteasomes (Figure 4.4 B and C and Figure 4.4.S C). With the replenished proteasomes loss of the branch point primarily results in an increase in Ub_{1-74}, whereas with wild type proteasomes debranching coincides with an increase in diGly-Ub_{1-74}. This could be due to differences in the isolated HMW chains or the activities of recombinant and endogenous proteasome-bound UCH37. Nevertheless, these results demonstrate that proteasome-bound UCH37 debranches Ub chains.

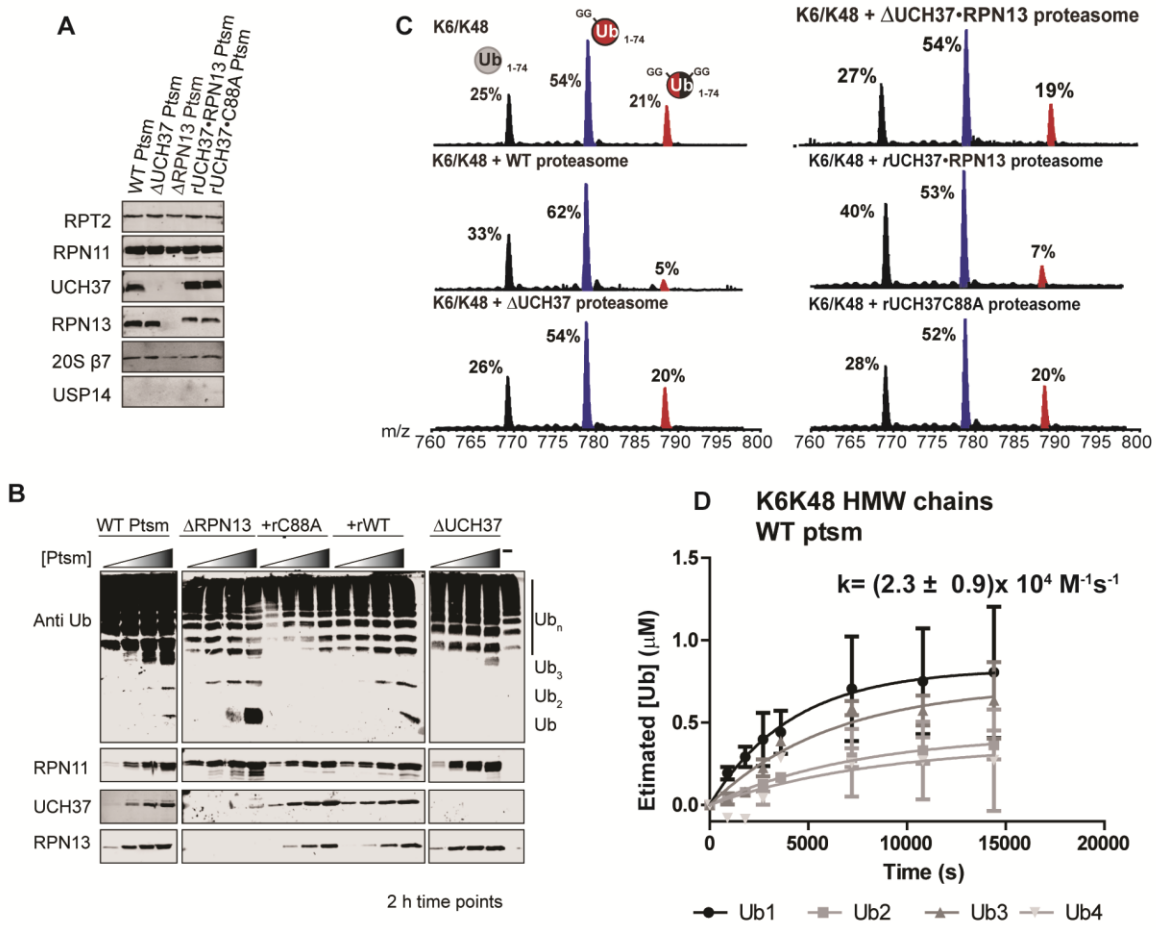

Figure 4. 4: Figure 5. Proteasome-Bound UCH37 Debranches Ub Chains. A) Western blot analysis of proteasome complexes used in this study. **B**) Western blot analysis of cleavage reactions with HMW K6/K48 chains (250 ng/μL) and varying amounts (1-10μg) of either WT proteasome, ΔUCH37 proteasome, ΔRPN13 proteasome, or replenished variants of the ΔRPN13 proteasome (+rC88A complex or + rWT complex). **C**) Ub MiD MS analysis of cleavage reactions with different proteasome complexes against K6/K48 linked Ub chains. The spectra correspond to the Ub^{11+} charge state for untreated HMW K6/K48 chains. Percentages correspond to the average relative quantification values of each Ub species: Ub_{1-74}, 1xdiGly-Ub_{1-74}, and 2xdiGly-Ub_{1-74}. **D**) Steady-state parameters obtained from the hydrolysis of K6K48 HMW chains. Analysis was done as described in Figure 4.3 E.

4.3.5 Proteasome Enhances the Debranching Activity of UCH37

Having detected chain debranching with purified proteasomes, we wanted to determine how the kinetics compare to the UCH37•RPN13 complex. To this end, we measured progress curves for the formation of lower MW species after adding HMW K6/K48 chains to wild type proteasomes (Figure 4.S.4 D). To account for the concentration of UCH37 in these reactions, quantitative western blotting was performed using recombinant UCH37 as a standard. The measured rate constant reveals a 7-fold increase relative to the UCH37•RPN13 complex (Figure 4.4 D and 4.S.4 B). Placing UCH37 on the proteasome therefore dramatically enhances its activity.

4.3.6 UCH37 Interacts with Branched Chains in Cells

As UCH37 debranches Ub chains, we hypothesized that UCH37 might act to recruit substrates tagged with branched chains to the proteasome. To date, several substrates have been shown to be marked for degradation by branched chains. Perhaps the most well characterized are substrates of the anaphase promoting complex (APC/C). APC/C drives progression through mitosis by decorating many cell cycle regulators with K11/K48 branched chains.[10]

To determine whether UCH37 interacts with APC/C substrates we performed pull down experiments with G2/M synchronized cells expressing flag-tagged UCH37 C88A or an empty vector. Cells were synchronized in G2/M phase using a thymidine-nocodazole block. To ensure that known binding partners can be detected, we first probed for RPN13. Western blot analysis shows that ectopically expressed, flag-tagged UCH37 C88A does indeed interact with endogenous RPN13 (Figure 4.5). Encouraged by these results, we then examined whether branched chains are enriched by UCH37 C88A. Using the recently reported K11/K48 branched chain specific antibody[52] we observed significant enrichment only with

UCH37 C88A (Figure 4.5). Lastly, we analyzed the pulldowns for the APC/C substrate p21, a cyclin dependent kinase inhibitor. We observed that ubiquitinated p21 is enriched by UCH37 C88A but not the empty vector (Figure 4.5). These results therefore suggest UCH37 interacts with substrates modified with branched chains in cells.

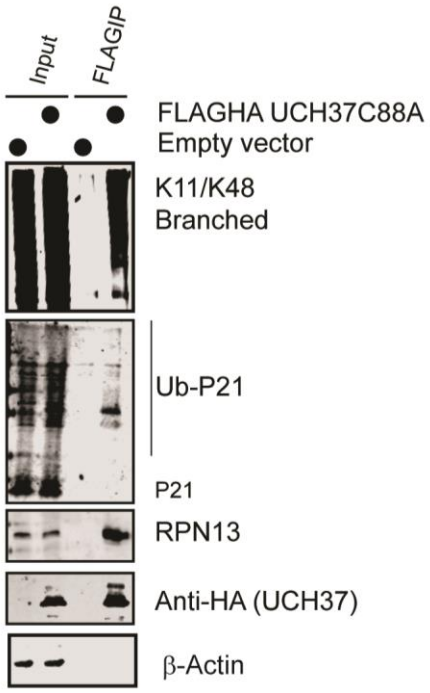

Figure 4. 5: UCH37 interacts with branched Ub chains and ubiquitinated substrates in cells. Cells were transfected with either a vector expressing only a FLAG-HA (empty vector) tag or FLAG-HA tagged UCH37C88A and were synchronized in prometaphase by thymidine-nocodazole block to induce K11/K48 branched chain formation. Cells were harvested and lysed and incubated with Anti-FLAG resin to immunoprecipitated FLAG tagged proteins. Proteins were separated by SDS-PAGE and visualized by western blot for the indicated antibodies.

4.3.7 UCH37 Displays Conflicting Roles in Regulating the Degradation of Branched Chains

Since UCH37 interacts with known proteasome substrates modified by branched Ub chains, we hypothesized that UCH37 could regulate their rate of degradation. To test this, we focused on substrates

of APC/C that are modified with K11/K48 branched chains, e.g., the cyclin-dependent kinase inhibitor p21. Degradation of p21 was monitored during mitosis by first arresting cells in the G2/M phase of the cell cycle using a thymidine-nocodazole block and followed by inhibition of translation by adding cycloheximide. Quantitative analysis of the western blot data shows that p21 levels decrease over time as expected (Figure 4.6A). Using siRNA to knockdown UBE2S, a component of the APC/C, results in the stabilization of p21 and reduces the levels of K11/K48 branched chains (Figure 4.6 A). This is consistent with a previous report showing that UBE2S works in conjunction with APC/C to build K11/K48 branched chains and promote protein degradation.[10] Surprisingly, however, knocking down both UCH37 and RPN13 also stabilizes p21 (Figure 4.6 A). These results suggest that UCH37 is important for promoting rather than inhibiting the degradation of proteins modified with branched chains.

Building on the siRNA results, we wanted to examine the stability of cell cycle regulators in the CRISPR/Cas9-derived UCH37 knockout cells. We therefore performed the same synchronization and cycloheximide chase as described above using HEK293 cells expressing the HTBH tagged RPN11 or the UCH37 CRISPR variant of this cell line and monitored the stability of p21 and NEK2A by western blot (Figure 4.6 B). Although the levels of p21 and NEK2A are lower in the UCH37 KO cells relative to the WT cell line, the degradation rates are not significantly different between the two cell lines (Figure 4.6 B). Degradation rates also do not change upon overexpressing the catalytically dead or active form of UCH37 in the KO cells. These data are not in agreement with the siRNA results.

Analyzing the same reactions with the K11/K48 branched chain antibody shows that K11/K48 branched chains are less abundant in synchronized UCH37 KO cells than the WT cells (Figure 4.6 B). These results are surprising, as it is unclear why a loss of UCH37 would afford lower steady-state levels of not only branched chains but also the cell cycle regulators p21 and NEK2A. One possible explanation is that UCH37 regulates global protein levels through its role in the INO80 chromatin remodeling complex, which is a key regulator of transcription.[53] This would be consistent with the observation that overexpressing

both UCH37 C88A and wild type UCH37 in the null background largely restores the levels of branched chains and cell cycle regulators, as the catalytic activity of UCH37 is not thought to be important for INO80 function.[28] Another possibility is the absence of UCH37 leads to an accumulation of branched chains in asynchronous cell populations, which is something we observed, and promotes aberrant protein degradation. This would lead to lower steady-state levels of proteins prior to synchronization. If this were the case, however, we would not expect inactive UCH37 to restore protein levels to the same extent as the active form. What is also puzzling is that the rate of p21 and NEK2A degradation is blind to the nature of UCH37. If branched chains are important for degradation, we would expect to observe differences in degradation rates when branched chains are depleted by active, but not inactive, UCH37.

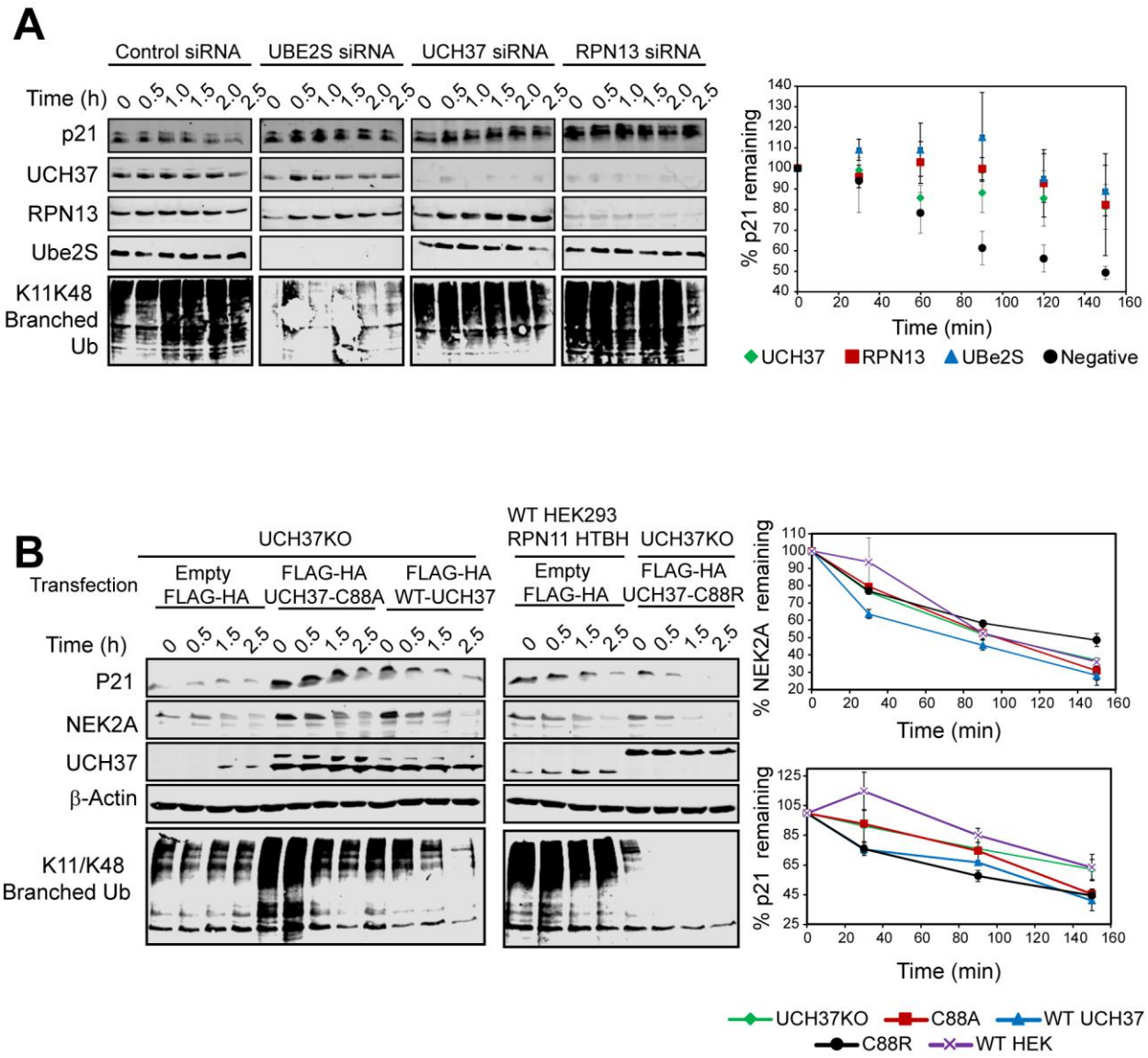

Figure 4. 6: The role of UCH37 in regulating protein degradation is unclear. A) Cycloheximide chase experiment looking at p21 stability in synchronized cells transfected with siRNA. HEK293FT Cells were transfected with siRNA against Ube2S, UCH37, RPN13 or a scrambled oligo and synchronized in prometaphase by thymidine-nocodazole block, upon which cycloheximide was added to shut off translation. Cells were harvested at the indicated timepoints and lysates were separated by SDS-PAGE and visualized with the indicated antibodies. Densitometry was performed on the bands for p21 and normalized to the total protein measured in each lane by total protein staining. The results are plotted on

the right. Error bars represent ± SEM (standard error of the mean) of three replicates. **B**) Cycloheximide chase experiment looking at p21 stability in synchronized HEK293 RPN11, UCH37 CRISPR KO or cells with UCH37 mutants transfected back in. WT or UCH37KO cells were transfected with either an empty FLAG-HA vector, or the indicated FLAG-HA UCH37 variant and synchronized as described above. Cells were treated with cycloheximide to shut off translation, harvested at the indicated timepoints, and lysates were separated by SDS-PAGE and visualized by western blot using the indicated antibodies. NEK2A and p21 levels were measured by densitometry and normalized to the total protein measured in each lane by total protein staining. The error bars represent ± SEM.

Branched chains linked through K11/K48 have also been implicated in regulating the degradation of misfolded proteins. One way to induce misfolded proteins is through the use of the translation inhibitor puromycin. This drug mimics aminoacylated tRNAs and is mistakenly incorporated into nascent polypeptides as they are synthesized by the ribosome.[54] This results in a truncated polypeptide that is often misfolded. These misfolded proteins are then targeted to the proteasome by the E3 ligases UBR4 and UBR5, which have been shown to build K11/K48 branched chains.[52] As these branched chains are required for degradation, we also thought that UCH37 might play an important role in the degradation of these substrates as well. To test this, we treated cells (either the WT HEK293 RPN11 HTBH cells, UCH37 CRISPR or RPN13 CRISPR) with puromycin and monitored the stability of the puromycinylated peptides by cycloheximide chase. The results of these assays are striking. Cells lacking UCH37 display greatly reduced levels of puromycinylated proteins at the early timepoints of the chase (Figure 4.7 A). When we analyzed the rate of degradation of these species however, we observed that the rates of degradation are the same in all three cell lines (Figure 4.7 A). This suggests that the reduced levels of puromycinylated proteins observed in the UCH37 KO and RPN13 KO cells is due to slower rates of protein synthesis rather than faster rates of degradation. We further compared the levels of puromycinylated proteins in UCH37 KO cells to cells in which wild type or inactive UCH37 had been reinstated. Overexpressing active UCH37

results in an increase in puromycinylated proteins, but the inactive form does not, suggesting that catalytically active UCH37 can recover the rates of protein synthesis (Figure 4.7 B).

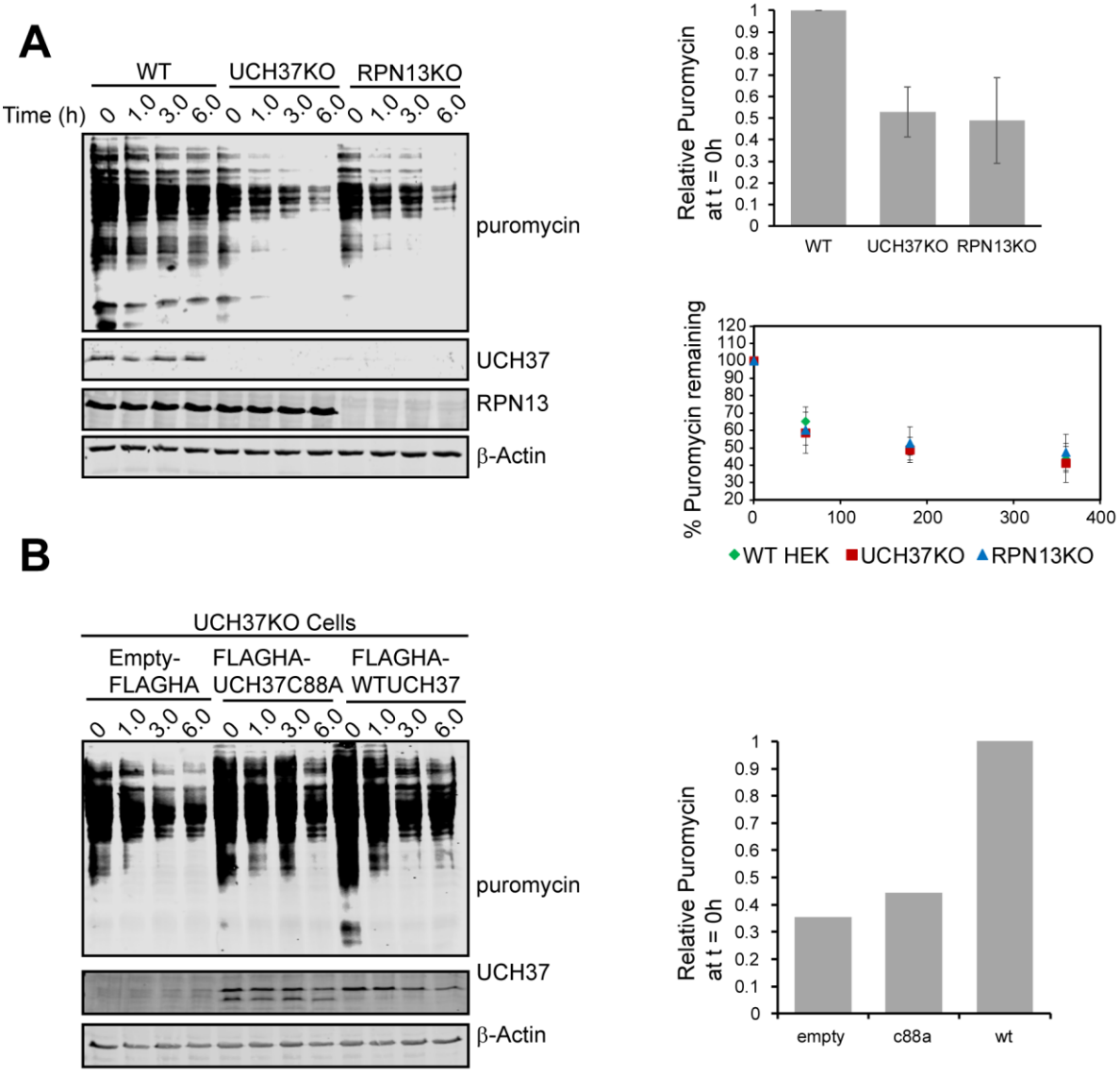

Figure 4. 7: UCH37 regulates levels of puromycinylated proteins and may play a role in regulating translation. A) HEK293 RPN11-HTBH cells (WT, UCH37KO, or RPN13KO) were treated with cycloheximide (5μg/mL) for one hour to allow for puromycin incorporation. This was followed by a chase with cycloheximide (50μg/mL) to shut off translation. Cells were harvested at the indicated timepoints and separated by SDS-PAGE and proteins visualized using the indicated antibodies. Levels of puromycin

incorporation was determined by densitometry, normalized to the total protein level in each lane as measured by total protein staining, and plotted as a function of time to obtain degradation rates. Bar graph shows the levels of puromycin at t=0 normalized to the amount of puromycin in the WT cells at t=0, showing lower levels of puromycin in KO cells. Error bars are representative of 4 separate measurements. **B**) Assay was performed as in A, but UCH37KO cells were used and transfected with the indicated DNA. Analysis was performed as in A.

Taken together, these results suggest that UCH37 plays a complicated role in regulating protein turnover. When treated with siRNA against UCH37 and RPN13, there was a clear enhancement of the stability of p21, relative to the negative control siRNA treatment. This however, was not observed when UCH37 was removed using the CRISPR/Cas9 system. As the CRISPR cell line is a stable knockout selected from a single clone, it is possible that these cells have evolved mechanisms to compensate for the loss of UCH37 in order to continue proliferating. Interestingly, we consistently observed lower levels of both p21 and NEK2A in the UCH37 CRISPR cell line, but their rates of degradation are not strongly affected by the loss of UCH37. This suggests that there may be a transcriptional/ translational response to the long-term loss of UCH37 resulting in the lowered levels of cell cycle inhibitors. This is consistent with our data looking at puromycinylated proteins, where cells lacking UCH37 display an overall lower level of puromycin incorporation into nascent peptides than the WT cells. As puromycin incorporation can also be used as a measurement of the rate of protein synthesis, this suggests that protein synthesis may be altered in the KO cells, and perhaps lowering rates of synthesis is a means to cope with impaired degradation. Aside from its role in the proteasome, UCH37 is also a member of the INO80 chromatin remodeling complex. This complex is a major regulator of transcription in eukaryotic cells and is required for the proper expression of many genes.[53] UCH37's role in this complex is essentially unknown but it has been shown that UCH37 is held in an inactive state while associated with the INO80 complex.[28, 49, 50] This activity can however, be transiently activated in the presence of proteasome subunits.[28] Thus, it is possible that the

cell can use UCH37 to communicate between the protein synthesis and degradation machinery, and the loss of UCH37 interferes with this regulation. It is also possible that the proteasome itself is differentially post-translationally modified these CRISPR cell lines to cope with the loss of UCH37 or RPN13 resulting in an enhanced ability to degrade proteins relative to the siRNA experiments. As siRNA gives temporal control over UCH37 levels, while the stable KO does not, it is possible that the KO cells are more greatly affected by UCH37 loss and display adaptive phenotypes that the siRNA cells do not have the time to develop. resulting in the discrepancy observed between depletion of UCH37 by siRNA and stable removal by CRISPR/Cas9. Future studies will be targeted towards looking into the potential of such an adaptive response by characterizing at the post-translational modifications of the proteasome as well as looking for biomarkers of downregulated protein synthesis (i.e. phosphorylation of eukaryotic translation initiation factor α eif2α).

4.4 Discussion

The proteasome is regulated by three DUBs, RPN11, USP14, and UCH37. Of these, both RPN11 and USP14 have been shown to regulate proteasomal degradation by removing Ub chains *en bloc* from substrates as they are degraded, albeit with different results.[55] RPN11 sits on the opening to the proteolytic pore and has been shown to facilitate degradation by removing chains *en bloc* as the substrate is translocated into the proteolytic chamber.[56] USP14 on the other attenuates degradation via the *en bloc* removal of Ub chains from substrates prior to the onset of degradation.[57] To date very little has been discovered about the substrate preferences of UCH37 and how it regulates protein degradation. In this study, we identify that UCH37 selectively cleaves branched Ub chains. This remarkable topological specificity coincides with linkage selectivity, as UCH37 prefers to cleave isopeptide bonds at position-48 of Ub. Moreover, UCH37 maintains this selectivity even when assayed against polydisperse HMW chains. When UCH37 is bound to RPN13 alone or in context of the proteasome, debranching activity is also

dramatically enhanced while selectivity remains. Hence, we propose that UCH37 removes K48 branch points from polyubiquitinated proteins once they have arrived at the proteasome.

Although its precise function has been unknown, the prevailing view is that UCH37 restricts proteasome-mediated degradation by acting before the commitment to proteolysis (Figure 4.8 A). [58] Our kinetic studies support this hypothesis, as the rate of debranching occurs with a turnover number of 16 min^{-1} for UCH37 bound to RPN13. A K48 branch point in a chain associated with the proteasome would therefore be removed within ~3.7 s ($1/k_{cat}$) (Figures 4.3 and 4.3.S). This is ample time for UCH37 to impede degradation considering it takes the proteasome tens of seconds to clear a ubiquitinated substrate, [59] and single-molecule studies have shown the delay between binding and commitment follows a modal distribution centered around 2 s. [33]

The modification of substrates with branched Ub chains however, has been shown to enhance their degradation in cells.[9, 10, 52, 60] Why then would the cell employ a debranching enzyme at the lid of the proteasome, as doing so would likely oppose the degradation of these substrates? When a protein is degraded by the proteasome, the chains that decorate that protein are removed prior to translocation into the catalytic chamber of the proteasome by RPN11.[55] This removal occurs *en bloc*, resulting in the release of an unanchored intact Ub chain. In the case of branched chains, they have been shown to enhance degradation of substrates by mediating high affinity interactions with proteasomal UBDs.[13] If a branched chain is released by RPN11 during the degradation process, it is therefore likely to remain bound to the proteasome, preventing new substrates from binding. As it has been suggested that chain branching can interfere with DUB hydrolysis,[11, 14] these unanchored branched chains might be long lived inside the cell. Thus, it is possible that the cell employs UCH37 as a specialized enzyme to clear these unanchored branched chains from the proteasome during degradation, thus allowing for the next generation of substrate to occupy the proteasome (Figure 4.7 B). There are also reports that binding of Ub chains to UCH37 can further enhance degradation by stimulating ATP hydrolysis.[61] Thus, UCH37 may

also potentiate the degradation of branched chain modified substrates by acting as branched chain receptor on the proteasome.

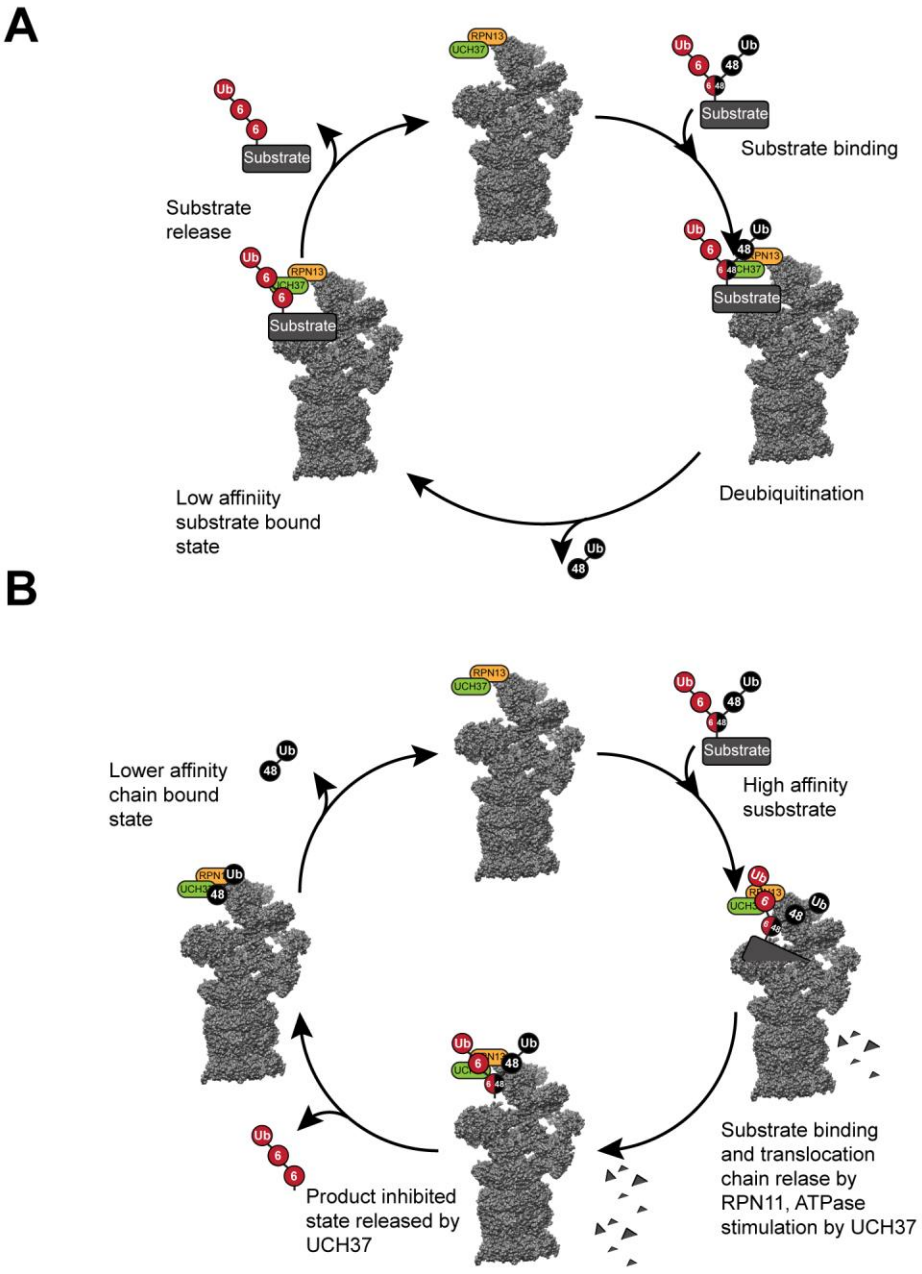

Figure 4. 8: Potential models for how UCH37 regulates proteasomal degradation. A) Prevailing view of UCH37 proteasomal degradation. UCH37 acts to antagonize substrates by removing Ub chains from substrates prior to their degradation. **B**) Model where UCH37 facilitates degradation of branched chain

substrates by aiding in the clearance of unanchored Ub chains formed during degradation of substrates. (Proteasome PDBID 5T0C).

For this to be true, we would expect that UCH37 interacts with branched Ub chains in the cell. Indeed, pull down assays showed a direct interaction between UCH37 and K11/K48 branched chains. Furthermore, we observed interactions between UCH37 and at least one substrate (p21) known to be targeted to the proteasome by branched Ub chains (Figure 4.5). For this model to also be true, we would further expect to observe a direct relationship between UCH37's debranching activity and proteasomal degradation. When we reduced levels of UCH37 or its binding partner RPN13 by siRNA, we did indeed observe reduced rates of p21 degradation in synchronized cells (Figure 4.6 A). This decrease in degradation was similar to the attenuation of degradation observed when we reduced levels of the APC/C component, Ube2S, which is necessary to promote p21 degradation in prometaphase. When we attempted to perform the same experiments in cells where UCH37 has been removed by CRISPR/Cas9 genome editing we surprisingly did not observe this same reduction in degradation rate. We did however observe a slight increase in the rate of both NEK2A and p21 degradation when UCH37 was overexpressed in this KO cell line. This increase in degradation coincided with an increase in the rate of branched chains clearance in these cells, suggesting that UCH37 may positively regulate protein degradation by clearing branched Ub chains.

This surprising result with the UCH37KO cell line suggests that cells grown under conditions of prolonged UCH37 abatement, may have found a way to compensate for the loss of UCH37. If UCH37 is responsible for mediating proteasomal degradation, then its loss may result in an upregulation of the unfolded protein response (UPR). One of the ways cells handle stress conditions is the downregulation of protein synthesis via the phosphorylation of eif2α.[62] Consistent with this, we found reduced rates of puromycin incorporation into newly synthesized proteins when we treat our UCH37 and RPN13 KO but

not the wild type cells with puromycin (Figure 4.7 A). As puromycin incorporation is a valid measurement of newly synthesized proteins,[63] it is possible that our KO cells are down regulating translation. Consistent with this, we observed lower levels of the Cyclin dependent kinase inhibitor, p21 in the UCH37KO lines. Analysis of degradation curves however revealed that this reduction in the levels of p21 was not due to a significant increase in degradation rate of this protein (Figure 4.6 B). As lower levels of p21 are have been shown to promote cell proliferation,[64] is it possible that the clonal population of UCH37KO cells we isolated have fine-tuned their p21 levels at the protein synthesis level to allow for their continued survival. Future studies will need to be performed to understand if this is indeed the case, including exploring the differences rates of cell cycle progression between cells that have been treated with UCH37 siRNA and our UCH37KO cell line. Furthermore, we will have to investigate if the unfolded protein response is upregulated in these cell lines and explore if we do indeed detect differences in the translational machinery in these cells i.e. phosphorylation of eif2α.

4.5 Acknowledgements

We thank Dr. Steve Eyles (UMass Amherst) and Prof. Ying Ge (UW-Madison) for assistance with high-resolution mass spectrometry. This work was funded by an NSF graduate research fellowship (GRFP1451512 to K.K.D.) and a grant from the NIH (RO1GM110543). The data described herein were acquired on an Orbitrap Fusion mass spectrometer funded by National Institutes of Health grant 1S10OD010645-01A1.

4.6 References

1. Hershko, A.; Ciechanover, A., The ubiquitin system. *Annu. Rev. Biochem.* **1998,** *67*, 425-79.

2. Komander, D.; Rape, M., The ubiquitin code. *Annu. Rev. Biochem.* **2012,** *81*, 203-29.

3. Chen, Z. J.; Sun, L. J., Nonproteolytic functions of ubiquitin in cell signaling. *Mol. Cell* **2009,** *33* (3), 275-86.

4. Komander, D.; Clague, M. J.; Urbe, S., Breaking the chains: structure and function of the deubiquitinases. *Nat. Rev. Mol. Cell. Biol.* **2009,** *10* (8), 550-63.

5. Clague, M. J.; Barsukov, I.; Coulson, J. M.; Liu, H.; Rigden, D. J.; Urbe, S., Deubiquitylases from genes to organism. *Physiol. Rev.* **2013,** *93* (3), 1289-315.

6. Damgaard, R. B.; Walker, J. A.; Marco-Casanova, P.; Morgan, N. V.; Titheradge, H. L.; Elliott, P. R.; McHale, D.; Maher, E. R.; McKenzie, A. N.; Komander, D., The Deubiquitinase OTULIN Is an Essential Negative Regulator of Inflammation and Autoimmunity. *Cell* **2016,** *166* (5), 1215-1230 e20.

7. Yau, R.; Rape, M., The increasing complexity of the ubiquitin code. *Nat. Cell Biol.* **2016,** *18* (6), 579-86.

8. Swatek, K. N.; Komander, D., Ubiquitin modifications. *Cell Res.* **2016,** *26* (4), 399-422.

9. Liu, C.; Liu, W.; Ye, Y.; Li, W., Ufd2p synthesizes branched ubiquitin chains to promote the degradation of substrates modified with atypical chains. *Nat. Commun.* **2017,** *8*, 14274.

10. Meyer, H. J.; Rape, M., Enhanced protein degradation by branched ubiquitin chains. *Cell* **2014,** *157* (4), 910-21.

11. Ohtake, F.; Saeki, Y.; Ishido, S.; Kanno, J.; Tanaka, K., The K48-K63 Branched Ubiquitin Chain Regulates NF-kappaB Signaling. *Mol. Cell* **2016,** *64* (2), 251-266.

12. Emmerich, C. H.; Ordureau, A.; Strickson, S.; Arthur, J. S.; Pedrioli, P. G.; Komander, D.; Cohen, P., Activation of the canonical IKK complex by K63/M1-linked hybrid ubiquitin chains. *Proc. Natl. Acad. Sci. U S A* **2013,** *110* (38), 15247-52.

13. Grice, G. L.; Lobb, I. T.; Weekes, M. P.; Gygi, S. P.; Antrobus, R.; Nathan, J. A., The Proteasome Distinguishes between Heterotypic and Homotypic Lysine-11-Linked Polyubiquitin Chains. *Cell Rep.* **2015,** *12* (4), 545-53.

14. Wertz, I. E.; Newton, K.; Seshasayee, D.; Kusam, S.; Lam, C.; Zhang, J.; Popovych, N.; Helgason, E.; Schoeffler, A.; Jeet, S.; Ramamoorthi, N.; Kategaya, L.; Newman, R. J.; Horikawa, K.; Dugger, D.; Sandoval, W.; Mukund, S.; Zindal, A.; Martin, F.; Quan, C.; Tom, J.; Fairbrother, W. J.; Townsend, M.; Warming, S.; DeVoss, J.; Liu, J.; Dueber, E.; Caplazi, P.; Lee, W. P.; Goodnow, C. C.; Balazs, M.; Yu, K.; Kolumam, G.; Dixit, V. M., Phosphorylation and linear ubiquitin direct A20 inhibition of inflammation. *Nature* **2015,** *528* (7582), 370-5.

15. Al-Shami, A.; Jhaver, K. G.; Vogel, P.; Wilkins, C.; Humphries, J.; Davis, J. J.; Xu, N.; Potter, D. G.; Gerhardt, B.; Mullinax, R.; Shirley, C. R.; Anderson, S. J.; Oravecz, T., Regulators of the proteasome pathway, Uch37 and Rpn13, play distinct roles in mouse development. *PLoS One* **2010,** *5* (10), e13654.

16. Fang, Y.; Fu, D.; Tang, W.; Cai, Y.; Ma, D.; Wang, H.; Xue, R.; Liu, T.; Huang, X.; Dong, L.; Wu, H.; Shen, X., Ubiquitin C-terminal Hydrolase 37, a novel predictor for hepatocellular carcinoma recurrence, promotes cell migration and invasion via interacting and deubiquitinating PRP19. *Biochim. Biophys. Acta.* **2013,** *1833* (3), 559-72.

17. Fang, Y.; Mu, J.; Ma, Y.; Ma, D.; Fu, D.; Shen, X., The interaction between ubiquitin C-terminal hydrolase 37 and glucose-regulated protein 78 in hepatocellular carcinoma. *Mol. Cell.l Biochem.* **2012,** *359* (1-2), 59-66.

18. Wicks, S. J.; Grocott, T.; Haros, K.; Maillard, M.; ten Dijke, P.; Chantry, A., Reversible ubiquitination regulates the Smad/TGF-beta signalling pathway. *Biochem. Soc. Trans.* **2006,** *34* (Pt 5), 761-3.

19. Wicks, S. J.; Haros, K.; Maillard, M.; Song, L.; Cohen, R. E.; Dijke, P. T.; Chantry, A., The deubiquitinating enzyme UCH37 interacts with Smads and regulates TGF-beta signalling. *Oncogene* **2005,** *24* (54), 8080-4.

20. Han, W.; Lee, H.; Han, J. K., Ubiquitin C-terminal hydrolase37 regulates Tcf7 DNA binding for the activation of Wnt signalling. *Sci. Rep.* **2017,** *7*, 42590.

21. Nishi, R.; Wijnhoven, P.; le Sage, C.; Tjeertes, J.; Galanty, Y.; Forment, J. V.; Clague, M. J.; Urbe, S.; Jackson, S. P., Systematic characterization of deubiquitylating enzymes for roles in maintaining genome integrity. *Nat. Cell Biol.* **2014,** *16* (10), 1016-26, 1-8.

22. Randles, L.; Anchoori, R. K.; Roden, R. B.; Walters, K. J., The Proteasome Ubiquitin Receptor hRpn13 and Its Interacting Deubiquitinating Enzyme Uch37 Are Required for Proper Cell Cycle Progression. *J. Biol. Chem.* **2016,** *291* (16), 8773-83.

23. Mazumdar, T.; Gorgun, F. M.; Sha, Y.; Tyryshkin, A.; Zeng, S.; Hartmann-Petersen, R.; Jorgensen, J. P.; Hendil, K. B.; Eissa, N. T., Regulation of NF-kappaB activity and inducible nitric oxide synthase by regulatory particle non-ATPase subunit 13 (Rpn13). *Proc. Natl. Acad. Sci. U S A* **2010,** *107* (31), 13854-9.

24. van Beekum, O.; Gao, Y.; Berger, R.; Koppen, A.; Kalkhoven, E., A novel RNAi lethality rescue screen to identify regulators of adipogenesis. *PLoS One* **2012,** *7* (6), e37680.

25. Hamazaki, J.; Iemura, S.; Natsume, T.; Yashiroda, H.; Tanaka, K.; Murata, S., A novel proteasome interacting protein recruits the deubiquitinating enzyme UCH37 to 26S proteasomes. *EMBO J.* **2006,** *25* (19), 4524-36.

26. Qiu, X. B.; Ouyang, S. Y.; Li, C. J.; Miao, S.; Wang, L.; Goldberg, A. L., hRpn13/ADRM1/GP110 is a novel proteasome subunit that binds the deubiquitinating enzyme, UCH37. *EMBO J.* **2006,** *25* (24), 5742-53.

27. Yao, T.; Song, L.; Xu, W.; DeMartino, G. N.; Florens, L.; Swanson, S. K.; Washburn, M. P.; Conaway, R. C.; Conaway, J. W.; Cohen, R. E., Proteasome recruitment and activation of the Uch37 deubiquitinating enzyme by Adrm1. *Nat. Cell. Biol.* **2006,** *8* (9), 994-1002.

28. Yao, T.; Song, L.; Jin, J.; Cai, Y.; Takahashi, H.; Swanson, S. K.; Washburn, M. P.; Florens, L.; Conaway, R. C.; Cohen, R. E.; Conaway, J. W., Distinct modes of regulation of the Uch37 deubiquitinating enzyme in the proteasome and in the Ino80 chromatin-remodeling complex. *Mol. Cell* **2008,** *31* (6), 909-17.

29. Lam, Y. A.; Xu, W.; DeMartino, G. N.; Cohen, R. E., Editing of ubiquitin conjugates by an isopeptidase in the 26S proteasome. *Nature* **1997,** *385* (6618), 737-40.

30. Anchoori, R. K.; Karanam, B.; Peng, S.; Wang, J. W.; Jiang, R.; Tanno, T.; Orlowski, R. Z.; Matsui, W.; Zhao, M.; Rudek, M. A.; Hung, C. F.; Chen, X.; Walters, K. J.; Roden, R. B., A bis-benzylidine piperidone targeting proteasome ubiquitin receptor RPN13/ADRM1 as a therapy for cancer. *Cancer Cell* **2013,** *24* (6), 791-805.

31. Bett, J. S.; Ritorto, M. S.; Ewan, R.; Jaffray, E. G.; Virdee, S.; Chin, J. W.; Knebel, A.; Kurz, T.; Trost, M.; Tatham, M. H.; Hay, R. T., Ubiquitin C-terminal hydrolases cleave isopeptide- and peptide-linked ubiquitin from structured proteins but do not edit ubiquitin homopolymers. *Biochem. J.* **2015,** *466* (3), 489-98.

32. Lu, X.; Nowicka, U.; Sridharan, V.; Liu, F.; Randles, L.; Hymel, D.; Dyba, M.; Tarasov, S. G.; Tarasova, N. I.; Zhao, X. Z.; Hamazaki, J.; Murata, S.; Burke, T. R., Jr.; Walters, K. J., Structure of the Rpn13-Rpn2 complex provides insights for Rpn13 and Uch37 as anticancer targets. *Nat. Commun.* **2017,** *8*, 15540.

33. Lu, Y.; Lee, B. H.; King, R. W.; Finley, D.; Kirschner, M. W., Substrate degradation by the proteasome: a single-molecule kinetic analysis. *Science* **2015,** *348* (6231), 1250834.

34. D'Arcy, P.; Brnjic, S.; Olofsson, M. H.; Fryknas, M.; Lindsten, K.; De Cesare, M.; Perego, P.; Sadeghi, B.; Hassan, M.; Larsson, R.; Linder, S., Inhibition of proteasome deubiquitinating activity as a new cancer therapy. *Nat. Med.* **2011,** *17* (12), 1636-40.

35. Tian, Z.; D'Arcy, P.; Wang, X.; Ray, A.; Tai, Y. T.; Hu, Y.; Carrasco, R. D.; Richardson, P.; Linder, S.; Chauhan, D.; Anderson, K. C., A novel small molecule inhibitor of deubiquitylating enzyme USP14 and UCHL5 induces apoptosis in multiple myeloma and overcomes bortezomib resistance. *Blood* **2014,** *123* (5), 706-16.

36. Valkevich, E. M.; Guenette, R. G.; Sanchez, N. A.; Chen, Y. C.; Ge, Y.; Strieter, E. R., Forging isopeptide bonds using thiol-ene chemistry: site-specific coupling of ubiquitin molecules for studying the activity of isopeptidases. *J. Am. Chem. Soc.* **2012,** *134* (16), 6916-9.

37. Trang, V. H.; Valkevich, E. M.; Minami, S.; Chen, Y. C.; Ge, Y.; Strieter, E. R., Nonenzymatic polymerization of ubiquitin: single-step synthesis and isolation of discrete ubiquitin oligomers. *Angew. Chem. Int. Ed. Engl.* **2012,** *51* (52), 13085-8.

38. Pham, G. H.; Rana, A. S.; Korkmaz, E. N.; Trang, V. H.; Cui, Q.; Strieter, E. R., Comparison of native and non-native ubiquitin oligomers reveals analogous structures and reactivities. *Protein Sci.* **2015**.

39. Crowe, S. O.; Pham, G. H.; Ziegler, J. C.; Deol, K. K.; Guenette, R. G.; Ge, Y.; Strieter, E. R., Subunit-Specific Labeling of Ubiquitin Chains by Using Sortase: Insights into the Selectivity of Deubiquitinases. *Chembiochem* **2016,** *17* (16), 1525-31.

40. Mevissen, T. E.; Hospenthal, M. K.; Geurink, P. P.; Elliott, P. R.; Akutsu, M.; Arnaudo, N.; Ekkebus, R.; Kulathu, Y.; Wauer, T.; El Oualid, F.; Freund, S. M.; Ovaa, H.; Komander, D., OTU deubiquitinases reveal mechanisms of linkage specificity and enable ubiquitin chain restriction analysis. *Cell* **2013,** *154* (1), 169-84.

41. Valkevich, E. M.; Sanchez, N. A.; Ge, Y.; Strieter, E. R., Middle-down mass spectrometry enables characterization of branched ubiquitin chains. *Biochemistry* **2014,** *53* (30), 4979-89.

42. Hospenthal, M. K.; Freund, S. M.; Komander, D., Assembly, analysis and architecture of atypical ubiquitin chains. *Nat. Struct. Mol. Biol.* **2013,** *20* (5), 555-65.

43. Lin, D. Y.; Diao, J.; Zhou, D.; Chen, J., Biochemical and structural studies of a HECT-like ubiquitin ligase from Escherichia coli O157:H7. *J. Biol. Chem.* **2011,** *286* (1), 441-9.

44. Bremm, A.; Freund, S. M.; Komander, D., Lys11-linked ubiquitin chains adopt compact conformations and are preferentially hydrolyzed by the deubiquitinase Cezanne. *Nat. Struct. Mol. Biol.* **2010,** *17* (8), 939-47.

45. Kristariyanto, Y. A.; Abdul Rehman, S. A.; Campbell, D. G.; Morrice, N. A.; Johnson, C.; Toth, R.; Kulathu, Y., K29-selective ubiquitin binding domain reveals structural basis of specificity and heterotypic nature of k29 polyubiquitin. *Mol. Cell* **2015,** *58* (1), 83-94.

46. Michel, M. A.; Elliott, P. R.; Swatek, K. N.; Simicek, M.; Pruneda, J. N.; Wagstaff, J. L.; Freund, S. M.; Komander, D., Assembly and specific recognition of k29- and k33-linked polyubiquitin. *Mol. Cell* **2015,** *58* (1), 95-109.

47. Nakasone, M. A.; Livnat-Levanon, N.; Glickman, M. H.; Cohen, R. E.; Fushman, D., Mixed-linkage ubiquitin chains send mixed messages. *Structure* **2013,** *21* (5), 727-40.

48. Kirkpatrick, D. S.; Hathaway, N. A.; Hanna, J.; Elsasser, S.; Rush, J.; Finley, D.; King, R. W.; Gygi, S. P., Quantitative analysis of in vitro ubiquitinated cyclin B1 reveals complex chain topology. *Nat. Cell Biol.* **2006,** *8* (7), 700-10.

49. Sahtoe, Danny D.; van Dijk, Willem J.; El Oualid, F.; Ekkebus, R.; Ovaa, H.; Sixma, Titia K., Mechanism of UCH-L5 Activation and Inhibition by DEUBAD Domains in RPN13 and INO80G. *Mol. Cell* **2015,** *57* (5), 887-900.

50. VanderLinden, R. T.; Hemmis, C. W.; Schmitt, B.; Ndoja, A.; Whitby, F. G.; Robinson, H.; Cohen, R. E.; Yao, T.; Hill, C. P., Structural Basis for the Activation and Inhibition of the UCH37 Deubiquitylase. *Mol. Cell* **2016,** *61* (3), 487.

51. Wang, X.; Chen, C.-F.; Baker, P. R.; Chen, P.-l.; Kaiser, P.; Huang, L., Mass Spectrometric Characterization of the Affinity-Purified Human 26S Proteasome Complex. *Biochemistry* **2007,** *46* (11), 3553-3565.

52. Yau, R. G.; Doerner, K.; Castellanos, E. R.; Haakonsen, D. L.; Werner, A.; Wang, N.; Yang, X. W.; Martinez-Martin, N.; Matsumoto, M. L.; Dixit, V. M.; Rape, M., Assembly and Function of Heterotypic Ubiquitin Chains in Cell-Cycle and Protein Quality Control. *Cell* **2017,** *171* (4), 918-933.e20.

53. Conaway, R. C.; Conaway, J. W., The INO80 chromatin remodeling complex in transcription, replication and repair. *Trends Biochem. Sci.* **2009,** *34* (2), 71-77.

54. Nathans, D., PUROMYCIN INHIBITION OF PROTEIN SYNTHESIS: INCORPORATION OF PUROMYCIN INTO PEPTIDE CHAINS. *Proc. Natl. Acad. Sci. USA* **1964,** *51* (4), 585.

55. de Poot, S. A. H.; Tian, G.; Finley, D., Meddling with Fate: The Proteasomal Deubiquitinating Enzymes. *J. Mol. Biol.* **2017,** *429* (22), 3525-3545.

56. Verma, R.; Aravind, L.; Oania, R.; McDonald, W. H.; Yates, J. R.; Koonin, E. V.; Deshaies, R. J., Role of Rpn11 Metalloprotease in Deubiquitination and Degradation by the 26S Proteasome. *Science* **2002,** *298* (5593), 611.

57. Lee, B.-H.; Lu, Y.; Prado, M. A.; Shi, Y.; Tian, G.; Sun, S.; Elsasser, S.; Gygi, S. P.; King, R. W.; Finley, D., USP14 deubiquitinates proteasome-bound substrates that are ubiquitinated at multiple sites. *Nature* **2016,** *532*, 398.

58. Collins, G. A.; Goldberg, A. L., The Logic of the 26S Proteasome. *Cell* **2017,** *169* (5), 792-806.

59. Peth, A.; Nathan, J. A.; Goldberg, A. L., The ATP costs and time required to degrade ubiquitinated proteins by the 26 S proteasome. *J. Biol. Chem.* **2013,** *288* (40), 29215-22.

60. Ohtake, F.; Tsuchiya, H.; Saeki, Y.; Tanaka, K., K63 ubiquitylation triggers proteasomal degradation by seeding branched ubiquitin chains. *Proc.Natl. Acad. Sci. USA* **2018,** *115* (7), E1401.

61. Peth, A.; Kukushkin, N.; Bossé, M.; Goldberg, A. L., Ubiquitinated Proteins Activate the Proteasomal ATPases by Binding to Usp14 or Uch37 Homologs. *J. Biol. Chem.* **2013,** *288* (11), 7781-7790.

62. Harding, H. P.; Zhang, Y.; Ron, D., Protein translation and folding are coupled by an endoplasmic-reticulum-resident kinase. *Nature* **1999,** *397*, 271.

63. Starck, S. R.; Green, H. M.; Alberola-Ila, J.; Roberts, R. W., A General Approach to Detect Protein Expression In Vivo Using Fluorescent Puromycin Conjugates. *Chem. Biol.* **2004,** *11* (7), 999-1008.

64. Spencer, Sabrina L.; Cappell, Steven D.; Tsai, F.-C.; Overton, K. W.; Wang, Clifford L.; Meyer, T., The Proliferation-Quiescence Decision Is Controlled by a Bifurcation in CDK2 Activity at Mitotic Exit. *Cell* **2013,** *155* (2), 369-383.

4.7 Supplemental Information

4.7.1 Supplemental Figures

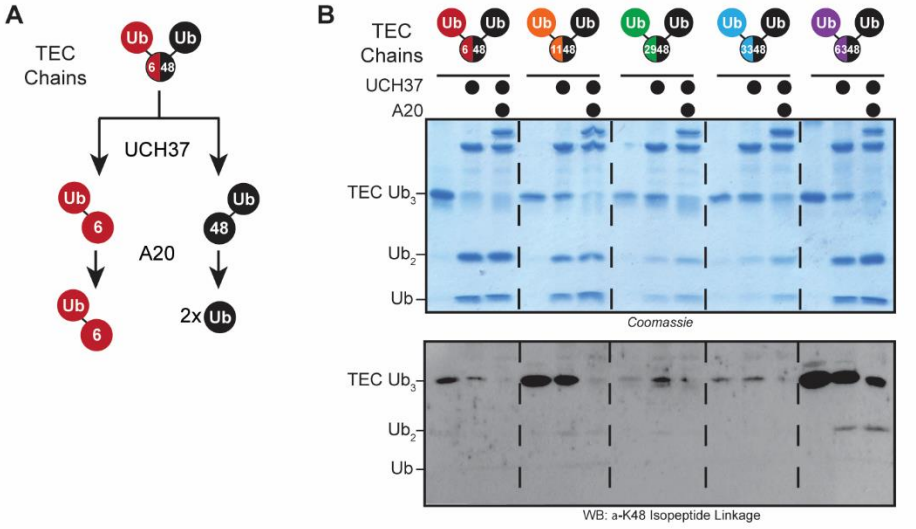

Figure 4.S. 1: Linkage Selectivity of UCH37 with TEC Trimers. A) Schematic showing the sequential DUB assay used to assess the linkage selectivity of UCH37 with thiol-ene coupling (TEC)-derived ubiquitin trimers. **B**) SDS-PAGE analysis of the sequential digests of Lys48 containing branched tri-Ub oligomers with UCH37 (5 µM) for 1 h followed by either A20 (5 µM) for 1 h. The linkage of the di-Ub species was confirmed by western blot utilizing the anti-Ubiquitin Lys48-selective antibody.

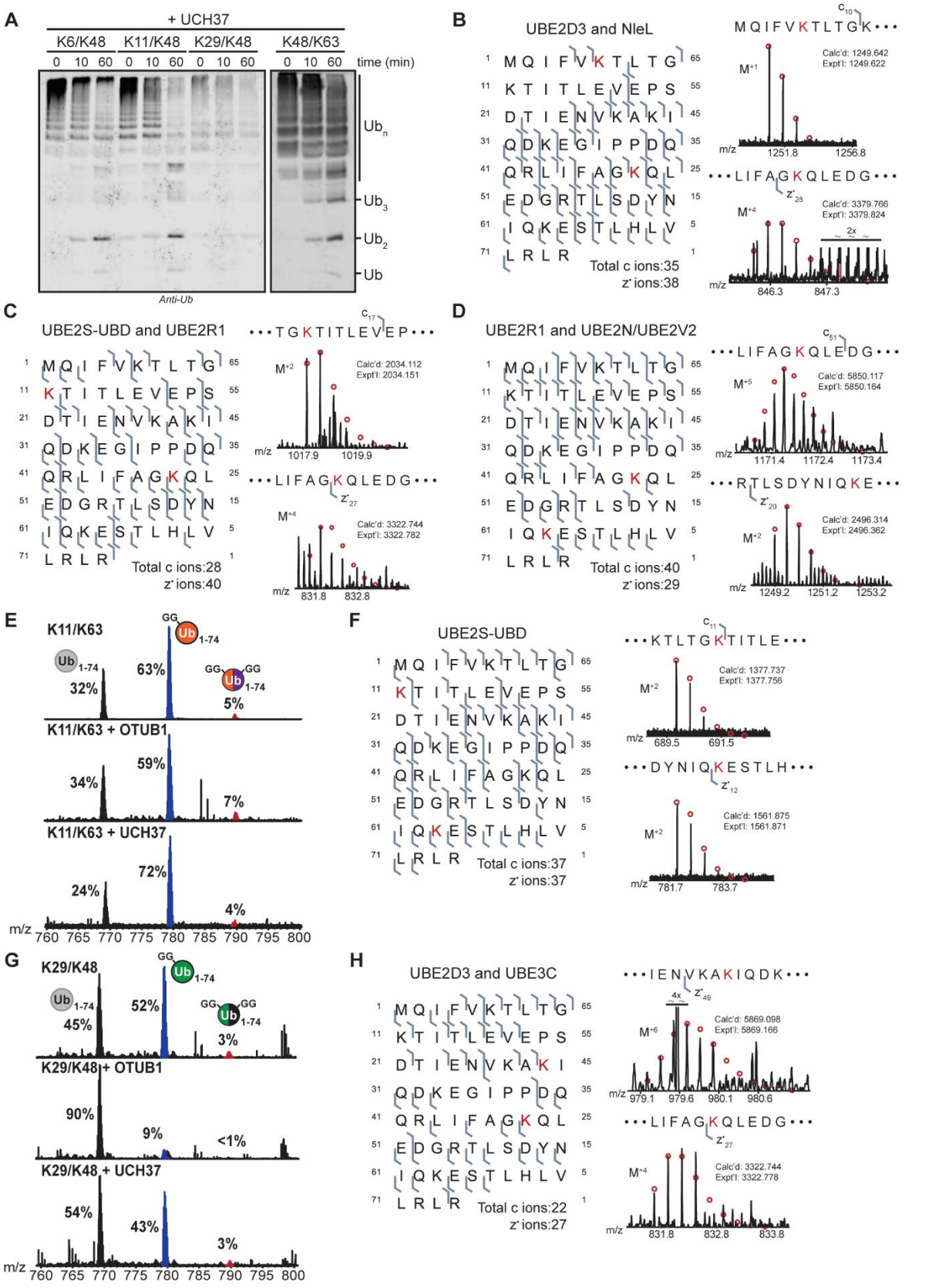
A
+ UCH37
K6/K48
K11/K48
K29/K48
K48/K63
0 10 60 0 10 60 0 10 60 0 10 60
time (min)
Ub$_n$
Ub$_3$
Ub$_2$
Ub
Anti-Ub
B
UBE2D3 and NleL
Total c ions:35
z˙ ions:38
Calc'd: 1249.642
Expt'l: 1249.622
Calc'd: 3379.766
Expt'l: 3379.824
C
UBE2S-UBD and UBE2R1
Total c ions:28
z˙ ions:40
Calc'd: 2034.112
Expt'l: 2034.151
Calc'd: 3322.744
Expt'l: 3322.782
D
UBE2R1 and UBE2N/UBE2V2
Total c ions:40
z˙ ions:29
Calc'd: 5850.117
Expt'l: 5850.164
Calc'd: 2496.314
Expt'l: 2496.362
E
K11/K63
K11/K63 + OTUB1
K11/K63 + UCH37
63%
32%
5%
59%
34%
7%
72%
24%
4%
m/z 760 765 770 775 780 785 790 795 800
F
UBE2S-UBD
Total c ions:37
z˙ ions:37
Calc'd: 1377.737
Expt'l: 1377.756
Calc'd: 1561.875
Expt'l: 1561.871
G
K29/K48
K29/K48 + OTUB1
K29/K48 + UCH37
52%
45%
3%
90%
9%
<1%
54%
43%
3%
m/z 760 765 770 775 780 785 790 795 800
H
UBE2D3 and UBE3C
Total c ions:22
z˙ ions:27
Calc'd: 5869.098
Expt'l: 5869.166
Calc'd: 3322.744
Expt'l: 3322.778

Figure 4.S. 2: Figure S2. Analysis HMW Chain Cleavage with UCH37. A) Western blot analysis of cleavage reactions with UCH37 (3 µM) and HMW K6/K48, K11/K48, K29/K48, and K48/K63 Ub chains (250 ng/µL). Time points were taken as indicated. **B**) Observed ETD fragments (c and $z^{\bullet}$ ions) mapped onto the Ub sequence containing a di-Gly modification at K6 and K48. ETD fragments showing the presence of a di-Gly modification at K6 and K48 labeled in red. Red circles represent theoretical isotopic abundance distributions of isotopomer peaks. Calc'd: calculated monoisotopic weight; expt'l: experimental monoisotopic weight. **C**) Observed ETD fragments (c and $z^{\bullet}$ ions) mapped onto the Ub sequence containing a di-Gly modification at K11 and K48. ETD fragments showing the presence of a di-Gly modification at K11 and K48 labeled in red. Red circles represent theoretical isotopic abundance distributions of isotopomer peaks. Calc'd: calculated monoisotopic weight; expt'l: experimental monoisotopic weight. **D**) Observed ETD fragments (c and $z^{\bullet}$ ions) mapped onto the Ub sequence containing a di-Gly modification at K48 and K63. ETD fragments showing the presence of a di-Gly modification at K48 and K63 labeled in red. Red circles represent theoretical isotopic abundance distributions of isotopomer peaks. Calc'd: calculated monoisotopic weight; expt'l: experimental monoisotopic weight. **E**) Middle-down MS analysis of HMW K11/K63 chains (top) followed by treatment with either OTUB1 (middle) or UCH37 (bottom). The spectra correspond to the Ub^{11+} charge state. Percentages correspond to the average relative quantification values of each Ub species: Ub1-74, ^{GG}Ub1-74, and ^{2xGG}Ub1-74 between the charge states of 8+ to 13+. **F**) Observed ETD fragments (c and $z^{\bullet}$ ions) mapped onto the Ub sequence containing a di-Gly modification at K11 and K63. ETD fragments showing the presence of a di-Gly modification at K11 and K63 labeled in red. Red circles represent theoretical isotopic abundance distributions of isotopomer peaks. Calc'd: calculated monoisotopic weight; expt'l: experimental monoisotopic weight. **G**) Middle-down MS analysis of HMW K29/K48 chains (top) followed by treatment with either OTUB1 (middle) or UCH37 (bottom). The spectra correspond to the Ub^{11+} charge state. Percentages correspond to the average relative quantification values of each Ub species: Ub1-74, ^{GG}Ub1-74, and ^{2xGG}Ub1-74 between the charge states of

8+ to 13+. **H**) Observed ETD fragments (c and $z^{\bullet}$ ions) mapped onto the sequence of Ub containing a di-Gly modification at K29 and K48. ETD fragments showing the presence of a di-Gly modification at K29 and K48 labeled in red. Red circles represent theoretical isotopic abundance distributions of isotopomer peaks. Calc'd: calculated monoisotopic weight; expt'l: experimental monoisotopic weight.

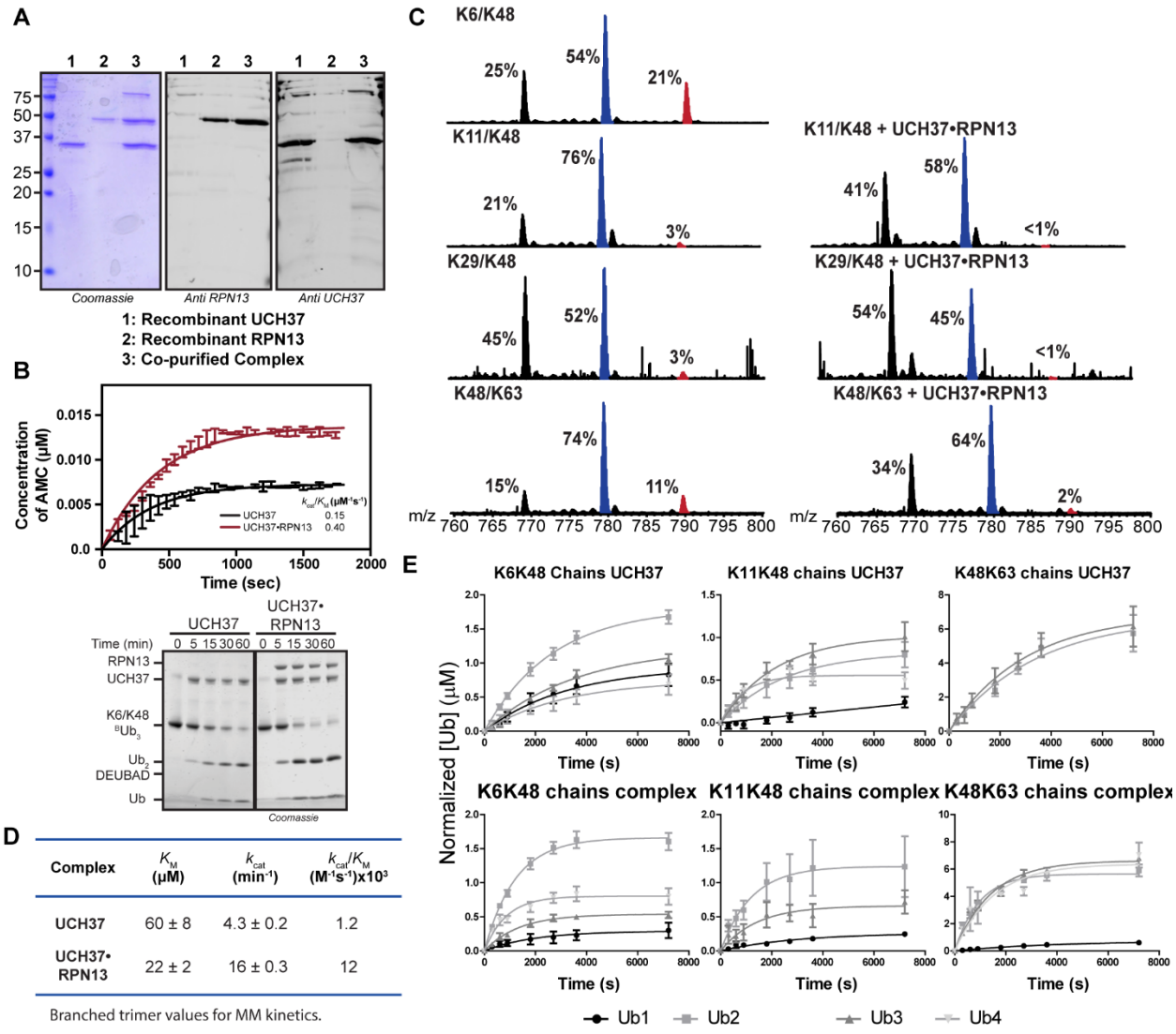

Figure 4.S. 3: Figure S3. Effects of RPN13 on Debranching Activity. A) Characterization of the UCH37•RPN13 co-purified complex: Coomassie-stained gel (left), anti-RPN13 immunoblot (middle), and anti-UCH37 immunoblot (right). 1 = recombinant UCH37, 2 = recombinant RPN13, 3 = co-purified complex. **B**) (Top) Ub-AMC hydrolysis of free UCH37 (black) and UCH37•RPN13 (red). Assays were performed in duplicate and k_{cat}/K_M values were derived by fitting to pseudo first-order kinetics: $Y = Y_{max}(1\text{-}e^{(kcat/Km)\bullet Eo\bullet t})$. (bottom) SDS-PAGE analysis of K6/K48 branched tri-Ub (10 μM) hydrolysis by UCH37 (1μM) and UCH37•RPN13 (1 μM) complexes. Time points were taken as indicated **C**) Ub MiD MS analysis of cleavage

reactions with the UCH37•RPN13 complex. The spectra correspond to the Ub^{11+} charge state. Percentages correspond to the average relative quantification values of each Ub species: Ub1-74, ^{GG}Ub1-74, and ^{2xGG}Ub1-74 between the charge states of 8+ to 13+. **D**) Michaelis-Menten kinetic parameters hydrolysis of native K6/K48 branched tri-Ub by either free UCH37 or UCH37•RPN13. **E**) Progress curves for the formation of mono-, di-, tri-, or tetra- Ub for the cleavage of HMW K6/K48, K11/K48, and K48/K63 HMW chains with either UCH37 (2.8 μM, 5 μM for HMW K11/K48 chains) or UCH37•RPN13 (1 μM). The products were visualized by western blot, normalized to an internal di-Ub standard and plotted as a function of time. This was fitted to the pseudo-first order kinetics expression. Error bars represent the standard deviation of three replicates.

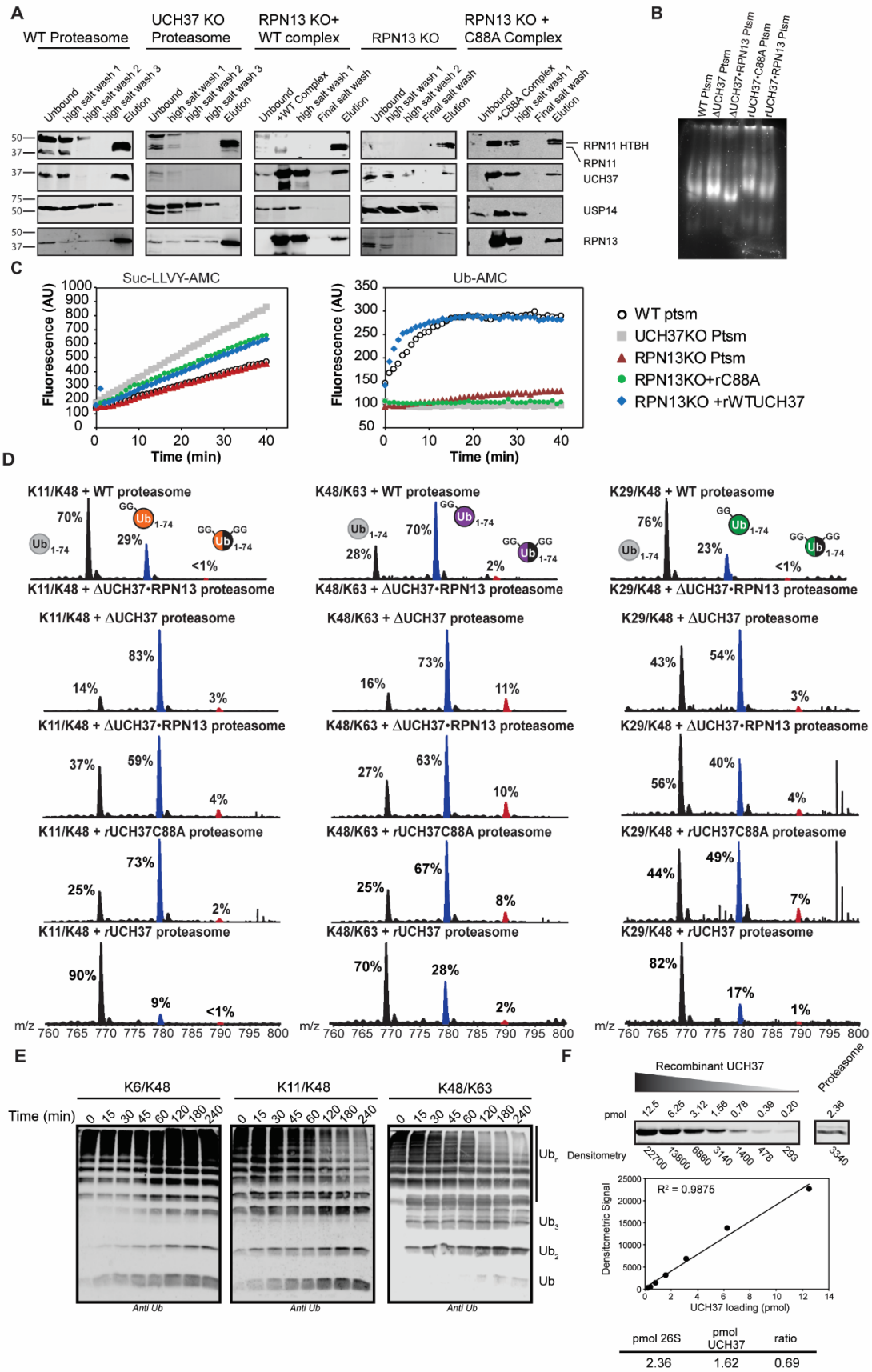
A
WT Proteasome
UCH37 KO Proteasome
RPN13 KO+ WT complex
RPN13 KO
RPN13 KO + C88A Complex
RPN11 HTBH
RPN11
UCH37
USP14
RPN13
B
WT Ptsm
ΔUCH37 Ptsm
ΔUCH37•RPN13 Ptsm
rUCH37•C88A Ptsm
rUCH37•RPN13 Ptsm
C
Suc-LLVY-AMC
Ub-AMC
Fluorescence (AU)
Time (min)
WT ptsm
UCH37KO Ptsm
RPN13KO Ptsm
RPN13KO+rC88A
RPN13KO +rWTUCH37
D
K11/K48 + WT proteasome
K48/K63 + WT proteasome
K29/K48 + WT proteasome
K11/K48 + ΔUCH37•RPN13 proteasome
K48/K63 + ΔUCH37•RPN13 proteasome
K29/K48 + ΔUCH37•RPN13 proteasome
K11/K48 + ΔUCH37 proteasome
K48/K63 + ΔUCH37 proteasome
K29/K48 + ΔUCH37 proteasome
K11/K48 + ΔUCH37•RPN13 proteasome
K48/K63 + ΔUCH37•RPN13 proteasome
K29/K48 + ΔUCH37•RPN13 proteasome
K11/K48 + rUCH37C88A proteasome
K48/K63 + rUCH37C88A proteasome
K29/K48 + rUCH37C88A proteasome
K11/K48 + rUCH37 proteasome
K48/K63 + rUCH37 proteasome
K29/K48 + rUCH37 proteasome
m/z
E
K6/K48
K11/K48
K48/K63
Time (min)
Ub_n
Ub_3
Ub_2
Ub
Anti Ub
F
Recombinant UCH37
Proteasome
pmol
Densitometry
Densitometric Signal
R² = 0.9875
UCH37 loading (pmol)
pmol 26S
pmol UCH37
ratio
2.36
1.62
0.69

Figure 4.S. 4: UCH37 is required for debranching by the proteasome. A) Western blot analysis showing the loss of USP14 during our purification. For KO cell lines the loss of UCH37 is also observed. For replenish experiments RPN13 and UCH37 are found in the final elution. **B**) Characterization of isolated proteasome complexes by native-PAGE and electrophoretic mobility shift. 5 μg of each proteasome was separated on a 3.5% native PAGE gel and stained with a 50 μM solution of the suc-LLVY-AMC peptide before fluorescence imaging. **C**) Characterization of 20S proteasome activity by suc-LLVY-AMC assay (left) or DUB activity by Ub-AMC assay (right). 1 μg of proteasome was warmed to 37^{o}C and added to 100 μL of prewarmed suc-LLVY-AMC (50μM) or Ub-AMC (500nM) and the production of fluorescence was monitored as a function of time. DUB activity is lost in both the UCH37KO and RPN13KO and proteasomes replenished with UCH37C88A suggesting that UCH37 is the only active DUB in our preps. **D**) Ub MiD MS analysis of K11/K48, K29/K48, and K48/K63 HMW chains treated with different proteasome variants. **E**) representative western blots for the cleavage of K6/K48, K11/K48, and K48/K63 HMW chains by WT proteasomes. **F**) Quantitative western blot analysis to determine concentration of UCH37 in WT proteasomes for kinetic analysis of cleavage reactions.

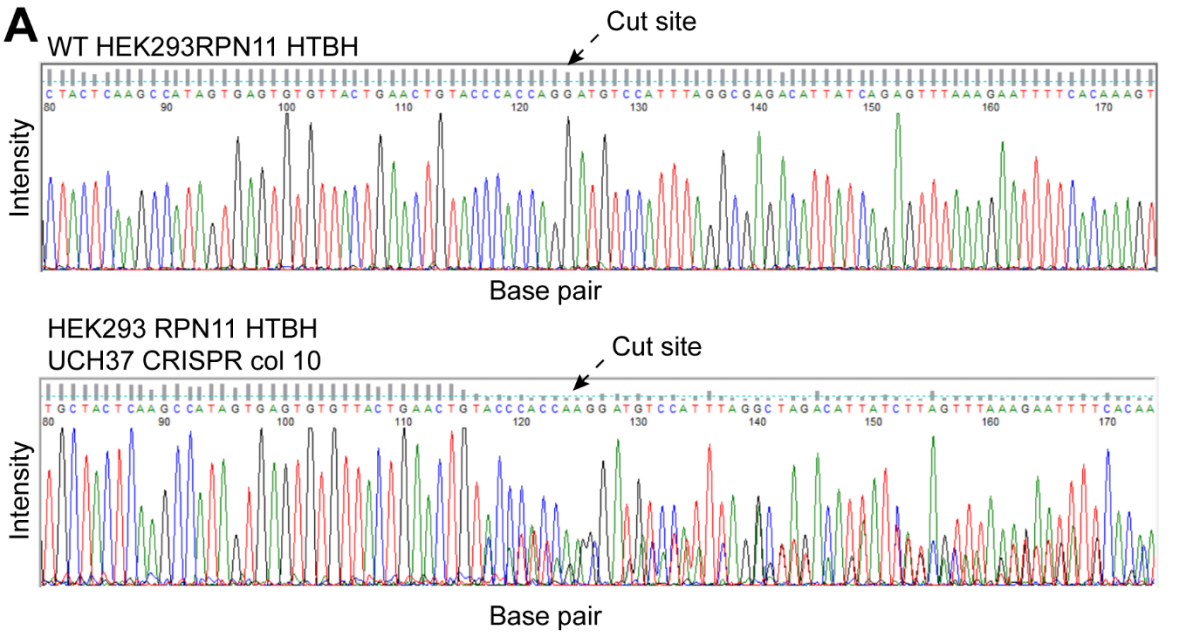
A
WT HEK293RPN11 HTBH
Cut site
Intensity
Base pair
HEK293 RPN11 HTBH
UCH37 CRISPR col 10
Cut site
Intensity
Base pair

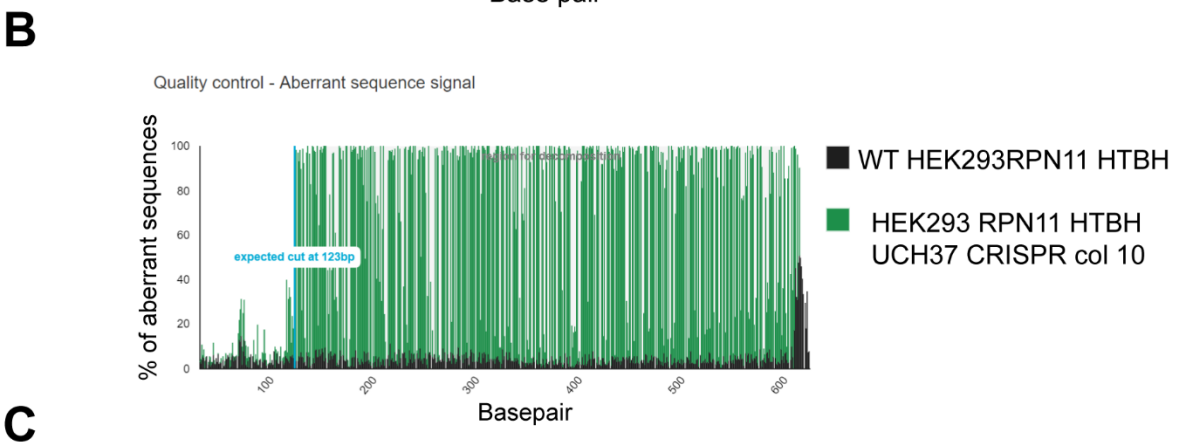
B
Quality control - Aberrant sequence signal
% of aberrant sequences
expected cut at 123bp
Basepair
WT HEK293RPN11 HTBH
HEK293 RPN11 HTBH
UCH37 CRISPR col 10

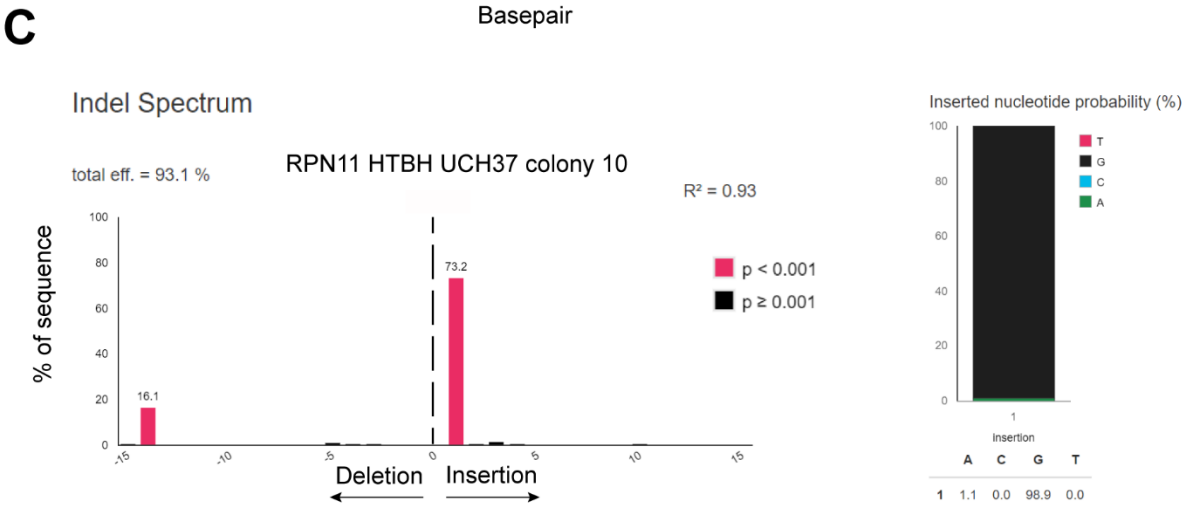
C
Indel Spectrum
total eff. = 93.1 %
RPN11 HTBH UCH37 colony 10
R² = 0.93
% of sequence
16.1
73.2
p < 0.001
p ≥ 0.001
Deletion
Insertion
Inserted nucleotide probability (%)
Insertion
A C G T
1 1.1 0.0 98.9 0.0

Figure 4.S. 5: Validating UCH37 CRISPR cell line by sequencing analysis by TIDE sequencing analysis[1]. A) Sanger sequencing trace analysis of region of the genome surrounding the expected cut site. (Top) shows the trace for cells treated with a negative control gRNA. (Bottom) shows the trace for colony 10 isolated from cells treated with a gRNA specific for UCH37. Arrow indicates expected cut site and site of trace decomposition. **B**) Histogram showing the percent of aberrant sequence reads between the negative control (black) and the isolated clone (green). Higher bars represent higher number of aberrant reads. **C**) Predicted locations of indels based on the sequence analysis. **D**) Predicted base of the insertion based on sequencing analysis.

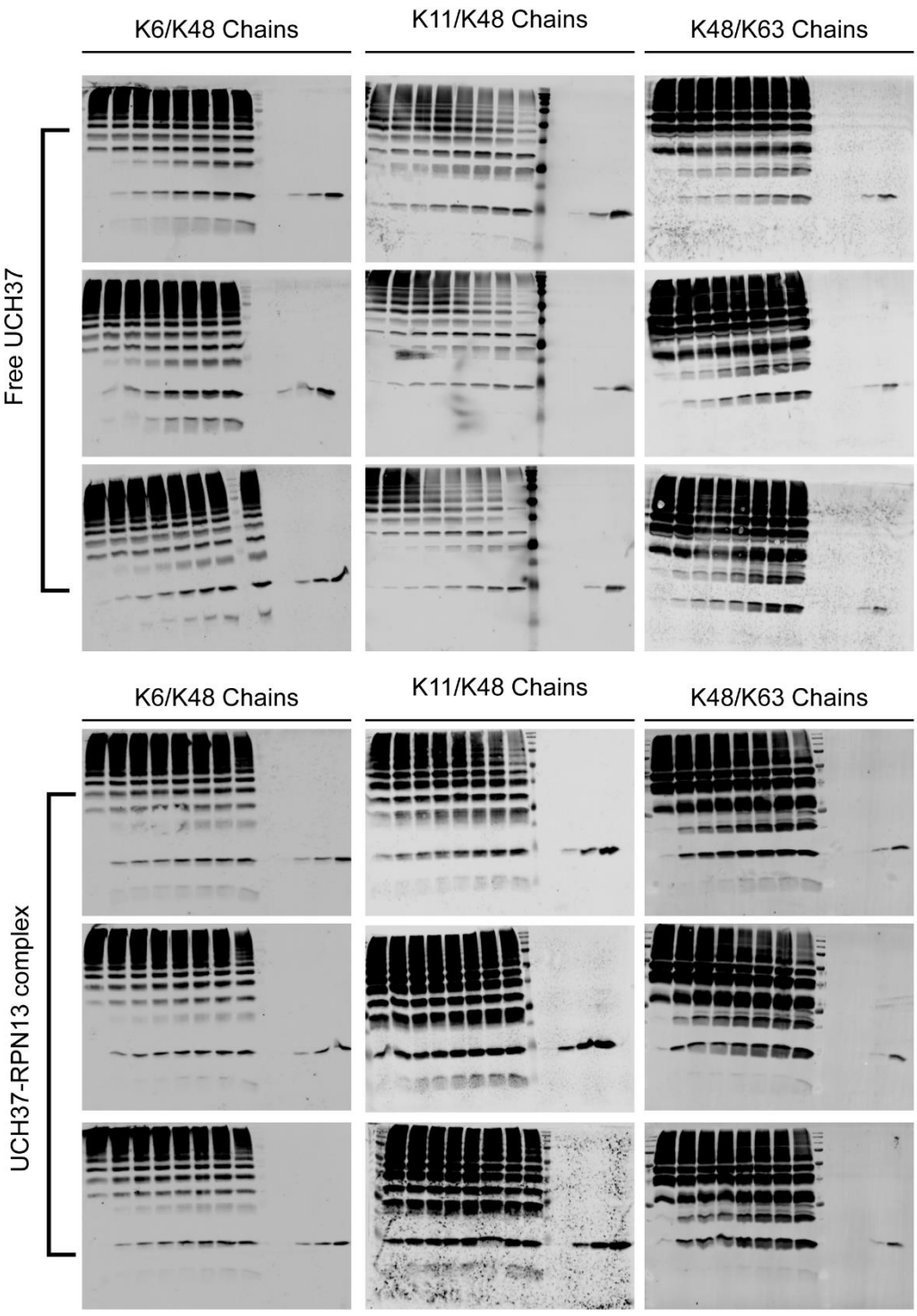

Figure 4.S. 6: Western blots used to calculate rate constant in Figure 4.4.

4.7.2 Methods and Materials

4.7.2.a Antibodies

The following antibodies were used in this study Anti UCH37 (Abcam, Cat. # ab124931) Anti RPN11 (Abcam, Cat. # ab109130) Anti RPN13 (Cell Signaling Technology, Cat # D9Z1U) Anti RPT2 (Abcam, Cat. # ab3317) Anti B7 (R&D Systems, Cat. #MAB7590) Anti USP14 (Cell Signaling Technology, Cat. # 11931S) Anti Ub (P4D1, Enzo Lifesciences, Cat. # BML-PW0930) Anti P21 (Cell Signaling Technology, Cat. # 2947S) Anti Cyclin B1 (Cell Signaling Technology, Cat. # 12231S) Anti NEK2A (BD Bioscience, Cat. # BDB610593) Anti Securin (Cell Signaling Technology, Cat. # 13445S) Anti K11K48 polyUb (Genentech) Anti β-Actin (Abcam, ab8227) Goat Anti Mouse IR Dye 800CW (LI-COR Biosciences) Goat Anti Rabbit IR Dye 680RD (LI-COR Biosciences) Anti-FLAG M2 Affinity gel (Sigma-Aldrich, Cat. # A2220-1ML)

4.7.2.b Chemicals, Peptides, and Recombinant Proteins

The following reagents were used in this study: His60 Ni Superflow resin (Clontech, Cat. # 635660) Glutathione resin (GenScript, Cat. # L00206) Amylose resin (NEB, Cat. # E8021S) Thymidine (Acros Organics, 226740050) Nocodazole (Acros Organics, 358240100) Cycloheximide (Sigma Aldrich, 01810-1G)

IU1 USP14 inhibitor (Selleck Chemicals, Cat. # S7134) b-AP15 DUB inhibitor (Selleck Chemicals, Cat. # S4920) Xfect transfection reagent (Clontech, Cat. # 631318) Lipofectamine RNAiMAX (Thermo Fisher, Cat# 13778030) Opti-MEM (Thermo Fisher, 31985062) ProBlock™ Gold Mammalian Protease Inhibitor Cocktail (Goldbio, Cat. # GB-331-5) Carfilzomib (Selleck Chemicals Cat. # S2853) STA-9090 (Selleck Chemicals Cat. # S1159) VER 155008 (Selleck Chemicals Cat. # S7751) Slide-A-lyzer MINI dialysis units (3.5kDa MWCO) (Thermo Scientific, Cat. # PI69552) 500mg SEP-PAK C_{18} column (Waters, Cat. # wat043395) SYPRO Ruby Stain (Fisher Scientific, Cat. # S12000) NuPAGE Novex 12% Bis-Tris Protein Gels (Fisher Scientific, Cat. # NPO343BOX) Trypsin (Promega, Cat. # V5113) AQUA peptides (Cell Signaling Technology, see Table S1)

4.7.2.c Protein Constructs

The following protein constructs were used in this study: UCH37 (DNASU, HsCD00084019) UCH37 C88A (this paper, N/A) FLAG-HA UCH37 (this paper) FLAG-HA UCH37C88A (this paper) FLAG-HA UCH37C88R (this paper) RPN13 or Adrm1 (Addgene, Plasmid #19423)[2] RPN13 DEUBAD domain (aa 268-407) (this paper) hRPN2 (aa 916-953)[3] (gifted from K. Walters) E1[4] NleL (aa 170-782)[5] UBE2D3[5] UBE2S-UBD (Addgene, Plasmid #66713)[6] AMSH (aa 219-424)[4] OTUD1 (Addgene, Plasmid #61405)[7] OTUB1[8] SortaseΔN25 (SrtA)[9] UBE3C (Addgene, Plasmid #66711)[10] UBE2R1[8] UBE2N/UBE2V2[8] Ub and Ub variants[11] Ub-AMC (Boston Biochem, Cat. # U-550) suc-LLVY-AMC (Boston Biochem, Cat. # S-280) Alt-R® S.p. Cas9 Nuclease 3NLS (IDT, Cat. # 1081058).

4.7.2.d Bacterial and Viral Strains

The following bacterial cell lines were used in this study: Rosetta 2(DE3)pLysS (EMD Millipore Novagen, Cat. # 71403-3) BL21(DE3)pLysS (Promega, Cat. # L1191).

4.7.2.e Experimental Models: Cell Lines

HEK293 Expressing Rpn11-HTBH (Applied Biological Materials, T6007) HEK293FT cell line (Thermofisher R70007).

4.7.2.f Recombinant DNA

The following recombinant proteins DNA was used in this study for transfections: FLAG-HA PCDNA3.1 (a gift from William Sellers (Addgene plasmid # 10792)), FLAG-HA UCH37, FLAG-HA UCH37C88A, FLAG-HA UCH37C88R.

4.7.2.g Software and Algorithms

The following software was used for data analysis: Typhoon FLA 9500 (GE Healthcare), Odyssey CLx Imager (LICOR), Image Studio software (LICOR Biosciences) Prism 6 (Graphpad Software) Xcalibur 3.0 (Thermo Fisher Scientific) Mash Suite (Guner et al., 2014)

4.7.3 Experimental Procedures

*All protein purifications were done at 4 °C unless indicated otherwise.

4.7.3.a Ub and Ub variants

Ub and Ub Kx/48C (where x is the mutated 6, 11, 29, 33 and 63 lysine position) variants were expressed as previously described.[12, 13]

4.7.3.b His-tagged proteins

1. E1, UBE2D3, UBE2R1, UBE2N/UBE2V2, and OTUB1 were expressed as previously described.[4, 5, 8]
2. N-terminally fused 6xHis-MBP UCH37[14] was grown in LB media supplemented with ampicillin (100μg/mL) to OD600 of 0.6-0.8 at 37 °C and then expressed overnight at 16 °C after induction with IPTG (250μM). Cells were pelleted at 5,000*xg* for 20min and resuspended in lysis buffer (20mM HEPES pH7.5, 200mM NaCl, 1mM EDTA, and 1mM TCEP). Cells were lysed by sonication, clarified by centrifugation at 30,000*xg* for 30min, and subsequently incubated with Ni-NTA resin for 2h. Resin was washed extensively with lysis buffer and proteins were eluted from resin with lysis buffer containing imidazole (300mM). The eluted protein was then buffer exchanged to TEV cleavage buffer (50mM HEPES pH7.5, 0.5mM EDTA, and 1mM TCEP) and cleaved overnight with TEV protease. UCH37 was then purified using anion exchange chromatography (Mono Q, GE Healthcare) in buffer A (20mM HEPES pH7.5, 1mM EDTA, and 2mM DTT) and buffer B (buffer A + 1M NaCl). Fractions containing UCH37 were identified by SDS-PAGE, combined, exchanged into storage buffer (50mM HEPES pH7.5, 50mM NaCl, 1mM EDTA, 1mM TCEP, and 10% glycerol), concentrated and flash frozen.
3. N-terminally fused His-SUMO UBE3C (aa 693-1083)[10] was purified similarly to UCH37; however, LB media was supplemented with kanamycin (50μg/mL) and cultures were induced with 400μM IPTG. After elution of the protein, 6xHis-SUMO UBE3C (aa 693-1083) was exchanged into storage

buffer (50mM Tris pH7.4, 50mM NaCl, 2mM DTT, and 10% glycerol), concentrated and flash frozen.

4. N-terminaly fused 6xHis SortaseΔN25 (SrtA) was expressed as described previously.[15]

4.7.3.c GST-tagged proteins

1. N-terminally fused GST UBE2S-UBD[6] was grown in LB media supplemented with ampicillin (100 μg/mL) to OD_{600} of 0.6-0.8 at 37 °C and then expressed overnight at 16 °C after induction with IPTG (250μM). Cells were pelleted at 5,000*xg* for 20 min and resuspended in lysis buffer (270mM sucrose, 50mM Tris pH8.0, 50mM NaF, and 1mM DTT). Cells were lysed by sonication, clarified by centrifugation at 25,000*xg* for 30min, and subsequently incubated with glutathione resin for 2h. Resin was washed extensively with high salt buffer (500mM NaCl, 25mM Tris pH8.0, 5mM DTT), low salt buffer (150mM NaCl, 25mM Tris pH8.0, 5mM DTT), and resuspended in 3C protease buffer for on-resin cleavage with HRV 3C protease overnight. UBE2S-UBD was exchanged into storage buffer (50mM Tris pH7.4, 75mM NaCl, 5mM DTT, 10% glycerol), concentrated and flash frozen.
2. N-terminally fused 6xHis-GST OTUD1[7] was grown LB was supplemented with kanamycin (50 μg/mL) to OD_{600} of 0.6-0.8 at 37 °C and then expressed overnight at 20 °C after induction with IPTG (250μM). Cells were pelleted at 5,000*xg* for20 min and resuspended in lysis buffer (25mM Tris pH8.5, 200mM NaCl, 5mM DTT, and EDTA free-complete inhibitor tablet). Cells were lysed by a French press (two passes at 18,000psi), clarified by centrifugation at 30,000*xg* for 45min, and subsequently incubated with glutathione resin for 2h. Resin was washed extensively with buffer (25mM Tris pH8.5, 200mM NaCl, and 5mM DTT) and resuspended in 3C protease buffer for on-resin cleavage with HRV 3C protease overnight. OTUD1 was then purified using anion exchange chromatography (Mono Q, GE Healthcare) in buffer A (25mM Tris pH8.0 and 1mM DTT) and buffer B (buffer A + 1M NaCl). Fractions containing OTUD1 were identified by SDS-PAGE, combined,

exchanged into storage buffer (50mM Tris pH8.0, 75mM NaCl, 5mM DTT, 10% glycerol), concentrated and flash frozen.

3. N-terminally fused GST NleL (aa 170-782) and AMSH (aa 219-424) were expressed as previously described.[4, 5]
4. The C-terminal 38 amino acids of human RPN2 was cloned into pGEX-6P-1 vector which contains an N-terminal GST tag followed by a 3C protease cleavage site. GST-hRPN2 (aa 916-953) was grown in in LB media supplemented with ampicillin (100 µg/mL) to OD_{600} ~0.5 at 37 °C and then expressed overnight at 18 °C after induction with IPTG (500µM). Cells were pelleted at 5,000*xg* for 20 min and resuspended in lysis buffer (50mM Tris pH7.5, 300mM NaCl, 2mM DTT, and 1mM PMSF). Cells were lysed by a French press (three passes at 20,000psi), clarified by centrifugation at 45,000*xg* for 30min, and subsequently incubated with glutathione resin for 2h. Resin was washed extensively with lysis buffer, high salt buffer (lysis buffer + 500mM NaCl), low salt buffer (lysis buffer + 50mM NaCl), and eluted with elution buffer (50mM Tris pH7.5, 150mM NaCl, 2mM DTT, and 50mM reduced glutathione). The eluted protein was then buffer exchanged to 3C cleavage buffer for cleavage with HRV 3C protease overnight. The cleavage reaction was quenched by adding 10% v/v acetic acid. The acidified solution was poured over a 500mg SEP-PAK C_{18} column (Waters) and washed with 3 mL 0.1% TFA in water followed by 1.5 mL each 10, 20, 30, 40, 50, 60, and 70% ACN in 0.1% TFA at room temperature. Fractions containing RPN2 peptide were identified by MALDI-TOF MS and lyophilized. The lyophilized peptide was then reconstituted in water.

4.7.3.d Co-Purification of UCH37 and RPN13

N-terminally fused His6-MBP UCH37 and N-terminally fused 6xHis RPN13 were grown in LB media supplemented with ampicillin (100 µg/mL) for both proteins (6L per protein). Cells were grown at 37 °C to

OD_{600} ~0.6 and expressed overnight at 16 °C after induction with IPTG (500µM). Cells were pelleted at 5,000*xg* for 20min and frozen at -80 °C until use. Cell pellets were thawed and resuspended in lysis buffer (25mM HEPES pH7.5, 200mM NaCl, 1mM EDTA, and 1mM TCEP), lysed by sonication, and clarified at 40,000*xg* for 30 min. UCH37•RPN13 complex was purified in three chromatographic steps. First, clarified lysate was incubated with amylose resin for 1 h, washed with lysis buffer followed by low salt buffer (25mM HEPES pH7.5, 50mM NaCl, 1mM EDTA, and 1mM TCEP), and eluted into amylose elution buffer (25mM HEPES pH7.5, 200mM NaCl, 1mM EDTA, 1mM TCEP, and 10mM maltose). The eluted protein was then incubated overnight with TEV protease to remove 6xHis-MBP tag from UCH37 resulting in a complex containing untagged UCH37 and His_6 tagged RPN13. Second, the complex was captured by incubation of the cleaved protein over Ni-NTA resin. The resin was then washed with low salt buffer, and the complex was eluted with elution buffer (25mM HEPES pH7.5, 200mM NaCl, 300mM imidazole, and 1mM TCEP). The eluted protein was then concentrated and exchanged into SEC buffer (50mM HEPES pH7.5, 50mM NaCl, 1mM EDTA, 1mM TCEP). Lastly, the complex was further purified by gel filtration using a Superdex 200 HiLoad size exclusion column (GE Healthcare) and isocratically eluted in SEC buffer. Fractions containing both UCH37 and RPN13 were identified by SDS-PAGE, combined, exchanged into storage buffer (50mM HEPES pH7.5, 50mM NaCl, 1mM EDTA, 1mM TCEP, and 10% glycerol), concentrated and flash frozen.

4.7.3.e Synthesis of Native K6/K48 Branched Trimers

K6/48R Ub (2mM), UbD77 (1mM), E1 (300nM), UBE2D3 (10µM), and NleL (aa 170-782, 1µM) were mixed in a reaction buffer (20mM ATP, 10mM $MgCl_2$, 40mM Tris-HCl pH7.5, 50mM NaCl, and 6mM DTT) overnight at 37 °C. The reaction was quenched by lowering the pH to <5 via addition of 5M ammonium acetate pH 4.4. Enzymes were then precipitated through multiple freeze thaw cycles and size exclusion chromatography was used for purification.

4.7.3.f Generation of High Molecular Weight (HMW) Ub chains

K6/K48 Ub chains were assembled in a reaction buffer (20mM ATP, 10mM $MgCl_2$, 40mM Tris-HCl pH 7.5, 50mM NaCl, and 6mM DTT) containing Ub (1 mM), E1 (150nM), UBE2D3 (5μM), and NleL (aa 170-782, 3μM). The resulting Ub chains were purified using size exclusion chromatography to isolate chains >35 kDa. *K11/48 Ub chains* were assembled in a reaction buffer (10mM ATP, 10mM $MgCl_2$, 40mM Tris pH 8.5, 100mM NaCl, 0.6mM DTT, and 10% (v/v) glycerol) containing Ub (0.6μM), E1 (150nM), and UBE2S-UBD (5μM). AMSH (aa 219-424, 3μM) and OTUD1 (0.5μM) were added after 3h and the mixture was left overnight at 37 °C. Prior to purification, an additional bolus of AMSH (aa 219-424, 3μM) and OTUD1 (0.5μM) was added, the mixture was incubated for 1 h at 37 °C and subjected to size exclusion chromatography to isolate chains with a mass >35 kDa. These HMW K11-linked chains were then added to Ub (0.6μM), E1 (150nM), and UBE2R1 (3μM) in the same reaction buffer. The resulting HMW Ub chains were further purified using size exclusion chromatography. *K48/K63 Ub chains* were assembled using Ub (1mM), E1 (150nM), UBE2R1 (5μM), and UBE2N/UBE2V2 (5μM). The resulting HMW Ub chains were also purified using size exclusion chromatography. *K11/K63 Ub chains* were assembled from Ub (1mM), E1 (150nM), UBE2S-UBD (5μM) as described above for K11/K48 chains. Finally, *K29/K48 chains* were generated from Ub (1mM), E1 (150nM), UBE2D3 (2μM), and UBE3C (aa 693-1083, 3μM) as previously described [16].

4.7.3.g Steady-State Measurements with K6/K48 Branched Trimer

Stock solutions of enzymes and K6/K48 branched trimer were prepared in assay buffer (50mM HEPES pH7.5, 50mM NaCl, and 2mM DTT) and warmed to 37 °C. Kinetic assays were performed by varying the concentration of K6/K48 branch trimer while maintaining a constant concentration of each enzyme: UCH37, or the UCH37•RPN13 complex (500nM). Reactions were performed at 37 °C and quenched by addition of 6X Laemmli loading buffer (6μL) at two time points: 2 and 5 min. Each sample along with a Ub and di-Ub standard (45μM and 15μM) were then separated on a 15% SDS-PAGE gel and followed by

SYPRO® Ruby staining. Gels were visualized on a Typhoon FLA 9500 (GE Healthcare) and densitometry was performed on the di-Ub product using Image Studio™. Initial velocities of di-Ub formation were converted to concentration of di-Ub per second by reference to di-Ub standard. These values were then fit to the Michaelis-Menten equation using nonlinear regression in Prism 6. Error bars represent the standard deviation of three trials for each reaction performed using UCH37 and the UCH37•RPN13 complex.

4.7.3.h Measuring Catalytic Efficiencies with HMW Chains

High molecular weight Ub chains (250ng/µL) were warmed to 37 °C in assay buffer (50mM HEPES pH7.5, 50mM NaCl, 10mM $MgCl_2$, 2mM DTT, and 2mM ATP) for 30 min. At the same time, UCH37, UCH37•RPN13 complex or WT proteasome were warmed to 37 °C in assay buffer. Reactions were initiated by the addition of DUB or proteasome mixture to achieve the final concentration of DUB indicated in each figure or proteasome (90µL final reaction volume). Time points were taken as indicated by removing 10µL aliquots of the reaction mixture and quenching with 6x Laemmli loading buffer (5µL). Reactions along with a concentration gradient of di-Ub standards as indicated were then separated on a 15% SDS-PAGE gel and visualized by western blot using the anti Ub antibody (P4D1). Western blots were visualized on a LI-COR Odyssey CLx imaging system and densitometry was performed on lower molecular weight products (Ub1-Ub4) using Image Studio™. The densitometry values for the di-Ub standards were used to create a standard curve for each western blot and the resulting curve was used to normalize the amount of lower molecular weight species. These values were then fit to Eq 1. using PRISM 6. The sum of the values obtained value for k_{obs} of the formation of all four lower molecular weight product error bars represent the standard deviation of three trials for each reaction performed using UCH37 and UCH37•RPN13 complex. For reactions using the proteasome, the error bars represent the standard deviation of two trials.

$$Y = Y_{max}\left(1 - e^{(k_{obs} \cdot E_o \cdot t)}\right) \quad \text{(Eq 1)}$$

4.7.3.i Ub Middle-down Mass Spectrometry (Ub MiD MS) Analysis

Minimal tryptic fragments of HMW K6/K48, K11/K48, K48/K63, K11/K63, and K29/48 Ub chains were either separated using an Ultimate 3000 UHPLC (Thermo Scientific) prior to analysis using Orbitrap Fusion Tribrid mass spectrometer (Thermo Scientific) or directly infused into the spectrometer. For separations, the UHPLC was equipped with a MASSPrep™ Micro Desalting VanGuard Pre-Column (2.1 x 5mm, Waters). Fragments were then separated using a linear gradient of 5% to 70% B over 18min and 70% to 95% B over 5min (solvent A: 0.1% formic acid (FA) in water, solvent B: 0.1% FA in ACN) using a flow rate of 10µL/min. The resolving power of the mass analyzer on the spectrometer was set at either 60000 or 120000. For tandem mass spectrometry (MS/MS) using ETD, individual charge states of protein molecular ions were isolated and dissociated by ETD using a 10ms reaction time, a 2.0e5 reagent ion target, and 10% supplemental collisionally induced dissociation (CID). All spectra were processed with in-house software (MASH Suite) using a signal-to-noise (S/N) threshold of 3 and a fit factor of 70% and then validated manually [17]. Percentages correspond to the average relative quantification values between the charge states of 9+ to 12+ for all three species: Ub_{1-74}, 1xdiGly-Ub_{1-74}, and 2xdiGly-Ub_{1-74}.

4.7.3.j Ubiquitin-AQUA High Resolution and Accurate Mass MS (HR/AM MS) Analysis

Full tryptic digests of HMW K6/K48, K11/K48, and K48/K63 Ub chains were separated on an Easy nLC 1000 UHPLC (Thermo Scientific) equipped with an Acclaim PepMap RSLC C18 (75µm x 15cm, Thermo Scientific). Using a flow rate of 300nL/min, the linear gradient was 0% to 50% over B for 20 min, 50% to 95% over B for 3min, and 95% hold over B for 7min (solvent A: 0.1% formic acid (FA) in water, solvent B: 0.1% FA in ACN). The LC system was coupled to the Orbitrap with a resolving power set at 60000. Spectra were recorded over a range 300 to 1500 m/z. For data-dependent MS/MS, the top four most intense ions with charge state of 2-5 were selected using an isolation window of 2 m/z. Fragmentation was achieved by CID at 35% nominal energy with product ion detection in the linear ion-trap. Ion chromatograms were extracted for each peptide of interest with an extraction window of 20ppm. Chromatograms were

smoothed using the Boxcar algorithm with a 7-point window. Integration was then performed using default parameters with manual adjustment as deemed appropriate. Results are normalized against total amount of Ub for each linkage type detected and are represented as means ± SEM of two replicates. For all points, asterisks represented are as follows: *P<0.025, **P<0.01 (student's t-test).

4.7.3.k Cell culture

HEK293FT cells, HEK293 cells stably expressing His-biotin affinity tagged human RPN11 (RPN11-HTBH)[18] and CRISPR variants were cultured at 37 °C under 5 % CO_2 in 150 mm TC treated plates using high glucose DMEM supplemented with 10% FBS, 1xGlutamax (Gibco), and 1xPen/Strep.

4.7.3.l Generation of CRISPR KO cell lines

Guide RNAs were designed for UCH37 and RPN13 using design tools from Harvard and the Broad Institute.[19, 20] The gRNA designed for UCH37 had the sequence (CGCCTAAATGGACATCCTGG), and the gRNA designed for ADRM1 had the sequence (CACGAACTCTCTGCGCTAGG). These gRNA designs were purchased from IDT to be used in their Alr-R® CRISPR-Cas9 system. CRISPR reactions were performed according to the protocol provided by IDT. Briefly, a 1:1 annealed complex of gRNA: tracrRNA was prepared by mixing 1μM of each RNA in nuclease-free duplex buffer (supplied by IDT), and warming to 95^{o}C for 5min before allowing to cool to room temperature on the bench. Once the annealed complex was prepared, a ribonucleotide-protein complex (RNP) was prepared by mixing the RNA complex with Alt-R® S.p. Cas9 Nuclease (60nM each) in Opti-MEM media (23μL) and incubating at room temp for 5 minutes. A transfection containing the RNP mixture was then prepared by diluting the RNP in 23.8μL Opti-MEM, adding 1.2μL Lipofectamine RNAimax, briefly vortexing, and allowing the mixture to incubate for 20min at room temp. The transfection mixture was then added to a 48 well plate, and 80,000 cells in antibiotic free media were added. These cells were allowed to grow for 2 days before trypsinization and dilution to single cell per well density in 96 well plates. Single colonies were identified and screened for protein

expression by western blot using appropriate antibodies. Colonies that showed loss of UCH37 or ADRM1 were further screened by sequencing and analysis using TIDE software.[1] Colonies with confirmed Indels were used in future experiments.

4.7.3.m Isolating WT, ΔUCH37 and ΔRPN13 proteasomes

Cells stably expressing RPN11-HTBH were grown, harvested and lysed by sonication. The lysate was clarified at 20,000*xg* for 20 min at 4 °C. Clarified lysate was incubated with streptavidin resin (GenScript) at 4 °C for O/N with rocking. The resin was then pelleted at 500*xg* for 2 min, the supernatant was discarded. The resin was further washed with 1.5mL portions of wash buffer (20mL total) rocking at 4°C for 5min during each wash, before pelleting at 500*xg* for 2min and discarding the washes. After washing, the resin was resuspended in 400μL storage buffer containing 2μM TEV protease and cleavage was allowed to proceed for 1.5h at room temp to elute the proteasome. Eluted proteasome was collected by pelleting the beads and saving the supernatant. The beads were further washed with 4x400μL portions of storage buffer, the supernatants were combined and concentrated to ~150μL before aliquoting and storing at -80°C. For UCH37 free and RPN13 free proteasomes, the same procedure was following using respective genome edited variants of the HEK293 RPN11 HTBH cell lines.

4.7.3.n Isolating proteasomes replenished with UCH37-RPN13 complexes

HEK293 RPN11HTBH RPN13 CRISPR cells were grown, harvested, lysed, and incubated with streptavidin resin as described in section 4.7.3.m. After overnight incubation with streptavidin beads, the beads were pelleted at 500*xg* for 5min and resuspended in 500μL lysis buffer + 5μM UCH37-RPN13 complex (or UCH37C88A-RPN13 complex) and incubated at 4°C for 4h with rocking. After 4h, the resin was pelleted at 500*xg* for 2min and supernatant discarded. The resin was then washed with 1.5mL portions of high salt wash buffer (20mL total) rocking 4°C for 5min during each wash, before pelleting at 700*xg* for 2min and discarding the washes. After washing, the resin was resuspended in 400μL storage buffer containing 2μM

TEV protease and cleavage was allowed to proceed for 1.5h at room temp to elute the proteasome. Eluted proteasome was collected by pelleting the beads and saving the supernatant. The beads were further washed with 4x400μL portions of storage buffer, the supernatants were combined and concentrated to ~150μL before aliquoting and storing at -80°C.

4.7.3.o Characterizing proteasome activity by AMC assay

Proteasomes were assayed for their DUB or proteolytic activity using either Ub-AMC or suc-LLVY-AMC quenched fluorescent reporter substrates respectively. Both assays were performed in black clear bottom 96 well plates. Reactions were performed by prewarming the AMC reagent (250nM for Ub-AMC or 50μM suc-LLVY-AMC) dissolved in assay buffer (50mM HEPES pH7.5, 50mM NaCl, 10mM $MgCl_2$, 2mM DTT, and 2mM ATP) in a 96 well plate at 37°C for 20min. At this point, proteasomes (0.5 or 1 μg) in assay buffer were added to added to the appropriate wells of a 96 well plate and hydrolysis was monitored continuously for 30min at 37 °C on a fluorescence plate reader (BioTek Synergy 2, λ_{ex} = 360nm, λ_{em} = 460nm).

4.7.3.p Immunoprecipitation of FLAG-HA UCH37C88A

Cells were synchronized in G2 as previously described.[21] Briefly, ~1.5 x 10^6 cells were plated in a 10cm dish and grown for 24h before being switched to media containing 2mM thymidine for 24h. At this point cells were transfected with either 30μg empty FLAGHA-pcDNA3 or FLAGHA-UCH37C88A pcDNA3 using Xfect transfection reagent according to the manufacturer's instructions. After 24h, cells were released into complete DMEM without inhibitors for 3h after which nocodazole (100ng/mL) was added and cells incubated a further 12h. After 12h, cells were removed from dish, pelleted at 300x*g* 5min, media removed and resuspended in PBS, pelleted again, PBS removed, and resuspended in 650μL ice cold IP lysis buffer (50mM HEPES, ph7.5, 150mM NaCl, 1mM EDTA, 1% Triton X-100, ProBlock™ Gold Mammalian Protease Inhibitor Cocktail, and 10 μM MG132. Cells were lysed by sonication and lysates were clarified at 21,000*xg*

for 20min. Clarified lysates (600μL) were incubated with 80μL Anti-FLAG M2 Affinity gel at 4°C for 5h with rocking. Resin was pelleted and washed 4x500μL IP lysis buffer. Proteins were eluted from resin by adding 2x non-reducing loading dye and incubating at 60°C for 15 minutes before being separated on an SDS-PAGE gel and immunoblotted using indicated antibodies.

4.7.3.q Monitoring the stability of cell cycle regulators by cycloheximide chase in cells treated with siRNA

The following siRNA systems were used: For UCH37 knockdown the TriFECTa DsiRNA Kit for UCHL5 (IDT: design ID hs.Ri.UCHL5.13) was used. This kit comes with three individual siRNA designs which were mixed in a 1:1:1 ratio to enhance knock down efficiency. For RPN13 knockdown the ON-TARGETplus HumanADRM1 (11047) siRNA - SMARTpool,5 nmol (Dharmacon item **#** L-012340-01 -0005). This kit comes with 4 premixed siRNA designs. For Ube2S the previously reported[21] siRNA with the sequence of GGCACUGGGACCUGGAUUUU was purchased from Dharmacon. Negative control dsiRNA was purchased from IDT (Cat# 51-01-14-03). Cells were reverse transfected with siRNA (30nM final concentrations) using lipofectamine RNAimax as described by the manufacturer's instructions and allowed to grow for 24-36h. Cells were then synchronized as described in section 4.7.3.p, after which cycloheximide (50μg/mL) was added to shut off translation. Cells were harvested at the indicated timepoints by pipetting cells from dish, pelleting at 1000*xg*, washing with PBS, pelleting again, and resuspending in 50μL RIPA buffer. Cells were lysed and clarified by repeated freeze-thaw lysis and centrifugation as described above. Lysates were normalized by Bradford assay before analysis by western blot using indicated antibodies.

4.7.3.r Monitoring the stability of cell cycle regulators by cycloheximide chase in transfected cells

Cells were synchronized and transfected with appropriate DNA (30μg/10cm dish) as described in section 4.7.3.o. After synchronization, cells were harvested from 10cm dish and separated into 4 equal portions in a 6-well dish, and cycloheximide (50μg/mL) was added to shut off translation. Cells were harvested at the indicated timepoints by pipetting cells from dish, pelleting at 1000*xg*, washing with PBS, pelleting

again, and resuspending in 50μL RIPA buffer. Cells were lysed and clarified by repeated freeze-thaw lysis and centrifugation as described above. Lysates were normalized by Bradford assay before analysis by western blot using indicated antibodies.

4.7.3.s Monitoring stability of puromycinylated proteins

Cells were plated in 6 well plates to approximately 80% confluency and then the media was replaced with fresh DMEM containing puromycin (5μg/mL) for 1h. After 1h, media was removed, and cells washed twice with PBS, before fresh DMEM containing cycloheximide (50μg/mL) was added to shut off translation. Cells were harvested at the indicated timepoints by pipetting cells from dish, pelleting at 1000*xg*, washing with PBS, pelleting again, and resuspending in 50μL RIPA buffer. Cells were lysed and clarified by repeated freeze-thaw lysis and centrifugation as described above. Lysates were normalized by Bradford assay before analysis by western blot using indicated antibodies. For reactions where cells were transfected, cells were plated to be approximately 30% confluency the next morning. Cells were then transfected with appropriate DNA (3.5μg/well) as described in section and allowed to grow 36h. After 36h cells were treated with puromycin and cycloheximide as described above.

4.7.5 Supplemental References

1. Brinkman, E. K.; Chen, T.; Amendola, M.; van Steensel, B., Easy quantitative assessment of genome editing by sequence trace decomposition. *Nuc. Acids Res.* **2014,** *42* (22), e168-e168.

2. Yao, T.; Song, L.; Xu, W.; DeMartino, G. N.; Florens, L.; Swanson, S. K.; Washburn, M. P.; Conaway, R. C.; Conaway, J. W.; Cohen, R. E., Proteasome recruitment and activation of the Uch37 deubiquitinating enzyme by Adrm1. *Nat. Cell Biol.* **2006,** *8*, 994.

3. Lu, X.; Liu, F.; Durham, S. E.; Tarasov, S. G.; Walters, K. J., A High Affinity hRpn2-Derived Peptide That Displaces Human Rpn13 from Proteasome in 293T Cells. *PLOS ONE* **2015,** *10* (10), e0140518.

4. Trang Vivian, H.; Valkevich Ellen, M.; Minami, S.; Chen, Y.-C.; Ge, Y.; Strieter Eric, R., Nonenzymatic Polymerization of Ubiquitin: Single-Step Synthesis and Isolation of Discrete Ubiquitin Oligomers. *Angew. Chem. Int. Ed.* **2012,** *51* (52), 13085-13088.

5. Valkevich, E. M.; Sanchez, N. A.; Ge, Y.; Strieter, E. R., Middle-Down Mass Spectrometry Enables Characterization of Branched Ubiquitin Chains. *Biochemistry* **2014,** *53* (30), 4979-4989.

6. Bremm, A.; Freund, S. M. V.; Komander, D., Lys11-linked ubiquitin chains adopt compact conformations and are preferentially hydrolyzed by the deubiquitinase Cezanne. *Nat. Struct. Mol. Biol.* **2010,** *17*, 939.

7. Mevissen, Tycho E. T.; Hospenthal, Manuela K.; Geurink, Paul P.; Elliott, Paul R.; Akutsu, M.; Arnaudo, N.; Ekkebus, R.; Kulathu, Y.; Wauer, T.; El Oualid, F.; Freund, Stefan M. V.; Ovaa, H.; Komander, D., OTU Deubiquitinases Reveal Mechanisms of Linkage Specificity and Enable Ubiquitin Chain Restriction Analysis. *Cell* **2013,** *154* (1), 169-184.

8. Pham Grace, H.; Rana Ambar, S. J. B.; Korkmaz, E. N.; Trang Vivian, H.; Cui, Q.; Strieter Eric, R., Comparison of native and non-native ubiquitin oligomers reveals analogous structures and reactivities. *Protein Sci.* **2015,** *25* (2), 456-471.

9. Ton-That, H.; Liu, G.; Mazmanian, S. K.; Faull, K. F.; Schneewind, O., Purification and characterization of sortase, the transpeptidase that cleaves surface proteins of Staphylococcus aureus at the LPXTG motif. *Proc. Natl. Acad. Sci. USA* **1999,** *96* (22), 12424.

10. Michel, Martin A.; Elliott, Paul R.; Swatek, Kirby N.; Simicek, M.; Pruneda, Jonathan N.; Wagstaff, Jane L.; Freund, Stefan M. V.; Komander, D., Assembly and Specific Recognition of K29- and K33-Linked Polyubiquitin. *Mol. Cell* **2015,** *58* (1), 95-109.

11. Valkevich, E. M.; Guenette, R. G.; Sanchez, N. A.; Chen, Y. C.; Ge, Y.; Strieter, E. R., Forging isopeptide bonds using thiol-ene chemistry: site-specific coupling of ubiquitin molecules for studying the activity of isopeptidases. *J. Am. Chem. Soc.* **2012,** *134* (16), 6916-9.

12. Pickart, C. M.; Raasi, S., Controlled Synthesis of Polyubiquitin Chains. In *Methods Enzymol.*, Academic Press: 2005; Vol. 399, pp 21-36.

13. Valkevich, E. M.; Guenette, R. G.; Sanchez, N. A.; Chen, Y.-c.; Ge, Y.; Strieter, E. R., Forging Isopeptide Bonds Using Thiol–Ene Chemistry: Site-Specific Coupling of Ubiquitin Molecules for Studying the Activity of Isopeptidases. *J. Am. Chem. Soc.* **2012,** *134* (16), 6916-6919.

14. Burgie Sethe, E.; Bingman Craig, A.; Soni Ameet, B.; Phillips George, N., Structural characterization of human Uch37. *Prot. Struct. Funct. Bioinfor.* **2011,** *80* (2), 649-654.

15. Crowe Sean, O.; Pham Grace, H.; Ziegler Jacob, C.; Deol Kirandeep, K.; Guenette Robert, G.; Ge, Y.; Strieter Eric, R., Subunit-Specific Labeling of Ubiquitin Chains by Using Sortase: Insights into the Selectivity of Deubiquitinases. *ChemBioChem* **2016,** *17* (16), 1525-1531.

16. Michel, M. A.; Elliott, P. R.; Swatek, K. N.; Simicek, M.; Pruneda, J. N.; Wagstaff, J. L.; Freund, S. M.; Komander, D., Assembly and specific recognition of k29- and k33-linked polyubiquitin. *Mol. Cell* **2015,** *58* (1), 95-109.

17. Guner, H.; Close, P. L.; Cai, W.; Zhang, H.; Peng, Y.; Gregorich, Z. R.; Ge, Y., MASH Suite: a user-friendly and versatile software interface for high-resolution mass spectrometry data interpretation and visualization. *J. Am. Soc. Mass. Spectrom.* **2014,** *25* (3), 464-70.

18. Wang, X.; Chen, C. F.; Baker, P. R.; Chen, P. L.; Kaiser, P.; Huang, L., Mass spectrometric characterization of the affinity-purified human 26S proteasome complex. *Biochemistry* **2007,** *46* (11), 3553-65.

19. Labun, K.; Montague, T. G.; Gagnon, J. A.; Thyme, S. B.; Valen, E., CHOPCHOP v2: a web tool for the next generation of CRISPR genome engineering. *Nuc. Acids Res.* **2016,** *44* (W1), W272-W276.

20. Montague, T. G.; Cruz, J. M.; Gagnon, J. A.; Church, G. M.; Valen, E., CHOPCHOP: a CRISPR/Cas9 and TALEN web tool for genome editing. *Nuc. Acids Res.* **2014,** *42* (W1), W401-W407.

21. Meyer, H.-J.; Rape, M., Enhanced Protein Degradation by Branched Ubiquitin Chains. *Cell* **2014,** *157* (4), 910-921.

Appendix A: Isolation of DUB-Free Proteasomes for the Study of Deubiquitinase Function

A.1 Introduction

Ubiquitin (Ub), is a small protein that acts as a post translational modification (PTM) of proteins, which displays broad functionality in the cell. Briefly, Ub is attached to lysine residues of substrate proteins in an ATP dependent process through the coordinated efforts of three classes of enzymes, E1, E2, and E3.[1] This process is also dynamic and is reversed by enzymes known as deubiquitinases (DUBs).[2] Many of the diverse functions that Ub displays results from the fact that Ub has eight reactive amines (Met1, Lys6, Lys11, Lys27, Lys29, Lys33, Lys48, and Lys63) that can all be further modified by Ub resulting in the formation of polymeric Ub chains. Ub chains linked through these modification sites results in eight structurally unique isomers of Ub chains, which encode the broad functionality found in Ub signaling.[3] This functionality is further enhanced because Ub chains can adopt multiple configurations including both unbranched (where Ub is modified at one positions) and branched (where a single Ub is modified at two or more positions) chains.

Once a protein is modified by an Ub chain, it can undergo one of several different fates. Perhaps the most well characterized of these, is degradation of the modified protein by the 26S proteasome. The proteasome is a 2.6 MDa complex that serves as the major protein degradation machine in eukaryotic cells. It consists of a 20S core particle (CP) which contains the proteolytic subunits and a 19S regulatory particle (RP) that ensures only the proper proteins are being degraded.[4] The human RP is decorated with three DUBs, RPN11, USP14, and UCH37. RPN11 is the only essential DUB associated with the proteasome and ablation of its activity inhibits proteasomal degradation and is lethal in cells.[5-7] USP14 and UCH37 on the other hand, are not necessary for proteasomal degradation and are thought to serve a regulatory role in this process. Of the two, more is known about how USP14 regulates the proteasome. This is largely due to USP14 being easily removed from the proteasome during purification by increasing the salt concentration in wash buffers, allowing for precise biochemical evaluation of its role in degradation.[8] To date, few methods of isolating UCH37 free proteasome have been reported, meaning that the biochemical

evaluation of its activity has lagged behind that of USP14. To isolate proteasomes free of UCH37, researchers typically purify the proteasome from red blood cells using biochemical fractionation techniques.[9] Proteasomes isolated from these cells do not appear to have UCH37, but isolation from these cells is time consuming due to the fractionation techniques required. Recently, an engineered HEK293 cell line stably expressing an affinity tagged variant of RPN11 (HEK293 RPN11-HTBH) has been described.[10] This cell line eases large-scale production of proteasomes for biochemical and biophysical studies. Using this cell line to study the activity of DUBs, however, typically involves removing DUB activity by incubating the proteasome with activity-based probes to block their catalytic site.[8] This approach is rather limited because there have been many reports of allosteric regulation of proteasomal degradation when DUBs are bound to Ub.[11-13] As these activity-based probes result in a covalent UCH37-DUB complex, this approach may affect studies as a result of this allosteric intervention. Our lab recently used the CRISPR-Cas9 system to genetically remove UCH37 from the HEK293 RPN11-HTBH cell line allowing for rapid isolation of proteasomes lacking UCH37 (Chapter 4). As genetic manipulation of an organism can have unforeseen consequences i.e., promoting PTMs of the proteasome to compensate for lost functionality, it would be ideal if UCH37 free proteasomes could be isolated from the same source as their UCH37-bound counterparts. The purpose of this appendix is to describe the work towards this goal.

UCH37 interacts with the proteasome via its interaction with the Ub receptor RPN13 (also known as ADRM1). RPN13 is a two-domain protein and interacts with UCH37 through its DEUbiquitinase ADaptor domain (DEUBAD). RPN13 docks onto the proteasome via its PRU (pleckstrin-like receptor for ubiquitin) domain, which interacts with the C-terminus of the scaffolding protein RPN2. Recently, it was reported that a small 38-mer peptide from the C-terminus of RPN2 ($RPN2_{916-953}$) competitively binds RPN13 with nM affinity, and this peptide when overexpressed in cells can displace RPN13 and UCH37 from the proteasome.[9] As this peptide can be used to remove RPN13 and UCH37 from the proteasome in cells we hypothesized that we could incorporate this into the purification of the proteasome to isolate

proteasomes depleted of the UCH37-RPN13 subcomplex. As methods to remove USP14 have already been described, we envision that this peptide would allow for the isolation of naked proteasomes lacking all non-essential DUBs allowing for precise characterization of DUB functionality.

A.2 Results

A.2.1 Isolation of Proteasomes Lacking Non-Essential DUBs

The HEK293 cell line stably expressing RPN11 with the C-terminal HTBH (His6 TEV cleavage biotin His6) affinity tag has greatly eased the isolation of human proteasomes for biochemical studies. As this cell line is now commercially available, it can easily be taken advantage of by any lab interested in the study of the proteasome. To gain a comprehensive understanding of DUB activity on the proteasome, however, methods to isolate the proteasome free of non-essential DUBs using this cell line is essential. To this end we envisioned purification strategy that combines high salt washes to remove USP14 with the $RPN2_{916\text{-}953}$ peptide to remove UCH37 (Figure A.1 A).

This purification strategy first requires access to the RPN2 peptide. A GST-tagged fusion bearing a precision protease-cleavage site between GST and the RPN2 peptide has been described previously, allowing for rapid generation of this peptide from E. coli.[9] Because of this, we also generated a GST-tagged fusion of this peptide and found that we can indeed isolate the RPN2 peptide from *E. coli* (Figure A.1 B). After protease cleavage to remove GST, we further isolated the peptide by reverse-phase chromatography.

With the peptide in hand we sought to purify proteasomes lacking USP14, and proteasomes lacking both USP14 and UCH37. As described previously, the proteasome subunit RPN11 is biotinylated in the HEK293 RPN11-HTBH cell line.[10] This allows for high quantities of proteasome to be isolated using a streptavidin pull down and can be eluted using the tobacco etch virus (TEV) protease. To isolate the proteasome, our lab typically grows 20, 15-cm plates of HEK293 RPN11 HTBH cells to confluency, harvests

the cells by scrapping, and resuspends and lyse the cells in 1 mL of lysis buffer per plate (see methods for buffer details). The proteasome can then be immobilized by incubation of the clarified lysate with streptavidin-agarose beads overnight. In agreement with previous reports, USP14 is readily removed from the proteasome by washing with high-salt buffers (200 mM NaCl).[8] Thus we can obtain proteasomes where the only non-essential DUB present is UCH37 (WT Ptsm, Figure A.1 E).

We next attempted to isolate proteasomes using the RPN2 peptide. We envisioned a purification strategy where we first immobilized the proteasome on resin prior to incubating with the peptide rather than adding the peptide directly to the lysate and displacing RPN13 prior to immobilization. This allows us to conserve the peptide because our preps are typically lysed in approximately 20 mL of buffer. By immobilizing first, we found that we could dispose of the lysate and resuspend the resin in small quantities of buffer (~1 mL) containing 10 μM RPN2 peptide saving a considerable amount of the peptide (~45 μg for 1 mL vs ~ 900 μg for 20 mL). Moreover, using this strategy we can perform several RPN2 washes to enhance depletion of the UCH37-RPN13 complex. Initially, we thought that it would be best to immobilize the proteasome on resin using a short incubation with streptavidin beads (~ 2 hours), followed by pelleting the resin and resuspension of the beads in RPN2 peptide buffer overnight to ensure displacement of RPN13 and UCH37. However, when we performed these isolations we found that our preps were lacking 20S subunits when analyzed by western blots. This was further confirmed using activity assays using the fluorogenic suc-LLVY-AMC peptide hydrolysis assay (Figure A.1 C). We did not observe this in our WT proteasome which was isolated with a longer incubation time during the immobilization step (Figure A.1 C) suggesting the incubation time of the resin with the lysate is critical. To test this, we immobilized the proteasome by incubating the resin with lysate for 8 h prior to pelleting and resuspension of the resin in RPN2 peptide buffer. This was further incubated overnight (~10 h) after which we followed this initial RPN2 wash with two more RPN2 washes and a series of 200 mM NaCl washes to remove USP14 (~50 resin volumes). When we performed purifications using this procedure we found that the 20S subunits

remained intact when analyzed by western blot (Figure A.1 D and E). Furthermore, analysis of these preps by western blot for other 19S subunits shows that USP14, UCH37, and RPN13 are indeed depleted by this treatment. Thus, we can isolate proteasomes lacking UCH37 and RPN13 using this method (ΔUCH37-RPN13 Ptsm, Figure A.1 E and F).

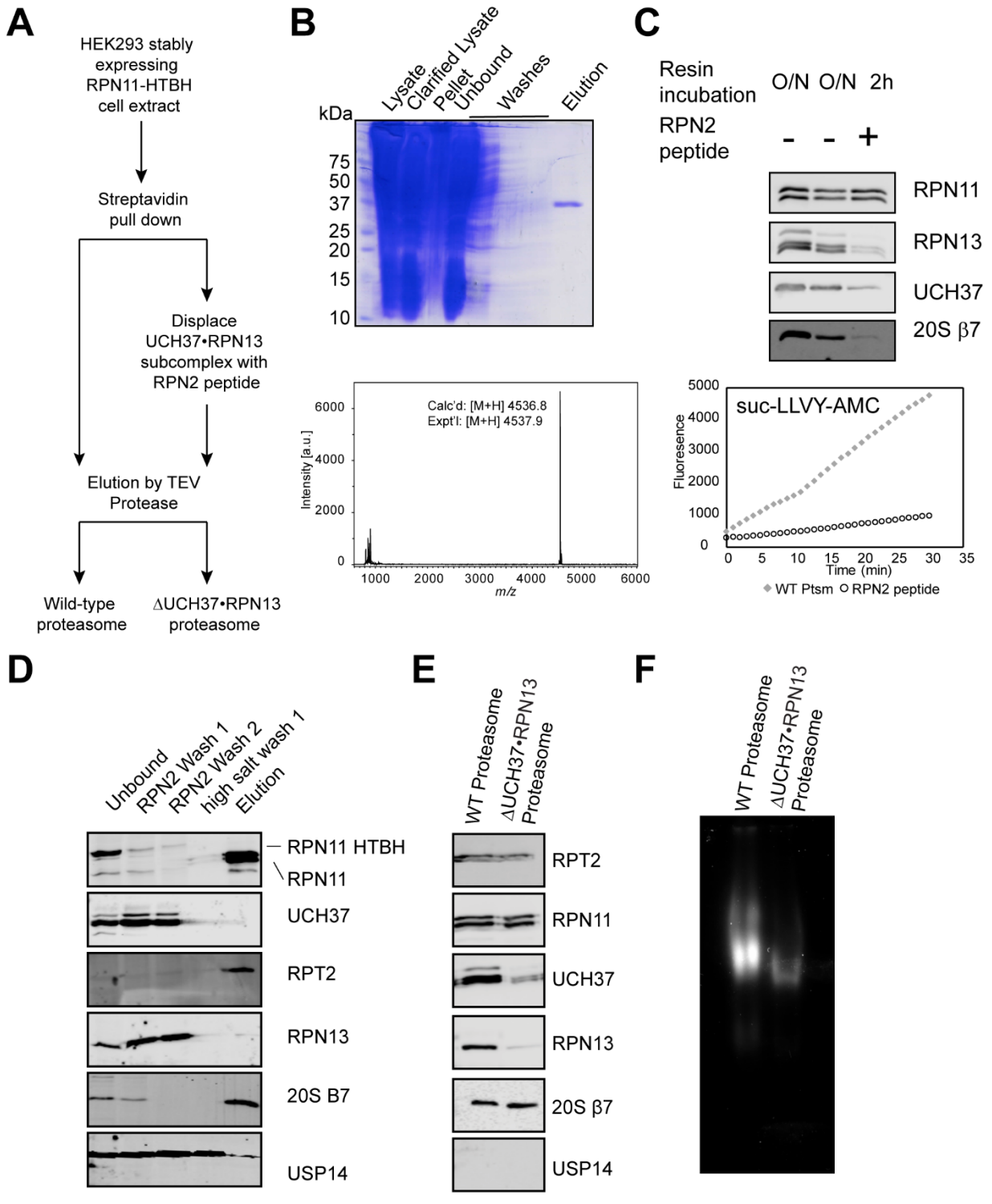

Figure A. 1: Purification of proteasomes lacking non-essential DUBs. A) Scheme for the purification of WT proteasomes and proteasomes lacking the UCH37-RPN13 subcomplex using the RPN2 peptide. **B)**

Coomassie stained gel for the purification of the $RPN2_{916-953}$ peptide is shown on the left and MALDI-TOF MS of the cleaved peptide is shown on the right. **C**) Top: western blot analysis showing that short incubation times of the resin with lysate results in loss of 20S subunits. Bottom: fluorescence reporter assay for 20S proteasome activity confirming that short resin incubation times results in the loss of 20S catalytic activity. **D**) Western blots for the purification of ΔUCH37-RPN13 proteasomes showing the removal of USP14 by high salt washes and the removal of the UCH37-RPN13 subcomplex by the RPN2 peptide wash. **E**) Western blot analysis of both WT and ΔUCH37-RPN13 proteasomes showing members of both the 19S and 20S subunits, and the loss of UCH37-RPN13 subcomplex. **F**) Native-PAGE and electrophoretic mobility shift analysis of isolated proteasome complexes. 5μg of proteasome was separated on a 3.5% native-PAGE gel and stained with a solution containing 50μM suc-LLVY-AMC peptide prior to fluorescence imaging.

A.2.2 Functional Evaluation of Isolated Proteasomes

With our two different proteasomes in hand we wanted to biochemically evaluate these preps. We first evaluated the proteolytic activity of our preps using the fluorogenic peptide substrate suc-LLVY-AMC, which is frequently used to assay the chymotrypsin-like activity of the 20S CP. Consistent with our western blot analysis, we found that both the WT Ptsm and the ΔUCH37-RPN13 Ptsm displayed similar reactivity against this substrate (Figure A.2 A). This suggests that the optimized purification does not interfere with the stability of the 26S proteasome aside from removing UCH37-RPN13. We also assayed the proteasomes using Ub-AMC, which is frequently used to assay for DUB activity. In our WT Ptsm prep, we observe robust activity against this substrate, however, proteasomes isolated using the RPN2 peptide do not show activity against this substrate (Figure A.2 B). This is consistent with both UCH37 and USP14 being removed in our ΔUCH37-RPN13 Ptsm confirming that we can indeed isolate proteasomes free of all non-essential DUBs.

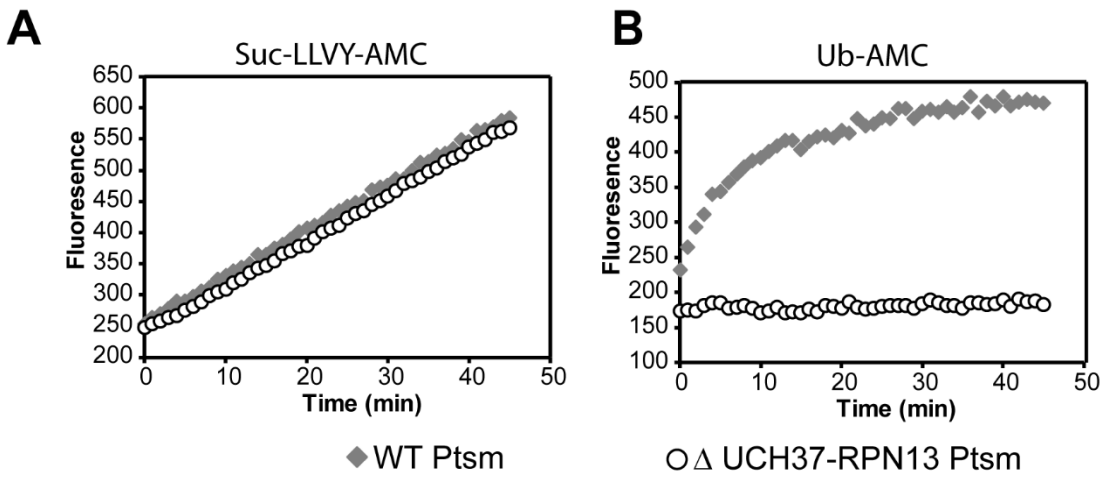

Figure A. 2: Characterization of Proteasome activity by AMC assay. A) Fluorescence reporter assay of 20S proteasome activity using the suc-LLVY-AMC substrate. **B**) Fluorescence reporter assay of DUB activity using the Ub-AMC substrate.

Our lab has demonstrated that UCH37 is a deubiquitinase that can selectively hydrolyze branched ubiquitin chains where one of the linkages in the branched chain contains a Lys48 linkage (Chapter 4). We have also shown that UCH37 retains this debranching activity while associated with the proteasome. With this information in hand, we decided to monitor the UCH37 dependent debranching activity of these preps. To this end, we first assayed the cleavage activity of these preps against high molecular weight (HMW) Ub chains generated with the bacterial E3 ligase NleL. Chains generated using this enzyme have been demonstrated to contain a high degree of branching bearing Lys6 and Lys48 linkages.[14] We have previously shown these HMW chains to be excellent substrates for both free UCH37 and proteasome bound UCH37 (Chapter 4). We titrated both our WT Ptsm and the ΔUCH37-RPN13 Ptsm into these chains and found that while the WT complex displayed DUB activity against these chains, the proteasome lacking UCH37 did not (Figure A.3 A). We further tested the ability of the proteasome to hydrolyze branched HMW chains linked through Lys48 and Lys63. Consistent with our results using NleL chains, we also observed activity against these chains when treated with our WT Ptsm, but this activity was lost when

treated with ΔUCH37-RPN13 Ptsm (Figure A.3 C). To further confirm that this activity was due to UCH37 and not the result of undetectable levels of USP14 or due to RPN11, we treated these preps with either b-AP15 or IU1. b-AP15 is a small molecule inhibitor of proteasome DUB activity that targets both UCH37 and USP14, while IU1 is an inhibitor that only inhibits USP14.[8, 15] Consistent with the observed activity being the result of UCH37, there was a concentration dependent loss in activity when treated with b-AP15 but not IU1 for both the NleL chains and the Lys48/Lys63 linked chains (Figure A.3 B and C).

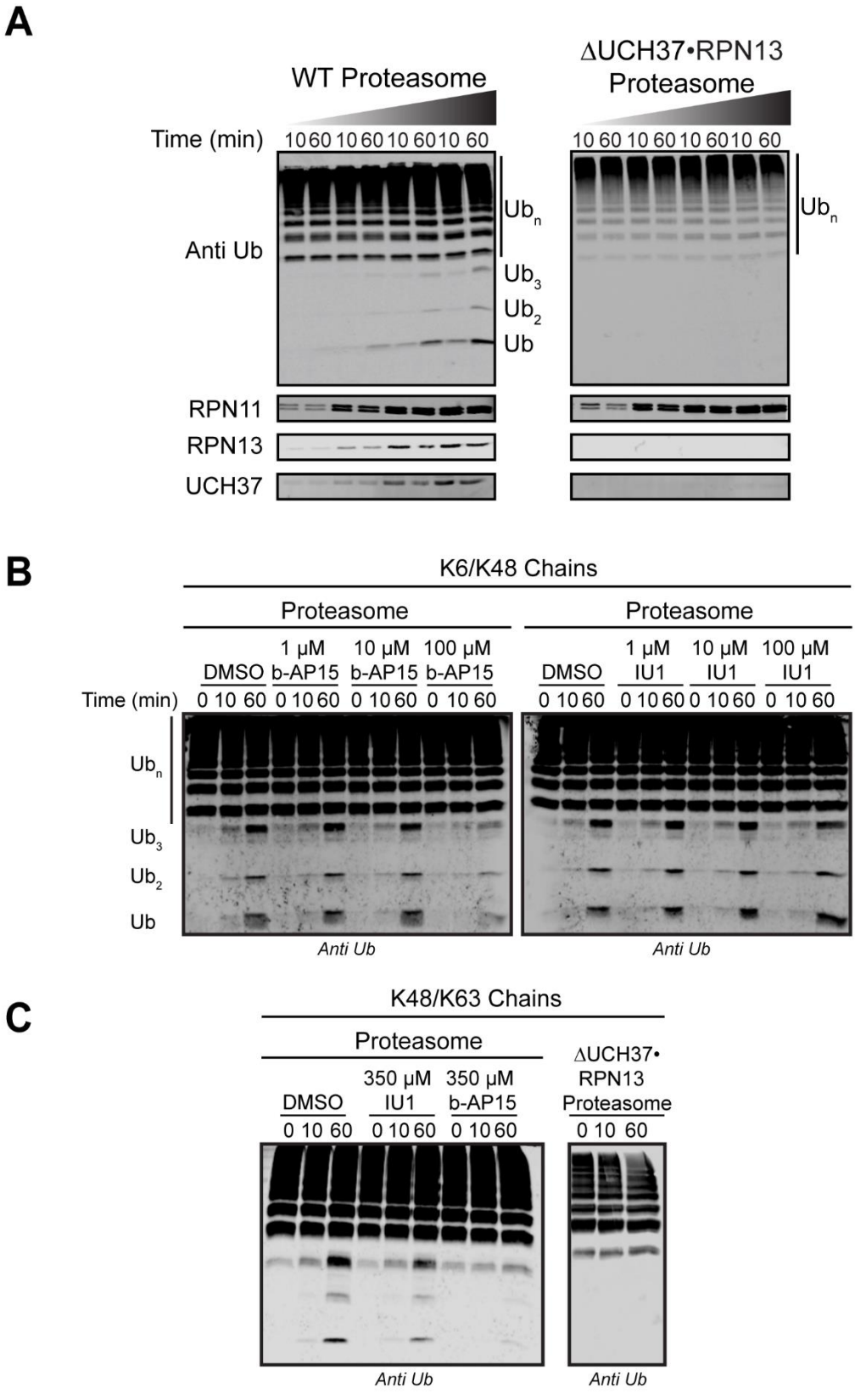
A
WT Proteasome
ΔUCH37•RPN13
Proteasome
Time (min)
10 60 10 60 10 60 10 60
10 60 10 60 10 60 10 60
Anti Ub
Ub_n
Ub_3
Ub_2
Ub
RPN11
RPN13
UCH37
B
K6/K48 Chains
Proteasome
Proteasome
DMSO
1 μM b-AP15
10 μM b-AP15
100 μM b-AP15
DMSO
1 μM IU1
10 μM IU1
100 μM IU1
Time (min)
0 10 60 0 10 60 0 10 60 0 10 60
0 10 60 0 10 60 0 10 60 0 10 60
Ub_n
Ub_3
Ub_2
Ub
Anti Ub
Anti Ub
C
K48/K63 Chains
Proteasome
DMSO
350 μM IU1
350 μM b-AP15
0 10 60 0 10 60 0 10 60
ΔUCH37• RPN13 Proteasome
0 10 60
Anti Ub
Anti Ub

Figure A.3: Characterizing proteasome DUB activity against HMW branched chains. A) Titration of WT Ptsm or ΔUCH37-RPN13 Ptsm into Lys6/Lys48 HMW chains. Lys6/Lys48 chains were incubated with increasing amounts (1, 2.5, 5, or 10 μg) of either WT Ptsm or ΔUCH37-RPN13 Ptsm for the indicated time prior to analysis by western blot with the indicated antibodies. **B**) Characterization of proteasome bound DUBs using the selective DUB inhibitors b-AP15 (inhibits both UCH37 and USP14) and IU1 (only inhibits USP14). Proteasomes were incubated with the indicated inhibitor for 30min prior to addition of Lys6/Lys48 linked chains. Reactions were quenched by SDS-loading buffer and separated on a 15% SDS-PAGE gel and visualized by western blot. **C**) Cleavage of Lys48/Lys63 linked branched chains with inhibitors and ΔUCH37-RPN13 Ptsm. Reactions were performed as in **B**.

We wanted to further confirm that the observed DUB activity was indeed due to chain debranching. To do this we turned to middle-down mass spectrometry (MS). Middle-down MS takes advantage of the limited ability of trypsin to cleave Ub under non-denaturing conditions.[16, 17] Under these conditions, trypsin cleaves Ub at a single site after Arg74, leaving the remaining core of the Ub protein intact (Ub_{1-74} fragment) and releasing Ub's C-terminal Di-Gly motif. When a Ub chain is subjected to this cleavage, the lysine residues that are modified by Ub in the chain retain this Di-Gly motif resulting in a $^{GG}Ub_{1-74}$ when an unbranched chain is present and a $^{2xGG}Ub_{1-74}$ fragment when a branch point is present. Because we can use this technology to look at individual populations of linear and branched chains in a complex mixture, we can use middle down MS to look at debranching activity of an enzyme as described in Chapter 4. Analysis of these preps by middle-down MS shows that the WT Ptsm does indeed display debranching activity, yielding a similar product ratio to free UCH37, while the ΔUCH37-RPN13 Ptsm loses the ability to debranch Ub chains (Figure A.4). Thus, we can use the RPN2 peptide to isolate proteasomes free of non-essential DUBs and begin to probe their functions.

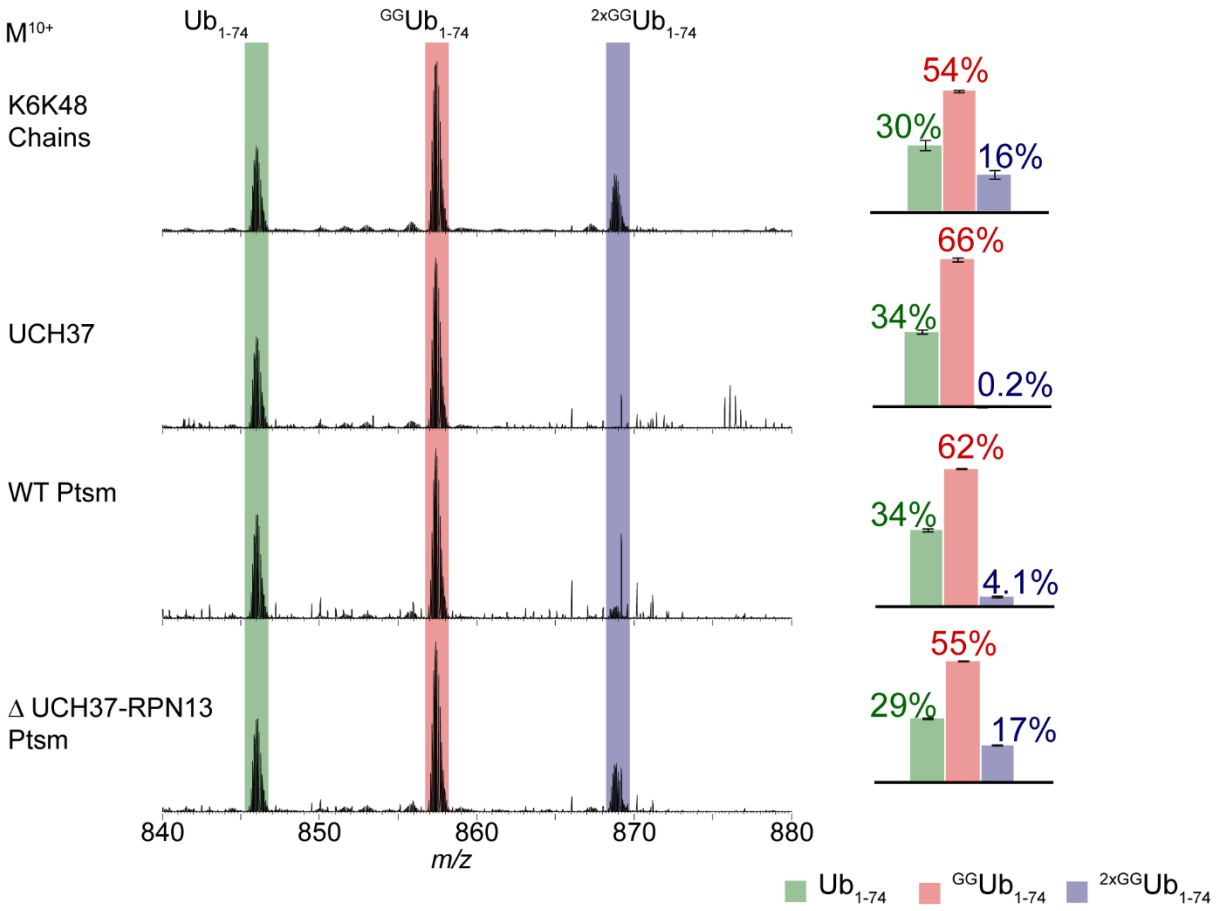

Figure A.4: Characterization of proteasome DUB activity by middle-down MS shows UCH37's debranching activity. NleL chains were incubated for 4h at 37°C with either recombinant UCH37 (5 μM), WT proteasome (10 μg), ΔUCH37-RPN13 Ptsm (10 μg), or buffer as a control. Chains were minimally trypsinized under native conditions prior to MS analysis. Peak highlighted in green corresponds to the Ub_{1-74} species indicative to mono-Ub or chain caps, peak highlighted in red corresponds to the $^{GG}Ub_{1-74}$ species indicative of linear chains, and the peak highlighted in blue corresponds to the $^{2xGG}Ub_{1-74}$ species indicative of chain branching. When treated with either free UCH37 or WT Ptsm, the branched chains decrease while the linear chains remain intact. When treated with ΔUCH37-RPN13 Ptsm however all the chains remain intact.

A.3 Conclusion and Future Directions

In conclusion, we have developed a method that allows us to isolate proteasome complexes where the non-essential DUBs have been removed. We have shown that this method does allow for the functional characterization of DUBs on the proteasome by confirming our previous observation that UCH37 acts as a debranching chain while associated with the 26S proteasome. This activity was present in our WT Ptsm preps but was lost upon depletion of the proteasome using the RPN2 peptide as observed by both western blot analysis and middle-down MS. Interestingly, our ΔUCH37-RPN13 Ptsm isolated using the RPN2 peptide did not display cleavage against the HMW NleL derived chains in our western blot assays. This result is different from the result in Chapter 4, where proteasomes isolated from an RPN13-CRISPR cell line displayed the formation of lower MW Ub species when assayed by western blot, and more work will have to be done to understand this discrepancy. This work now sets the stage for studying the roles of human proteasome bound DUBs in isolation. To date, removal of UCH37 has remained technically difficult. As a result, the study USP14's DUB activity has relied on inhibition of UCH37 using Ub-activity based probes.[8] As both UCH37 and USP14 have been implicated in allosteric regulation of proteasomal AAA+ ATPase activity when bound to Ub, the ability to remove UCH37 and USP14 will be helpful in gaining a better understanding of how these DUBs influence proteasomal degradation.[11-13] With this strategy in hand, the next stage will be to replenish the DUB-free proteasomes with recombinant USP14, UCH37-RPN13 complex, or both so we can further investigate the roles of these non-essential DUBs.

A.4 Experimental Procedures

A.4.1 Materials and Reagents

The following antibodies were used: Anti UCH37 (Abcam, Cat. # ab124931), Anti RPN11 (Abcam, Cat. # ab109130), Anti RPN13 (Cell Signaling Technology, Cat # D9Z1U), Anti RPT2 (Abcam, Cat. # ab3317), Anti B7 (R&D Systems, Cat. #MAB7590), Anti USP14 (Cell Signaling, Cat. # 11931S), Anti Ub (P4D1, Enzo

Lifesciences, Cat. # BML-PW0930), Goat Anti Mouse IR Dye 800CW secondary (LI-COR Biosciences), Goat Anti Rabbit IR Dye 680RD secondary (LI-COR Biosciences). Streptavidin beads and glutathione resin were purchased from Genscript (Cat. #'s L00353 and L00206 respectively). Cells were cultured in DMEM (Genesee Scientific, Cat. # 25-501N) supplemented with 10% FBS (Genesee Scientific, Cat. # 25-514H), 1x Glutamax (Thermofisher, Cat. # 35050061) and 1x pen/strep. Mass spectrometry grade trypsin was purchased from Promega, (Promega, Cat. # V5113). Small molecule inhibitors b-AP15 and IU1 were purchased from Selleck Chemicals (Cat. #'s S7134 and S4920 respectively). Ub-AMC and suc-LLVY-AMC were purchased from Boston Biochem (Cat. #'s U-550 and S-280 respectively).

A.4.2 Protein Expression and Purification

A.4.2.a Expression and Purification of RPN2$_{916-953}$

The C-terminal 38 amino acids of human RPN2 was cloned into pGEX-6P-1 vector which contains an N-terminal GST tag followed by a 3C protease cleavage site. GST-hRPN2 (aa 916-953) was grown in in LB media supplemented with ampicillin (100 µg/µL) to OD_{600} ~0.5 at 37 ^{o}C and then expressed overnight at 18 °C after induction with IPTG (500 µM). Cells were pelleted at 5,000*xg* for 20 min and resuspended in lysis buffer (50 mM Tris pH7.5, 300 mM NaCl, 2 mM DTT, and 1 mM PMSF). Cells were lysed by a French press (three passes at 20,000 psi), clarified by centrifugation at 45,000*xg* for 30 min, and subsequently incubated with glutathione resin for 2 h. Resin was washed extensively with lysis buffer, high salt buffer (lysis buffer + 500 mM NaCl), low salt buffer (lysis buffer + 50 mM NaCl), and eluted with elution buffer (50 mM Tris pH7.5, 150 mM NaCl, 2 mM DTT, and 50 mM reduced glutathione). The eluted protein was then buffer exchanged to 3C cleavage buffer for cleavage with HRV 3C protease overnight. The cleavage reaction was quenched by adding 10% v/v acetic acid. The acidified solution was poured over a 500 mg SEP-PAK C_{18} column (Waters Cat. # wat043395) and washed with 3 mL 0.1% TFA in water followed by 1.5 mL each 10, 20, 30, 40, 50, 60, and 70% ACN in 0.1% TFA at room temperature. Fractions containing RPN2

peptide were identified by MALDI-TOF MS and lyophilized. The lyophilized peptide was then reconstituted in water.

A.4.3 Isolation of WT Proteasomes

HEK293 cells stably expressing His-biotin affinity tagged human RPN11 (RPN11-HTBH) were cultured in 150 mm tissue culture treated plates to a confluency of 80-90%. After reaching confluency, the media was removed, cells were washed with cold PBS and scraped into lysis buffer (50 mM HEPES pH7.5, 50 mM NaCl, 10 mM $MgCl_2$, 2 mM ATP, 2 mM DTT, and 10% glycerol; 1 mL per 150 mm dish), and the harvested cells were stored at -80 ^oC. For each prep, cells from 20x150 mm plates were used. Frozen cells were thawed, lysed by sonication, and the lysate was clarified at 20,000*xg* for 20 min at 4 ^oC. The clarified lysate was incubated with 400 μL streptavidin resin (pre-equilibrated with lysis buffer) overnight at 4 ^oC with rocking. The resin was then pelleted at 500*xg* for 2 min and the supernatant was discarded. The resin was washed with 50 resin volumes of wash buffer (lysis buffer + 200 mM NaCl; 2 mL). Washes were performed by resuspending the resin in 1.5 mL of wash buffer, rocking for 5 mins at 4^oC, pelleting the beads 500*xg* for 2 min, and discarding the supernatants and repeating until the resin had undergone 50 resin volumes of wash (20mL). After washing, the immobilized proteasome was eluted by resuspending the beads in 300 μL elution buffer (2 μM TEV protease in 50 mM HEPES pH7.5, 50 mM NaCl, 10 mM $MgCl_2$, 2 mM ATP, and 10% glycerol) and rocking the resin at room temperature for 2h. After TEV cleavage, the resin was pelleted at 500*xg* for 2 min and the supernatant was collected. The resin was then washed 4 more times with storage buffer (500 μL) and all the supernatants were combined and concentrated to ~150 μL. The concentration of proteasome was estimated by BCA assay, aliquoted into 15 μL portions, and stored at -80 ^oC.

A.4.4 Isolation of ΔUCH37-RPN13 Ptsm

Culturing, harvesting, lysis and clarification of lysate were all identical to the procedure used for WT proteasomes. After clarification, the lysate was incubated with 400µL streptavidin beads for 8h at 4°C with rocking. After 8h the beads were collected by centrifugation at 500*xg* for 2min. The resin was then resuspended in 1mL of lysis buffer, and $RPN2_{916-953}$ was added to a final concentration of 10µM and the resin was further incubated overnight at 4°C with rocking. The following morning the resin was pelleted by centrifugation at 500*xg* for 2min, and further washed two more times with 500µL of 10µM RPN2 in lysis buffer. From here high salt washes, washes, elution, concentration, and storage was identical to the procedure described for WT proteasomes.

A.4.5 Measuring Proteasome Activity by AMC Assay

Proteasome proteolytic activity was followed by using the suc-Leu-Leu-Val-Tyr-AMC (LLVY-AMC) peptide substrate and proteasome deubiquitinase activity was monitored using Ub-AMC. Prior to the start of the reaction, suc-LLVY-AMC (50 µM) or Ub-AMC (250 nM) were warmed to 37 °C in assay buffer (50 mM HEPES pH7.5, 50 mM NaCl, 10 mM $MgCl_2$, 2 mM DTT, and 2 mM ATP) for 30 min. At the same time, the proteasome (wild type or UCH37 free) was warmed to 37 °C in assay buffer for 30 min. The reaction was initiated by the addition of the entire proteasome mixture to the AMC peptide substrate and Ub-AMC substrate. AMC hydrolysis was monitored at 37 °C in 1 min intervals (45 min total) on a fluorescent plate reader (BioTek Synergy 2, λ_{ex} = 360nm, λ_{em} = 460nm).

A.4.6 Measuring Proteasome Activity by Western Blot

High molecular weight Ub chains (250 ng/µL) were warmed to 37 °C in assay buffer (50 mM HEPES pH7.5, 50 mM NaCl, 10 mM $MgCl_2$, 2 mM DTT, and 2 mM ATP) for 30 min. At the same time, the proteasome (4 µg) was incubated with the indicated concentration of DUB inhibitor or DMSO for 30 min at 37 °C. Reactions were initiated by the addition of proteasome-inhibitor mixture (final reaction volume: 35 µL).

Time points were taken as indicated in the figures by removing 10 µL aliquots of the reaction mixture and quenching with 6x Laemmli loading buffer (5 µL). Reactions were separated on a 15% SDS-PAGE gel and visualized by western blot using the anti Ub antibody (P4D1).

A.4.7 Middle-Down MS Analysis of Proteasome Activity

Stock solutions of the proteasome (10 µg) and HMW Ub chains (250 ng/µL) were diluted in assay buffer (50 mM HEPES pH7.5, 50 mM NaCl, 10 mM $MgCl_2$, 2 mM DTT, and 2 mM ATP) and warmed to 37 ^oC. Debranching assays were initiated by adding the proteasome to the chain mixture and incubated for 4h at 37^oC. After 4h, the reactions were quenched by the addition of sequencing grade-modified trypsin (1 µg) to begin the minimal trypsinolysis. This was allowed to proceed for 2h at 37^oC before the reactions were quenched by addition of 10% v/v of acetic acid. All samples were dissolved in a water/acetonitrile (ACN)/acetic acid (45:45:10) solution. Ub_{1-74} species were separated from the mixtures by pouring the acidified mixture over a 100 mg SEP-PAK C_{18} column (Waters Cat. # WAT036935) and washed with 3 mL 0.1% TFA in water followed by 1.5 mL each 10, 20, 30, 40, 50, 60, and 70% ACN in 0.1% TFA at room temperature. Fractions containing Ub_{1-74} species were identified by MALDI-TOF MS and lyophilized. The lyophilized protein was reconstituted in 45:45:10 H_2O: acetonitrile: acetic acid. These were then directly infused into an Orbitrap Fusion Tribrid Mass Spectrometer (Thermo Scientific™ Inc), where the resolving power of the mass analyzer was set at 60000. All spectra were processed using the MASH suite software package[18] using a signal-to-noise (S/N) threshold of 3 and a fit factor of 70% and then validated manually. Percentages correspond to the average relative quantification values of each Ub species: Ub1-74, 1xdiGly-Ub1-74, and 2xdiGly-Ub1-74 between the charge states of 7+ to 12+.[19, 20]

A.5 References

1. Hershko, A.; Ciechanover, A., The Ubiquitin System. *Annu. Rev. Biochem.* **1998,** *67* (1), 425-479.

2. Komander, D.; Clague, M. J.; Urbé, S., Breaking the chains: structure and function of the deubiquitinases. *Nat. Rev. Mol. Cell Biol.* **2009,** *10*, 550.

3. Komander, D.; Rape, M., The Ubiquitin Code. *Annu. Rev. Biochem.* **2012,** *81* (1), 203-229.

4. Bard, J. A. M.; Goodall, E. A.; Greene, E. R.; Jonsson, E.; Dong, K. C.; Martin, A., Structure and Function of the 26S Proteasome. *Annu. Rev. Biochem.* **2018,** *87* (1), 697-724.

5. de Poot, S. A. H.; Tian, G.; Finley, D., Meddling with Fate: The Proteasomal Deubiquitinating Enzymes. *J. Mol. Biol.* **2017,** *429* (22), 3525-3545.

6. Finley, D.; Sadis, S.; Monia, B. P.; Boucher, P.; Ecker, D. J.; Crooke, S. T.; Chau, V., Inhibition of proteolysis and cell cycle progression in a multiubiquitination-deficient yeast mutant. *Mol. Cell. Biol.* **1994,** *14* (8), 5501-5509.

7. Verma, R.; Aravind, L.; Oania, R.; McDonald, W. H.; Yates, J. R.; Koonin, E. V.; Deshaies, R. J., Role of Rpn11 Metalloprotease in Deubiquitination and Degradation by the 26S Proteasome. *Science* **2002,** *298* (5593), 611.

8. Lee, B.-H.; Lee, M. J.; Park, S.; Oh, D.-C.; Elsasser, S.; Chen, P.-C.; Gartner, C.; Dimova, N.; Hanna, J.; Gygi, S. P.; Wilson, S. M.; King, R. W.; Finley, D., Enhancement of proteasome activity by a small-molecule inhibitor of USP14. *Nature* **2010,** *467*, 179.

9. Chen, X.; Lee, B.-H.; Finley, D.; Walters, K. J., Structure of Proteasome Ubiquitin Receptor hRpn13 and Its Activation by the Scaffolding Protein hRpn2. *Mol. Cell* **2010,** *38* (3), 404-415.

10. Wang, X.; Chen, C.-F.; Baker, P. R.; Chen, P.-l.; Kaiser, P.; Huang, L., Mass Spectrometric Characterization of the Affinity-Purified Human 26S Proteasome Complex. *Biochemistry* **2007,** *46* (11), 3553-3565.

11. Peth, A.; Besche, H. C.; Goldberg, A. L., Ubiquitinated Proteins Activate the Proteasome by Binding to Usp14/Ubp6, which Causes 20S Gate Opening. *Mol. Cell* **2009,** *36* (5), 794-804.

12. Peth, A.; Kukushkin, N.; Bossé, M.; Goldberg, A. L., Ubiquitinated Proteins Activate the Proteasomal ATPases by Binding to Usp14 or Uch37 Homologs. *J. Biol. Chem.* **2013,** *288* (11), 7781-7790.

13. Kim, H. T.; Goldberg, A. L., The deubiquitinating enzyme Usp14 allosterically inhibits multiple proteasomal activities and ubiquitin-independent proteolysis. *J. Biol. Chem.* **2017,** *292* (23), 9830-9839.

14. Hospenthal, M. K.; Freund, S. M. V.; Komander, D., Assembly, analysis and architecture of atypical ubiquitin chains. *Nat. Struct. Mol. Biol.* **2013,** *20*, 555.

15. Tian, Z.; D'Arcy, P.; Wang, X.; Ray, A.; Tai, Y.-T.; Hu, Y.; Carrasco, R. D.; Richardson, P.; Linder, S.; Chauhan, D.; Anderson, K. C., A novel small molecule inhibitor of deubiquitylating enzyme USP14 and

UCHL5 induces apoptosis in multiple myeloma and overcomes bortezomib resistance. *Blood* **2014,** *123* (5), 706.

16. Xu, P.; Peng, J., Characterization of Polyubiquitin Chain Structure by Middle-down Mass Spectrometry. *Anal. Chem.* **2008,** *80* (9), 3438-3444.

17. Valkevich, E. M.; Sanchez, N. A.; Ge, Y.; Strieter, E. R., Middle-Down Mass Spectrometry Enables Characterization of Branched Ubiquitin Chains. *Biochemistry* **2014,** *53* (30), 4979-4989.

18. Guner, H.; Close, P. L.; Cai, W.; Zhang, H.; Peng, Y.; Gregorich, Z. R.; Ge, Y., MASH Suite: A User-Friendly and Versatile Software Interface for High-Resolution Mass Spectrometry Data Interpretation and Visualization. *J. Am. Soc. Mass Spectrom.* **2014,** *25* (3), 464-470.

19. Peng, Y.; Gregorich, Z. R.; Valeja, S. G.; Zhang, H.; Cai, W.; Chen, Y.-C.; Guner, H.; Chen, A. J.; Schwahn, D. J.; Hacker, T. A.; Liu, X.; Ge, Y., Top-down Proteomics Reveals Concerted Reductions in Myofilament and Z-disc Protein Phosphorylation after Acute Myocardial Infarction. *Mol. Cell. Proteomics* **2014,** *13* (10), 2752-2764.

20. Chen, Y.-C.; Ayaz-Guner, S.; Peng, Y.; Lane, N. M.; Locher, M. R.; Kohmoto, T.; Larsson, L.; Moss, R. L.; Ge, Y., Effective Top-Down LC/MS+ Method for Assessing Actin Isoforms as a Potential Cardiac Disease Marker. *Anal. Chem.* **2015,** *87* (16), 8399-8406.